Intestinal epithelial and microbial interactions at cellular resolution

by

Reegan J Willms

A thesis submitted in partial fulfillment of the requirements for the degree of

Doctor of Philosophy

in

Immunology

Department of Medical Microbiology and Immunology

University of Alberta

Abstract

The intestinal epithelium is a complex tissue monolayer composed of regionally and functionally specialized cells. Given epithelial exposure to harsh and varied luminal conditions, epithelial cells continuously regenerate to sustain the barrier against environmental factors, including microbial invaders. Both host factors and microbial input contribute to intestinal epithelial growth, differentiation, and function. However, the epithelium contains a complex mixture of secretory and absorptive cell types, and it is unclear how each of these cell populations responds to microbial signals or contributes to epithelial homeostasis.

To determine how microbes alter cell type-specific processes in the intestine, I employed a zebrafish model and single-cell RNA sequencing (scRNA-seq) of the intestine to measure microbe-dependent transcriptional changes at the cellular level. First, I describe genetic markers for cell types in the zebrafish gut under conventional conditions in larvae and adults, establishing homeostatic cell profiles of the zebrafish intestine at two developmental stages. Next, I compare these conventional scRNA-seq datasets to respective cell profiles of intestines from fish larvae raised without microbes, or adults exposed to pathogenic *Vibrio cholerae*, an aquatic bacterium that infects the gastrointestinal tract, and for which zebrafish are natural hosts. Lastly, I employ these single-cell profiles of the zebrafish intestine to identify the receptor activator of nuclear factor kappa light-chain-enhancer of activated B cells (RANK), as a developmental regulator of cells with genetic similarity to microbe-sensing tuft cells in mammals. Taken together, this thesis provides a framework for how commensal and pathogenic microbes impact IEC transcriptional programmes, and explores regulatory infrastructure underlying development of a candidate microbe-sensing cell type.

Preface

This thesis contains original work from Reegan Willms, as well as the work of Lena Jones, Dr. Minjeong Shin, and Dr. Edan Foley. Some of the work herein and listed below is reproduced from published sources and is reused with permission. Dr. Edan Foley is the supervisory author involved in concept formation and manuscript composition.

- o **Willms RJ**, Foley E. (2023). Mechanisms of epithelial growth and development in the zebrafish intestine. *Biochem. Soc. Trans.*
  - o Written content is included in Chapter 1. RW and EF wrote the manuscript.

- o **Willms RJ**, Jones LO, Hocking JC, and Foley E. (2022). A cell atlas of microbe-responsive processes in the zebrafish intestine. *Cell Reports*.
  - o Written content is included in Chapters 1-4. RW and EF wrote the manuscript.
  - o Data from this manuscript are shown in Chapters 3, 4, and 5. RW performed all experiments and analysis included in this thesis, except 16S rRNA gene sequencing and analysis performed by LJ (Tables 4.2 and 4.3 herein). LJ also assisted with larval intestinal dissections for Nanostring gene expression analysis and the second replicate of larval scRNA-seq. Figures reproduced in this thesis include Figures 3.1, 3.2, 3.3, 4.1, 4.2, 4.3, 4.4, 4.5, and 4.6. Data published in this paper, but included in modified form, are shown in Tables 3.1 and 4.1 (cell type markers), as well Figures 3.7 (integrated analysis of larval and adult scRNA-seq data) and 5.6 (TEM of tuft-like cell).

This work also contains a portion of the original work by Lena Jones, Reegan Willms, Minjeong Shin, and Edan Foley presently in preprint form and under review at *Cell Reports*.

- o Jones LO, **Willms RJ**, Shin M, Xu X, Graham RDV, Eklund M, Foley E. (2023). Single cell resolution of the adult zebrafish intestine under conventional conditions, and in response to an acute, natural infection. *bioRxiv.*

o   Written content is included in Chapters 2-4. RW, LJ, and EF wrote the manuscript.

o   Data from this manuscript are shown in Chapters 3 and 4. Data reproduced in this thesis include Figures 3.4, 3.5 and 4.7. LJ performed scRNA-seq of adult intestines, RW and EF analyzed scRNA-seq data. All data and figures included in this thesis (Chapters 3 and 4) were compiled by RW excepting Figure 3.4D (IHC performed by LJ), Figure 3.5 (leukocyte transcriptional analysis performed by EF), Figure 4.7A-C (Vc CFU analysis performed by MS) and Figure 4.7D-G (Adult H&E performed by LJ). Data contained in this paper, but included in modified form, are shown in Tables 3.2 and 4.4 (cell type markers), as well Figures 3.6 (integrated analysis of larval and adult scRNA-seq data) and 4.8 (feature plot of ISG-enriched ECs).

All data included in Chapter 5 are unpublished, except for Figure 5.6B (TEM of tuft-like cell). Analysis of adult intestinal scRNA-seq data in Figures 5.1A and 5.5A employs the abovementioned adult scRNA-seq dataset (Jones et al., 2023).

Acknowledgements

Table of Contents

List of Tables

List of Figures

Chapter 5: RANK drives tuft-like cell development

Chapter 6: Discussion

List of Abbreviations

In order of appearance:

IECs: intestinal epithelial cells

IBDs: inflammatory bowel diseases

scRNA-seq: single-cell RNA sequencing

RANK: receptor activator of nuclear factor kappa light-chain-enhancer of activated B cells

hpf: hours post-fertilization

dpf: days post-fertilization

wpf: weeks post-fertilization

ISC: intestinal stem cell

TA: transit amplifying

BMP: Bone Morphogenetic Protein

NF-κB: nuclear factor kappa light-chain-enhancer of activated B cells

TCF: T-cell factor

APC: Adenomatous Polyposis Coli

TNF: Tumor Necrosis Factor

FAE: follicle-associated epithelium

RANKL: RANK ligand

LGR4: leucine-rich repeat-containing G-protein-coupled receptor 4

TRAF: tumor necrosis factor receptor-associated factor

ILCs: innate lymphoid cells

EEC: enteroendocrine

EC: enterocyte

LRE: lysosome-rich enterocyte

TEM: transmission electron microscopy

M cell: microfold cell

PRRs: pattern recognition receptors

MAMPs: microbe-associated molecular patterns

DAMPS: damage-associated molecular patterns

TLRs: Toll-like receptors

NLRs: NOD-like receptors

LPS: lipopolysaccharide

GF: germ-free

CR: conventionally reared

CV: conventionalized

GO: gene ontology

dgRNA: double guide RNA

ECM: extracellular matrix

Vc: *Vibrio cholerae*

IFN: interferon

IFN-ECs: interferon-enriched ECs

ISG: interferon-stimulated gene

FISH: fluorescent *in situ* hybridization

RNP: ribonucleoprotein

Broad SCP: Broad Institute Single Cell Portal

Chapter 1: Introduction

This chapter contains content from the following sources:

- o **Willms RJ**, Foley E. (2023). Mechanisms of epithelial growth and development in the zebrafish intestine. *Biochem. Soc. Trans.*
- o **Willms RJ**, Jones LO, Hocking JC, and Foley E. (2022). A cell atlas of microbe-responsive processes in the zebrafish intestine. *Cell Reports*.

1.1 Overview

The gastrointestinal tract captures nutrients and energy essential for animal development and health. At the same time, the intestine maintains an intimate relationship with a complex consortium of microbes residing on the intestinal surface, collectively referred to as the gut microbiota (Bengmark, 1998; Bäckhed et al., 2005; Neish, 2009). This microbial multitude is dynamic, containing bacteria, viruses, and fungi whose populations fluctuate according to hereditary and environmental factors (Bennet et al., 2018; Chassaing et al., 2017; Claesson et al., 2012; David et al., 2014). Moreover, the intestine is invariably exposed to pathogenic microbes that damage the host and disrupt the commensal microbiota (Bäumler and Sperandio, 2016). Accordingly, the intestine must balance the need for nutrient uptake, commensal microbe tolerance, and pathogen elimination.

The intestinal epithelium lies at the host-environment interface, forming a single cell layer that harvests dietary nutrients and responds to altered luminal status, including nutrient availability and microbial composition (Bäumler and Sperandio, 2016; den Besten et al., 2013; Gensollen et al., 2016; Natividad and Verdu, 2013). To accomplish this extraordinary feat, the intestinal epithelium contains specialist cell types that contribute in variable capacities to environmental sensing, nutrient acquisition, microbial deterrence, and immune activation (Gehart and Clevers, 2019). However, continuous epithelial exposure to the luminal environment eventually drives mature intestinal epithelial cells (IECs) to programmed cell death (Patankar and Becker, 2020). Thus, the epithelium regenerates continuously, replacing cells that succumb to mechanical or environmental forces (Clevers, 2013; van der Flier and Clevers, 2009; Vermeulen and Snippert, 2014). Maintaining epithelial homeostasis is critical to host health, where dysregulation is associated with impaired microbial containment, intestinal cancers, inflammatory bowel diseases (IBDs) and immune or metabolic disorders (Belkaid and Hand, 2014; Sekirov et al., 2010; Zitvogel et al., 2015). Thus, it is critical to understand intrinsic and extrinsic factors shaping epithelial growth and function.

Over the last few decades, researchers have applied animal models and microbial manipulation to investigate organismal responses to commensal and pathogenic microbes (Bry et al., 1996; Cebra, 1999; Hooper et al., 2001; Hooper et al., 2003; Husebye et al., 1994; Kelly et

al., 2004; Macpherson et al., 2000; Stappenbeck et al., 2002; Uribe et al., 1997). Such studies showed that microbes influence intestinal growth and differentiation, nutrient metabolism, and innate and adaptive immune processes, all of which have broader impact on host health (Bry et al., 1996; Cebra, 1999; Hooper et al., 2001; Hooper et al., 2003; Husebye et al., 1994; Kelly et al., 2004; Macpherson et al., 2000; Stappenbeck et al., 2002; Uribe et al., 1997). Moreover, researchers implemented genetic approaches to identify molecular pathways mediating intestinal responses to microbes (Arora et al., 2018; Haber et al., 2017; Hooper et al., 2001; Koch et al., 2018; Rawls et al., 2004; Reikvam et al., 2011). While this research provided tremendous insight into host-microbe interactions, most investigations focused on the entire gut, or intestinal regions. Thus, a knowledge gap exists in our understanding of intestinal cell-type-specific processes altered by microbial signals. This is a critical unknown given that the intestine contains spatially and functionally specialized cell types with diverse roles in gut function and homeostatic maintenance.

To begin this work, **I hypothesized that microbes alter cell-type-specific processes in the intestine** (Figure 1.1). To test this hypothesis, I employed a zebrafish model and single-cell RNA sequencing (scRNA-seq) of the intestine to measure microbe-dependent transcriptional changes at the cellular level. First, I describe genetic markers for cell types in the zebrafish gut under conventional conditions in larvae and adults, establishing homeostatic cell profiles of the zebrafish intestine at two developmental stages (Chapter 3). Next, I compare these conventional scRNA-seq datasets to respective cell profiles of intestines from fish larvae raised without microbes, or adults exposed to pathogenic *Vibrio cholerae*, an aquatic bacterium that infects the gastrointestinal tract, and for which zebrafish are natural hosts (Chapter 4). Lastly, I employ these single-cell profiles of the zebrafish intestine to identify the receptor activator of nuclear factor kappa light-chain-enhancer of activated B cells (RANK), as a developmental regulator of cells with genetic similarity to microbe-sensing tuft cells in mammals (Chapter 5). Taken together, this thesis provides a framework for how commensal and pathogenic microbes impact IEC transcriptional programmes, and explores regulatory infrastructure underlying development of a candidate microbe-sensing cell type. In this introduction, I explore intestinal structure, mechanisms of epithelial growth and development, and microbe-dependent processes in the vertebrate gut, to

contextualize cell type identifications in the zebrafish intestine (Chapter 3), RANK as a developmental regulator in the intestinal epithelium (Chapter 5), and cell type-specific, microbe-dependent processes in the intestine (Chapter 4).
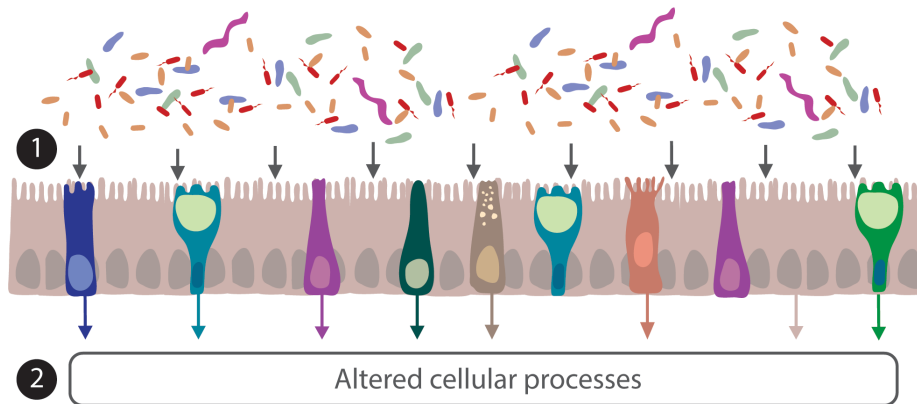
Figure 1.1. Do microbes regulate cell-type-specific processes in the intestine? Microbes are depicted in the lumen of the intestine. (1) Gray arrows represent microbial signals detected by the intestinal epithelium. Specialist IECs (described in this chapter) are represented by unique shape and colour. (2) I predict that microbial signals modulate processes specific to each specialist IEC type, where coloured arrows represent cell-type-specific alterations mediated by microbes.

1.2 Introduction to the zebrafish intestinal model

Regulators of epithelial development and growth have been uncovered through decades of investigation in models as far-ranging as the vinegar fly, rodents, pigs, chickens, and organoids, each sharing common blueprints for intestinal formation and function (Barker, 2014; Buchon et al., 2013b; Ferguson and Foley, 2022; Myers and Schat, 1990; Sato et al., 2009; Zhang et al., 2013). Another emerging and potent model of intestinal development and immunity is the zebrafish, *Danio rerio* (Brugman, 2016), originally established by developmental biologists as a vertebrate model of embryonic development, differentiation, and growth (Grunwald and Eisen, 2002).

Zebrafish offer several advantages, including tremendous fecundity and the developmental conveniences of rapid *ex utero* growth, translucency, small size, and genetic tractability (Westerfield, 2000). Foundational studies in the late 1990's and early 2000's demonstrated that zebrafish and mammalian intestines share structural, functional, and developmental similarities (Crosnier et al., 2005; Ng et al., 2005; Pack et al., 1996; Wallace and Pack, 2003; Wallace et al., 2005), validating the utility of fish to uncover fundamental principles of gut biology. Since then, zebrafish have emerged as a powerful system to study intestinal inflammation and host-microbe interactions (Brugman, 2016; Flores et al., 2020; López Nadal et al., 2020), and genetic analyses have expanded our understanding of fish gut physiology, revealing transcriptional overlap between fish and mammalian intestines (Davison et al., 2017; Lickwar et al., 2017; Wang et al., 2010b). These studies revealed that regional subdivisions and mucosal composition of the zebrafish gut are highly similar to mammalian intestines. Despite these advances, the zebrafish intestine remains under-characterized relative to other models, obscuring the potential of zebrafish for studies of intestinal development, growth, and host-microbe interactions. For instance, researchers lack a complete picture of intestinal epithelial cell types and their markers, and regulators of epithelial development remain incompletely understood (Crosnier et al., 2005; Flasse et al., 2013; Flores et al., 2008; Haramis et al., 2006; Muncan et al., 2007; Ng et al., 2005; Olden et al., 2008; Pack et al., 1996; Roach et al., 2013; Wallace and Pack, 2003; Wallace et al., 2005). Given the known similarities across vertebrate intestinal development, structure, and transcriptional regulation, it is likely that zebrafish will be useful to uncover both regulators of intestinal development, as well as cell type-specific responses to environmental stressors, as considered in this work. Throughout this chapter, I explore zebrafish intestinal biology, drawing comparisons to mammals in an effort to highlight similarities and unknowns related to the use of the zebrafish model.

1.3 Intestinal segmentation and architecture

Intestinal tracts are regionally specialized to optimize the harvest of usable energy sources (Thompson et al., 2018). Along the gut tube, both host organisms and commensal microbes secrete digestive enzymes that catabolize dietary nutrients into simple peptides,

sugars, and fatty acids that are then absorbed across the intestinal epithelium (Perrigoue et al., 2014; Perrone et al., 2010; Rooks and Garrett, 2016). Nutrient digestion along the intestinal length is regionally dependent and corresponds to distinct epithelial composition and function (Thompson et al., 2018). In mammals, the proximal intestine (duodenum) facilitates chemical digestion, the jejunum specializes in protein, carbohydrate, and lipid absorption, the ileum is immune-competent and reabsorbs bile acids, and the colon specializes in water and salt retention (Figure 1.2). Functional specializations also correlate with other regional features; for example, the small intestine contains a single loose mucous layer that enables nutrient absorption, while the colon has both attached and loose mucous layers that support a vast consortium of commensal microbes (Johansson et al., 2013). Microbiota repression in the proximal intestine is further achieved through higher antimicrobial peptide expression relative to the colon (Gubatan et al., 2021).

The zebrafish intestine is segmented, though less complex, than the mammalian gut. While the zebrafish does not possess an acidic digestive domain like the human stomach, it has three major intestinal regions defined as the anterior intestinal bulb, the middle intestine, and the posterior intestine (Crosnier et al., 2005; Ng et al., 2005; Pack et al., 1996; Wallace and Pack, 2003; Wallace et al., 2005), with up to seven transcriptionally distinct regions therein (Lickwar et al., 2017; Wang et al., 2010b). Prevailing evidence indicates that the anterior bulb and middle intestine are akin to the mammalian duodenum and jejunum, mediating lipid, carbohydrate, and protein uptake, while the distal middle intestine recovers bile salts like the ileum, and the posterior mediates ion and water absorption like the colon (Brugman, 2016; Lickwar et al., 2017; Ng et al., 2005; Wallace et al., 2005; Wang et al., 2010b) (Figure 1.2). The zebrafish also has an esophagus and pharynx that comprise the foregut, and a cloaca or hindgut that may be comparable to the mammalian rectum, though these tissues have yet to be thoroughly investigated. Some work indicates the proximal digestive tract exhibits developmental congruence with the stomachs of mammals and birds, where early formation requires the transcription factor Sox2 (Muncan et al., 2007).

Zebrafish and mammalian intestines exhibit moderate structural overlap. Both contain a serous membrane underlying layers of longitudinal and circular muscle (Wallace and Pack, 2003).

6

However, unlike mammals that have a submucosa and muscularis mucosa underlying the mucosa, the zebrafish mucosa sits directly over the musculature with an attenuated layer of connective tissue beneath the epithelium (Wallace et al., 2005). Zebrafish also possess a simplified enteric nervous system of a single myenteric layer with neurons and glia that regulates gut peristalsis, hormone secretion, and nutrient absorption (Wallace et al., 2005).

The zebrafish mucosa itself is comparable to humans, with folded structures referred to as villar ridges, or rugae (Figure 1.2). Here, the zebrafish mucosa is elongated relative to mammalian finger-like villi, and rugae lack infolded crypts (Pack et al., 1996; Wallace et al., 2005; Wang et al., 2010b). The lamina propria of both rugae and villi contain immune and stromal cells, as well as a dense network of blood and lymphatic vessels that quickly disseminate available nutrients (Wallace and Pack, 2003). The epithelium overlays the lamina propria, contacting the lumen, where distinct IEC populations contribute to regional and functional gut specializations (Wallace and Pack, 2003).
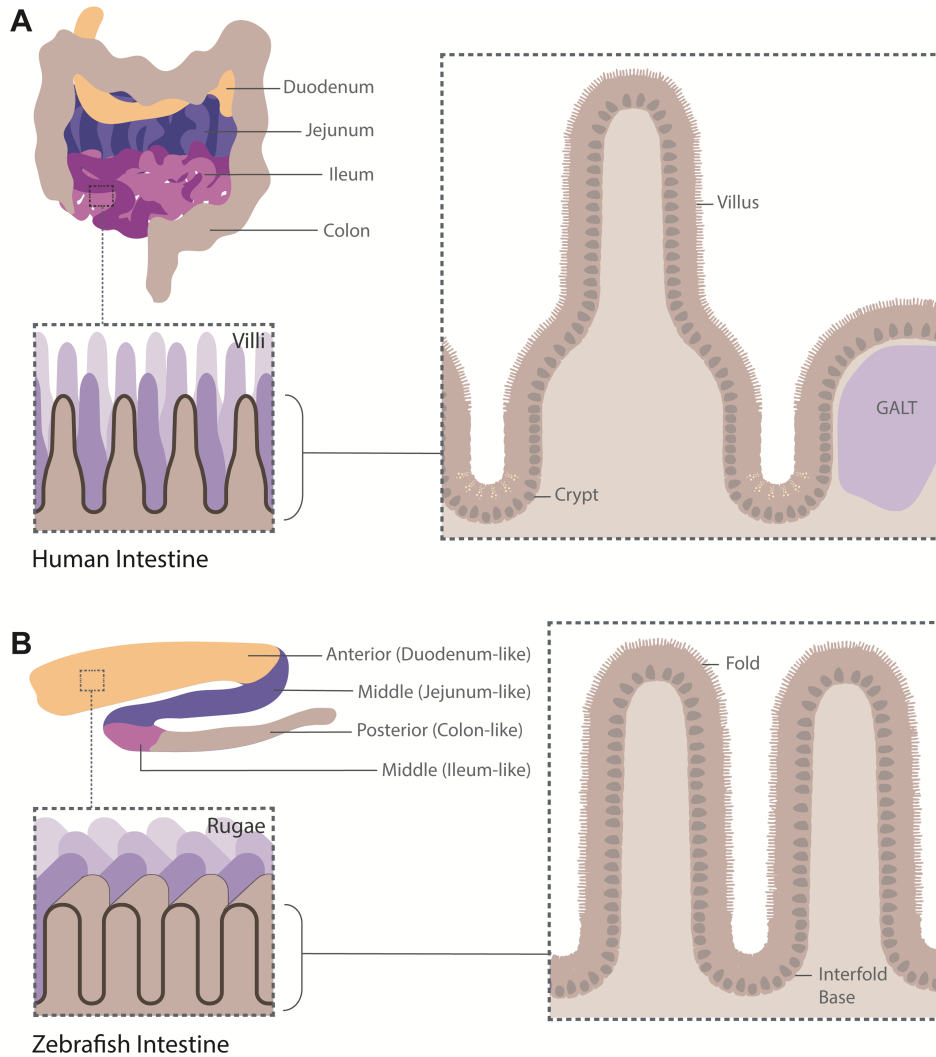
Figure 1.2. Comparison of intestinal structure in humans and zebrafish. **A)** The human intestine is composed of the small intestine (duodenum, jejunum, ileum) and large intestine (colon). The small intestine contains villi, with an epithelium organized into villus-crypt structures. The human intestine also possesses dedicated epithelia overlying gut-associated lymphoid tissue (GALT). **B)** The zebrafish intestine is segmented into the anterior, middle, and posterior regions that exhibit functional and genetic similarity to the mammalian intestine. Epithelia are arranged into folded structures termed rugae.

1.4 Zebrafish intestinal formation

Zebrafish gut tube formation begins at mid somite stages (Wallace and Pack, 2003) and completes morphogenesis by 34 hours post-fertilization (hpf) (Wallace et al., 2005). The gut tube then grows substantially and forms a polarized epithelium between 34 and 120 hpf, coincident with early nutrient acquisition from the yolk as well as exogenous feeding around 120 hpf (Wallace and Pack, 2003; Wallace et al., 2005). Initially, the epithelium is highly proliferative to facilitate growth, however division rates decrease from 74 to 120 hpf, with dividing cells and nascent IECs restricted to the base of newly formed epithelial folds (Crosnier et al., 2005; Wallace et al., 2005). It is unclear what drives decreased proliferative potential after 74 hpf, however researchers have proposed that smooth muscle formation at this time encourages epithelial folding and simultaneously confines proliferation to the fold base (Li et al., 2020; Olden et al., 2008; Wallace et al., 2005). Thus, by 5 days post-fertilization (dpf) zebrafish have fully functional intestines with maturing epithelial folds and basally restricted epithelial growth.

Between 6 and 33 dpf, the intestine matures substantially, with a burst of growth and intestinal folding occurring 19 to 26 dpf (Li et al., 2020; Wallace et al., 2005). From 6 to 19 dpf, proliferative IECs and their progeny remain at the base of modestly sized epithelial folds; however, the rapid growth period from 20 to 26 dpf is accompanied by increased epithelial proliferation, fold elongation, and apical migration of differentiating IECs (Li et al., 2020). At this time, new IECs primarily contribute to epithelial fold lengthening, with limited apoptosis until 2 months of age (Li et al., 2020). Thus, the postembryonic period appears to be divided into three stages of epithelial growth: 1) an immature stage of steady growth from 6 to 19 dpf, where new cells are restricted to the fold base; 2) epithelial maturation from 20 to 33 dpf, where new cells migrate apically and epithelial folds elongate; and 3) the mature adult form where epithelial cells undergo homeostatic cell replacement (Li et al., 2020). Further work is needed to understand stem cell division and differentiation dynamics, as well as functional IEC alterations that accompany these disparate developmental stages.

1.5 Growth and renewal of the intestinal epithelium

At the heart of epithelial growth are multipotent intestinal stem cells (ISCs) that undergo self-renewing divisions, followed by differentiation to generate regionally specialized mixtures of absorptive and secretory cell types (Barker et al., 2007). Stem cell dynamics and terminal cell maturation are highly responsive to endogenous and external stimuli, where inter-IEC communication and molecular pattern sensing trigger cell division and differentiation to maintain an epithelial barrier (van der Flier and Clevers, 2009).

Mammalian small intestinal ISCs reside at the base of epithelial invaginations called crypts of Lieberkühn, within a protected niche formed by neighbouring epithelial, stromal and muscle cells (Gehart and Clevers, 2019). These ISCs, referred to as crypt base columnar cells, are marked by Lgr5 expression and divide frequently under homeostatic conditions to regenerate the entire small intestinal epithelium every 3-5 days (Barker et al., 2007; Darwich et al., 2014). Lgr5+ crypt base columnar cells simultaneously self-renew while giving rise to highly proliferative transit-amplifying (TA) cells that exit the crypts and migrate apically as they differentiate (Barker et al., 2007; Bjerknes and Cheng, 1999; Winton and Ponder, 1990). Differentiated cells continue moving toward the villus tip as they age, until environmental stress drives them to programmed cell death, at which stage they are shed from the epithelium (Gilmore, 2005). There is some controversy over the existence of quiescent, reserve ISC populations that inhabit the niche periphery and re-populate the stem cell niche if crypt base columnar cells are compromised, for example due to genomic instability (Barker et al., 2012; Gehart and Clevers, 2019). Given the uncertainty in this area, I will confine my discussion of ISCs to crypt base columnar cells, and hereafter refer to them simply as "ISCs." Likewise, I will use the term "progenitors" in reference to ISCs and TA cells collectively.

Studies in the zebrafish intestine uncovered a cycling basal epithelial cell, analogous to the mammalian ISC, that drives epithelial development in larvae and adults (Crosnier et al., 2005; Li et al., 2020; Wallace et al., 2005; Wang et al., 2010b). Despite this important similarity, a major barrier to harnessing zebrafish as a model for intestinal biology has been the lack of genetic markers and tools to manipulate this ISC population. The zebrafish genome does not encode Lgr5 or Ascl2, two Wnt pathway genes highly expressed by mammalian ISCs. However, recent studies

uncovered characteristics of the progenitor compartment in fish guts, such as basally-localized Stat3-responsive cells (Peron et al., 2020), or Prmt1-expressing cells that generate both secretory and absorptive lineages (Tavakoli et al., 2022), though it is unclear if these are the same cell type, or if these cells are present throughout development. While validated markers for a multipotent cell type that generates all epithelial lineages have yet to be described, a growing body of evidence demonstrates that pathways regulating progenitor dynamics are shared across mammals and zebrafish, including Wnt, Bone Morphogenetic Protein (BMP) and Notch signaling. In this section, I discuss regulatory pathways foundational to understanding cell types and genetic markers identified in Chapter 3. Furthermore, I consider the role of RANK-mediated activation of the nuclear factor kappa light-chain-enhancer of activated B cells (NF-κB) pathway and cell specification in the gut to provide context for investigating RANK function in Chapter 5.

1.5.1 Wnt/β-catenin signals drive ISC maintenance and renewal

The Wnt/β-catenin signaling pathway is essential for mammalian stem cell renewal and maintenance (van de Wetering et al., 2002). Wnt ligands are secreted glycoproteins that bind to members of the Frizzled receptor family, where Wnt pathway activation leads to β-catenin nuclear translocation and association with T-cell factor (TCF) family transcription factors that initiate Wnt effector molecule transcription (Alok et al., 2017; Behrens et al., 1996; Molenaar et al., 1996; Nusse and Clevers, 2017). In mammals, intestinal Wnt activity is restricted to crypts, where stromal-derived Wnt ligands bind the Frizzled and LRP5/6 receptors that prevent β-catenin degradation by the Adenomatous Polyposis Coli (APC) destruction complex (Nusse and Clevers, 2017). Low level Wnt signals are then enhanced by R-spondins that bind leucine-rich repeat-containing G protein-coupled receptors to promote ISC renewal and maintenance (Carmon et al., 2011; de Lau et al., 2011; Glinka et al., 2011; Kim et al., 2005; Sato et al., 2009). Wnt signals diminish as proliferating cells exit the niche to facilitate progenitor cell differentiation (Nusse and Clevers, 2017).

Wnt also functions in the zebrafish intestinal epithelium, though its mechanism of action has yet to be fully uncovered, and disparities are apparent between larval and adult IECs. For example, zebrafish larvae lacking the Wnt co-activator Tcf4 fail to develop a class of Stat3-

responsive cells with stem-like character (Peron et al., 2020), and lose some proliferative capacity (Cheesman et al., 2011). Conversely, larvae with overactive Wnt, achieved through depletion of the β-catenin destruction complex component Axin1, exhibit excess cell proliferation (Cheesman et al., 2011). Thus, it appears that Wnt has a moderate pro-proliferative and cell maintenance role in the larval zebrafish gut but is not absolutely required for epithelial maintenance or growth. In contrast, juvenile *tcf4* null mutants exhibit severely diminished cell division at the fold base four weeks post-fertilization, leading to premature death by six weeks (Muncan et al., 2007), while adults deficient for the Wnt antagonist APC develop spontaneous intestinal tumours (Haramis et al., 2006). Together, these studies reveal that Wnt drives proliferation in the zebrafish intestine, although Wnt may only become essential as fish mature to adulthood. Further work using conditional, cell type-specific gene inactivation will uncover requirements for Wnt in ISC maintenance and epithelial growth, and remove possible confounding effects of whole animal knockouts or maternally-provided gene products in mutant larvae.

Additional studies report the expression of putative Wnt receptors and targets in zebrafish IECs, though their role in Wnt signaling and epithelial homeostasis remains speculative. For example, the Tcf4 target (Blache et al., 2004) and candidate stem cell marker *sox9b* is expressed at the fold base of the adult zebrafish intestine (Cheesman et al., 2011; Peron et al., 2020), indicating a probable role in ISC niche maintenance. Furthermore, *ascl1a*, though not a confirmed target of Wnt in zebrafish, is highly expressed in larval epithelial progenitors (Flasse et al., 2013), and may be functionally equivalent to mammalian Wnt target and ISC marker *Ascl2*. Finally, the Wnt receptors *fzd5* and *fzd8a* were detected in the developing gut at 30 hours post-fertilization (hpf) (Nikaido et al., 2013), while *lgr4* could be detected at 96 hpf (Hirose et al., 2011), though their roles in IEC homeostasis are not known.

1.5.2 Bone morphogenetic protein signaling: an unknown factor in zebrafish IEC differentiation

BMPs are members of the Transforming Growth Factor Beta superfamily that regulate epithelial cell differentiation in the mammalian gut (Cichy et al., 2014; Howe et al., 1998). BMP gradients act in opposition to Wnt signals, increasing apically along the basal-apical villus axis to inhibit proliferation and promote differentiation (He et al., 2004). In mice, mesenchyme-derived

BMPs promote absorptive cell differentiation, whereas depletion of endogenous BMP drives neoplastic stem cell overgrowth (Auclair et al., 2007; He et al., 2004; Qi et al., 2017). Factors involved in mouse IEC differentiation include BMP2 and BMP4 that bind epithelial BMPR1A to initiate a phosphorylation cascade that drives SMAD complex formation, nuclear translocation, and transcriptional regulation (Gehart and Clevers, 2019).

BMP is involved in early endoderm specification in zebrafish (Chung et al., 2010), though we know little about BMP function in zebrafish IECs. BMP2b-deficient zebrafish exhibit developmental defects in intestinal smooth muscle and enteric nervous system formation (Huang et al., 2019), while conditional BMP inhibition impedes cloaca development (Pyati et al., 2006). These findings implicate BMP in intestinal development, although we do not know which cells are involved in signal transduction, and we lack information on BMP involvement in the development of larval or adult intestinal epithelia.

1.5.3 Notch-mediated differentiation: the binary enforcer

Intestinal Notch signals are critical for progenitor cell fate choices between secretory and absorptive lineages, where high Notch activity blocks secretory cell differentiation in favor of absorptive cell production (Fre et al., 2005; Micchelli and Perrimon, 2006; Ohlstein and Spradling, 2006; van Es et al., 2005). In mammals, Notch signaling occurs in ISCs and basal TA cells, where a Paneth or secretory precursor cell presents membrane-bound Dll1 or Dll4 to neighboring progenitors that express the Notch receptor (Pellegrinet et al., 2011; Sato et al., 2011; Stamataki et al., 2011). Receptor activation prompts γ-secretase-dependent cleavage and nuclear translocation of the Notch intracellular domain, followed by binding with transcriptional activator Rbpj and induction of the secretory cell differentiation factor Atoh1, which also represses Dll1 and Dll4 ligand production in Notch-expressing cells (Kim et al., 2014). Thus, Notch activation is reinforced in absorptive progenitors while preventing Notch activation in adjacent ligand-presenting cells, solidifying their secretory fate. This binary mechanism of lateral inhibition ensures consistent ratios of absorptive and secretory cell production, alongside stem cell maintenance.

Notch signaling also plays a critical role in zebrafish IEC differentiation. For example, Notch regulators are highly expressed in the larval gut, including the Delta and Serrate ligands, as well as several Notch receptors (Crosnier et al., 2005). The intestinal epithelium of zebrafish with a null mutation in the *Dll1* orthologue *deltaD* has moderately increased secretory cell numbers, while depletion of an E3 ubiquitin ligase and pan-Delta activator, *mib1*, produced epithelia dominated by secretory cells (Crosnier et al., 2005). These findings indicate that Delta-Notch signals suppress secretory cell fate choices in the zebrafish intestine, and that several Notch ligands collaborate to activate Notch. In support of a role for Notch in secretory fate choices, inhibition of Notch via expression of a dominant-negative Rbpj elevated endocrine-specified secretory cell numbers (Troll et al., 2018). Additional work showed that loss of the mRNA alternative splicing regulator heterogeneous nuclear ribonucleoprotein I (hnRNP I) prevented degradation of the Notch intracellular domain, leading to overactive Notch, goblet cell deprivation, and epithelial overgrowth (Yang et al., 2009). Finally, several studies revealed that the γ-secretase inhibitor DAPT increased secretory cell abundance (Flasse et al., 2013; Roach et al., 2013), and prevented specification of absorptive cells such as vacuolated lysosome-rich enterocytes (Rodríguez-Fraticelli et al., 2015). Together, these findings indicate that Notch induces IECs to adopt an absorptive fate, whereas Notch inhibition is sufficient for secretory lineage determination.

Some evidence suggests that zebrafish Notch signaling employs an alternate bHLH transcription factor to specify secretory cells. While mammals rely on Atoh1 to drive Notch ligand transcription, concurrent studies of *ascl1a* mutants demonstrated that Ascl1a may fulfill this role in zebrafish, driving secretory cell differentiation by inducing expression of *deltaD*, as well as downstream endocrine cell specification factors (Flasse et al., 2013; Roach et al., 2013). While these findings need to be reconciled with research showing that *atoh1b* can partially rescue secretory cell production when overexpressed in *ascl1a* mutants (Reuter et al., 2022), it remains unclear if upstream Notch regulators Rbpj and Hes1 inhibit bHLH transcription factor expression. Recent work found *Hes1* orthologues *her6* and *her9*, as well as *Hes5* orthologue *her15.1*, are expressed in the gut (Rodríguez-Fraticelli et al., 2015), and one paper revealed an IEC subset co-labeled by fluorophores under the control of Rbpj-mediated transcription and an *her6* enhancer

respectively (Lickwar et al., 2017). These findings implicate Hes-related family members in Notch activation, though additional work is needed to clarify the role of specific Notch signaling pathway components in zebrafish IECs.

1.5.4 RANK and NF-κB as regulators of cell specification

RANK is a Tumor Necrosis Factor (TNF) receptor superfamily member (*TNFRSF11A*) involved in a broad spectrum of host developmental processes, including bone homeostasis (Li et al., 2022), immune cell differentiation (Li et al., 2022), mammary gland epithelial development (Fata et al., 2000), medullary thymic epithelial development (Rossi et al., 2007), and specification of antigen transporting M cells in the intestinal follicle-associated epithelium (FAE) (Knoop et al., 2009), a cell layer overlying lymphoid follicles that specializes in antigen uptake. While it is not yet clear how RANK function compares in these tissues, a requirement for RANK activity in such diverse contexts implicates RANK as a fundamental mediator of development.

RANK is activated through trimerization that occurs upon binding with RANK ligand (RANKL), a TNF superfamily member that exists in both soluble and membrane-bound forms (Hikita et al., 2006; Man et al., 2018). RANK can also trimerize and self-activate independently of RANKL binding (Crockett et al., 2011; Kanazawa and Kudo, 2005), though the relative contribution of self-activated RANK to *in vivo* functioning requires further study. Given that RANK activation is thwarted by the presence of alternate RANKL receptors, RANK-RANKL interactions appear to be the primary mechanism of RANK activation. Specifically, osteoprotegerin (OPG) and leucine-rich repeat-containing G-protein-coupled receptor 4 (LGR4) both limit RANK activation by binding to RANKL (Li et al., 2022; Luo et al., 2016), at least in the context of bone homeostasis.

RANK activation through RANKL binding drives association of the RANK intracellular domain with tumor necrosis factor receptor-associated factor (TRAF) family members that induce numerous signaling pathways, including NF-κB (Nakashima et al., 2012). NF-κB is an industrious transcription factor that responds to many inputs, such as microbial and inflammatory signals, and activates various downstream processes including cell survival and innate immune pathways (Taniguchi and Karin, 2018). Given the prolific roles of NF-κB and my focus on intestinal

development, I will limit further consideration of NF-κB to known involvement in intestinal cell specification.

NF-κB activation is well known as a developmental regulator of the mammalian FAE, where innate lymphoid cells (ILCs) and stromal cells produce cytokines that bind to epithelial tumor necrosis factor receptor superfamily members to activate NF-κB. Specifically, ILC3 cells produce lymphotoxin alpha that binds to epithelial TNFR (Debard et al., 2001; Dejardin et al., 2002), and stromal cells produce RANKL that binds to epithelial RANK (Kanaya et al., 2012; Kanaya et al., 2018; Knoop et al., 2009), resulting in specification of M cells from lymphoid follicle-adjacent ISCs. While additional roles for NF-κB in vertebrate IEC development remain unclear, work in *Drosophila* demonstrated that the Immune Deficiency (IMD) pathway, a relative of the TNF-receptor signaling pathway, activates NF-κB family member *relish* to increase enterocyte production by upregulating Notch pathway components (Liu et al., 2022). Moreover progenitor-specific inactivation of the IMD pathway shifts epithelial composition across development (Shin et al., 2022), implicating NF-κB activity in IEC differentiation. Thus, while the role of RANK has not been investigated in the context of villus IEC differentiation (as distinct from FAE differentiation), it may not be surprising that RANK-mediated NF-κB activation regulates aspects of IEC development, as purported in Chapter 5 of this work.

1.6 IEC lineages and specification factors

The mature human intestinal epithelium has at least seven specialist cell types that develop from multipotent ISCs. Cells of the secretory lineage include Paneth, enteroendocrine cells (EECs), goblet, and tuft cells, while the absorptive lineage includes enterocytes (ECs), M cells, and recently identified BEST4-positive enterocytes (Parikh et al., 2019; Smillie et al., 2019). While zebrafish possess clear absorptive and secretory IEC populations, and transcriptional overlap is evident between humans and zebrafish intestinal epithelia (Crosnier et al., 2005; Ng et al., 2005; Wallace et al., 2005), zebrafish IEC subtypes remain poorly defined (Figure 1.3), hindering cell type-specific investigations of development or host-microbe interactions.
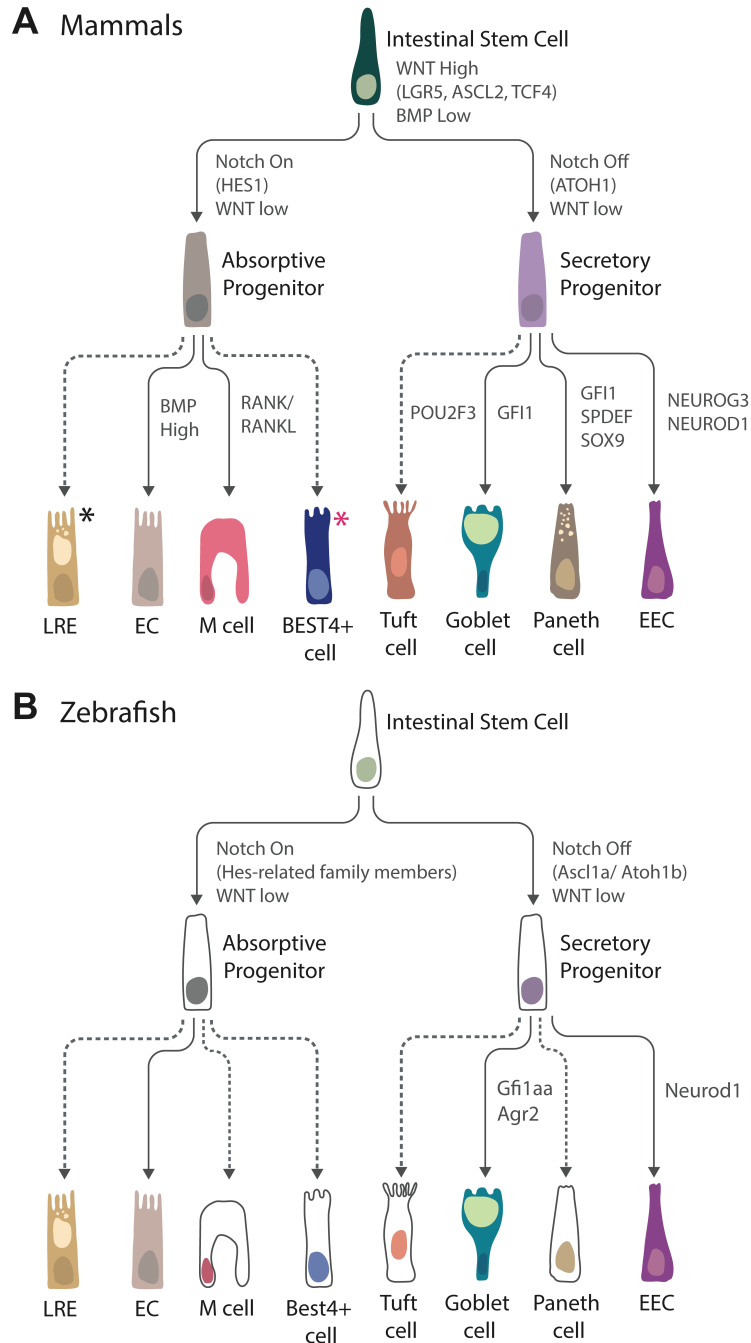
Figure 1.3 Comparison of intestinal epithelial cell development in mammals and zebrafish. A) In mammals, specialized epithelial cells differentiate from intestinal stem cells that generate absorptive or secretory progenitors, where a combination of Wnt, BMP and Notch signals determine cell fate. Dashed arrows indicate tentative lineages. *LREs (Lyososome-rich enterocytes) are only present in mammalian neonates. *BEST4+ cells are present in humans but have not been identified in mice. **B)** Zebrafish intestinal stem cells generate absorptive and

secretory lineages dependent on Notch and Wnt signals. Dashed arrows indicate tentative lineages. Non-coloured cells indicate cell types that have not been identified in zebrafish (absorptive progenitors, secretory progenitors, M cells, BEST4+ cells, tuft cells, and Paneth cells).

1.6.1 Secretory cell lineages

From flies to fish and mammals, Notch is the primary determinant of progenitor fate, where cells default to a secretory cell state in the absence of Notch activity (Gehart and Clevers, 2019). Vertebrate secretory cells generally arise from a common progenitor under the direction of Atoh1 (perhaps Ascl1a in zebrafish), although the exact combination of differentiation signals needed to specify secretory cell subtypes requires clarification.

1.6.1.1 Paneth cells

Mammalian Paneth cells are crypt-resident specialists that protect stem cells by preventing microbiota infiltration and providing growth cues to neighbouring ISCs (Sato et al., 2011). Unusual among IECs, these long-lived cells traverse downward from the niche periphery to interdigitate with ISCs, where they survive up to 2 months (Batlle et al., 2002; Genander et al., 2009). Paneth cells maintain crypt sterility by secreting antimicrobial peptides, and manage ISC maintenance and differentiation by producing Wnt and Notch ligands that support the stem cell niche and drive secretory cell production (Gehart and Clevers, 2019). Paneth cells are the default fate for committed secretory precursors in mammals, where high fibroblast growth factor signals and Wnt-dependent *Sox9* expression direct Paneth cell differentiation (Bastide et al., 2007; Mori-Akiyama et al., 2007; Vidrich et al., 2009). Initial specification of both Paneth and goblet cells depends on *Gfi1* (Shroyer et al., 2005), while the Wnt-responsive gene *Spdef* guides terminal differentiation of both cell types (Gregorieff et al., 2009; Noah et al., 2010).

Histological analysis and transmission electron microscopy (TEM) studies indicate that larval and adult zebrafish intestines lack Paneth cells (Brugman, 2016). However, zebrafish IECs at the fold base express *sox9b*, orthologous to Paneth cell specification factor *Sox9* (Cheesman et al., 2011; Peron et al., 2020). This observation reveals a greater need to understand the role of *sox9b* in zebrafish IEC specification, as well as ISC niche maintenance in the absence of Paneth

cells. In this respect, it is plausible that zebrafish ISCs rely on stromal factors, specialist sentinel goblet cells, and additional crypt-resident secretory cells to form a stable niche (Birchenough et al., 2016; Sasaki et al., 2016).

1.6.1.2 Goblet cells

The most abundant secretory cell type in mammals and zebrafish is the goblet cell, whose role is to produce a protective mucous layer that prevents microbial invasion of the host layer. As in mammals, zebrafish goblet cells are concentrated in the distal mid-intestine, akin to the ileum and colon (Crosnier et al., 2005; Ng et al., 2005; Wallace et al., 2005), although regionally-specialized goblet cell subtypes are apparent (Crosnier et al., 2005). Specifically, wheat-germ agglutinin-positive goblet cells are found in the anterior and posterior intestine, and can be differentially labeled via immunostaining (Crosnier et al., 2005). At present, we have limited knowledge of goblet cell differentiation in zebrafish, or factors that might influence regional subtypes. The transcription factor *cdx1b*, functionally equivalent to mouse *cdx2*, regulates specification of several IEC types including goblet cells (Chen et al., 2009; Flores et al., 2008). Notch signals also regulate goblet cell specification, where overexpression of *ascl1a* or *atoh1b* rescued goblet cell deficiency but not EEC production in *ascl1a* mutants (Reuter et al., 2022). As in mammals, zebrafish *agr2* is required for mucus production, though zebrafish *agr2* additionally promotes terminal goblet cell differentiation (Chen et al., 2012). Finally, GFP expressed under the control of *Gfi1* orthologue *gfi1aa* labels intestinal goblet cells (Thambyrajah et al., 2016) implicating *gfi1aa* in zebrafish goblet cell production. Given the immediate link between goblet cell function and microbiota containment, zebrafish are an attractive organism to dissect effects of pathogenic microbial communities on goblet cell development and function.

1.6.1.3 Enteroendocrine cells (EECs)

In zebrafish and mammals, peptide-hormone secreting EECs guide metabolite sensing, nutrient intake, digestive enzyme production, appetite, and intestinal motility (Flasse et al., 2013; Gribble and Reimann, 2016; Lavergne et al., 2020; Roach et al., 2013). EEC subtypes exhibit unique peptide hormone secretion profiles, producing variable combinations of the 15 or more intestinal

peptide hormones (Bates et al., 2006; Chen et al., 2009; Flasse et al., 2013; Gribble and Reimann, 2016; Moran-Ramos et al., 2012; Roach et al., 2013; Wallace et al., 2005). Mammalian EEC fate is determined by *Neurog3* expression in secretory precursor cells, where *Neurog3* is downstream of *Atoh1*, and *Neurog3* mutant mouse guts are devoid of EECs (Jenny et al., 2002). Further work has shown that *Neurod1* is also important for specification of EECs in mice, downstream of *Neurog3* (Li et al., 2011; Ray and Leiter, 2007). While *neurod1* is also an excellent marker for differentiated zebrafish EECs (Ye et al., 2019), and is essential for EEC development (Reuter et al., 2022), a role for *neurog3* has not been established in the zebrafish gut. Moreover, factors involved in specifying vertebrate EEC subtypes more broadly are largely unknown.

1.6.1.4 Tuft cells

Finally, mammalian intestines possess a rare IEC type called tuft cells that control the epithelial response to helminth encounter (Gerbe et al., 2016; von Moltke et al., 2016). While tuft cells are typically counted among the secretory lineage, tuft cell generation does not require *Atoh1* (unlike other secretory cell types) and specification relies on the transcription factor *Pou2f3*, with further encouragement from interleukins 4 and 13 (Bjerknes et al., 2012; Gerbe et al., 2016; von Moltke et al., 2016). It is known that mammalian tuft cells arise from ISCs (Gerbe et al., 2011), though it is unclear if tuft cells are produced from a common secretory progenitor.

Zebrafish are not thought to possess a tuft cell population. However, numerous studies in zebrafish and other teleost species described an enigmatic cell population, termed the rodlet cell, that is immunologically active and particularly responsive to helminth infection (Abd-Elhafeez et al., 2020a; Reite, 2005; Sayyaf Dezfuli et al., 2018; Sayyaf Dezfuli et al., 2022). These similarities have led to comparisons between tuft cells and rodlet cells, and some researchers speculate that they share developmental origins (Montoro et al., 2020). Although rodlet cells were first described over 130 years ago (Thélohan, 1892) and clearly inhabit the zebrafish gut epithelium, their origin and developmental regulation remain obscure. Based upon work in Chapter 5 of this thesis, I believe rodlet cells and tuft cells are functionally and developmentally related.

1.6.2 Absorptive cell lineages

1.6.2.1 Enterocytes

Enterocytes are the dominant cell type of the intestinal epithelium, where EC abundance corresponds to their essential role as the primary absorptive cells that produce digestive enzymes and absorb catabolized fats, carbohydrates, and peptides, as well as water and ions (Ross and Pawlina, 2006). Across the animal kingdom, Notch activation induces EC precursor formation, where mammals also require BMP collaboration with the transcription factor hepatocyte nuclear factor 4α (HNF4α) to generate mature ECs (Auclair et al., 2007; Beumer et al., 2018; Chen et al., 2019b; Heppert et al., 2021). Additional work is needed to understand mechanisms that guide EC subtype formation, including formation of regionally-restricted ECs, and ECs specialized for selective nutrient absorption. Zebrafish and pre-weaned mammals also possess a highly endocytic EC subpopulation of lysosome-rich enterocytes (LREs) that digest dietary protein via receptor-mediated endocytosis and lysosomal degradation (Harper et al., 2011; Muncan et al., 2011; Park et al., 2019). While mouse LRE production requires the transcriptional repressor *Prdm1* (Harper et al., 2011; Muncan et al., 2011), additional factors governing LRE specification in vertebrates are largely unclear. LREs are only specified in mammalian neonates, however zebrafish LREs persist into adulthood, providing a larger window of opportunity for investigating LRE development.

1.6.2.2 BEST4+ cells

Single-cell RNA sequencing of human intestinal epithelia uncovered a previously undescribed cell type enriched for expression of the ion channels BEST4, OTOP2, and CFTR, variably referred to as BEST4/OTOP2 cells, BEST4+ cells, or BEST4, CFTR high-expressor (BCHE) cells (Busslinger et al., 2021; Parikh et al., 2019; Smillie et al., 2019, #59790). The expression of *OTOPETRIN* family members and *CFTR* in *BEST4*-expressing cells is regionally-dependent (Busslinger et al., 2021; Parikh et al., 2019; Smillie et al., 2019, #59790), indicating functional divergence of BEST4+ subtypes along the gut. Original studies suggest that duodenal BCHE cells are involved in high-volume fluid secretion (Busslinger et al., 2021), while colonic BEST4+ cells may regulate pH sensing and electrolyte balance (Parikh et al., 2019; Smillie et al., 2019, #59790).

BEST4-expressing cells have been counted among the absorptive lineage, although it is unclear if they differentiate from an absorptive progenitor, an alternate progenitor, or directly from ISCs. BEST4+ cells are enriched for the NOTCH2 receptor and NOTCH2NL (Parikh et al., 2019), which enhances NOTCH2 activity (Fiddes et al., 2018), suggesting a distinct Notch activation cascade mediates BEST4+ enterocyte development. It was previously unknown if zebrafish have a population of *Best4*-expressing IECs, however I uncover a population of Best4 and Otop2 positive cells in Chapter 3 of this work. Given the recent discovery and unknown function of these cells in humans, fish may serve as an excellent model for investigating BEST4+ cell function and development.

1.6.2.3 M cells

The FAE of mammalian gut-associated lymphoid tissue (GALT) boasts an additional absorptive cell, the microfold (M) cell, dedicated to transepithelial transport of luminal antigens to underlying lymphocytes. As discussed previously, M cell differentiation depends on RANK activation by RANKL (Knoop et al., 2009), where GALT-localized stromal cells produce RANKL and other cytokines to drive production of specialized enterocytes and M cells from neighbouring ISCs (Debard et al., 2001; Dejardin et al., 2002; Kanaya et al., 2012; Kanaya et al., 2018; Knoop et al., 2009). Zebrafish do not possess a clear M cell population, although cells of the distal zebrafish gut can transport bacteria across the epithelium (Løvmo et al., 2017). These findings suggest that zebrafish intestines may develop a cell type analogous to mammalian M cells, though it has not previously been demonstrated that *tnfrsf11a* (encoding RANK; for simplicity and continuity, I refer to the *tnfrsf11a* gene as *rank* throughout this thesis) is expressed in the fish gut or contributes to development of any zebrafish IEC subset. Because larval zebrafish lack organized GALT and rely solely on germline-encoded defenses against pathogenic challenges, zebrafish provide opportunity to characterize immune modulators such as RANK in IEC development and homeostasis, independent of complex, secondary adaptive responses. In this thesis, I characterize a novel role for RANK in driving development of a tuft-like cell subset in the zebrafish intestine (Chapter 5). Accordingly, it will be necessary to reconcile the role for mammalian RANK in M cell

development, and the role of the zebrafish RANK orthologue in specification of a dissimilar cell type.

1.7 Epithelial immunity in the zebrafish intestine

Zebrafish and mammals both employ a combination of germline-encoded innate defenses, cellular defenses, and humoral defenses to control commensal and pathogenic microbes. For the first four to six weeks of life, zebrafish rely solely on innate immune signals (Flores et al., 2020; Lam et al., 2004; Willett et al., 1999), allowing for independent investigation of innate immune function during development of a model vertebrate. After this time, efficacious adaptive immunity arises, including systemic dispersal of diverse lymphocyte populations, like B and T cell subsets that produce antigen-specific immunoglobulins (Flores et al., 2020). In this section, I discuss what is known about epithelial immunity and host-microbe interactions in the zebrafish intestine.

1.7.1 Microbe sensing in the epithelium

To establish a healthy mutualistic relationship with commensal microbes, host organisms must recognize and tolerate beneficial microbes while warding off pathogens. IECs provide a physical barrier that impedes immediate microbial access to the host and minimizes activation of immune cells (Garrett et al., 2010). The host further employs germline-encoded pattern recognition receptors (PRRs) to detect microbe-associated molecular patterns (MAMPs) derived from luminal microbes, or damage-associated molecular patterns (DAMPs) produced by damaged host cells (Burgueño and Abreu, 2020; Garrett et al., 2010). While vertebrates possess a variety of PRRs, two signaling receptor families mediate most molecular pattern sensing in the mammalian gut epithelium: Toll-like receptors (TLRs) and NOD-like receptors (NLRs) (Garrett et al., 2010).

TLRs are cell surface receptors that interact with molecules derived from gram-positive and gram-negative bacteria, fungi, single-stranded and double-stranded RNA, viruses, unmethylated DNA, and various DAMPs (Kawai and Akira, 2011; Medzhitov et al., 1997; Schaefer, 2014). TLR-ligand binding leads to receptor dimerization and subsequent interaction of the

intracellular domain with adapter proteins like myeloid differentiation primary response protein 88 (Myd88) that mediate NF-kB activation and pro-inflammatory cytokine production (Burgueño and Abreu, 2020; Garrett et al., 2010). Similarly, NLRs are cytosolic PRRs that detect intracellular MAMPs, leading to NF-kB activation and cytokine production (Claes et al., 2015). In this way, TLR and NLR-dependent microbe-sensing modulate immune cell recruitment and activation as well as epithelial growth and differentiation (Burgueño and Abreu, 2020; Claes et al., 2015). While zebrafish possess as many as 20 TLR and 421 NLR family members, many remain poorly characterized, and orthologues to mammalian LPS-sensing TLR4 are not functionally equivalent (Li et al., 2017; Sullivan et al., 2009). Given that zebrafish generate a MyD88-dependent inflammatory response to bacterial LPS (Bates et al., 2007; Koch et al., 2018), it is likely that alternate TLR receptors have assumed this role.

1.7.2 Epithelial response to microbes

High fecundity and ex utero development in the chorion make zebrafish highly amenable to germ-free derivation, generation of gnotobiotic animals, and host-microbe interaction studies. Zebrafish hatch from their protective chorion at 2 dpf, followed by opening of the mouth at 3 dpf, which invites colonization of the gut lumen by water-borne microbes (Bates et al., 2006). Intestinal microbiota composition is dependent on developmental stage and husbandry practices, however the zebrafish intestinal environment selects for Gram-negative Proteobacteria and Fusobacteria, and researchers have identified several core microbial species (Bates et al., 2006; Rawls et al., 2004; Roeselers et al., 2011; Stephens et al., 2016).

Zebrafish are a proven model for host-microbe interaction studies. Transcriptional comparisons of intestines from 6 dpf germ-free (GF) zebrafish to those reared with a conventional microbiome (CV) revealed at least 212 genes regulated by the microbiota, including orthologues to 59 microbe-responsive genes identified in mice intestines (Hooper et al., 2001; Koch et al., 2018; Rawls et al., 2004; Reikvam et al., 2011). These gene expression changes provide evidence that microbes regulate a broad range of intestinal processes across vertebrates such as cell proliferation, development, metabolism, and innate immunity. *In vivo* studies support a role for the microbiota in vertebrate developmental processes including epithelial renewal, secretory

cell differentiation, and gut motility (Cheesman et al., 2011; Troll et al., 2018; Wiles et al., 2016). In addition to functional and developmental alterations, microbes educate the immune systems of fish and mammals, inducing mucosal inflammation and myeloid cell recruitment through Myd88-dependent TLR signals (Galindo-Villegas et al., 2012; Koch et al., 2018; Takeda and Akira, 2005). Finally, experimental evidence in fish revealed that epithelial alkaline phosphatase detoxifies lipopolysaccharide (LPS), a finding later corroborated in mice (Bates et al., 2007; Goldberg et al., 2008). These findings demonstrate that zebrafish, alongside other models, can inform our understanding of microbial impacts on host development and disease.

1.7.3 Zebrafish infection model of gastrointestinal pathogens

In addition to understanding the host response to the gut microbiota, zebrafish are a commonly utilized infectious disease model, where researchers have successfully colonized the fish intestine with numerous gastrointestinal pathogens including members of the *Edwardsiella* and *Aeromonas* genera*,* as well as various *Salmonella enterica* and *Vibrio cholerae* strains, among others (Flores et al., 2020). Moreover, in many cases it appears that pathogen colonization induces comparable disease phenotypes to humans. For example, zebrafish infected with *S. enterica* serovar typhimurium experience inflammation and swelling of the GI tract, as well as neutrophil recruitment to inflamed tissues (Varas et al., 2017), while fish infected with *V. cholerae* experience increased mucin production and shedding, as well as profuse diarrhea, akin to humans (Mitchell et al., 2017).

Like mammals, fish neutralize pathogenic bacteria via epithelial production of reactive oxygen species and antimicrobial peptides (Flores et al., 2010; Katzenback, 2015). However, the molecular response to pathogen infection remains largely unknown. While researchers have shown that expression of antibacterial factors and major histocompatibility complex (MHC) components depends on NLR signals in some cases (Wu et al., 2019), such studies lack resolution, and the specific tissues and cell types mediating the pathogen response are unclear. Given that zebrafish are an excellent model for several gastrointestinal pathogens, providing detailed resolution of cellular responses to intestinal infection will be valuable for understanding the host response to disease.

1.8 Objective

The intestinal epithelium faces a complex luminal environment and must simultaneously respond to extrinsic signals while preserving a barrier to commensal and pathogenic microbes. To support these efforts, intestinal stem cells at the base of epithelial folds respond to intrinsic and extrinsic cues to produce a complex mixture of regionally and functionally specialized IECs. However, it is largely unclear how microbes, either commensal or pathogen, influence the genetic landscape, including the development and function, of these individual IEC types. Moreover, it is unclear how individual cell types in turn might influence the luminal environment.

In this study, I first use the zebrafish intestinal model to investigate cell type-specific responses to intestinal microbes. Because the cellular composition and genetic makeup of the zebrafish intestine is relatively under-characterized, I begin by profiling single cells from the intestines of zebrafish at 6 dpf, and in mature adults. Following this analysis, I perform transcriptional cell-type-specific comparisons between both CV and GF larvae, as well as CV adults to those infected with the pathogen *V. cholerae*. In this way, I define intestinal responses to microbes at greater resolution than has yet been achieved in vertebrates. Next, I describe the role of RANK in specification of a cell subset with homology to mammalian microbe-sensing tuft cells, and investigate how loss of RANK function, and resultant loss of tuft-like cells, influences intestinal homeostasis, as well as the luminal environment.

Chapter 2: Materials and Methods

This chapter contains content from the following sources:

- **Willms RJ**, Jones LO, Hocking JC, and Foley E. (2022). A cell atlas of microbe-responsive processes in the zebrafish intestine. *Cell Reports*.
- Jones LO, **Willms RJ**, Shin M, Xu X, Graham RDV, Eklund M, Foley E. (2023). Single cell resolution of the adult zebrafish intestine under conventional conditions, and in response to an acute, natural infection. *bioRxiv.*

2.1 Zebrafish maintenance

Zebrafish were raised and maintained using protocols approved by the Animal Care & Use Committee: Biosciences and Health Sciences (#3032) at the University of Alberta, operating under the guidelines of the Canadian Council of Animal Care. TL strain zebrafish were used for single-cell RNA-sequencing experiments, Nanostring gene expression analysis, transmission electron microscopy, 16S rDNA sequencing, histological analysis of wild-type fish, and *Vibrio cholerae* experiments. *Tg*(*kdrl:mCherry*) fish (Wang et al., 2010a) were used for analysis of intestinal vasculogenesis. TL/AB mixed background zebrafish were used for all other experiments, including experiments with transgenic and mutants strains generated herein. Adult fish were raised and maintained within the University of Alberta fish facility at 29°C in tank water (Instant Ocean Sea Salt dissolved in reverse osmosis water for a conductivity of 1000µS and pH buffered to 7.4 with sodium bicarbonate) under a 14 hour/10 hour light/dark cycle as previously described (Westerfield, 2000). Adult zebrafish used for experimentation were fasted for ~20h prior to intestinal dissection. Embryos raised to larvae were housed at 29°C under a 14 hour/10 hour light/dark cycle until 6 days post fertilization.

2.2 Generating germ-free zebrafish

Fish embryos were made germ-free (GF) essentially as in (Melancon et al., 2017). A clutch of embryos was collected then washed and split into two cohorts. The conventionally reared (CR) cohort was kept in sterile EM, while the GF cohort was kept in sterile EM supplemented with ampicillin (100 µg/mL), kanamycin (5 µg/mL), amphotericin B (250 ng/mL), and gentamicin (50 µg/mL). Embryos were washed every 2 hours with EM or EM plus antibiotics for CR and GF cohorts respectively. Once at 50% epiboly, the GF cohort was successively washed three times in EM, then 2 minutes in 0.1% polyvinylpyrrolidone-iodine (PVP-I) in EM, followed by three EM washes, then a 20-minute incubation with 0.003% sodium hypochlorite (bleach) in EM. Embryos were washed three more times then transferred into tissue culture flasks with sterile EM. The CR cohort received the same number and duration of washes, using EM in lieu of dilute PVP-I or bleach. All work was performed in a biosafety cabinet sterilized first with 10% bleach, followed by 70% ethanol. We tested for bacterial contamination in GF flasks at 4 days post-fertilization,

according to established protocol (Melancon et al., 2017). EM was collected from CR and GF culture flasks to test for bacteria by plating on TSA, as well as PCR against bacterial 16S rDNA. Parental tank water and sterile filtered water were used as a positive and negative control respectively, where bacteria were positively identified in parental tank water and confirmed absent from sterile water. CR and GF flasks with bacteria present or absent respectively were used for subsequent analysis. Where GF fish were conventionalized (CV), GF flasks were inoculated with 100 μL parental tank water at 3 dpf.

2.3 Infection with *Vibrio cholerae* by immersion.

V. cholerae V52 was streaked from a glycerol stock onto LB agar supplemented with streptomycin (100μg/mL final) and grown overnight at 37°C. A single clonal colony was grown overnight with aeration at 37°C in LB broth supplemented with streptomycin (100μg/mL final). Bacteria were washed with 1xPBS (pH 7.4) then resuspended to an OD600 of 1 (~10^8CFU/mL) in 1xPBS. Five fish were incubated in a 400-mL beaker containing 1mL of the OD600 = 1 culture or 1mL of 1xPBS ('uninfected') in 200mL sterile tank water (filtered through a 0.22μm filter) at 29°C and 14h/10h light/dark cycle. To enumerate *V. cholerae* CFU in the intestine and tank water over time, fish were infected with GFP-expressing strains and fluorescence used to count *V. cholerae* colonies. Fish were transferred to fresh, sterile tank water and fed daily until the end of the experiment.

2.4 Generating single-cell suspensions for larval single-cell RNA-sequencing

Fish from the same embryo clutch were derived CV or GF as described. Five larvae were euthanized at a time in PBS plus 5X tricaine (300 mg/L), then intestines were immediately dissected with sterilized equipment and placed into 200 μL sterile PBS in a 1.5 mL microfuge tube on ice, alternating five CV and five GF intestines until 25 intestines (replicate 1) or 55 intestines (replicate 2) were collected per condition (80 intestines total per condition). Total dissection time was kept below 2 hours for each replicate. Immediately following dissections, intestines were incubated in 1.5 mL microfuge tubes with 200 μL of dissociation cocktail containing 1 mg/mL fresh collagenase A, 40 μg/mL proteinase k, and 0.25% trypsin in PBS for 30 minutes at 37°C, pipetting up and down 40X every 10 minutes to aid digestion. Then, either (Replicate 1) ZombieAqua

viability dye (BioLegend) was added at the beginning of dissociation to a final concentration of 1:1000 to stain dead and dying cells, 10% non-acetylated BSA in PBS was added to the dissociation cocktail (final concentration of 1%) to stop digestion, cells were spun for 15 minutes at 0.3 RCF and 4 °C to pellet cells, cells were gently re-suspended in 200 μL PBS+0.04% BSA (non-acetylated) and spun down through a 40 μm cell strainer (Pluriselect) at 0.3 RCF for 1 minute at 4 °C, then filtered cells were sorted on a BD FACS Aria III to collect live single cells (ZombieAqua negative); or (Replicate 2) 10% non-acetylated BSA in PBS was added to the dissociation cocktail (final concentration of 1%) to stop digestion, and the cells were spun for 15 minutes at 0.3 RCF and 4 °C to pellet cells. Cells were then gently re-suspended in 200 μL PBS+0.04% non-acetylated BSA and spun down through a 40 μm cell strainer (Pluriselect) at 0.3 RCF for 1 minute at 4°C. Live cells were collected using OptiPrep^{TM} Density Gradient Medium (Sigma, D1556-250ML). Briefly, a 40% (w/v) iodixanol working solution was prepared with 2 volumes of OptiPrep^{TM} and 1 volume of 0.04 %BSA in 1XPBS/DEPC-treated water. This working solution was used to prepare a 22% (w/v) iodixanol solution in the same buffer. One volume of working solution was mixed with 0.45 volume of cell suspension via gentle inversion. The solution mixture was transferred to a 15ml conical tube then topped up to 6 ml with working solution. The solution was overlaid with 3 ml of the 22% (w/v) iodixanol and the 22% iodixanol layer was overlaid with 0.5 ml of PBS+0.04% BSA. Viable cells were separated by density gradient created by centrifuging at 800xg for 20 min at 20°C. Viable cells were harvested from the top interface, which was then diluted in PBS+0.04% BSA. Live cells were pelleted at 0.3 RCF for 10 min at 4°C. Supernatant was decanted and cells were resuspended in PBS+0.04% BSA. (Both Replicates): Cell suspensions were then counted with a hemocytometer. Viability, as determined with Trypan blue, was >95% for all CV and GF samples. The single cell suspensions were immediately run through the 10X Genomics Chromium Controller with Chromium Single Cell 3' Library & Gel Bead Kit v3.1. Libraries were constructed by the High Content Analysis core facility at the University of Alberta, according to 10X Genomics Chromium Single Cell 3' Library & Gel Bead Kit v3 protocol. Libraries were sent to Novogene, where QC was performed by Nanodrop for quantitation, agarose gel electrophoresis to test for library degradation/ contamination, and Agilent 2100 analysis for library integrity and

quantitation. Paired-end sequencing was performed on the Illumina Hiseq platform with a read length of PE150 bp at each end.

2.5 Generating single-cell suspensions for adult single-cell RNA-sequencing

Five fish were infected or treated with 1xPBS for 16h as described above. Zebrafish intestines were dissected, surrounding organs removed, then minced into smaller pieces with Vannas scissors. Minced intestinal tissue was washed in 10mL 1xPBS (5 minutes, 300rcf, 4°C). The tissue was digested in a dissociation cocktail containing fresh collagenase A (1mg/mL), 40µg/mL Proteinase K, and Tryple (Gibco 12605-010, diluted 1:1000 [final]) in 1xPBS for 30 min in a 37°C water bath. Tissue was mechanically disrupted by gentle pipetting 40X every 10 minutes to aid in digestion. A 10% stock of non-acetylated bovine serum albumin (BSA) was added at a final concentration of 1% in PBS to stop the dissociation after 30 minutes. Cell suspensions were diluted in 5mL ice-cold PBS then filtered through 40µm filter fitted on a 50mL conical. Cells were pelleted (15min, 300rcf, 4°C) then pellet resuspended in 450µL PBS + 0.04% BSA and live cells collected using OptiPrep™ Density Gradient Medium (Sigma, D1556-250ML). OptiPrep™ Application Sheet C13 was followed to remove dead cells. Briefly, a 40% (w/v) iodixanol working solution was prepared by diluting 2 volumes of OptiPrep™ in 1 volume of 1xPBS + 0.04% BSA. The working solution was used to prepare a 22% (w/v) iodixanol solution in PBS + 0.04% BSA. One volume of working solution was carefully mixed with 0.45 volume of cell suspension by gentle inversion. The cell suspension mixture was transferred to a 15mL conical and topped up to 6mL with working solution. The working solution was then overlaid with three milliliters of 22% (w/v) iodixanol diluted PBS + 0.04% BSA. Finally, the 22% iodixanol solution was overlaid with 0.5mL PBS + 0.04% BSA. Live cells were separated by centrifuging at 800g for 20 minutes at 20°C. Viable cells were collected from the top interface (top 500µL). Cells were washed in 1mL PBS + 0.04% BSA (10min, 300rcf, 4°C), supernatant removed, then resuspended in 50µL PBS + 0.04% BSA. Cell suspensions were filtered through a 40µm filter fitted on a 1.5mL tube. Filter was washed with 20µL PBS + 0.04% BSA. Viability and cell counts were determined by staining dead cells with Trypan blue and counting with a hemacytometer. Cell suspensions were then diluted to a concentration of 1200 cell/µL and immediately run through the 10X Genomics Chromium

Controller with Chromium Single Cell 3' Library & Gel Bead Kit v3.1. Libraries were constructed by the High Content Analysis core facility at the University of Alberta. Library QC and sequencing was performed by Novogene using the Illumina HiSeq platform.

2.6 Bioinformatics

2.6.1 Processing and analysis of single-cell RNA-seq data

For single cell analysis, Cell Ranger v3.0 (10X Genomics) was used to demultiplex raw base call files from Illumina sequencing and to align reads to the Zebrafish reference genome (Ensembl GRCz11.96).

For larval datasets, Cell Ranger output matrices were analyzed using the Seurat R package version 3.1 (Butler et al., 2018) in RStudio. Cells possessing fewer than 200 unique molecular identifiers (UMis), greater than 2500 UMIs, or greater than 50% mitochondrial reads were removed to reduce the number of low-quality cells and doublets. Seurat was then used to normalize expression values and perform cell clustering on integrated datasets at a resolution of 1.0 with 26 principal components (PCs), where optimal PCs were determined using JackStraw scores (Macosko et al., 2015; Macosko et al., 2015) and elbow plots. After using the "FindMarkers" function in Seurat to identify marker genes for each cluster, clusters were annotated according to known cell type markers in zebrafish, or orthologous markers in mammals.

For adult datasets, Cell Ranger output matrices were analyzed using the Seurat R package version 4.1 (Hao et al., 2021) in RStudio. Cells possessing fewer than 200 unique molecular identifiers (UMis), greater than 2500 UMIs, or greater than 25% mitochondrial reads were removed to reduce the number of low-quality cells and doublets. Seurat was then used to normalize expression values and perform cell clustering on individual or integrated datasets at a resolution of 0.8 with 50 principal components (PCs), where optimal PCs were determined using JackStraw scores (Macosko et al., 2015; Macosko et al., 2015) and elbow plots. After using the "FindMarkers" function in Seurat to identify marker genes for each cluster, clusters were annotated according to known cell type markers in zebrafish, or orthologous markers in mammals.

For differential expression testing between single-cell RNA-seq datasets, significant changes were determined in Seurat with a non-parametric Wilcoxon rank sum test with Bonferroni correction, except for analysis of populations with low cell numbers in the larval datasets, for which Wilcoxon rank sum tests were performed. In each case, significance was defined as p value <0.05.

For lineage trajectory analysis over pseudotime, Cell Ranger output matrices for conventional adult data were analyzed using the Moncole3 R package version 1.3.1 (Cao et al., 2019). Clusters were identified by known genetic markers, and putative progenitor and tuft-like cells were manually isolated to perform trajectory analysis. The root node was assigned within the progenitor cluster, followed by manual analysis of gene expression (*rank, pou2f3, her15.1*) over pseudotime.

2.6.2 Gene ontology (GO) enrichment analysis of single-cell RNA-seq data

Marker genes (p-value cut-off < 0.05), as well as down-regulated gene lists from the integrated dataset (p-value cut-off < 0.05) were analyzed in GOrilla (*Gene Ontology enRIchment anaLysis and visuaLizAtion tool)* to determine GO term enrichment (Eden et al., 2009). Genes were analyzed in a two-list unranked comparison using the whole dataset gene list as background. To remove redundant GO terms, enriched terms with associated p-values from GOrilla were run through REVIGO (REduce and VIsualize Gene Ontology) using SimRel semantic similarity metric with an allowed similarity of 0.4 (Supek et al., 2011). Bar plots were manually generated using ggplot2 in RStudio.

2.7 NanoString nCounter gene expression analysis

For larval analysis, fish from the same embryo clutch were derived CR or GF as in Melancon et al., 2017. Fifteen 6 dpf zebrafish were taken per flask, with four replicates per condition. Larvae were euthanized in PBS plus 5X tricaine, then intestines were immediately dissected with sterile equipment and placed into 250 μL TRIzol™ (Invitrogen Cat# 15596026) in a 1.5 mL microfuge tube on ice. Once 15 intestines were collected, samples were homogenized and stored at -80°C. After freezing, samples were thawed, and standard TRIzol™-chloroform

extraction was used to isolate RNA. Sample concentrations and quality were measured on an Agilent Bioanalyzer 2100 prior to shipping to NanoString Technologies for gene expression analysis using the nCounter® Elements™ platform.

For adult analysis, RNA was extracted from zebrafish intestinal tissue using TRIzol™ Reagent (Invitrogen Cat# 15596026) as follows. Three zebrafish intestines were dissected, surrounding tissue removed, then quickly homogenized in 250μL TRIzol™. The intestinal homogenates were topped up to 1mL with TRIzol™. Homogenized tissue was stored at -70°C prior to RNA extraction. Four hundred microliters of chloroform were added to destabilize the aqueous phase, gently vortexed for 15 seconds then incubated at room temperature for 3 minutes. Chloroform extraction was repeated with the upper aqueous phase at a 1:1 ratio. Sodium acetate (3M, pH 5.2) was added at one tenth the volume of the collected aqueous phase (50μL sodium acetate). Ninety-five percent ethanol was added at two times the volume (1mL) then incubated overnight at 4°C to precipitate salts and nucleic acids. Nucleic acids were pelleted by centrifuging at 12,000rcf, 10min 4°C. Ethanol was carefully removed. RNA pellet was washed twice with 0.5mL 75% ethanol (7500rcf, 10min, 4°C). RNA pellet was allowed to dry 4 minutes then resuspended in 50μL nuclease-free water. RNA concentrations were determined by Nanodrop then diluted to 10μL at 100ng/μL for Nanostring hybridization using the nCounter® Elements™ platform.

2.8 16S rRNA gene sequencing

For larval analysis, 5 dpf intestines were dissected, using aseptic technique, and collected in 200 μl of Microbead Solution. A total of thirty guts were collected, with ten guts pooled per replicate. For adult intestinal analysis, single intestines were dissected into sterile PBS, then transferred into 250 μl Microbead Solution. For both pooled larval and single adult intestines, the MoBio UltraClean Microbial DNA Isolation kit (Cat No. 12224-250) was used to extract microbial DNA. To assess the intestinal bacterial community composition, the V4 variable region of the 16S rRNA gene encompassed by the 515 forward primer and 806 reverse primer (Caporaso et al., 2011) was sequenced. Quality control and sequencing was performed by Novogene Corporation using illumina Novaseq Platform PE250. Sequences were processed with QIIME2-2019.10 (Bolyen et al., 2019). The DADA2 pipeline was used to join paired-end reads, remove chimeric sequences,

and to generate the feature table used to resolve amplicon sequence variants using default parameters. Amplicon sequence variants (ASVs) represented by fewer than 200 reads across all samples were removed. A naïve Bayes classifier trained on SILVA132_99% full-length reference sequences was used to assign taxonomy. Taxonomy assignments were verified using NCBI blast. The sequence table was then filtered to exclude any sequences that were unassigned, not assigned past phylum level, or assigned as eukaryote.

2.9 Imaging and quantifying intestinal vasculature

Tg(kdrl:mCherry) fish (Wang et al., 2010a) were raised under CR or GF conditions for 6 dpf, then euthanized with tricaine and fixed overnight at 4 °C. Larvae were washed 3X in PBS then embedded in 0.7% UltraPure low melting point agarose (Invitrogen 16520) on a glass bottom dish. Tile and Z-stack images (5 µm sections) of whole fish were captured on a Leica Falcon SP8 equipped with a 25x 0.95NA Water HC Fluotar objective lens. Images were stitched with Leica Application Suite X software (Leica) and imported to Fiji (Schindelin et al., 2012) to produce maximum intensity Z-projection images that were adjusted for brightness and contrast, as well as false color manipulations. To quantify intestinal vasculature, corresponding brightfield images were used to set intestinal boundaries in FIJI. Fluorescent images were then converted to binary images and the area of kdrl:mCherry signal relative to the area of the whole intestine was measured.

2.10 Histology

Zebrafish intestines were fixed in 4% neutral buffered formalin at room temperature. Intestinal segments were processed for paraffin embedding and 5µm sections collected on slides. Tissue was deparaffinized then stained with Alcian Blue for 20 minutes (in experiments with goblet cells labeled), followed by Hematoxylin Gill III (Leica Ca.# 3801542) for two minutes followed by an eosin counterstain (Leica Cat# 3801602). Sections were dehydrated, cleared in toluene, then mounted in DPX. Histological samples were imaged on a ZEISS AXIO A1 compound light microscope with a SeBaCam 5.1MP camera.

2.11 Immunofluorescence

Zebrafish intestines were fixed in 4% PFA (EMS Cat #15710, 16% paraformaldehyde diluted in 1xPBS) overnight at 4°C. Intestines were washed twice in 1xPBS. The desired intestinal segments were cut from the rest of the intestine then cryoprotected in 15% (w/v) sucrose/PBS at room temperature until sunk followed by sinking in 30% (w/v) sucrose/PBS (overnight at 4°C). Intestines were mounted in Optimal Cutting Temperature Embedding Medium (Fisher Scientific Cat#23-730-571), then frozen on dry ice. 5 µm sections were collected on Superfrost Plus (Fisherbrand Cat# 22-037-246) slides. After allowing sections to adhere onto slides, slides were immersed in PBS for 20 minutes at room temperature. Tissue was blocked for 1h at room temperature in 3% (w/v) BSA dissolved in PBST (1xPBS + 0.2% (v/v) Tween-20). Primary antibodies were diluted in blocking buffer and layered onto sections. Sections were incubated in primary antibody solution overnight in a humid chamber at 4°C. Excess primary antibody was washed by immersing slides in fresh PBST for 1.5h. Sections were incubated in secondary antibody solution (prepared in blocking buffer) for 1h at room temperature in a humid chamber, protected from light. Secondary solution was removed then sections incubated in Hoechst (Molecular Probes Cat# H-3569) diluted 1:2000 in PBST for 10 minutes protected from light. Slides were washed in PBST by brief immersion followed by a 30-minute incubation in fresh PBST protected from light. Slides were mounted in Fluoromount™ Aqueous Mounting Medium (Sigma F4680-25ML).

2.12 Immunohistochemistry

Zebrafish intestines were fixed at 4°C in BT fixative: 4% PFA, 0.15mM CaCl2, 4% Sucrose in 0.1 M phosphate buffer (pH 7.4) (Cheesman et al., 2011). Posterior intestinal segments were processed for paraffin embedding and 5µm sections collected on Superfrost Plus slides. Tissue was deparaffinized, rehydrated, then boiled in 10mM sodium citrate pH 6, 0.05% Tween-20 for 20 min at 98°C to unmask antigen. After cooling sections to room temperature for 30min, sections were incubated in 3% hydrogen peroxide for 10 minutes, washed twice in dH_2O, and once in PBST (PBS + 0.5% Triton-X 100). Sections were then blocked for 1h at room temperature in 10% (v/v) normal goat serum (NGS)/PBSt followed by overnight incubation in primary antibody solution (prepared in blocking buffer) in a humid chamber at 4°C. Slides were washed three times in PBSt

and tissue incubated in SignalStain® Boost Detection Reagent (HRP, Rabbit or Mouse) for 30 min at room temperature. Colorimetric detection was done by incubating in SignalStain® DAB Chromogen solution (Cell Signaling Technology #8059) for 5 minutes. Slides were immersed in dH$_2$O then counterstained in ¼-strength Hematoxylin Gill III for 30 seconds. Finally, sections were dehydrated in ethanol, cleared with toluene and mounted in DPX. Histological samples were imaged on a ZEISS AXIO A1 compound light microscope with a SeBaCam 5.1MP camera.

2.13 HCR RNA fluorescent *in situ* hybridization

For adult analysis in tissue sections: whole zebrafish intestines were fixed in 4% PFA in PBS overnight at 4°C, then washed in PBS. Intestines were then positioned in OCT (Fisher Scientific 4585) in base molds (Fisher Scientific 22-363-552) and frozen on dry ice. After tissue sectioning (5 μm sections), slides were stored at -70°C until processing. Tissue was then prepared according to established protocols (Molecular Instruments). Briefly, tissue was immersed in ice-cold 4% PFA for 15 min at 4°C. Tissue was then dehydrated with a graded ethanol wash series (50%/70%/100%/100%), followed by two PBS washes. For larval analysis: 6 dpf larval intestines were dissected and fixed in 4% PFA in PBS overnight at 4°C, then washed in PBS. Larval and adult samples were then processed as follows. Samples were then pre-hybridized with probe hybridization buffer (Molecular Instruments) at 37°C for 15 minutes. Next, tissue was incubated overnight at 37°C with probes in hybridization buffer. Probes were then removed, and samples were washed with probe wash buffer (Molecular Instruments), followed by a series of 15-minute washes at 37°C with probe wash buffer/ 5X SSCT (75/25; 50/50; 25/50; 0/100). After an additional wash with 5X SSCT (0.1% Tween-20) at room temperature, samples were incubated with amplification buffer (Molecular Instruments) for 30 minutes at room temperature. At the same time, hairpin amplifiers were heated to 95°C for 90 seconds and snap-cooled to room temperature for 30 minutes. Hairpins were mixed in amplification buffer, and samples were incubated with hairpin solution (covered with parafilm) overnight in a humid chamber at room temperature. The next day, samples were washed in 5X SSCT and counter-stained with Hoechst 33258 (Molecular Probes Cat# H-3569) diluted 1:2000 in 5X SCCT before mounting in Fluoromount™ Aqueous Mounting Medium (Sigma F4680-25ML).

2.14 EdU treatment and detection

Tissue samples were processed according to the manufacturer's protocol (Invitrogen Click-iT™ EdU Cell Proliferation Kit; C10337). For larval analysis, 6 dpf larvae were incubated for 8 hours at 29°C with 50 µM EdU in EM supplemented with 1% DMSO. Whole larval intestines were dissected and processed directly following the 8-hour EdU pulse. For adult analysis, adult zebrafish were incubated at 29°C in 25 µM EdU in facility water supplemented with 1% DMSO for 16 hours (ON), then intestines were dissected and processed to generate tissue sections. Whole larval guts or adult tissue sections were processed through the HCR RNA fluorescent *in situ* hybridization protocol (as in section 2.13) prior to EdU detection. For EdU detection, samples were incubated for 30 minutes with a Click-iT reaction cocktail containing 1X Click-iT reaction buffer, $CuSO_4$, Alexa Fluor Azide, and reaction buffer additive. Samples were then counterstained with Hoechst (1:2,000) in PBT, then washed with PBT before mounting with Fluoromount™ Aqueous Mounting Medium (Sigma F4680-25ML).

2.15 Larval succinate treatment

Sodium succinate dibasic (Sigma 224731) was dissolved in water to make 1M and 10mM stock solutions. Respective succinate stock solution was added to EM to achieve 10 µM, 100 µM, 1 mM, 10 mM, or 100 mM concentrations. 3 dpf larvae (15-20 per condition) were immersed in 8 mL EM + succinate in a 6 well plate. Media was changed at 4 dpf and 5 dpf, then larvae were dissected at 6 dpf. Intestines were processed using FISH protocol (section 2.13).

2.16 Transmission electron microscopy of adult zebrafish intestines

To prepare samples for TEM, the posterior intestine was isolated and fixed in 2.5% glutaraldehyde, 2% PFA and 0.1M phosphate buffer solution for several days. Samples were then washed in 0.1M phosphate buffer, treated in 1% osmium tetroxide in 0.1M phosphate buffer, followed by additional washes. Intestines were subsequently dehydrated through a graded ethanol series, followed by infiltration with Spurr's resin. Infiltrated samples were then embedded in flat molds in Spurr's resin and cured overnight at 70°C. Blocks were then sectioned (70-90 nm thickness) on a Rechert-Jung UltracutE Ultramicrotome, and sections were stained

with uranyl acetate, followed by lead citrate. Images were acquired using a FEI-Philips Morgagni 268 Transmission Electron Microscope operating at 80 kV and equipped with a Gatan Orius CCD camera.

2.17 Generating transgenic zebrafish

Tg(tnfrsf11a:GFP) zebrafish were generated using the Tol2kit (Kwan et al., 2007). A 3,441 base pair fragment upstream of the of the *tnfrsf11a* transcription start site was amplified by PCR from zebrafish genomic DNA, then subcloned into the 5' entry vector using KpnI and SacII restriction sites. The p5E-3.4-*tnfrsf11a* construct was confirmed via restriction digest, and gateway cloning was used to combine the 5' entry, middle entry (pME-EGFP), and 3' (p3E-polyA) entry clones into the destination vector (pDestTol2CG2). The final construct was confirmed via restriction digest. To generate transgenics, 1-cell stage embryos were injected with approximately 50 pg DNA and 25 pg transposase RNA. Injected embryos were screened for *cmlc2:GFP* expression (heart GFP marker), and positive larvae were raised to adulthood, then outcrossed to identify founders that produced progeny with GFP+ hearts.

2.18 CRISPR-Cas9 mutagenesis

CRISPR-Cas9 mutagenesis was carried out as in (Hoshijima et al., 2019). Guide RNA (gRNA) and diagnostic primers were designed against the third exon of the *rank* gene (Table 2.1) (I refer to the *tnfrsf11a* gene as *rank* throughout this thesis). A gRNA targeting a restriction site (MslI) was chosen to enable quick diagnosis of target site mutagenesis (by loss of DNA restriction). Double guide RNA was generated using the Alt-R CRISPR-Cas9 System (IDT). Here, trans-activating crispr RNA (tracrRNA; IDT 1072533) and crispr RNA (crRNA) from IDT were dissolved to 100 μM in duplex buffer (IDT; 11-05-01-03) to make double guide RNA (dgRNA), then equal volumes tracrRNA and crRNA were duplexed by incubating at 95°C for 5 minutes, cooling and incubation at 25°C for 5 minutes, and rapid cooling to 4°C. The Cas9:dgRNA complex was prepared by mixing 1 ul 50μM crRNA:tracrRNA duplex with 2 ul 25μM Cas9 stock, and 7 ul nuclease-free H_2O. Prior to microinjection, the RNP complex solution was incubated at 37°C for 5 minutes and then placed at room temperature during injections. Approximately one nanoliter of dgRNA:Cas9 RNP complex

was injected into the cytoplasm of one-cell stage embryos from the *rank:GFP* strain (TL/AB mixed background). Cutting efficiency was assessed by PCR and amplicon digestion with the restriction enzyme MslI (NEB), where lack of digestion indicated disruption of the recognition sequence by the RNP complex. To generate stable mutants, injected embryos were reared to adulthood, then several single adults were outcrossed to AB wild-type fish. F1 progeny were reared, in-crossed and genotyped by fin clipping (NemaMatrix Genotyping Kit) to search for F2 generations bearing a frame-shift mutation. PCR amplicons were sequenced at the Molecular Biology Services Unit at the University of Alberta.

Table 2.1 CRISPR gRNA and related primers

Oligo	Sequence
rank gRNA	CACGTACTTGAACATTGCAA
rank diagnostic forward primer	CACACACGCACATGAACTATAACC
rank diagnostic reverse primer	GTCTTAAAGTGACACGAACCC

2.19 Data visualization and statistical analysis

Figures were constructed using R studio version 1.1.442 with ggplot2 version 3.4.1. Statistical analysis was performed in R. For boxplots containing outliers, outliers were determined to be datapoints that fall outside of 1.5 * IQR, where IQR is the inter-quartile range, or distance between the first and third quartiles. Figures were assembled in Adobe Illustrator CC 2019.

2.20 Data and code availability

- o Larval scRNA-seq data are available for visualization and analysis on the Broad Single Cell Portal
  - o https://singlecell.broadinstitute.org/single_cell/study/SCP1623/zebrafish-intestine-conventional-and-germ-free-conditions.
- o Raw larval scRNA-seq data are available on the NCBI GEO database
  - o https://www.ncbi.nlm.nih.gov/geo/query/acc.cgi?acc=GSE161855

- Adult processed single-cell RNA-seq data are available for visualization and analysis on the Broad Single Cell Portal
    - https://singlecell.broadinstitute.org/single_cell/study/SCP2141/adult-zebrafish-intestine
- Raw adult scRNA-seq data will soon be available on the NCBI GEO database (GSE230044).
- All code for analysis of scRNA-seq datasets, dataset markers, and differential gene expression analyses are available on Github:
    - https://github.com/rjwllms/Thesis-scripts

Chapter 3: Cellular Characterization of the Zebrafish Intestine

This chapter contains content from the following sources:

- o **Willms RJ**, Jones LO, Hocking JC, and Foley E. (2022). A cell atlas of microbe-responsive processes in the zebrafish intestine. *Cell Reports*.

- o Jones LO, **Willms RJ**, Shin M, Xu X, Graham RDV, Eklund M, Foley E. (2023). Single cell resolution of the adult zebrafish intestine under conventional conditions, and in response to an acute, natural infection. *bioRxiv.*

3.1 Summary

Developmental, transcriptional, and functional studies have revealed broad similarities between fish and mammalian intestines (Bates et al., 2006; Cheesman et al., 2011; Crosnier et al., 2005; Davison et al., 2017; Ng et al., 2005; Pack et al., 1996; Rawls et al., 2004; Wallace and Pack, 2003; Wallace et al., 2005; Wang et al., 2010b). Across vertebrates, intestinal epithelia contain mixtures of specialist secretory and absorptive cell types arranged into folded projections to maximize surface area at the lumen (Gehart and Clevers, 2019). While IEC composition in mammalian models is increasingly defined (Haber et al., 2017; Parikh et al., 2019; Smillie et al., 2019), we have an incomplete picture of fish IEC composition and arrangement within the gut. The zebrafish intestine possesses mucin-producing goblet cells and regulatory enteroendocrine cells (Crosnier et al., 2005; Ng et al., 2005; Wallace et al., 2005), however there are no reports of immune-modulatory Paneth or tuft cells. Moreover, our understanding of absorptive lineages remains incomplete. The fish intestinal epithelium includes regionally specialized enterocytes that harvest nutrients from the lumen (Lickwar et al., 2017; Ng et al., 2005; Park et al., 2019; Wallace et al., 2005; Wang et al., 2010b), however the extent of functional heterogeneity within enterocyte populations is unexamined, and we do not know if the intestinal epithelium houses specialized absorptive cells such as antigen-capturing M cells, or recently described Best4/Otop2 cells (Parikh et al., 2019; Smillie et al., 2019). Likewise, despite experimental evidence for the existence of cycling progenitors (Crosnier et al., 2005; Li et al., 2020; Peron et al., 2020; Rawls et al., 2004; Wallace et al., 2005), we lack expression markers that permit identification and manipulation of this essential cell type. Combined, these deficits have hampered our ability to harness the full potential of the zebrafish as a model of intestinal biology and host-microbe interactions.

Single cell profiling is a powerful tool to unlock cell heterogeneity in complex tissues, and scRNA-seq analyses have provided unprecedented genetic resolution of intestinal cell types and subtypes in the gut (Burclaff et al., 2022; Busslinger et al., 2021; Haber et al., 2017; Parikh et al., 2019; Smillie et al., 2019). For example, characterization of the mouse intestine by Haber et al. revealed two unique tuft cell subsets with distinct immune-related gene signatures, as well as twelve EEC progenitors and subtypes distinguished by peptide hormone expression profiles

(2017). Such experiments demonstrate that scRNA-seq has tremendous potential to unlock fundamental cellular traits and resolve cell heterogeneity within complex tissues.

In this chapter, I performed scRNA-seq of larval and adult zebrafish intestines to describe the cellular composition of the zebrafish intestine on a transcriptional level, and to establish homeostatic cell profiles of the zebrafish intestine at two developmental stages under conventional conditions. I identified previously unknown cell types of the zebrafish intestine conserved throughout development including progenitor cell subsets, tuft-like cells, and Best4/Otop2 cells. In addition, I identified genetic markers for all known cell types, and described genetic heterogeneity within cell types. This cellular characterization of the zebrafish intestine will further zebrafish as a model for investigations of intestinal development and host-microbe interactions, and has additional potential to unlock compositional and genetic differences between IECs from immature and mature stages of intestinal development.

3.2 The larval zebrafish intestine contains genetically and functionally specialized cell populations

To generate single-cell transcriptional profiles of digestive tracts from 6 dpf zebrafish larvae raised under conventional conditions, I dissected and dissociated intestines for scRNA-seq using the 10X Genomics platform. This experiment was performed in replicate with a total of 80 intestines per condition (alongside germ-free intestines, analyzed in Chapter 4), to control for technical and biological variability. My results include tissues that exist in close association with the gut, such as the pancreas and liver.

After filtering for dead cells and doublets, I determined gene expression profiles for 8,036 individual cells from CV zebrafish intestines and associated tissue (Table 3.1 and Figure 3.1A). To advance our understanding of cellular heterogeneity within the intestine, I used graph-based clustering to identify genetic markers for transcriptionally similar cells (Table 3.1). I identified 35 distinct clusters (Table 3.1), which I initially grouped into 18 cell types based on expression of known markers and cluster similarity (Figure 3.1A-B).

Table 3.1 CV intestinal scRNA-seq cell identifiers based on unbiased clustering.

Cell Type	Captured Cells	Top Gene Expression Markers
Progenitor-like 1	164	dld, her15.2, atoh1b, her15.1, dla
Progenitor-like 2	83	si:dkey-96g2.1, zgc:193726, zgc:113142, stm, si:rp71-17i16.6
Endocrine 1	202	ccka, si:zfos-2372e4.1, insl5a, scg3, si:ch73-359m17.9
Endocrine 2	102	pnoca, scgn, scg3, scg5, slc45a2
Tuft-like	151	gng13a, calb2a, ponzr6, gnb3a, rgs1
Goblet 1	445	si:ch211-153b23.5, lect2l, malb, si:ch211-139a5.9, cldnh
Goblet 2	120	si:ch211-153b23.5, cldnh, si:ch211-139a5.9, krt92, cnfn
Goblet-like	276	tcnba, cnfn, zgc:92380, CABZ01068499.1, s100a10b, muc5.3
EC1	519	apoa1a, chia.2, fabp2, rbp2a, apoa4b.2.1
EC2	360	chia.1, chia.2, fabp1b.1, apoa4b.2.1, apoa1a
EC3	660	si:ch211-142d6.2, elovl2, mogat2, lta4h, sult1st3
EC4	607	anpepb, mep1b, mep1a.1, si:dkey-219e21.2, clca1
EC5	165	tmprss15, neu3.3, si:ch211-113d11.6, pdx1, tcnba
LRE 1	64	si:dkey-194e6.1, pdzk1ip1, lrp2a, slc5a12, mfsd4ab
LRE 2	39	ctsbb, dab2, fabp6, lrp2b, mtbl
Best4/Otop2	98	otop2, cftr, ptger4c, tacr2, best4
Mesenchymal 1	494	zgc:153704, si:ch211-106h4.12, si:ch211-251b21.1, col1a1a, pmp22a
Mesenchymal 2	352	aqp1a.1, podxl, cavin2b, cavin1b, rhag
Mesenchymal 3	134	fgfbp2b, col2a1a, matn1, cnmd, col9a2
Mesenchymal 4	41	colec10, colec11, agtr2, angptl6, cidea
Muscle	68	actc1b, mylpfa, nme2b.2, tnnt3b, pvalb4
Vasc. Sm. Muscle	236	tagln, acta2, BX088707.3, mylkb, desmb
Vasc. Endothelial	146	cdh5, plvapb, kdrl, fgd5a, clec14a
Leukocyte 1	163	fcer1gl, si:dkey-5n18.1, si:ch211-147m6.1, si:ch211-194m7.3, spi1b
Leukocyte 2	129	ccl36.1, ccl38.6, ccl20a.3, ccr9a, coro1a
Neuronal	28	elavl4, elavl3, sncb, phox2a, phox2bb
Hepatocytes 1	358	hamp, ces2, serpina1l, si:dkeyp-73d8.9, fgg
Hepatocytes 2	312	hpda, si:dkey-86l18.10, ambp, zgc:112265, c3a.1
Hepatocytes 3	356	gc, serpina1, apom, zgc:123103, serpina1l
Acinar 1	191	prss1, ctrb1, prss59.2, CELA1 (1 of many), prss59.1
Acinar 2	220	si:ch211-240l19.5, cel.2, CELA1 (1 of many).5, pdia2, c6ast3
Acinar 3	183	pla2g1b, si:ch211-240l19.5, cpa4, si:dkey-14d8.7, cel.2
Epidermis 1	127	krt1-19d, ponzr5, zgc:165423, icn2, anxa1c
Epidermis 2	246	cldni, aqp3a, cxl34b.11, col4a5, si:rp71-77l1.1
Epidermis 3	197	cyt1l, krt17, zgc:111983, cyt1, si:dkey-247k7.2

The dataset was dominated by expression profiles for IECs. For example, I identified secretory peptide hormone-producing enteroendocrine cells expressing endocrine-specific *neurod1*

(Reuter et al., 2022; Ye et al., 2019), as well as goblet cells marked by expression of the goblet cell differentiation factor *anterior gradient 2* (*agr2*) (Chen et al., 2012), and *sstr5* (Figure 3.1B), a gene product that stimulates Mucin 2 production in the mouse colon (Song et al., 2020). I also uncovered a goblet-like cluster that upregulated *pdx1* and *muc5.3* (Table 3.1, Figure 3.1B), enriched in secretory cells of the foregut and pancreas (Jevtov et al., 2014; Lavergne et al., 2020). Besides endocrine and goblet cell lineages, I identified an unexpected cluster with pronounced transcriptional similarity to mammalian intestinal tuft cells, including expression of tuft cell marker genes *Gng13, Trpm5, Avil*, and the tuft cell specification master regulator *Pou2f3* (Gerbe et al., 2016; Haber et al., 2017) (Figure 3.1B).

The majority of IECs were absorptive cells and included canonical enterocyte (EC) lineages that expressed genes required for nutrient acquisition and metabolism, as well as recently described LREs (Figure 3.1A-B), thought to mediate protein degradation (Park et al., 2019). Separately, I discovered a population of Best4/Otop2 cells (Figure 3.1A-B), an absorptive lineage recently described in humans (Parikh et al., 2019; Smillie et al., 2019), and uncharacterized in zebrafish. Like human Best4/Otop2 cells (Parikh et al., 2019; Smillie et al., 2019), the fish counterparts were marked by enhanced expression of *notch2* and Notch-responsive *hes-related* family members (Figure 3.1B). Additionally, zebrafish Best4/Otop2 cells expressed the chloride/bicarbonate transporter *cftr* (Figure 3.1B), suggesting possible functional similarities with human duodenal BCHE cells (Busslinger et al., 2021).

While prior studies in the zebrafish intestine demonstrated that fish possess cycling basal epithelial cells analogous to mammalian ISCs (Crosnier et al., 2005; Li et al., 2020; Wallace et al., 2005; Wang et al., 2010b), progenitor cell markers have not been uncovered. Zebrafish do not encode Wnt pathway genes highly expressed by mammalian ISCs, including Lgr5 and Ascl2, though Wnt and Notch and pathway components are expressed in basal zebrafish IECs (Bates et al., 2006; Cheesman et al., 2011; Crosnier et al., 2005; Lickwar et al., 2017; Muncan et al., 2007; Peron et al., 2020). Apart from absorptive and secretory lineage, my initial clustering uncovered two populations that displayed features associated with intestinal progenitor cells, including expression of Notch pathway components *dld* and *dla* (Crosnier et al., 2005)*,* and *HES5* othologues *her15* and *her2* (de la Pompa et al., 1997) (Table 3.1 and Figure 3.1B). A more detailed

analysis resolved the putative progenitor pool into four sub-clusters with distinct transcriptional hallmarks (Figure 3.1C-D). Of these four, I believe cluster one is hepatic in origin, as it is marked by expression of liver-associated genes *apoa2* and *fabp10a* (Venkatachalam et al., 2009) (Figure 3.1D). In contrast, cells from clusters zero, two, and three expressed genes affiliated with intestinal progenitors in mammals, or basal IECs in zebrafish. For instance, cluster zero was marked by expression of the gut-associated genes *onecut1* (Matthews et al., 2004) and *notch3* (Crosnier et al., 2005) in addition to *sox9b* (Figure 3.1D), an ISC marker in medaka fish (Aghaallaei et al., 2016), and a marker of basal columnar IECs in adult zebrafish (Peron et al., 2020). Additionally, cluster zero cells expressed elevated amounts of *epcam* (Figure 3.1D), a gene linked with intestinal epithelial proliferation in vertebrates (Ouchi et al., 2021). Cluster two cells expressed intestinal epithelial cell markers *cldn15la* (Alvers et al., 2014) and *vil1* (Abrams et al., 2012; Thakur et al., 2014), as well as regulators of intestinal progenitor cell division and differentiation, such as *cdx1b* (Flores et al., 2008) and *atoh1b* (Reuter et al., 2022) (Figure 3.1D). Furthermore, fluorescence imaging of intestines from *Tg(rank:GFP)* fish that expressed GFP under control of the promoter for cluster two marker *rank* showed that, like intestinal progenitors (Li et al., 2020; Ng et al., 2005), cluster two cells appear to reside at the base of intestinal folds (Figure 3.1E). Intriguingly, *rank*, like other progenitor markers, is also expressed in a subset of Best4/Otop2 cells, demonstrating a need to better understand the developmental relationship between candidate progenitors and Best4/Otop2 cells. Finally, we identified cluster three as a cycling population that actively expressed proliferation markers of mammalian transit amplifying cells (Haber et al., 2017), such as *mki67*, *cdk1*, and *top2a* (Figure 3.1D). Thus, our transcriptional and *in vivo* data identified a previously undescribed pool of IECs with hallmarks of intestinal progenitors, although lineage tracing studies are required for confirmation. In sum, I have identified a panel of expression markers that distinguish major lineages of the larval zebrafish digestive tract, including previously undescribed tuft-like cells, Best4/Otop2 cells, and possible markers of intestinal progenitor subsets.
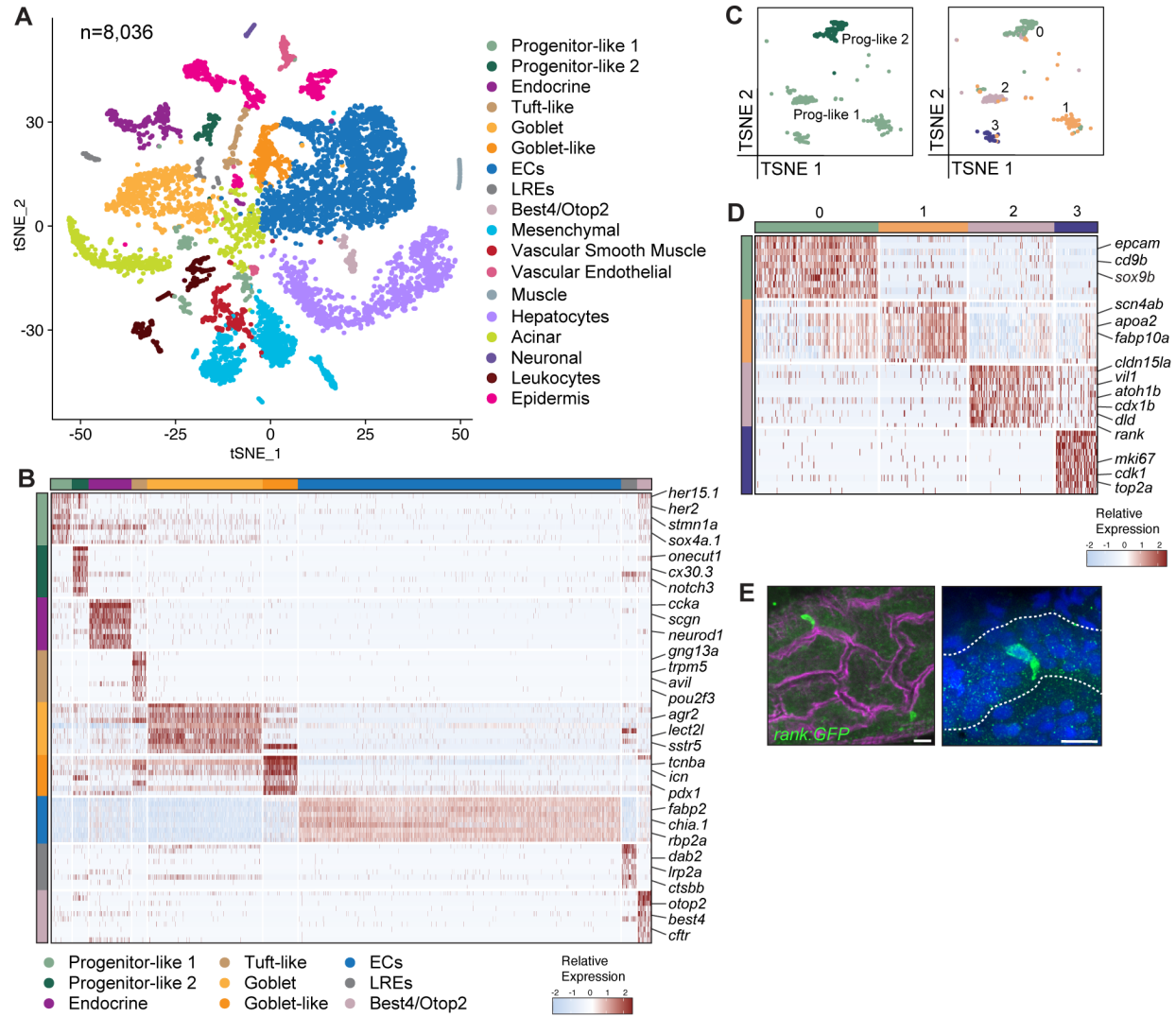
Figure 3.1 Transcriptionally distinct cell populations in the larval zebrafish intestine. A) 2D t-SNE projections of profiled intestinal cells from 6 dpf CV larvae color coded by cell type. **B)** Heatmap of IEC cluster markers colored by relative gene expression. Cell types are indicated by colored bars on the left and top. Several top markers for each cluster are shown on the right axis of the heatmap. **C)** t-SNE plots of progenitor-like clusters 1 and 2 from original graph-based analysis (left) and further re-clustering (right), color coded by cell type. **D)** Heatmap of cell markers for putative progenitor-like clusters, colored by relative gene expression. Cell types are indicated by colored bars on the left and top. Several top markers for each cluster are shown on the right axis of the heatmap. **E)** Optical section of a whole gut from 6 dpf *Tg(rank:GFP)* zebrafish, stained with

phalloidin to visualize filamentous actin (magenta) and Hoechst to visualize nuclei (blue). Right panel is a magnified image of a GFP positive cell from the left panel. Scale bars = 10 μm.

3.2.1 Identification of absorptive cell subsets in the larval zebrafish gut

Like most animals, the zebrafish intestinal epithelium primarily contains absorptive cells that acquire material from the gut lumen. In fish, metabolite acquisition relies on specialist enterocyte and protein-acquiring LRE lineages (Lickwar et al., 2017; Ng et al., 2005; Park et al., 2019; Wallace et al., 2005; Wang et al., 2010b). To characterize functional specializations within the absorptive lineage, I analyzed gene expression in absorptive cell subsets. Moreover, I assigned regional identities based on previously established regional markers of the fish intestine (Lickwar et al., 2017; Wang et al., 2010b). I identified five enterocyte clusters (Table 3.1 and Figure 3.2A), of which clusters one to four were enriched for markers of the anterior intestine (Figure 3.2D) and expressed genes required for lipid, carbohydrate, chitin, and small molecule metabolism (Table 3.1 and Figure 3.2B-C). Cluster five cells were a distinct subset, specialized in the metabolism of xenobiotic compounds (Figure 3.2C), and transport of vitamin B12 by *transcobalamin beta a* (*tcnba*) (Figure 3.2B). Alongside enterocytes, I captured expression profiles for three separate absorptive lineages, two of which had expression profiles consistent with LREs (Park et al., 2019). LRE1 cells were relatively rare and expressed pronephros markers such as *lrp2a*, *zgc:64022* and *tspan35* (Anzenberger et al., 2006; Thisse and Thisse, 2004) (Table 3.1 and Figure 3.2B), suggesting that LRE1 cells are renal. In contrast, LRE2 cells appear mid-intestinal (Figure 3.2D), enriched for expression of genes required for peptide catabolism, in agreement with a role for mid-intestinal LREs in protein digestion (Park et al., 2019). Lastly, I identified a previously unknown lineage analogous to recently characterized human colonic BEST4/OTOP2 cells, assigned to the absorptive lineage (Parikh et al., 2019; Smillie et al., 2019). Like the human equivalent, zebrafish Best4/Otop2 cells appear enriched in the posterior intestine (Figure 3.2D), and expressed genes required for ion transport (*cftr*, *ca2*, *best4*) (Bagnat et al., 2010; Lin et al., 2008), suggesting that they regulate intestinal ion concentrations. Collectively, these data indicates that IECs from larval zebrafish include a sophisticated organization of absorptive lineages.

Figure 3.2 The larval zebrafish intestine possesses regionally specified absorptive cells. A) t-SNE plot of absorptive cells color coded by cell state. **B)** Heatmap of cluster markers for absorptive cells, colored by relative gene expression. Cell types are indicated by colored bars on the left and top. Several top markers for each cluster relative to other absorptive cell populations are shown on the right axis of the heatmap. **C)** Gene ontology enrichment analysis of absorptive cells based on genetic markers from the conventional single-cell RNA sequencing dataset. Top 5 non-redundant GO terms are shown for each cell state. Enrichment score is represented by bar length and p-value is indicated with white circles. **D)** Heatmap showing relative expression of established

regional marker genes (Lickwar et al., 2017; Wang et al., 2010b) in each absorptive cell type. BO = Best4/Otop2 cells.

3.2.2 Identification of stromal and leukocyte subsets in the larval zebrafish gut

In addition to epithelial cells, I uncovered transcriptionally discrete leukocyte and mesenchymal populations in the larval intestine. I first characterized two highly distinct larval leukocyte clusters (Table 3.1 and Figure 3.3A-B). Cluster one was a mixed phagocyte population that expressed known macrophage and neutrophil markers such as *spi1b*, *mpeg1.1*, and *mpx* (Bennett et al., 2001) (Figure 3.3B-C). This is in alignment with many studies showing macrophages and neutrophils inhabit the larval intestine by 6 dpf (Brugman, 2016; Flores et al., 2020; López Nadal et al., 2020). In contrast, cluster two cells expressed classical markers of developing T cells (Ma et al., 2013), such as *ikaros* (*ikzf1*), *runx3* and *ccr9a*, as well as the *T-cell receptor alpha/delta variable 14.0* gene segment (*tradv14.0*) (Figure 3.3B-D). While this could indicate that T cells seed the intestine by 6 dpf, it is also plausible that these cells originated from kidney tissue attached to the gut, and the site of hematopoiesis. It is also possible that leukocyte cluster two cells represent an ILC population, given the transcriptional overlap between T cells and ILCs (Robinette et al., 2015). In mice, ILCs develop during early embryogenesis, and are involved in intestinal lymphoid tissue formation (Eberl et al., 2004). Recent work showed that adult zebrafish also have intestinal ILC subsets (Hernández et al., 2018), though it is unclear when these cells develop or migrate to the intestine. Since ILC intestinal localization precedes adaptive responses in mammals, it may not be surprising if ILCs are present in the intestines of 6 dpf zebrafish. Thus, future work is required to determine the identity of leukocyte 2 cells, and to determine if T cells or ILCs have already seeded the larval intestine by day six.

Mesenchymal cells segregated into four distinct clusters (Figure 3.3E), of which cluster one represented a fibroblast population that expressed extracellular matrix (ECM) components such as *col1a1a* and *col1a2*, and the fibroblast marker *vimentin* (*vim*) (Farnsworth et al., 2020) (Figure 3.3F). The identity of mesenchymal cluster two is unclear; however, it was marked by expression of ammonia transporter *rhag,* and *aqp1a.1* (Figure 3.3F) involved in ammonia, water, and CO_2 transport (Horng et al., 2015; Talbot et al., 2015), implicating these cells in regulating gas and ion

movement. Similar gene expression markers are found in vasculature-derived cells from whole larval single-cell analysis (Farrell et al., 2018), suggesting these cells could also be vascularly derived. Cluster three cells were marked by ECM components *matrilin 1* (*matn1*) and several collagens, as well as *fibroblast growth factor binding protein 2b* (*fgfbp2b*), also indicative of fibroblast identity (Farnsworth et al., 2020) (Figure 3.3F). Finally, mesenchyme cluster four was marked by expression of soluble pattern recognition receptors from the collectin family (Table 3.1), and vasculature markers *angptl6* and *agtr2* (Figure 3.3F), indicating that cluster four likely represents perivascular fibroblasts that contribute to blood vessel formation (Rajan et al., 2020). Collectively, these data indicate that distinct leukocyte and stromal cell subtypes inhabit the larval gut. Together with the epithelial analysis, our data reveals that the larval zebrafish intestine contains a complex mixture of functionally and regionally specialized immune, stromal and epithelial cell types by 6 dpf, and provides unprecedented resolution of cell subsets underpinning intestinal composition and function in the post-embryonic intestine.
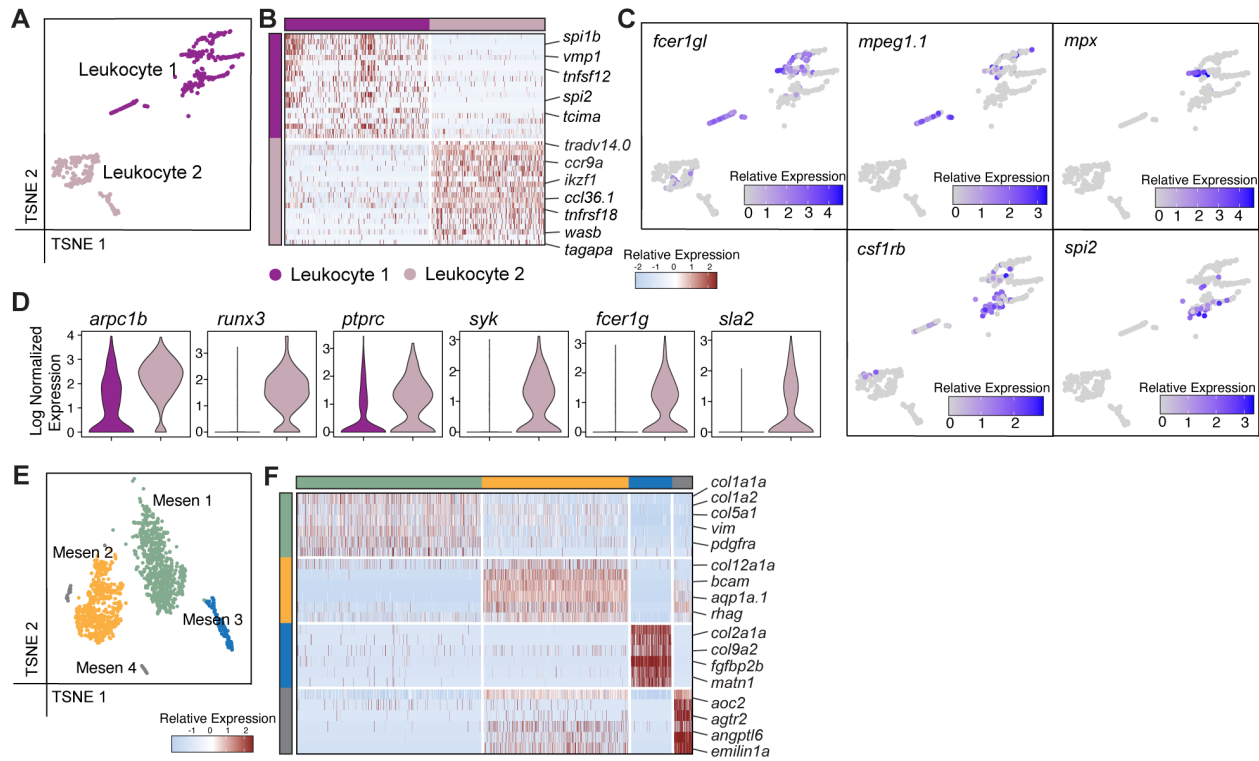
Figure 3.3 Stromal and leukocyte populations in the larval gut. A) t-SNE plot of leukocytes, color coded by cell cluster. **B)** Heatmap of cluster markers for leukocytes, colored by relative gene expression. Cell types are indicated by colored bars on the left and top. Several top cluster markers relative to the other leukocyte population are shown on the right axis of the heatmap. **C)** t-SNE plots of leukocytes showing cell-specific expression of leukocyte subset markers. **D)** Violin plots showing log normalized expression of marker genes for leukocyte 2 cells. **E)** t-SNE plot of color-coded mesenchymal clusters. **F)** Heatmap of cluster markers for mesenchymal cells, colored by relative gene expression. Cell types are indicated by colored bars on the left and top. Several top cluster markers relative to the other mesenchymal population are shown on the right axis of the heatmap.

3.3 The adult intestine contains a complex population of spatially and functionally specialist epithelial cells.

Most studies of the zebrafish intestine utilize larvae 5-7 dpf. Accordingly, the adult zebrafish intestine remains under-characterized relative to larvae, and to mature intestines of other animal models. To uncover the range of cell states encoded within such a complex structure, we determined the transcriptomes of single cells purified from healthy adult fish guts. We successfully generated high-quality expression data for 18,358 cells, where unbiased graph-based clustering identified 30 cell clusters (Table 3.2) that could be partitioned into 16 unique transcriptional states (Figure 3.4A). I assigned cellular identities to each state based on expression of established cell type markers in fish and mammals (Table 3.2 and Figure 3.4B). Among the transcriptional clusters, I identified leukocytes, differentiated stromal cells, and nine IEC types that included, as in larvae, a cycling population enriched for the Notch mediator *her15.1* (Figure 3.4B), a pan-stem cell marker in zebrafish (Raj et al., 2020; Sigloch et al., 2023; Steiner et al., 2014). Fluorescence *in situ* hybridization showed that *her15.1+* cells are proliferative residents of the interfold base (Figure 3.4C), as expected for intestinal stem cells. My transcriptional identification of a second cluster of cycling cells (Figure 3.4A-B), alongside our immunohistochemical characterization of multiple proliferative cells (PCNA+) at each fold base (Figure 3.4D) indicates that, like mammals, the adult fish intestine contains a population of basal, undifferentiated, transit amplifying (TA) cells.

I also identified transcriptional profiles for secretory enteroendocrine, goblet, and tuft-like cells, as well as absorptive enterocytes, lysosome-rich enterocytes (LREs), and Best4/Otop2 cells (Figure 3.4B). I found that *pou2f3+* IECs did not express the endocrine marker *neurod1*, and lacked the distinct mucous compartment of goblet cells (Figure 3.4E), confirming the existence of distinct tuft-like cells in adult fish guts. To fully characterize IEC types, I systematically analyzed gene expression profiles of all secretory and absorptive lineage for specialist subsets. In this manner, I resolved the enteroendocrine population (Figure 3.4B) into eight subtypes based on their unique peptide-hormone expression profiles (Figure 3.4G). For example, I identified two distinct clusters resembling mammalian L cells that express *pyy* and proglucagon (Haber et al., 2017), where cluster 1 exclusively expressed *pyyb* and cluster 7 expressed glucagon paralogues *gcga* and *gcgb*

(Figure 3.4G). These data suggest that zebrafish EECs are highly specialized for production of specified hormones in adulthood, in contrast to mouse EEC subtypes that display overlapping peptide hormone distribution (Haber et al., 2017). I also identified two tuft-like cell subsets distinguished by expression of *alox5a*, involved in production of leukotrienes from arachidonic acid (Brash, 1999), and *si:dkey-61f9.1*, a C-type lectin domain-containing protein homologous to human secretory phospholipase A2 receptor *PLA2R1*, involved in release of arachidonic acid (Triggiani et al., 2005) (Figure 3.4H). These data indicate that zebrafish tuft-like cells may mediate type 2 immune responses and leukocyte recruitment through leukotriene biosynthesis, comparable to mammalian tuft cells (McGinty et al., 2020).

Upon examination of enterocytes, I identified four unique clusters. EC1 was the dominant EC cluster, expressing classical markers of lipid, carbohydrate, chitin, and small-molecule metabolism. Cells within cluster two were enriched for expression of the bile acid binding protein gene *fabp6* (Oehlers et al., 2011); cluster three cells expressed high levels of endopeptidases including *meprin* subunits; and cluster four cells expressed interferon-response genes (Levraud et al., 2019), such as *ifit14*, *isg15* and *rsad2* (Figure 3.4I), suggesting that zebrafish intestines possess a dedicated enterocyte population with enhanced immune activity. I also discovered transcriptionally distinct LRE and Best4+ populations (Figure 3.4J-K), where LRE cluster three and Best4+ cluster two closely resembled canonical enterocytes, suggesting that these absorptive subtypes may arise from a common progenitor. *In vivo* visualization of the Best4/Otop2 cell marker *cftr* showed that *cftr*-positive cells generally resided in the lower half of intestinal folds (Figure 3.4F), signifying a spatially restricted requirement for Best4/Otop2 cells. In sum, our imaging and transcriptional data reveal the adult fish gut as an integrated community of spatially organized specialist cells that act in concert to support animal health and protect from infection.

Table 3.2 CV adult intestinal scRNA-seq cell identifiers based on unbiased clustering.

Cell Type	Captured Cells	Top Gene Expression Markers
Progenitor	938	her15.1, si:ch211-222l21.1, si:ch211-213d14.2, dld, neurl1aa
TA	220	mcm5, si:ch211-156b7.4, mcm6, nasp, lig1
Endocrine 1	494	syt1a, pax6b, cbln8, ccl19a.1, tango2
Endocrine 2	385	neurod1, plcvd3, scg3, pdyn, egr4
Endocrine 3	249	sst1.1, ins, ppdpfb, dkk3b, g6pcb
Endocrine 4	235	penka, adcyap1a, nmbb, hbegfb, adgrg4a
Endocrine 5	156	gcga, gcgb, pnoca, dkk3b, si:dkey-14d8.6
Goblet	1273	agr2, si:dkey-203a12.9, CABZ01080550.1 (muc2), fabp3, cd63
Goblet-like	303	cuzd1.2, si:ch211-173a9.6.1, si:ch211-173a9.6, pdia2, si:ch211-255i20.3
Tuft-like	635	si:ch211-270g19.5, si:dkey-61f9.1, adgrf3a, pdia2, ckbb, pou2f3
EC1	2275	chia.3, ucp1, rbp2a, chia.1, fabp1b.1
EC2	801	cd36, lct, slc6a19b, enpp7.1, chia.2, fabp2
EC3	1579	slc26a3.2, cd36, si:ch211-196f2.3, zgc:77439, zanl
LRE 1	2000	fabp6, ifi30, ctsl.1, tmigd1, slc10a2
LRE 2	1138	tmigd1, slc10a2, dabp2, fabp6, ctsl.1
LRE 3	184	ctsbb, ctsl.1, slc15a2, lrp2b, slc10a2
Best4/Otop2 1	1523	ndrg2, zgc:172079.2, tcnba, lhfpl2b, metrnla, otop2
Best4/Otop2 2	166	fam92a1, otop2, cftr, ca4b, cfd, ca2, notch2
Leukocyte 1	1704	si:dkey-185m8.2, si:ch211-119e14.1, ccl36.1, lgals2b, ccr9a
Leukocyte 2	392	zgc:123107, ms4a17a.10, cxcl19, spi1b, sftpbb
Leukocyte 3	319	ccl20a.3, FP236331.1, cebpb, nitr5, sla2
Leukocyte 4	257	si:ch211-152c2.3, spi2, spic, plekho2, si:dkey-56m19.5
Leukocyte 5	153	gata2, nitr6a, FP236331.1, si:ch211-231m23.4, il17a/f3
Leukocyte 6	116	ponzr6, ighv1-4, rnaset2l, igic1s1, zgc:153659
Leukocyte 7	44	spi1b, npsn, timp2b, cd7al, fcer1gl
Stromal 1	129	podxl, dcn, mmp2, anxa1a, ifitm1, rbp4, col1a2, vim
Stromal 2	63	cdh5, lyve1a, mrc1b, gas6, pros1
Pancreatic	93	si:dkey-14d8.7, c6ast4, c6ast3, pglyrp6, dnase1
Epidermal	70	zgc:66473, zgc:101810, tppp3, lsp1b, anxa1a
Unknown 1	217	acsl4b, oclnb, ftr83, tmprss13b, sstr5
Unknown 2	129	BX855618.1, zgc:193726, cbln11, pvalb6, noxo1a
Unknown 3	118	syt10, syt4, oaz2b, tnc, clip2
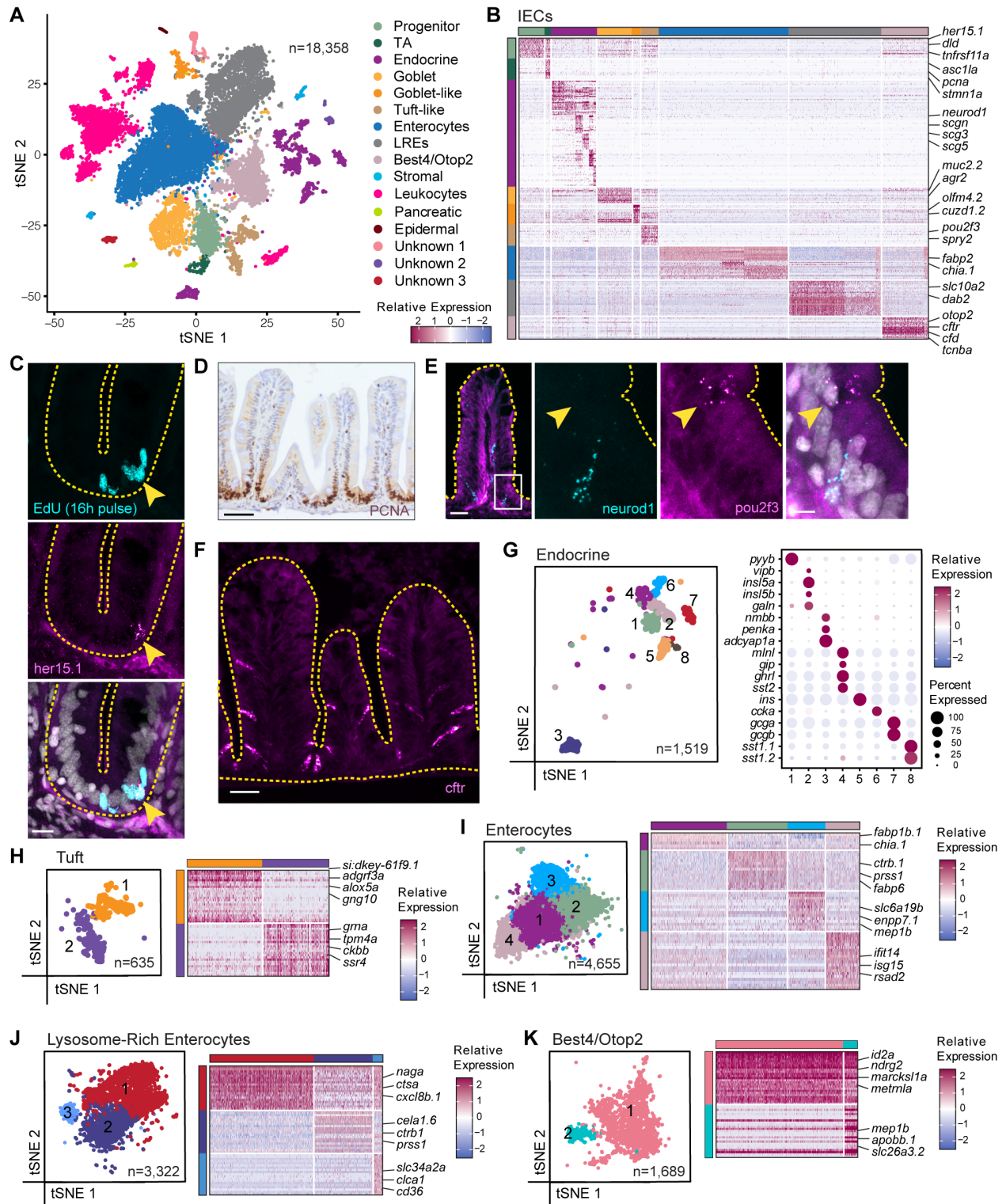
Figure 3.4 The intestinal epithelium contains a complex mix of proliferative and mature specialist epithelial cells. (A) 2D t-SNE projections of 18,358 intestinal cells color coded by cell type. (B) Heatmap of IEC cluster markers colored by relative gene expression and arranged

according to cell type. Cell types are indicated by colored bars on the left and top. Prominent markers for each cluster are shown on the right y-axis of the heatmap. (C) Fluorescence visualization of EdU-positive cycling cells (cyan), and her15.1 positive cells (magenta) in an intestinal fold base. In the merged image all nuclei are labeled in white and a her15.1/EdU double-positive cell is marked with a yellow arrowhead. Scale bar = 10μm. (D) Immunohistochemical images of a sagittal posterior intestine section stained for PCNA. Scale bar = 50 μm. (E) Fluorescence visualization of *neurod1*-positive endocrine cells (cyan), and *pou2f3*-positive tuft cells (arrowhead, magenta) in an intestinal fold. In the merged image all nuclei are labeled in white. Scale bar = 25μm for left panel and 5μm for inset. (F) Fluorescence in situ hybridization showing expression pattern of the Best4/Otop2 cell marker *cftr* in three intestinal folds. Scale bar = 25μm. (G) t-SNE plot of enteroendocrine cells color coded by subset type. Bubble plot shows the relative expression levels for eighteen peptide hormones across all eight cell types (H-K) t-SNE plots of Tuft (H), Enterocyte (I), Lysosome-Rich Enterocytes (J) and Best4/Otop2 clusters (K) from original graph-based analysis, re-clustered and color coded by cell type. In each instance, heatmaps show expression of subset cell markers colored by relative gene expression. Cell types are indicated by colored bars on the left and top. Markers for each subset are shown on the right y-axis of each heatmap.

3.4 Identification of stromal and leukocyte subsets in the adult zebrafish gut

Intriguingly, the adult scRNA-seq dataset contained few mesenchymal cells and a large number of gut-associated leukocytes. Differences between larvae and adults may reflect population differences across development, where the ratio of IECs and leukocytes to stromal cells increases over time, or technical disparities during sample preparation. Since we have limited knowledge of stromal and immune cell populations that support epithelial cells and mediate humoral immunity in the adult gut, we analyzed these cells more closely. Unbiased clustering revealed two small stromal clusters (Table 3.2 and Figure 3.5A), where stromal 1 cells were marked by expression of collagen proteins, and fibroblast markers *rbp4* and *vim* (Table 3.2). A subset of stromal 1 cells also highly expressed cytokine and complement genes (supplementary spreadsheet: conventional adult scRNA-seq unbiased cluster markers), indicating that stromal

cluster 1 contains a mixed fibroblast population, with some specialist immune activators. Stromal cluster 2 was marked by expression of vasculature genes *cdh5* and *kdrl* (Sumanas et al., 2005), alongside lymphatic vessel marker *lyve1a* (Chen et al. 2013) (Table 3.2) indicating that stromal 2 cells likely represents a mixture of vascular and lymphatic vessel-derived cells.

Initial unbiased clustering also revealed seven leukocyte clusters (Table 3.2). Through manual analysis, we re-classified these into five cell types based on known expression markers: a dominant population of T cells (leukocytes 1-3), alongside B cells (leukocyte 6), macrophages (leukocyte 4), granulocytes (leukocyte 7) and dendritic cells (leukocyte 5) (Figure 3.5A-B). Each cluster had a unique gene expression profile (Figure 3.5B) that implicate specialist, cell type-specific contributions to intestinal innate and adaptive defenses. Collectively, this data indicates that the adult intestine contains complex mixtures of stromal and leukocyte cells that support epithelial function and protect the epithelial barrier.
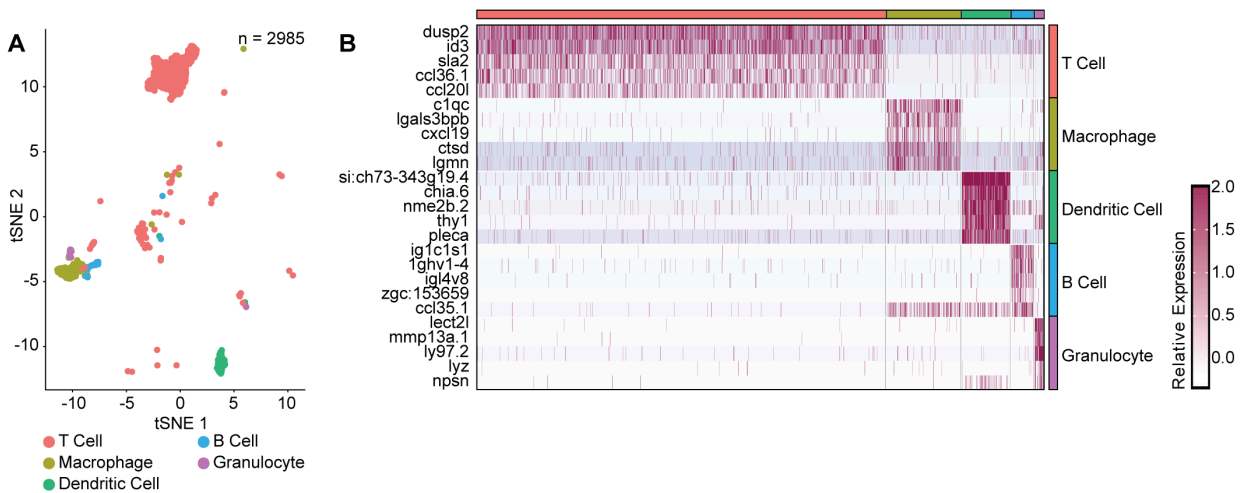
Figure 3.5 The adult intestine contains protective lymphoid and myeloid cells. A) 2D t-SNE projection of gut-associated leukocytes color coded by cell type. B) Heatmap of leukocyte cluster markers colored by relative gene expression and arranged according to cell type. Cell types are indicated by colored bars on the right and top. Markers for each cluster are labeled on the y-axis of the heatmap.

3.5 Larval and adult intestines are genetically comparable

Single cell profiling of larval and adult intestines revealed that numerous cell types and genetic markers are shared across intestinal development, though the extent of compositional and genetic overlap is unclear. To assess compositional and genetic similarity between conventional larval and adult digestive tracts, I spatially aligned cell gene expression profiles through dataset integration (Figure 3.6). A majority of cells were aligned across datasets (Figure 3.6A), especially between IECs (Figure 3.6A-B), suggesting that zebrafish IECs generally possess highly similar transcriptional states throughout development. Notable disparities in IEC populations include limited goblet cell, goblet-like 2, LRE3, and tuft-like cell representation in the larval intestinal dataset, and the emergence of interferon-enriched ECs (IFN-ECs), and clearer TA cell population in larvae. This likely indicates that IFN-ECs and TA cells are present in larvae, but that low cell abundance precluded detection during independent analysis of the larval dataset. Future work will be necessary to validate cell populations *in vivo* and to determine the significance of population variability, as differences here may reflect technical discrepancies related to cell isolation from larval versus adult tissue. Intriguingly, a significant fraction of larval tuft cells clustered near epidermal cells in the integrated dataset, in contrast to adult tuft cells that cluster with intestinal progenitors, suggesting that a subset of larval tuft cells originated from the epidermis, not the intestine. Future investigation may therefore yield insight into genetic distinctions across tuft cells from different tissues, and between comparable cell types of mature and immature intestines.
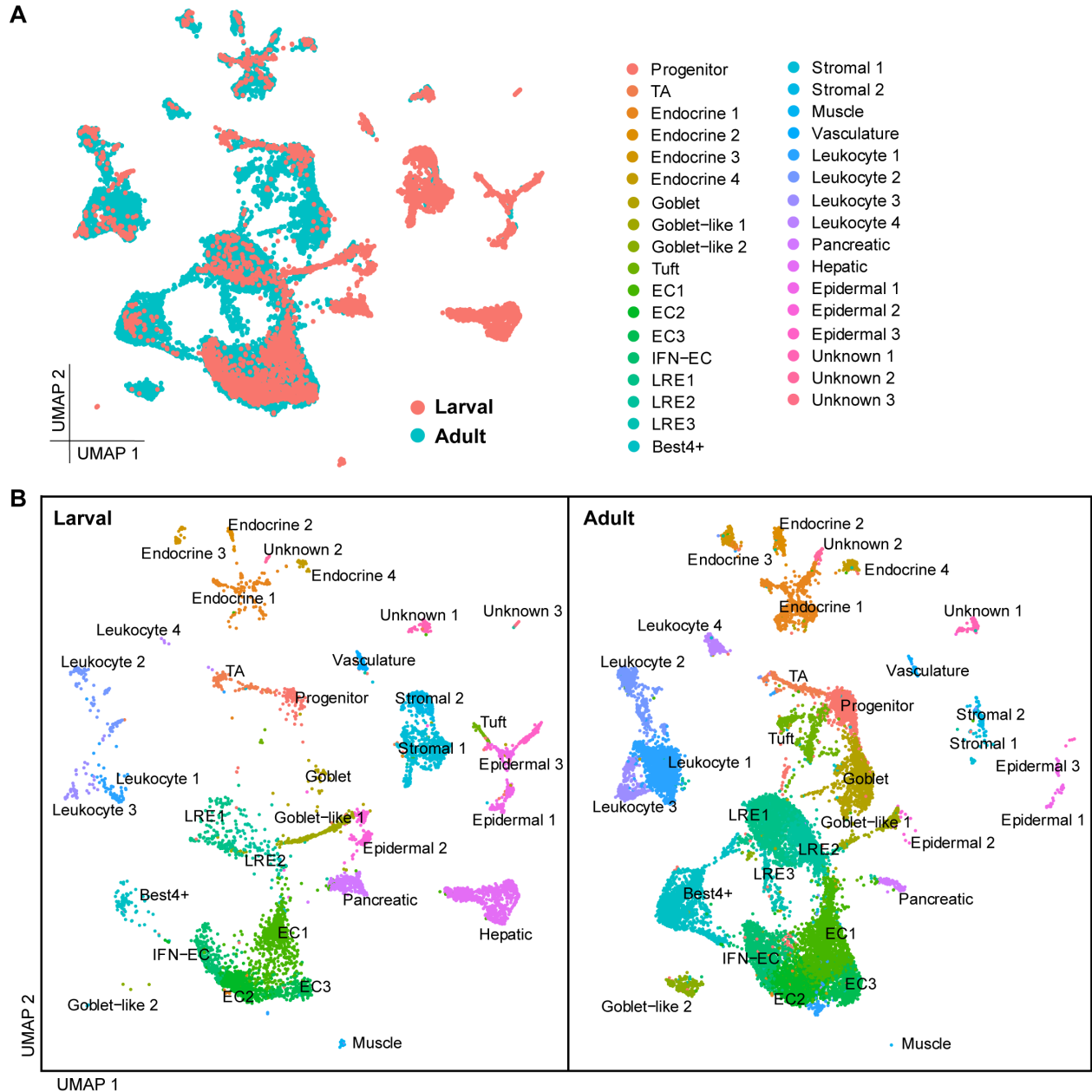
Figure 3.6 Alignment of larval and adult single cell profiles. A) Overlapping 2D UMAP projections of integrated cells from larval and adult conventional scRNA-seq datasets, colored by origin. B) 2D UMAP projections of integrated cells split across larval and adult conventional scRNA-seq datasets, color coded according to cell type and annotated according to markers in Tables 3.1 and 3.2.

3.6 Conclusions

The molecular and genetic networks that determine intestinal development are highly similar between zebrafish and mammals (Davison et al., 2017; Heppert et al., 2021; Lickwar et al., 2017). Thus, discoveries made with fish have the potential to reveal foundational aspects of intestinal development and function across vertebrates. However, important knowledge gaps prevent us from maximizing the value of the zebrafish model. In particular, we know less about cellular composition within the zebrafish intestinal epithelium compared to mice and humans, and we lack genetic markers that allow us to identify or isolate defined cell populations for experimental characterization. To bridge these deficits, we prepared single cell atlases of the larval and adult intestines raised under conventional conditions. We identified transcriptionally distinct cells in the gut and associated tissue that are conserved across development, including cell types that have not been described to date. We believe these findings constitute a valuable resource, and I have made our datasets publicly accessible for user-friendly visualization on the Broad Single Cell Portal, a web-based resource (see Chapter 2: Materials and Methods).

Looking at the intestinal epithelium, I identified progenitor cell subsets, including cells in both larvae and adults that express classical intestinal stem cell markers, such as the Delta-like ligand *dld*, Notch pathway components *ascl1a* and *atoh1b* (Crosnier et al., 2005; Flasse et al., 2013; Reuter et al., 2022; Roach et al., 2013), and Notch-responsive *hes-related* transcription factor family members, such as *her2* and *her15.1* (Rodríguez-Fraticelli et al., 2015). These data raise the possibility that I have uncovered ISC markers in the zebrafish intestine. In the future, it will be of interest to perform lineage tracing with candidate progenitor cells identified in this study, as well as cells that express the stemness marker *sox9b* (Peron et al., 2020), to test their ability to generate a mature epithelium. In addition to candidate stem cells, I uncovered basally localized proliferative cells marked by cell cycle regulators such as *pcna*, *mcm5*, and *mki67*, comparable to mammalian TA cells (Haber et al., 2017). Collectively, these data argue that zebrafish possess interfold base-localized ISCs that generate differentiated progeny through TA cell intermediaries.

Separate to transit amplifying and Notch-positive cells, I identified transcriptional markers for secretory cell subsets, including enteroendocrine cells, mucin-producing goblet cells, and a

novel cell type comparable to mammalian tuft cells. Examination of endocrine populations in both larvae and adults revealed a spatially complex pattern of hormone production within the intestinal epithelium. This was especially apparent in adults, where I resolved eight distinct patterns of peptide hormone expression in endocrine cells. In addition, I observed transcriptionally distinct mucin-producing lineages across development, perhaps reflecting functional or regional disparities in goblet cell function. This observation of transcriptionally distinct goblet cell subtypes in the adult aligns with observations of regionally distinct goblet cell subtypes in the fish epithelium (Crosnier et al., 2005). Additional work is needed to understand functional and regional differences between goblet-related cell populations. Perhaps most intriguing, I also uncovered cells that are enriched for expression of markers highly associated with mammalian intestinal tuft cells, including the *pou2f3* master regulator, and regulators of leukotriene biosynthesis, important for recruitment and activation of immune cells (Jo-Watanabe et al., 2019; McGinty et al., 2020). Tuft cells are a relatively under-characterized cell type thought to activate mucosal type II immune responses, and believed to share developmental trajectories with secretory lineages. At present, it is unclear if zebrafish tuft-like cells are involved in mucosal defenses, or arise through the IEC secretory lineage, though these will be important lines of inquiry given the frequent contact of aquatic vertebrates to parasitic pathogens.

Absorptive cell subsets comprised the bulk of our scRNA-seq datasets, where I identified ECs with distinct regional and functional gene expression profiles, as well as extensive gene expression profiles for LRE subsets thought to mediate protein absorption and metabolism (Park et al., 2019). To my surprise, I also uncovered a population of Best4/Otop2 cells previously unknown in zebrafish. Best4/Otop2 cells are a minimally characterized cell type only recently discovered in the human gut and thought to regulate ion transport, though their function(s) remains speculative (Parikh et al., 2019; Smillie et al., 2019). Given the utility of zebrafish for examination of gut development, particularly in the context of host-microbe interactions, fish will be of considerable value for *in vivo* characterization of Best4 and Otop2 positive cells. Moreover, identification of Best4/Otop2 and tuft-like cells within the zebrafish intestinal epithelium underscores the similarities between fish and mammalian intestines.

Since I analyzed intestines from immature 6 dpf fish and mature adult fish, our transcriptional profiles further enabled comparisons between two distinct stages of intestinal development. Overall, this analysis revealed that IEC composition is highly preserved from early intestinal growth stages through intestinal maturation. In the future, it will be of interest to assess all stages of intestinal development simultaneously (including those not considered here) to avoid technical discrepancies and enable accurate assessment of differentially expressed genes between developmentally shared cell types. Such analysis would likely reveal stage-specific regulators of intestinal morphogenesis and growth.

Chapter 4: Microbe-responsive processes in the zebrafish intestine

This chapter contains content from the following sources:

- **Willms RJ**, Jones LO, Hocking JC, and Foley E. (2022). A cell atlas of microbe-responsive processes in the zebrafish intestine. *Cell Reports*.

- Jones LO, **Willms RJ**, Shin M, Xu X, Graham RDV, Eklund M, Foley E. (2023). Single cell resolution of the adult zebrafish intestine under conventional conditions, and in response to an acute, natural infection. *bioRxiv.*

4.1 Summary

Microbe-dependent processes have been assessed at the level of whole intestinal tissue in a variety of animal models, demonstrating that gut microbial products influence a medley of developmental and functional processes including growth, differentiation, and nutrient metabolism (Bates et al., 2006; Camp et al., 2014; Hooper et al., 2001; Rawls et al., 2004; Reikvam et al., 2011; Sekirov et al., 2010). However, we lack system-wide understanding of both cell-specific responses to the microbiome, and molecular mechanisms underpinning inflammation and infection responses that accompany pathogen colonization. Zebrafish have emerged as a valuable tool to identify key regulators of host-microbe interactions (Brugman, 2016; Flores et al., 2020; López Nadal et al., 2020). Zebrafish embryos develop within a protective chorion that shields them from environmental microbes up to forty-eight hours post fertilization (hpf). Once larvae exit the chorion, water-borne microbes colonize the gut lumen (Bates et al., 2006; Stephens et al., 2016; Wallace et al., 2005), where they influence host development and organ function (Bates et al., 2006; Cheesman et al., 2011; Kanther et al., 2011; Koch et al., 2018). Additionally, researchers have simple protocols to generate large numbers of germ-free larvae, or larvae associated with defined microbial communities (Melancon et al., 2017; Pham et al., 2008), allowing expedient investigations of microbial impact on physiology in a relevant vertebrate model. Moreover, zebrafish and mammals exposed to pathogenic microbes often exhibit comparable responses to intestinal infection (Flores et al., 2020), making zebrafish an ideal tool to uncover host responses to pathogen challenge.

In this chapter, I first profiled cell transcriptomes from the intestine, and associated tissue, of zebrafish larvae raised in the absence of a microbiome, and compared these to profiles from conventionally reared siblings of the same embryo clutch (characterized in Chapter 3). By comparing conventional to germ-free profiles, I mapped the IEC transcriptional response to commensal microbes at cellular resolution. I revealed intricate degrees of cellular specificity in host responses to the microbiome that included regulatory effects on patterning, metabolic and immune activity. For example, I showed that the absence of microbes hindered pro-angiogenic signals in the developing vasculature, causing impaired intestinal vascularization.

Next, I compared transcriptional profiles from conventional adult intestines (characterized in Chapter 3) to profiles from siblings infected with the aquatic bacterium and natural zebrafish pathogen *Vibrio cholerae* (*Vc*) (Mitchell et al., 2017; Mitchell and Withey, 2018; Nag et al., 2018; Runft et al., 2014). *Vc* is the causative agent of the severe diarrheal disease, cholera, that claims approximately 100,000 lives per year, predominantly in areas with limited access to clean drinking water (Ali et al., 2015; Camacho et al., 2018; Piarroux et al., 2022). However, our understanding of the host intestinal response to *Vc* challenge, including molecular and cell-specific responses, remains incomplete.

Vc infections are commonly modeled in organisms such as *Drosophila*, rabbits, and mice. While *Drosophila* are useful for understanding commensal-pathogen interactions during disease (Davoodi and Foley, 2019; Fast et al., 2018; Fast et al., 2020; Jugder et al., 2021; Jugder et al., 2022), they are limited by differences in intestinal structure and cell composition relative to humans. The guts of rabbits and mice exhibit greater similarity to human intestines, but *Vc* infection is difficult to achieve in mature animals, requiring arduous experimental manipulation to drive host disease (Herrington et al., 1988; Klose, 2000; Olivier et al., 2009; Spira et al., 1981). In recent years, zebrafish have emerged as an alternate model for *Vc* infection. Zebrafish are natural hosts for a variety of *Vibrio* strains and may be vectors of transmission for pathogenic *Vc* in endemic regions (Halpern and Izhaki, 2017; Senderovich et al., 2010). Moreover, zebrafish intestines are easily colonized by *Vc* through animal immersion in *Vc*-laden fish water (Mitchell et al., 2017; Mitchell and Withey, 2018; Nag et al., 2018), leading to host disease marked by diarrhea and mild intestinal inflammation akin to humans (Mitchell et al., 2017; Mitchell and Withey, 2018; Nag et al., 2018; Runft et al., 2014). Thus, zebrafish provide an excellent opportunity to assess molecular responses to *Vc* infection in a natural host. By comparing single cell profiles of challenged and unchallenged zebrafish, I determined the host IEC response to primary *Vc* infection at the molecular level, which included globally suppressed interferon signaling and increased antigen capture by host IECs.

4.2 Cell type-specific effects of gut microbes on host gene expression

Despite critical roles for microbial factors in regulating host physiology, we have made sporadic progress charting cell type-specific responses to the microbiome. To address this disparity, I performed single cell profiling of GF larval zebrafish digestive tracts alongside CV counterparts from the same embryo clutch. Zebrafish embryos were derived GF using established protocols, where I tested for bacteria by plating on tryptic soy agar plates, as well as PCR against bacterial 16S rDNA (Melancon et al., 2017). After filtering for dead cells and doublets, I determined gene expression profiles for 10,309 individual GF cells, where clustering analysis revealed subsets of progenitor-like, secretory, and absorptive IECs, as well as stromal, immune, and extra-intestinal cells conserved across CV and GF datasets (Tables 3.1 and 4.1). Notably, our fish primarily host gamma- and alpha-proteobacteria (Tables 4.2 and 4.3), akin to zebrafish from other facilities (Roeselers et al., 2011). Therefore, I believe that comparisons between our GF and CV data may uncover relevant cell-specific responses to the microbiome.

Table 4.1 GF larval intestinal scRNA-seq cell identifiers based on unbiased clustering.

Cell Type	Captured Cells	Top Gene Expression Markers
Progenitor-like 1	154	dld, her15.2, gig2h, her15.1, dla
Progenitor-like 2	149	si:dkey-96g2.1, zgc:193726, zgc:113142, stm, si:rp71-17i16.6
Endocrine 1	254	ccka, egr4, insl5a, scg3, si:ch73-359m17.9
Endocrine 2	85	pnoca, scgn, scg3, scg5, pax6b
Tuft-like	68	gng13a, calb2a, ponzr6, gnb3a, rgs1
Goblet 1	785	si:ch211-153b23.5 , malb, si:ch211-139a5.9, cldnh, ponzr1
Goblet 2	414	si:ch211-153b23.5, cldnh, si:ch211-139a5.9, krt92, cnfn
Goblet-like	248	tcnba, cnfn, zgc:92380, CABZ01068499.1, s100a10b
EC1	841	apoa1a, chia.2, fabp2, rbp2a, fabp1b.1
EC2	470	chia.1, chia.2, fabp1b.1, apoa4b.2.1, fabp2
EC3	568	si:ch211-142d6.2, elovl2, mogat2, lta4h, sult1st3
EC4	660	anpepb, mep1b, mep1a.1, si:dkey-219e21.2, clca1
EC5	134	tmprss15, neu3.3, si:ch211-113d11.6, pdx1, meis1a
LRE 1	67	lrp2a, slc5a12, mfsd4ab, slc22a7b.1, slc13a3
LRE 2	55	ctsbb, dab2, fabp6, slc15a2, si:ch211-214j8.1
Best4/Otop2	106	otop2, cftr, ptger4c, tacr2, best4
Mesenchymal 1	311	zgc:153704, si:ch211-106h4.12, si:ch211-251b21.1, col1a1a, pmp22a
Mesenchymal 2	285	aqp1a.1, podxl, cavin2b, cavin1b, rhag
Mesenchymal 3	50	fgfbp2b, col2a1a, matn1, cnmd, col9a2

Mesenchymal 4	41	colec10, colec11, agtr2, angptl6, lhx9
Muscle	54	mylpfa, nme2b.2, tnnt3b, mylz3, tnni2a.1
Vasc. Sm. Muscle	232	tagln, acta2, BX088707.3, mylkb, desmb
Vasc. Endothelial	134	cdh5, plvapb, kdrl, fgd5a, clec14a
Leukocyte 1	146	fcer1gl, si:dkey-5n18.1, si:ch211-147m6.1, si:ch211-194m7.3, spi1b
Leukocyte 2	114	ccl36.1, ccl38.6, ccr9a, coro1a, CR753876.1
Neuronal	51	elavl4, elavl3, sncb, phox2a, phox2bb
Hepatocytes 1	497	hamp, ces2, serpina1l, si:dkeyp-73d8.9, fgg
Hepatocytes 2	558	hpda, si:dkey-86l18.10, ambp, zgc:112265, c3a.1
Hepatocytes 3	994	gc, serpina1, tfa, zgc:123103, serpina1l
Acinar 1	802	prss1, ctrb1, prss59.2, CELA1 (1 of many), prss59.1
Acinar 2	316	si:ch211-240l19.5, cel.2, CELA1 (1 of many).5, pdia2, c6ast3
Acinar 3	289	pla2g1b, si:ch211-240l19.5, cpa4, si:dkey-14d8.7, cel.2
Epidermis 1	111	krt1-19d, ponzr5, zgc:165423, icn2, anxa1c
Epidermis 2	117	cldni, aqp3a, cxl34b.11, col4a5, si:rp71-77l1.1
Epidermis 3	119	cyt1l, krt17, zgc:111983, cyt1, si:dkey-247k7.2

Table 4.2 Classification of 16S rRNA gene sequence datasets. Relative abundance is shown after removal of taxa that were <1% abundant.

Phylum	Firmicutes		Proteobacteria							
Class	Bacilli		Alpha-proteobacteria		Beta-proteobacteria		Gammaproteobacteria			
Order	Baci-llales	Lacto-Bacill-ales	Acetoba-cterales	Rhizo-biales	Burkho-lderiales	Neiss-eriales	Altero-mona-dales	Aero-mona-dales	Pseudo-mona-dales	Vibrio-nales
CV1	0.78	6.20	4.91	0.25	0.58	0.26	0.46	0.72	1.64	84.21
CV2	1.07	22.25	6.26	2.90	1.56	2.53	2.71	12.32	12.37	36.03
CV3	0.56	35.06	2.76	1.18	1.18	3.09	2.28	3.75	6.06	43.69

Table 4.3 Description of 16s rRNA gene sequencing datasets used in this study and associated metadata.

Sample Name	# Input Reads	Reads post-filtration	Target	515F-Primer	816R-Primer	Barcode-F	Barcode-R
CV1	174987	153739	16S-V4	GTGCCAGCM GCCGCGGTAA	GGACTACHVG GGTWTCTAAT	CCAACA	CGATGT
CV2	163143	148080				CCAACA	TGACCA
CV3	172703	139893				CCAACA	GCCAAT

I first confirmed that our data reproduce known effects of GF growth on host gene expression by comparing aggregated cell gene expression profiles across samples. Among the top globally differentially expressed genes in GF fish relative to CV controls, I identified microbe-dependent effects on expression of host genes previously identified by whole-gut RNA sequencing of CV and GF zebrafish intestines (Rawls et al., 2004), including *gpx1b*, *socs3a*, *mlnl*, and *cfd* (Figure 4.1A). In addition to previously uncovered genes with microbe-dependent expression changes, I uncovered changes to a range of host genes in GF fish, such as decreased expression of *plac8.1* and *tmem176l.2*, both thought to modulate ERK/MAPK signaling (Li et al., 2014; Li et al., 2018), and drastically increased expression of numerous endopeptidases in GF fish such as *ela2* and *prss59.1*. To independently validate effects of the microbiome on expression of host genes observed in our single-cell data, I used Nanostring quantitative analysis. Consistent with our single-cell analysis (Figure 4.1A), *plac8.1*, *tmem176l.2, muc13b* and *tcnba* were significantly downregulated, while *prss59.1* and *ela2* showed moderately increased expression under GF growth conditions (Figure 4.1B). Increased expression of digestive enzymes is an intriguing finding given that such gene products are largely generated by the exocrine pancreas, packaged into vesicles, and delivered to the intestinal lumen; however, follow-up work on whole-larvae has since corroborated this finding, showing that microbes stimulate production of digestive enzymes, at least in the pancreas (Massaquoi et al., 2023). It is plausible that increased production of digestive enzymes signifies increased reliance on protein catabolism in the absence of a microbiome. Collectively, these observations argue that our gene expression data accurately report effects of the microbiome on gut function.
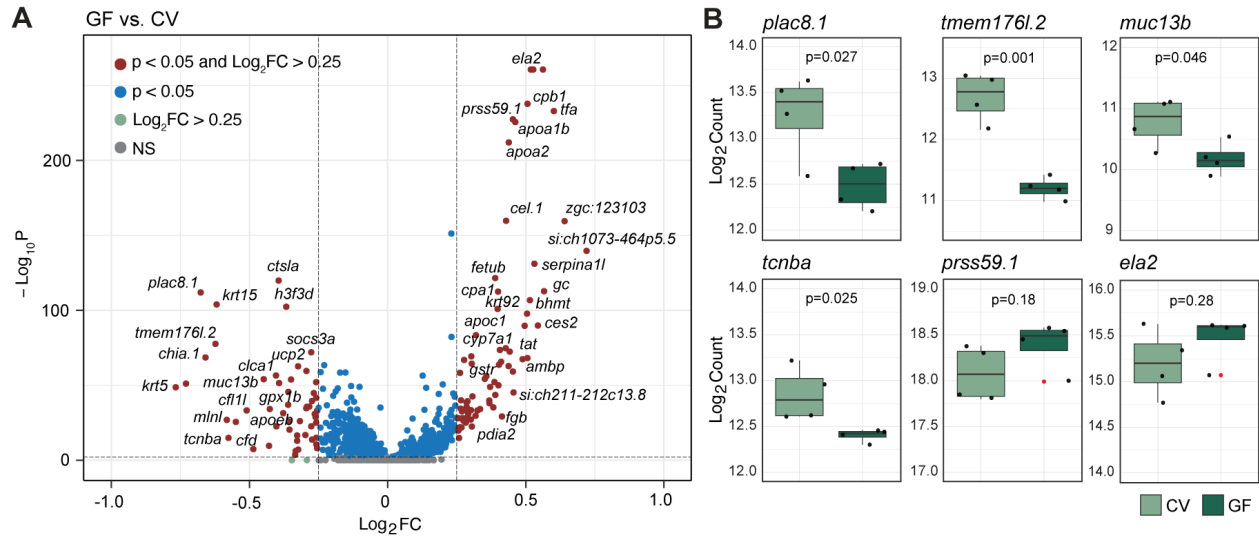
Figure 4.1 Microbial control of host gene expression. A) Volcano plot of differentially expressed genes in GF relative to CV cells, treated in aggregate. Significance (adjusted P-value) was determined in Seurat using the non-parametric Wilcoxon rank sum test with Bonferroni correction. B) Quantitative gene expression analysis from dissected whole guts. Four replicates (n=15 guts per replicate) were analyzed per condition. Outliers are indicated with red dots. Significance was determined using a Student's *t*-test.

4.2.1 Microbes stimulate specialized processes in progenitor-like cell subsets

Single cell profiling of larval and adult IECs revealed a cell subset with progenitor-like properties, including expression of cell cycle regulators and Notch pathway components. While I identified and analyzed several progenitor-like subsets, I believe progenitor-like cluster 2 is intestinally derived, and most likely to represent an ISC population (see section 3.2). To begin exploring cell-type specific microbiome responses, I first characterized the transcriptional programs of progenitor-like cells (Figure 3.1C,D) raised under CV and GF conditions. I selected progenitors, as microbes are established modifiers of proliferation and differentiation, including Notch pathway components (Crosnier et al., 2005; Flasse et al., 2013; Roach et al., 2013; Troll et al., 2018; Yang et al., 2009). I observed remarkable cellular specificity in the responses of putative progenitor clusters to GF growth (Figure 4.2). For example, cells from progenitor-like cluster two downregulated Notch-responsive transcription factors *atoh1b* and *her15.1*, as well as the intestinal Notch ligand *delta D* (*dld*) when grown in the absence of a microbiome (Figure 4.2B,D).

This result is particularly intriguing since the zebrafish microbiome is a known promoter of secretory cell differentiation through Notch inhibition (Troll et al., 2018), though specific regulators of this process have not been identified. Therefore, reduced expression of *dld* and *atoh1b*, known regulators of secretory IEC development, implicates these genes in microbe-dependent secretory cell differentiation. Microbes are also established modifiers of intestinal proliferation in zebrafish, through MyD88-dependent TLR signals. Intriguingly, I observed decreased expression of *interferon-related developmental regulator 1* (*ifrd1*) in progenitor-like cluster two (Figure 4.2D), an immune response gene that regulates gut epithelial proliferation (Yu et al., 2010), suggesting that *ifrd1* may mediate microbe-dependent proliferation changes in zebrafish intestinal progenitors downstream of MyD88. Taken together, my data indicate that a specific subset of candidate progenitors are particularly sensitive to the impacts of microbial factors on Notch activity and growth regulators. Moreover, my results align with studies demonstrating that microbes alter intestinal stem cell proliferation and differentiation dynamics throughout the animals kingdom (Bates et al., 2006; Broderick et al., 2014; Buchon et al., 2013a; Ferguson and Foley, 2022; Kandori et al., 1996; Sommer and Bäckhed, 2013; Troll et al., 2018), and provide specific mediators of these processes in a vertebrate model.

4.2.2 Microbes alter immune gene expression across intestinal cell types

To test the utility of our data for cell-specific mapping of signaling pathway activity in the presence or absence of microbes, I visualized relative expression of microbial sensors, NF-κB pathway components, cytokines and chemokines in CV and GF fish. In CV larvae, I detected cell-restricted expression of key immune sensors and effectors (Figure 4.3). For example, leukocytes expressed immune-regulatory cytokines such as *cxcl8a*, *il1b,* and *tnfa* (Secombes et al., 2001), whereas the vasculature was characterized by enriched expression of microbial sensor *tlr4ba* (Meijer et al., 2004), cytokine *tgfb1b* (Maehr et al., 2013) and the inflammation regulator *ahr2* (Hennig et al., 2002). Like mammals, CV hepatocytes expressed the *hamp* antimicrobial peptide (Shike et al., 2004), while mesenchymal cells were characterized by enriched expression of *cxcl8b* isoforms, *cxcl12*, and the *tgfb1a*, *tgfb2* and *tgfb3* cytokines. Within the intestinal epithelium, most enterocyte subtypes produced *alpi.2*, a phosphatase required for detoxification of bacterial

lipopolysaccharide (Bates et al., 2007), whereas enteroendocrine cells expressed *il22*, a cytokine that activates epithelial innate defenses (Dudakov et al., 2015). In agreement with previous reports (Kanther et al., 2011), *serum amyloid A* (*saa*) was expressed in mid-intestinal LREs and goblet cells. Intriguingly, I also saw enhanced *nod1, nod2* and *myd88* expression in CV tuft-like cells, consistent with proposed roles for Nod1 and Nod2 in type 2 immunity in tuft cells (Magalhaes et al., 2011). Removal of the microbiome significantly impacted organization of immune pathways in developing larvae. In particular, I noted greatly diminished expression of *il22* from endocrine cells and leukocytes; *nod1* from progenitors, mesenchyme, and vasculature; *tgf* isoforms from mesenchymal cells, vasculature, and leukocytes; *ifit14* and *ifit15* (*IFIT1* orthologues) from enterocytes; and *stat2* across IECs. Decreased IFN signals in GF absorptive cells is highly intriguing given that I observed IFN-enriched ECs in conventional single-cell datasets (Chapter 3). It is tempting to speculate that microbes encourage differentiation of these candidate immune-involved cells. Combined, my data uncovered a sophisticated partitioning of immune gene expression patterns across CV cell types, many of which indicate shared microbe-response pathways in zebrafish and mammals.
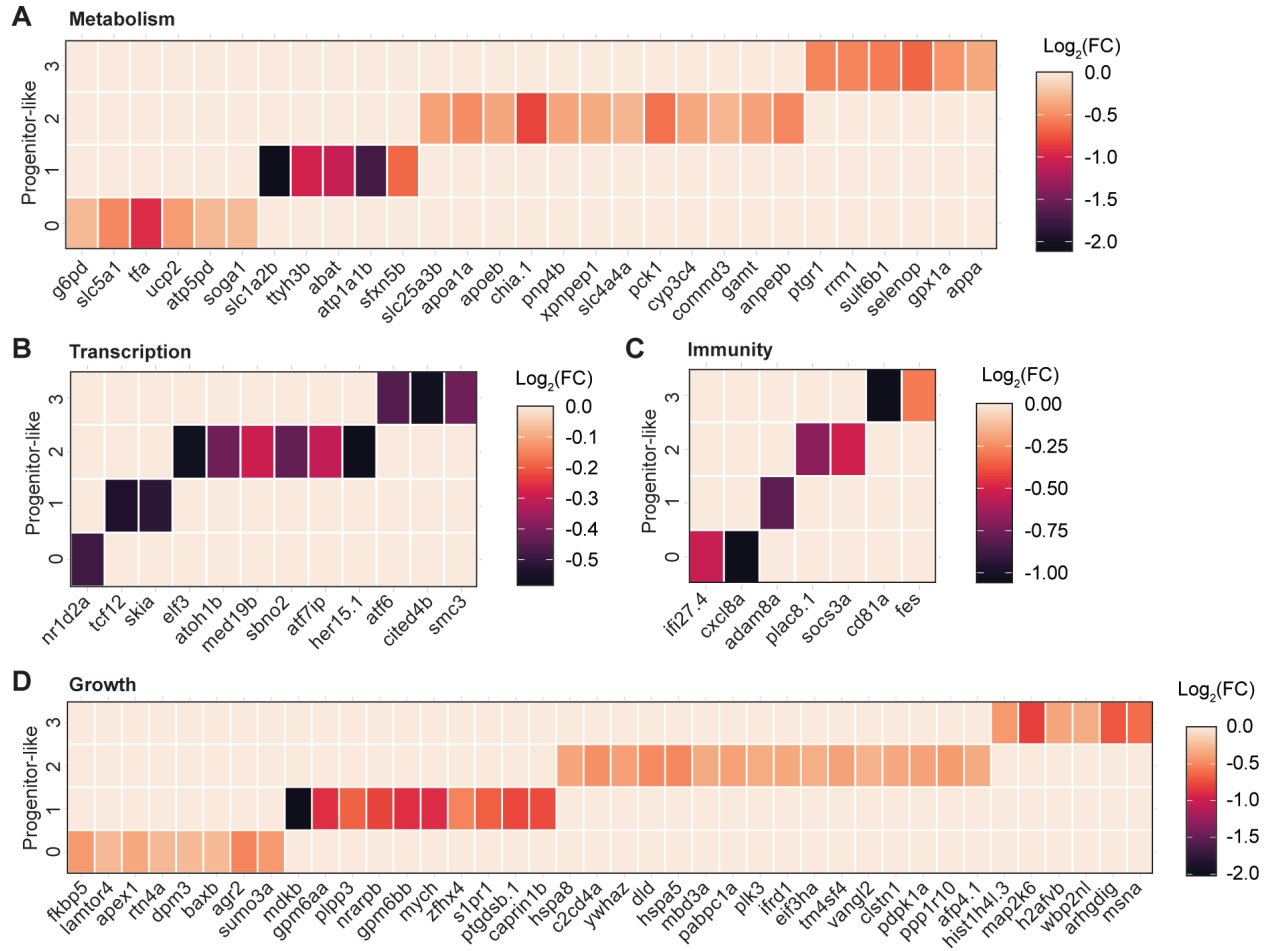
Figure 4.2 Microbes stimulate specialized processes in progenitor-like cell subsets. Heatmaps of differentially expressed genes (GF vs. CV, p<0.05) involved in metabolism (A), transcription (B), immunity (C) and growth (D), in progenitor-like subsets 0-3 (from Figure 3.1C,D), color coded according to Log$_2$(FC). All non-zero value expression changes are significant (p<0.05) as determined with a non-parametric Wilcoxon rank sum test.
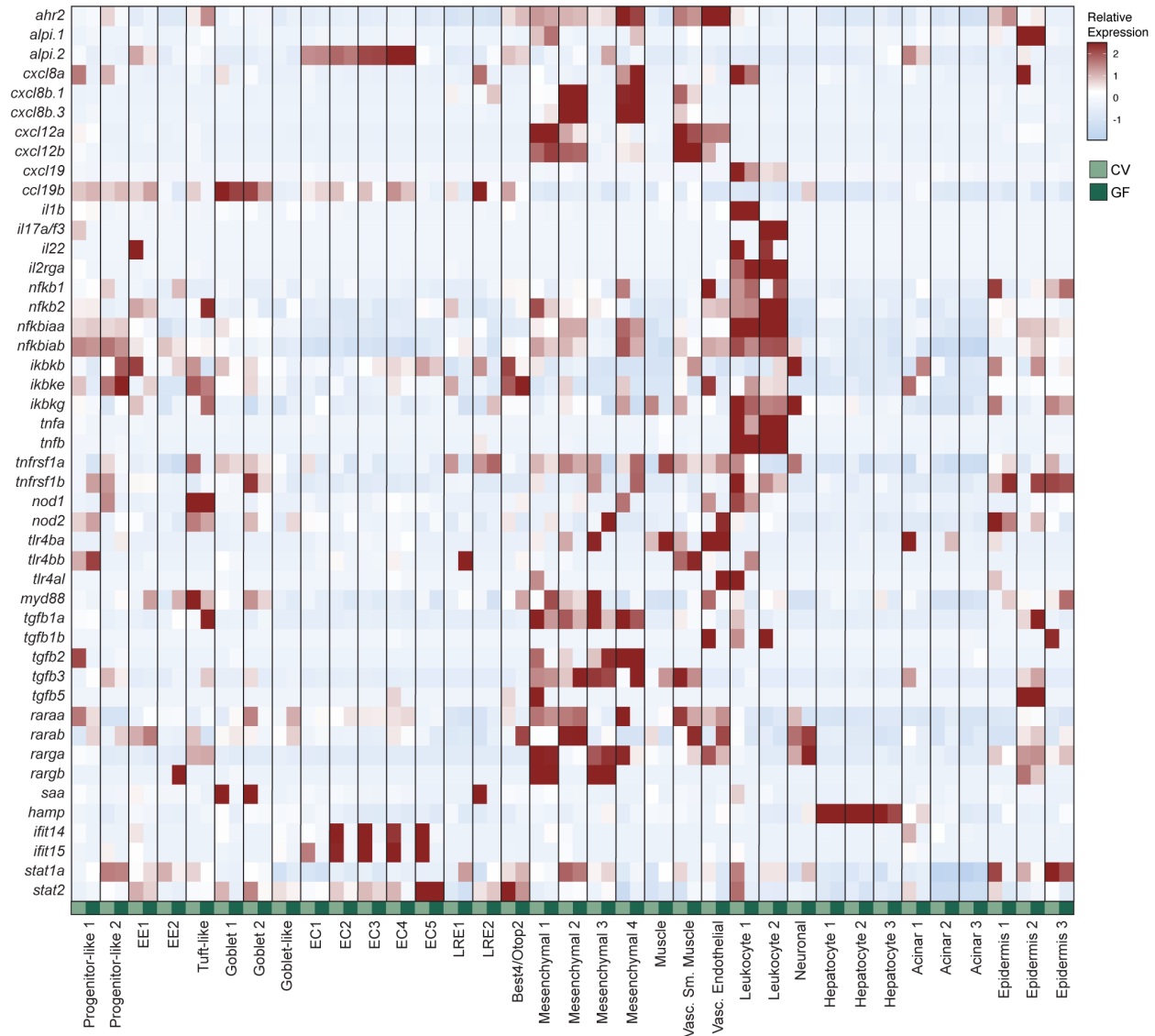
Figure 4.3 Immune gene expression across CV and GF cell populations. Heatmap showing relative expression of a representative set of microbial sensors, NF-kB pathway components, cytokines and chemokines in CV and GF cell types.

4.2.3 Microbes drive lineage-dependent processes in the larval intestine

I next investigated the mature IEC response to microbial encounter. Since mature IECs directly contact the luminal environment, I expected to uncover significant transcriptional differences across cell types. To understand how endocrine cells interact with a conventional

microbiome, I generated a transcriptional atlas of secretory cells from CV and GF fish (Figure 4.4). Among the enteroendocrine population, I uncovered six distinct transcriptional cell states, each marked by a unique pattern of peptide hormone production (Figure 4.4A-B). For example, CV enteroendocrine cluster five cells were characterized by production of *ccka* and *cckb*, regulators of gut motility, satiety, and lipid and protein digestion (Le et al., 2019; Rehfeld, 2017). By contrast, enteroendocrine cluster three cells were the predominant source of the motility regulator *vipb*, and the multifunctional peptide *galn*. Larval peptide hormone distributions across cell subsets were therefore distinct from adult EECs (Figure 3.4G), suggesting zebrafish modify intestinal secretion profiles with age, perhaps to accommodate dietary and metabolic changes. I observed modest effects of GF growth on expression of most peptide hormones (Figure 4.4B), suggesting that enteroendocrine lineage specification is broadly insensitive to microbial exposure. However, I detected instances where microbial presence affected hormone expression profiles of distinct enteroendocrine lineages. In particular, I observed moderately diminished expression of *gip* and *gcgb* within cluster four enteroendocrine cells (Figure 4.4B), supporting a role for microbes in modifying levels of *gip* and *glucagon*, incretin hormones that regulate glucose metabolism and insulin secretion (Gribble and Reimann, 2016). These results also align with a study in mice showing that microbes modify the transcriptomic profiles of glucagon and peptide YY producing L cells (Arora et al., 2018).

I was intrigued by apparent changes to immunity in GF goblet and absorptive cells relative to CV counterparts (Figure 4.3), so I further examined immune gene expression within these subsets. Re-clustering of integrated GF and CV data revealed three goblet cell subsets differentiated by *agr2* and *muc5.3* expression levels (Figure 4.4D), consistent with the presence of distinct mucus-producing cells throughout the gut (Crosnier et al., 2005), and described in chapter 3). Notably, removal of the microbiome had cluster-specific impacts on several immune regulators in goblet-related cells. For example, microbiome elimination resulted in significantly diminished expression of the putative LPS-binding molecule and anti-microbial peptide *ly97.2* (Liu et al., 2017; Wang et al., 2016) in goblet cell clusters 1 and 2, as well as the inflammation mediators *irg1l* (Hall et al., 2014; van Soest et al., 2011) and *lect2l* (Gonçalves et al., 2012) in goblet cell cluster 1 (Figure 4.4E). In contrast, GF growth led to diminished expression of *interferon*

alpha inducible protein 27 (*IFI27*) orthologues across all goblet cells, whereas absence of the microbiome exclusively attenuated expression of *CCL19* orthologues in cluster one cells (Figure 4.4E). These data suggest that a subset of zebrafish intestinal goblet cells mediates aspects of innate immune function in response to microbes. Since zebrafish do not possess a clear Paneth cell population, this could further indicate that microbe-responsive goblet cells sense bacteria and protect vulnerable cells at the fold base, akin to sentinel goblet cells in mice (Birchenough et al., 2016).

Within absorptive cells, enterocyte clusters one to five (Figure 3.2) had similar transcriptional responses to GF growth, including downregulation of *plac8.1* and *cathepsin La* (*ctsla*)*,* while ECs 2-4 also showed downregulation of the interferon pathway element *socs3a*, and *elf3* (Figure 4.4F). While these genes have putative innate immune function, the significance of these gene expression changes in enterocytes is not entirely clear. It is plausible that diminished immune signals in ECs contribute to previously described reductions in immune cell recruitment and inflammation of GF intestines (Kanther et al., 2011; Murdoch et al., 2019; Rolig et al., 2015). LRE1 cells did not display significant changes in GF fish, consistent with localization in the kidney and reduced exposure to microbial metabolites. However, intestinal LRE2 cells exhibited dramatic changes following microbial elimination, including significant downregulation of *prdx1*, *lect2l*, *saa*, and numerous interferon-stimulated genes (Figure 4.4F). Remarkably, these and other gene expression differences in GF LRE2 cells were highly similar to the GF response of cluster one goblet cells, suggesting that intestinal LRE2 and goblet one clusters have overlapping immune responses to microbial encounters, and may therefore cooperate in the bacterial response. Given regional specializations across the gut tube, I feel it is likely that LRE2 and goblet one clusters cell co-localize within an intestinal region. In line with this, intestinal *saa* is specifically expressed in the distal mid-intestine (Kanther et al., 2011), and mediates neutrophil activation and bacterial killing following microbial colonization (Kanther et al., 2011). Since *saa* is downregulated in both LRE2 and goblet cells, it is likely that these cells mediate decreased neutrophil recruitment and activation from the distal midgut. In addition to my single-cell analysis, I validated microbiome-dependent expression changes to several gene expression changes observed in goblet and absorptive cell subsets by whole-tissue quantitative gene expression analysis, including *IFI27*

orthologues, *irg1l,* and *ccl19b* (Figure 4.4G), further supporting a role for goblet and absorptive cell-mediated IFN and inflammatory signaling in response to commensal microbes. Collectively, these data indicate that mature zebrafish IEC types collaborate to support specialized immune responses to gut microbes.
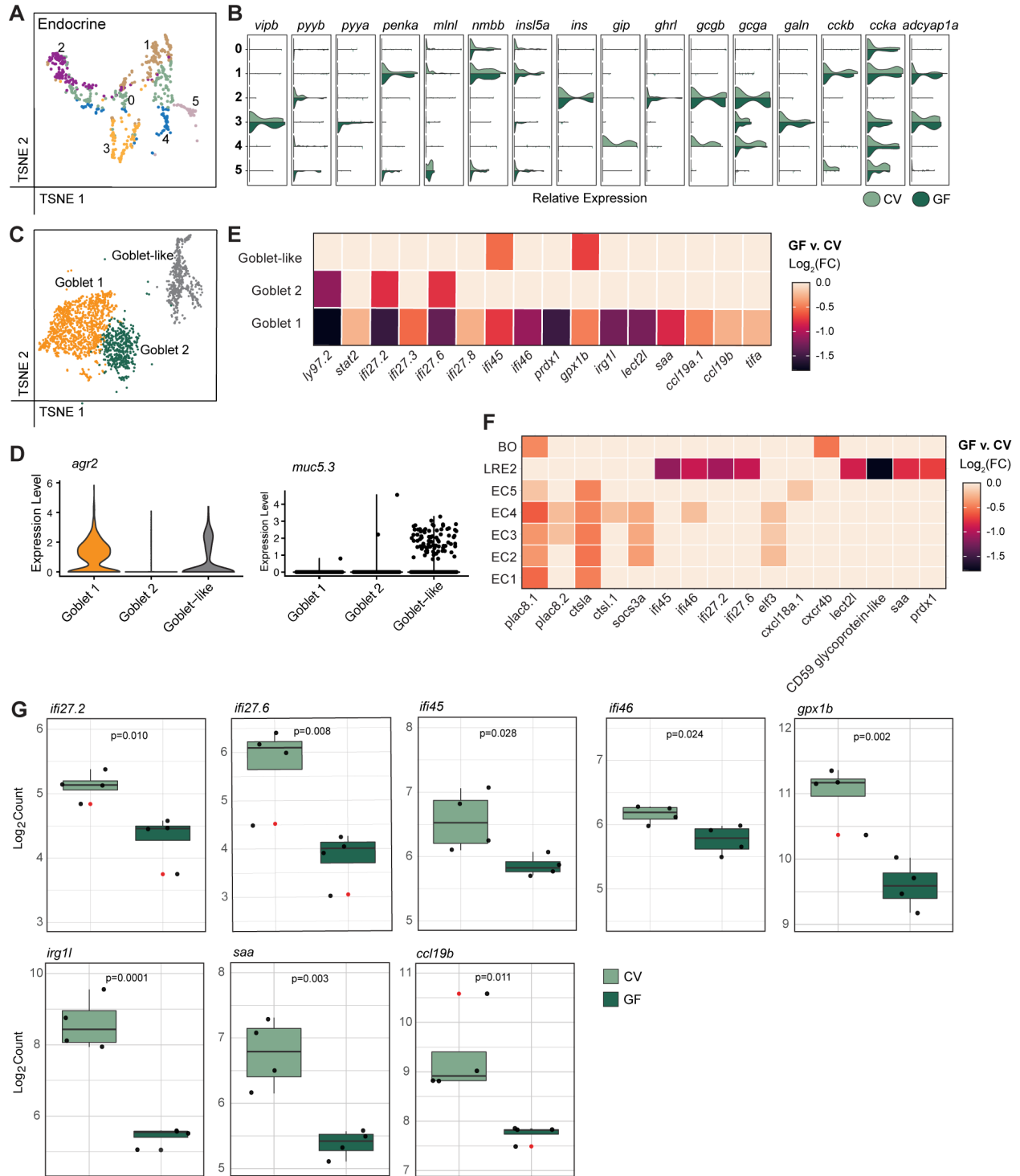
Figure 4.4 Germ-free growth alters peptide hormone expression in enteroendocrine cells and immune signaling in goblet and absorptive cells. (A) t-SNE plot of enteroendocrine cells after re-clustering, color coded by cell type. (B) Violin plots for expression of zebrafish peptide hormones, as expressed in enteroendocrine clusters 0-5. (C) t-SNE plot of goblet and goblet-like cell clusters

color coded by cell type. D) Violin plots for *agr2* and *muc5.3* expression in goblet and goblet-like clusters. E-F) Heatmaps of differentially expressed immune related genes in GF relative to CV goblet-related cells (E) or absorptive cell subsets (F), color coded according to Log$_2$(FC). All non-zero value expression changes are significant (adjusted p-value <0.05) as determined with a non-parametric Wilcoxon rank sum test with Bonferroni correction. LRE 1 showed no significant differential immune gene expression and was therefore not included. BO = Best4/Otop2 cells. G) Boxplots of Nanostring gene expression analysis from dissected whole guts. Four replicates (n=15 guts per replicate) were analyzed per condition. Outliers are indicated with red dots. Significance was determined using a Student's *t*-test.

4.2.4 Cell-specific effects of microbial exposure on leukocyte and stromal activity

As my data included non-epithelial lineages, I expanded my study to map relationships between microbiome colonization and gene activity in leukocytes and stromal cells, critical regulators of host-microbe interactions. I uncovered two highly distinct larval leukocyte clusters, including a mixed phagocyte population (leukocyte 1) and a putative T cell or ILC subset (leukocyte 2) (Figure 3.3A-D). The microbiome primarily impacted gene expression within phagocytes, where GF growth led to significantly diminished expression of interferon and cytoskeletal components relative to CV controls (Figure 4.5A), and attenuated production of key immune regulators such as *stat1a* and *stat2*, and the pro-inflammatory cytokines *il1b*, *tnfa* and *tnfb* (Figure 4.5C). While previous work has demonstrated increased intestinal myeloid cell recruitment and activation in response to microbiota colonization (Kanther et al., 2011; Koch et al., 2018; Murdoch et al., 2019; Rolig et al., 2015), these data provide candidate immune genes and regulators likely to regulate myeloid cell recruitment and activation following microbial colonization. Intriguingly, I also observed decreased expression of neutrophil marker *mpx* in GF zebrafish, which could represent a shift to a macrophage-dominated myeloid cell population, or decreased redox regulation in myeloid cells in the absence of microbes. Significantly decreased *mpx* expression is notable, since this is the dominant marker used to identify neutrophils, including in GF zebrafish.

Among the mesenchymal clusters, removal of the microbiome primarily attenuated expression of genes associated with metabolism (Figure 4.5A). In contrast, GF growth had sizable

80

effects on gene expression in vascular smooth muscle and endothelial cells. Relative to CV controls, GF vascular cells expressed significantly lower amounts of genes that regulate leukocyte migration, cell proliferation, and sprouting angiogenesis. (Figure 4.5A). Furthermore, unlike mesenchymal cell-types, vascular smooth muscle cells exhibited significantly decreased chemokine expression under GF growth conditions (Figure 4.5B,C), implicating vascular cells as an intermediary in microbe-dependent leukocyte recruitment. Consistent with a role for vascular cells in mediating microbial recruitment of leukocytes, I found that, compared to CV controls, vascular smooth muscle cells from GF fish downregulated expression of the lymphocyte chemotactic regulator *cxcl12b* (Glass et al., 2011), and the granulocyte chemotaxis regulator *cxcl18b* (Torraca et al., 2017), while vascular endothelial cells downregulated *cd99* (Figure 4.5C), a promoter of trans-endothelial leukocyte migration (Schenkel et al., 2002). In summary, larval intestinal leukocyte and stromal cell subtypes exhibit differential degrees of microbial sensitivity, where vascular cells are probable agents of microbe-responsive leukocyte migration.

A Downregulated Processes (GF v. CV)

Legend:
- Leukocyte 1
- Leukocyte 2
- Mesen 1
- Mesen 2
- Mesen 3
- Mesen 4
- Vasc. Smooth Muscle
- Vasc. Endothelial

B

Legend:
- Mesen 1
- Mesen 2
- Mesen 3
- Mesen 4
- Vasc. Smooth Muscle
- Vasc. Endothelial
- CV
- GF

C
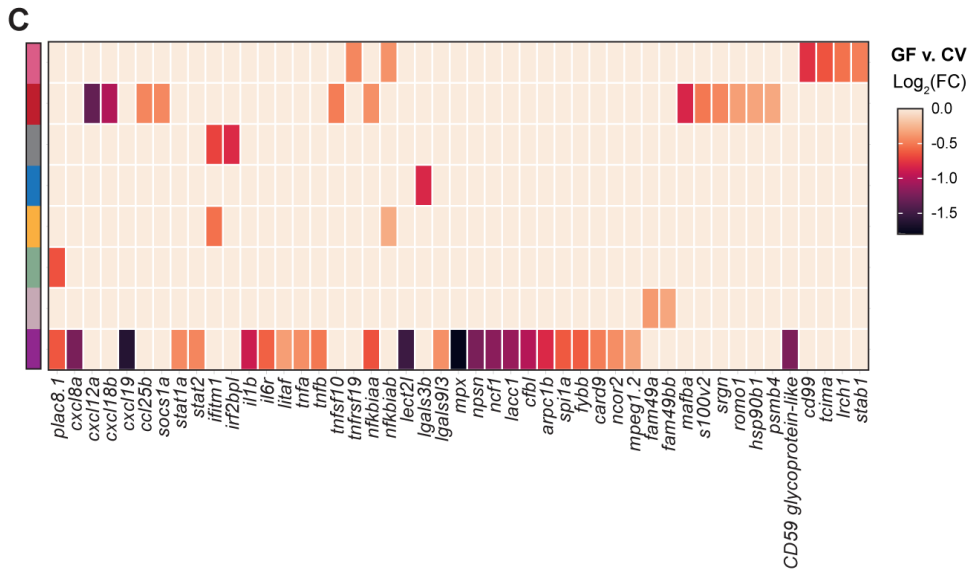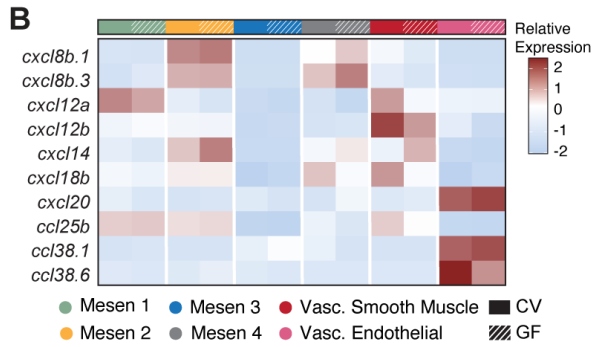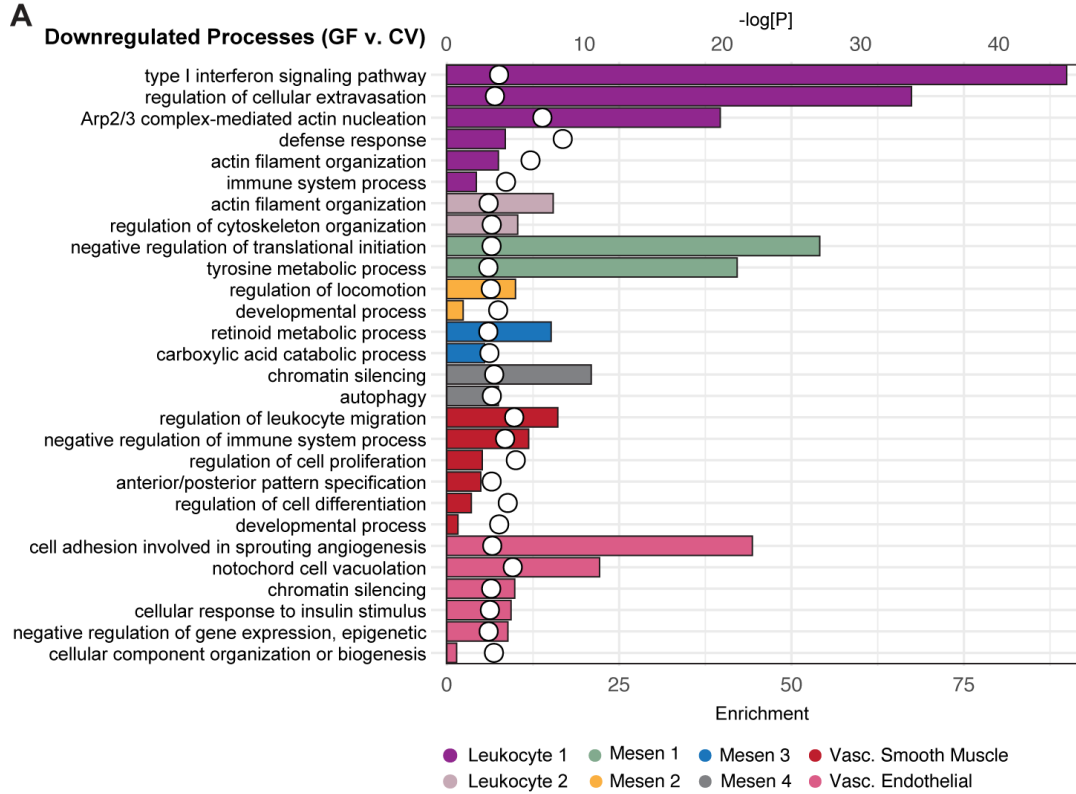
Figure 4.5 Stromal and leukocyte populations have subtype-specific responses to commensal microbes. A) GO enrichment analysis of downregulated genes in GF relative to CV stromal and leukocyte populations. Enrichment score is represented by bar length and p-value is indicated with white circles. B) Heatmap showing relative expression of chemokines in CV or GF stromal subsets. C) Heatmap of differentially expressed immune related genes in GF relative to CV leukocyte and stromal cell populations, color coded according to Log_2(FC). All non-zero value expression changes are significant ($p<0.05$) as determined with a non-parametric Wilcoxon rank sum test.

4.2.5 The microbiome is essential for intestinal vascularization.

Integrated analysis of CV and GF data revealed microbe-dependent gene expression changes in vascular endothelial and smooth muscle populations, including significantly diminished expression of vasculature developmental regulators (Figure 4.5). Thus, I reasoned that, like mice (Reinhardt et al., 2012; Stappenbeck et al., 2002), microbes may promote zebrafish intestinal angiogenesis. A closer look at vascular cells showed that larvae raised in GF conditions expressed lower amounts of pro-angiogenic factors such as *moesin a* (*msna*) and *cdh5* (Wang et al., 2010a), as well as BMP regulators involved in vascular morphogenesis (He and Chen, 2005; Mouillesseaux et al., 2016), such as *smad5* and *smad6a* (Figure 4.6A). Likewise, I detected significant drops in expression of *angptl4* and transcriptional regulators *pre-B-cell leukemia homeobox 1a* (*pbx1a*) and *pbx4* in vascular smooth muscle (Figure 4.6A), known regulators of vascular development (Cvejic et al., 2011; Kao et al., 2015). Combined, these data raise the possibility that GF growth has detrimental consequences for formation of gut-associated vascular tissue. Intestinal vasculogenesis commences approximately three days after fertilization (Isogai et al., 2001), a time that matches microbial colonization of the lumen. At this stage, angioblasts migrate ventrally from the posterior cardinal vein, establishing the supra-intestinal artery, and a vascular plexus that gradually resolves into a parallel series of vertical vessels and the sub-intestinal vein (Goi and Childs, 2016; Lenard et al., 2015; Nicenboim et al., 2015). The gut vasculature delivers nutrients from the intestine to the hepatic portal vein, supporting growth and development. To determine if the microbiome affects intestinal vasculogenesis, I used

kdrl:mCherry larvae to visualize the vasculature of fish raised in the presence, or absence of a conventional microbiome for six days (Figure 4.6B,C). I did not observe effects of the microbiome on formation or spacing of the supra-intestinal artery and the sub-intestinal vein, VEGF-independent processes. In both groups, the artery and vein effectively delineated the dorsal and ventral margins of the intestine (Figure 4.6B,C). In contrast, removal of the microbiome had significant effects on development of connecting vessels, a VEGF-dependent event. Consistent with this, I observed a near 50% reduction of intestinal *kdrl:mCherry* signal in GF larvae compared to CV counterparts (Figure 4.6D). Thus, I conclude that microbial factors are essential for proper development of intestinal vasculature in larval zebrafish.

A

Vasc. Endothelial Cells		Vasc. Smooth Muscle	
Gene	log2(FC)	Gene	log2(FC)
pank2	-0.55	cxcl12a	-1.16
ptprb	-0.48	id1	-0.55
ldb2a	-0.45	grem2b	-0.44
celsr1a	-0.44	angptl4	-0.42
csnk1a1	-0.42	igf2b	-0.42
stab1	-0.42	sap30l	-0.35
cemip2	-0.40	nr2f2	-0.34
tnfrsf19	-0.39	hopx	-0.33
nrarpb	-0.38	serpine1	-0.32
hspa12b	-0.38	vcam1b	-0.32
smad5	-0.38	pbx1a	-0.31
adgra2	-0.35	pbx4	-0.29
ecscr	-0.35	ftr82	-0.28
msna	-0.33	gspt1l	-0.27
cdh5	-0.33	ntn1a	-0.26
pkma	-0.30	ramp2	-0.26
rap1b	-0.27	myh11a	-0.26
smad6a	-0.27	cd63	-0.25
rap1aa	-0.26		
acvrl1	-0.25		

Figure 4.6 Microbes promote pro-angiogenic factor expression and intestinal vasculogenesis. A) Downregulated expression of pro-angiogenic factors in GF relative to CV vascular endothelial and vascular smooth muscle populations (p<0.05). Significance was determined with a non-parametric Wilcoxon rank sum test. B-C) Expression of kdrl:mCherry in zebrafish 6 dpf raised under CV (B) or GF (C) conditions. Corresponding brightfield images were used to identify the

intestine, outlined in blue. Bottom panels in B and C show enlarged region of middle to posterior intestine within yellow boxes of respective upper panels. PCV- posterior cardinal vein; SIA- supra-intestinal artery; SIV- sub-intestinal vein. Scale bars = 100 μm. D) Box and whisker plot showing the area of intestinal kdrl:mCherry signal relative to total intestinal area. n=14 and n=13 for CV and GF fish respectively. Outlier is indicated with red dot. Significance was determined via Student's *t* test.

4.3 *Vibrio cholerae* infection drives inflammatory and protective responses from adult IECs

Alongside the analysis of conventional adult intestines, I analyzed IEC responses to overnight immersion with the damaging enteric pathogen *Vibrio cholerae*. Environmental *Vc* exposure resulted in stable colonization of all intestinal regions (Figure 4.7A-C), where challenged fish experienced disrupted epithelial integrity, shedding of intestinal cells into the lumen, breached epithelial barriers, and internalization of microbial cells with *Vc*-like morphology (Figure 4.7D-H). Thus, in our hands, *Vc* infected zebrafish exhibit equivalent disease outcomes to mammalian models and humans (Mitchell et al., 2017; Mitchell and Withey, 2018; Nag et al., 2018; Runft et al., 2014). Given comparable *Vc*-mediated disease states across vertebrates, I believe zebrafish will be a valuable model to decipher previously unknown molecular responses to *Vc* infection at the intestinal mucosa. In this way, we may establish relevant disease markers and identify targets for therapeutic intervention.

Intestinal cells from *Vc* infected fish possessed comparable gene expression profiles to conventional adult controls (Figure 4.7I, Tables 3.2 and 4.4), allowing differentially gene expression analysis between IECs of challenged and unchallenged fish. The global IEC immune response was characterized by increased expression of proinflammatory genes like *grn1*, thought to be a pro-survival gene in response to colonization by other *Vibrio* pathogens (Wu et al., 2018), as well as suppression of interferon-stimulated genes (ISGs) like *isg15*, *ifit15*, *rsad2* (Figure 4.7J). While ISGs were downregulated across mature IECs in *Vc* infected fish (Figure 4.7K), expression of ISGs were enriched in immune-dedicated ECs of the uninfected fish (Figure 3.4I), where this cell population largely disappeared upon *Vc* infection (Figure 4.8). These data suggest that

reduced IFN signaling is a hallmark of *Vc* disease, where therapeutic IFN stimulation may provide an avenue for reducing disease severity (discussed further in Chapter 6).

Cell type-specific analysis further revealed that *Vc* moderately upregulated genes with putative roles in zebrafish antigen-presentation (Figure 4.7M), while suppressing expression of genes involved in leukocyte recruitment, most notably in Best4/Otop2 cells (Figure 4.7L). Specifically, Best4/Otop2 cells are high-expressors of *ccl25a* under homeostatic conditions (Broad SCP2141), where *ccl25a* is downregulated during *Vc* infection. Interestingly, the chemokine encoded by *ccl25a* is involved in zebrafish hematopoiesis and lymphocyte migration downstream of CFTR (Lin et al., 2021), where CFTR is known to increase susceptibility to severe cholera (Rodman and Zamudio, 1991). This could suggest that aberrant leukocyte recruitment and inflammation during *Vc* infection is secondary to dysregulated CFTR. In line with this, whole dataset analysis and independent analysis of Best4/Otop2 cells revealed *cftr* to be among the most downregulated of all genes following *Vc* infection (Figure 4.7J,N). This is notable both because Best4/Otop2 cells are localized high-expressors of *cftr* (Figure 3.4), and because cholera toxin indirectly activates CFTR, leading to epithelial chloride expulsion and massive water loss that culminates in severe diarrhea (Thiagarajah et al., 2015). Taken together, these findings indicate that in response to substantial chloride imbalance, mediated by CFTR activation during *Vc* infection, Best4/Otop2 cells specifically downregulate *cftr* to decrease membrane permeability and re-establish ion homeostasis. This may secondarily lead to decreased chemokine expression and attenuated inflammation. To support this natural response, it is possible that therapeutic CFTR inactivation in Best4/Otop2 cells could alleviate severe diarrhea and mild inflammation associated with *Vc* infection. Consistent with this notion, a recent study demonstrated that administration of a CFTR small molecule inhibitor blocked acute diarrhea in a suckling mouse *Vc* model (Rivera-Chávez et al., 2022). Given that mice do not possess Best4/Otop2 cells and therefore do not exhibit localized *cftr* expression, it remains unclear if this strategy will also be effective in humans, or a zebrafish model. One study showing that ion channels are the subject of natural selection in areas where cholera is endemic (Karlsson et al., 2013), supports the notion that ion channels (specifically CFTR) may be valid therapeutic targets for cholera. However, further work will be necessary to elucidate the role of Best4/Otop2 cells

and cell-specific *cftr* expression during *Vc* infection, and to determine the efficacy of therapeutic approaches that target these cells (or ion channels) during human infection. Of note, I also observed diminished expression of genes linked with mucin production in enterocytes, including decreased chloride channel accessory (*clca1*) expression. While the role of *clca1* during *Vc* infection is unclear, it is possible that this gene may also serve as a point of therapeutic intervention for cholera.

Overall, the most prominent epithelial response to infection was a suppression of genes associated with the interferon response in mature, differentiation IECs, as well as decreased expression of ion conductors and leukocyte recruitment factors in absorptive cell subsets. Alterations to these pathways during *Vc* infection may therefore be relevant biomarkers of disease as well as candidate targets for therapeutic intervention. Future work will be necessary to translate these findings *in vivo*, and investigate related avenues for cholera treatment and prevention.
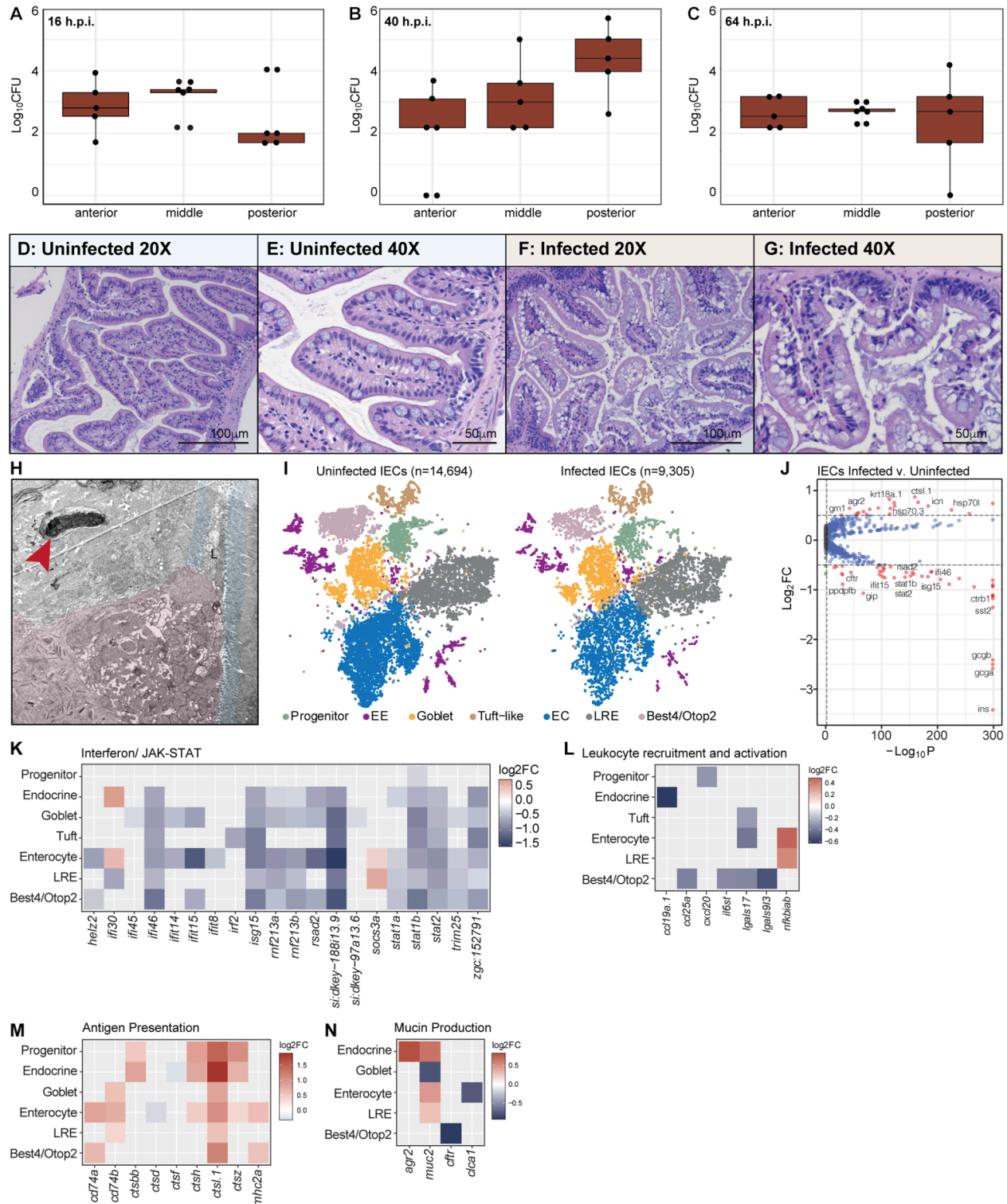
Figure 4.7 *Vibrio cholerae* activates inflammatory responses while suppressing interferon signaling in IECs. A-C) CFU Counts of gut-associated Vc in anterior, middle, and posterior

intestinal sections of infected fish, 16h (A), 40h (B) and 64h post-infection (h.p.i.). D-G) H&E stains of sagittal posterior intestinal sections from uninfected (D-E) and infected adult zebrafish (F-G). Scale bars are indicated in all panels. H) Transmission Electron Microscopy image from a sectioned, infected adult intestine. An internalized microbe with a *Vc*-like morphology is indicated with a red arrowhead. I) t-SNE projections of profiled cells from an integrated data set generated from uninfected and infected IECs color-coded by cell type. The left panel shows uninfected IECs and the right panel shows infected IECs. J) Volcano plot of differentially expressed genes in infected epithelial relative to uninfected controls. Y-axis shows the relative expression changes on a log2 scale, and x-axis shows significance values as a -log10 value. K-N) Heatmaps showing differentially expressed genes related to interferon signaling (K), leukocyte recruitment (L), antigen presentation (M), and mucin production (N) in infected cells relative to uninfected counterparts.

Table 4.4 *Vc* infected adult intestinal scRNA-seq cell identifiers based on unbiased clustering.

Cell Type	Captured Cells	Top Gene Expression Markers
Progenitor	455	her6, si:ch211-222l21.1, si:ch211-213d14.2, dld, gig2h, her15.1
TA	190	aspm, cdk1, top2a, aurkb, zgc:110540
Endocrine 1	282	etv1, neurod1, cabp2a, rims2a, isl1
Endocrine 2	267	neurod1, plcvd3, scg3, pdyn, egr4
Endocrine 3	20	sst1.1, ins, ppdpfb, dkk3b, g6pcb
Endocrine 4	173	adcyap1a, trpa1b, mfge8a, grhprb, scg3
Endocrine 5	16	g6pcb, ndufa4l2a, c9, gpr158a, mnx1
Goblet	1338	agr2, si:dkey-203a12.9, CABZ01080550.1 (muc2), fabp3, cd63
Goblet-like	267	cuzd1.2, si:ch211-173a9.6.1, si:ch211-173a9.6, pdia2, si:ch211-255i20.3
Tuft-like	474	calm1b, pou2f3, anxa4, hmx3a, hes2.2, alox5a
EC1	1292	chia.3, ucp1, rbp2a, chia.1, fabp1b.1
EC2	223	apobb.1, apoa1a, apoa4b.2.1, chia.3, apoea
EC3	896	slc6a19b, chia.2, cd36, fabp2, enpp7.1
LRE 1	1412	fabp6, slc15a2, ctsl.1, tmigd1, slc10a2
LRE 2	553	ifi30, ctsl.1, ctsz, fabp6, ctsh
LRE 3	515	fabp6, si:ch211-139a5.9, cxcl8b.1, slc10a2, tmigd1
Best4/Otop2 1	719	tcnba, cfd, ca4b, fam92a1, id2a
Best4/Otop2 2	88	tcnba, ca4b, cfd, fam92a1, chia.1
Leukocyte 1	282	dusp2, pfn1, tmsb4x, wasb, ccr9a, cd74a

Leukocyte 2	99	ms4a17a.10, tmsb4x, fcer1gl, c1qa, cd74a
Leukocyte 3	94	ccl20a.3, FP236331.1, pfn1, nitr5, sla2
Leukocyte 4	208	si:ch211-152c2.3, spi2, spic, plekho2, si:dkey-56m19.5
Leukocyte 5	153	il1fma, spi1a, crfb15, ly86, il12bb
Leukocyte 6	157	igl3v5, rnaset2l, swap70a, ebf3a, hlx1
Stromal	182	rbp4, fn1b, sparc, aoc2, c4b
Pancreatic	42	si:dkey-14d8.7, c6ast4, c6ast3, pglyrp6, dnase1
Epidermal	115	cnfn, agr1, etf1a, sptssb, oclnb
Unknown 1	109	acsl4b, oclnb, ftr83, tmprss13b, sstr5
Unknown 2	43	BX855618.1, zgc:193726, cbln11, pvalb6, noxo1a
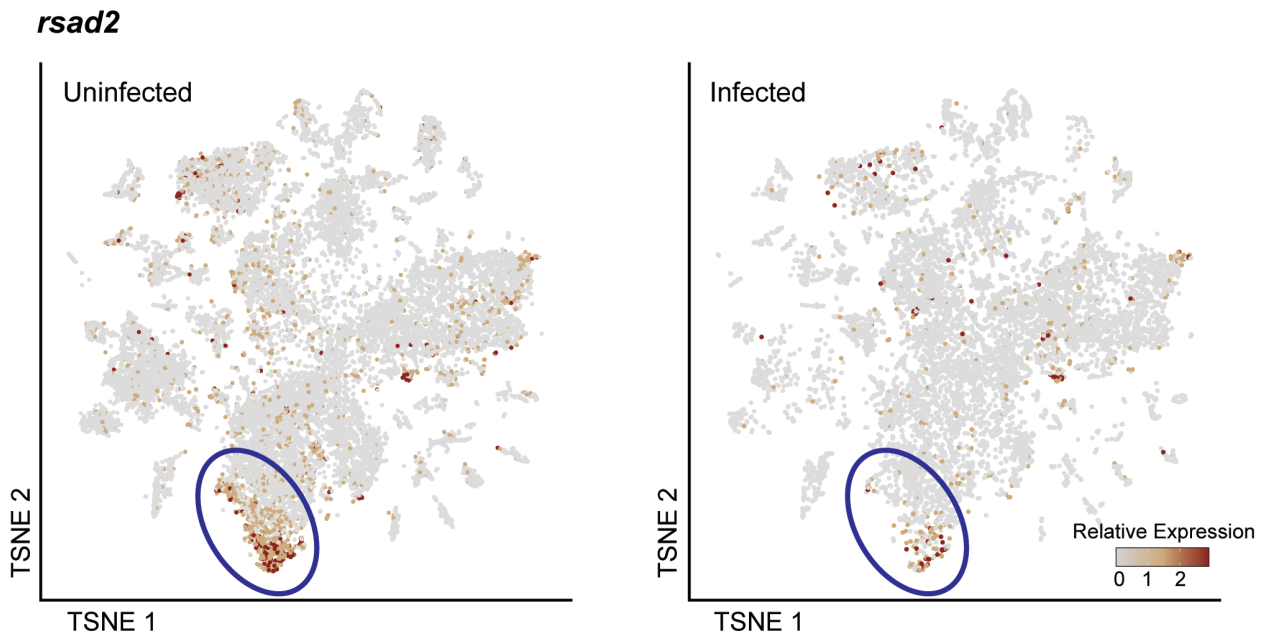
rsad2

Figure 4.8 *Vc* infected fish have fewer ISG-enriched ECs. Feature plot showing relative expression of EC subset 4 marker *rsad2* (Figure 3.4I) across datasets. Immune-dedicated/ interferon-enriched ECs (based on the uninfected dataset) are encircled in blue.

4.4 Conclusions

Gut microbial factors are critical determinants of animal development (Sekirov et al., 2010). Comparative studies with CV and GF zebrafish larvae uncovered numerous microbial effects on the host, including impacts on proliferation, cell fate specification, and metabolism (Bates et al., 2006; Hooper et al., 2001; Rawls et al., 2004; Reikvam et al., 2011). Importantly, the molecular and genetic networks that determine intestinal development are highly similar between zebrafish and mammals (Davison et al., 2017; Heppert et al., 2021; Lickwar et al., 2017). Thus, discoveries made with fish have the potential to reveal foundational aspects of host-microbe relationships.

To determine host responses to microbial colonization at cellular resolution, I first prepared single-cell atlases of intestines from larval zebrafish raised under conventional or germ-free conditions. Comparisons between datasets allowed me to delineate impacts of the microbiome on growth, patterning, immune, and metabolic processes in each cell type. While it is possible that some of the cell-specific changes observed result from GF derivation, my recapitulation of known microbe-responsive processes makes this unlikely to be a major confounding factor. Moreover, recent whole-larvae scRNA-seq comparison of CV and GF animals corroborated many gene expression changes reported herein (Massaquoi et al., 2023). Importantly, the resolution provided by single-cell approaches allowed us to uncover a large number of unknown microbe-driven processes in the host, and resolve each process to the level of distinct cell types. Our work shows that microbiota-dependent control of growth, developmental, metabolic and immune processes display remarkable cellular specificity. To provide one example, I will discuss effects of the microbiota on host immune activity; however, I note our data permit identification of microbial impacts on many physiological processes.

This work revealed a hitherto unknown complexity of germline-encoded immune gene expression patterns in CV fish, suggesting a refined partitioning of immune functions among intestinal epithelial cell types. Absorptive intestinal epithelial cells expressed enriched amounts of detoxifying alkaline phosphatases (Bates et al., 2006), and myeloid-activating *serum amyloid A* (Kanther et al., 2011; Murdoch et al., 2019). In contrast, progenitor and tuft-like cells expressed elevated levels of the bacterial peptidoglycan sensor *nod2* and core NF-kB pathway elements,

whereas enteroendocrine cells and leukocytes expressed larger amounts of *il22*, a cytokine that activates epithelial defenses (Dudakov et al., 2015). Phagocytes were characterized by elevated expression of pro-inflammatory cytokines such as *il1b, tnfa* and *tnfb*, whereas mesenchymal cells were prominent sources of immune-regulatory TGF-beta class cytokines. Comparisons between CV and GF fish uncovered a remarkable input from the microbiome on all these processes, with cell-specific expression of many immune effectors and mediators declining, relocating, or disappearing almost entirely in GF fish. Future work will be needed to elucidate impacts of cell-specific immune signals on intestinal homeostasis.

To test developmental consequences of microbial removal on larvae, I focused on intestinal vasculogenesis. In fish, the intestinal vasculature arises from angioblasts that migrate ventrally from the posterior cardinal vein, and establish a plexus that gradually resolves into the dorsal supra-intestinal artery, the ventral sub-intestinal vein, and a series of parallel vessels that connect artery and vein (Goi and Childs, 2016; Isogai et al., 2001; Lenard et al., 2015; Nicenboim et al., 2015). I noted diminished expression of key angiogenesis regulators in GF larvae, particularly VEGF-class receptors with established roles in formation of connecting vessels (Goi and Childs, 2016). Examination of GF fish showed that the microbiota is dispensable for positioning and spacing of the artery and vein. In contrast, removal of the microbiota had deleterious effects on connecting vessels, confirming a role for the microbiome in establishing the intestinal vasculature. These results match observations from mice, where germ-free growth also diminishes villus angiogenesis (Reinhardt et al., 2012; Stappenbeck et al., 2002), suggesting a shared requirement for microbial cues to direct intestinal angiogenesis in vertebrates. I believe the advances made in this study will allow us to trace the molecular, and cellular networks that control intestinal vasculogenesis in a developing vertebrate.

Next, I assessed IEC responses to the pathogenic bacteria Vc. Members of the *Vibrio* genus are common members of the zebrafish gut microbiota, and zebrafish are a natural host for the aquatic pathogen *Vibrio cholerae,* allowing us to determine primary host responses to *Vc* challenge at cellular resolution, and therefore identify possible disease biomarkers and therapeutic targets. In our hands, *Vc* infection caused predictable disease, including disrupted barrier integrity and increased cell shedding into the lumen. In response to *Vc* challenge, mature

IECs exhibited overlapping transcriptional responses dominated by suppressed ISG expression, increased expression of genes associated with antigen capture, and suppressed expression of leukocyte recruitment factors and ion channels. Type I IFNs are important inhibitors of proliferation that also prevent apoptosis, thereby sustaining the epithelial barrier (Katlinskaya et al., 2016; Mirpuri et al., 2010). Accordingly, diminished IFN in IECs upon *Vc* challenge may be an important mechanism for *Vc*-mediated barrier disruption that drives disease associated with *Vc* infection. Secondarily, I observed decreased expression of several ion channels (*clca1* in ECs, and *cftr* in Best4/Otop2 cells) in *Vc* infected intestines. Given that ion channels are exploited host factors during *Vc* infection, and that the natural host response to infection includes downregulation of these channels, it is possible that ion channel targeting could be an effective approach to cholera intervention. While additional work will be necessary to understand the consequences of IFN pathway and ion channel suppression during host infection, this study sheds light on the involvement of each IEC type in the mucosal response to *Vc*, and identifies key molecular factors modulated by *Vc* infection.

Chapter 5: RANK drives tuft-like cell development

This chapter contains content from the following sources:

- o **Willms RJ**, Jones LO, Hocking JC, and Foley E. (2022). A cell atlas of microbe-responsive processes in the zebrafish intestine. *Cell Reports*.

5.1 Summary

Single cell profiling of larval and adult IECs revealed a cell subset with progenitor-like properties, including expression of cell cycle regulators and Notch pathway components (Chapter 3). Intriguingly, this progenitor-like cell population highly expressed *tnfrsf11a,* encoding RANK (Chapter 3), a TNF receptor superfamily member involved in a broad spectrum of host developmental processes, including bone homeostasis (Li et al., 2022), immune cell differentiation (Li et al., 2022), mammary gland epithelial development (Fata et al., 2000) and medullary thymic epithelial development (Rossi et al., 2007) (For the sake of simplicity and continuity, I refer to the *tnfrsf11a* gene as *rank* throughout this thesis). Within the mammalian intestine, RANK-dependent activation of the NF-κB signaling pathway promotes antigen-capturing M cell development from progenitor compartments adjacent to lymphoid follicles (Debard et al., 2001; Dejardin et al., 2002; Kanaya et al., 2012; Kanaya et al., 2018; Knoop et al., 2009). Because RANK is a critical developmental regulator in numerous contexts, and RANK transcripts are abundant in a zebrafish intestinal progenitor cell subset, I surmised that RANK has an additional role in zebrafish intestinal epithelial development. RANK function in non-lymphoid intestinal tissue has not been described under homeostatic conditions in vertebrates. However, given shared regulatory infrastructure underlying intestinal development, zebrafish may be useful to uncover the role of RANK in vertebrate IEC development.

To investigate RANK function in the gut epithelium, I first performed lineage trajectory analysis of our conventional adult single cell data, where I determined that RANK is upregulated in the tuft-like IEC lineage. I validated expression of RANK in tuft-like cells using a combination of fluorescent *in situ* hybridization (FISH) and genetic reporter analyses, which further supported a role for RANK in tuft-like cell formation. Next, I generated and analyzed *rank* mutants, and determined that RANK is critical for the generation of the zebrafish tuft-like cell lineage. My results therefore identify a novel role for RANK signals in IEC development, which may have broader implications for IEC development in mammals. Given that tuft cells are crucial regulators of mammalian type 2 immune responses, identification of factors involved in tuft cell specification may provide a more comprehensive understanding of the role tuft cells play in intestinal homeostasis and disease.

5.2 *rank* is upregulated in the tuft-like cell lineage

Single cell analysis of conventional larval and adult zebrafish IECs revealed candidate progenitor cells highly expressing the developmental regulator *rank* (Figures 3.1 and 3.4). Accordingly, I surmised that RANK mediates aspects of zebrafish intestinal epithelial development. To test this assertion, I first performed lineage trajectory analysis of IECs from our conventional adult scRNA-seq dataset, where we captured a significant number of *rank+* progenitors (Figure 5.2A). Because scRNA-seq allows unbiased capture of cells likely to be at different states of the differentiation process within a cell type, where these cells are distinguished by transcriptional changes, single-cell trajectory analysis can order cells in various states within a developmental lineage over "pseudotime", based on their relative gene expression profiles. Gene expression analysis over pseudotime showed two transcriptionally divergent tuft-like cell subsets derived from Notch-positive progenitors (*her15.1+*), and revealed increased *rank* expression during development of *pou2f3+* tuft-like cells (Figure 5.1A,B). To validate lineage analysis, I first performed FISH against *pou2f3*, *rank*, and progenitor-like cell marker *her15.1* on whole-mounted larval intestines. I observed both *her15.1+ rank+* cells and *rank+ pou2f3+* cells (Figure 5.1C), consistent with *rank* expression in progenitor and tuft-like IECs. I further validated gene expression data by quantifying *pou2f3+* cells in *rank:GFP* larvae (Figure 5.1D-F), where a greater number of *pou2f3* or *rank:GFP* positive cells expressed both markers (Figure 5.1E). Notably, I observed few *pou2f3* single-positive cells (Figure 5.1E), though trajectory analysis predicted this as a significant cell fraction (Figure 5.1A). Despite this anomaly, FISH and *rank* reporter data largely aligned with trajectory analysis, supporting increased *rank* expression along the progenitor to tuft-like cell axis. Intriguingly, supplementary visualization of f-actin revealed a fraction of *pou2f3+ rank:GFP+* cells with prominent cortical actin and distinct pear-shaped morphology (Figure 5.1F), suggesting that tuft-like cells exhibit variable morphology, perhaps in alignment with earlier-described transcriptionally divergent tuft-like populations (Figures 3.4H, 5.1A). Notably, one tuft-like cell subset was marked by expression of ENSDART00000020282.6 (CU929145.1; Broad SCP2141), with homology to Myeloid-associated differentiation marker-like proteins that regulates the cortical cytoskeleton and controls inflammatory responses (Aranda et al., 2013). Furthermore, it is intriguing that intestinal rodlet cells have been described as actin-

rich, pear-shaped cells (Dalum et al., 2021; Sayyaf Dezfuli et al., 2022), which could indicate that tuft-like cells and rodlet cells are an equivalent cell type. Visualization of adult anterior intestinal tissue sections aligned with larval analysis, revealing cells of variable morphology co-expressing *pou2f3* and *rank* (Figure 5.1G,H). While my FISH protocol precluded actin visualization in adult tissue sections (and therefore f-actin and *pou2f3* co-labeling), f-actin+ *rank:GFP+* cells were also evident in adults (see Figure 5.4). Taken together, these data indicate that tuft-like cells exhibit variable morphologies, perhaps representing transcriptionally distinct subsets, and further establish *rank* as a marker of the tuft-like cell lineage across development.
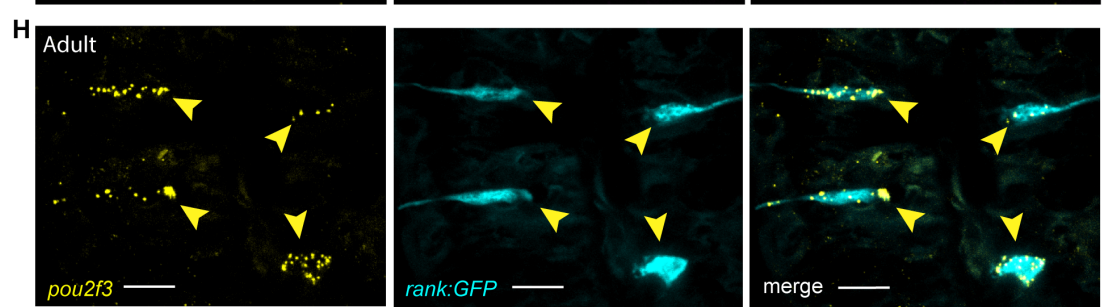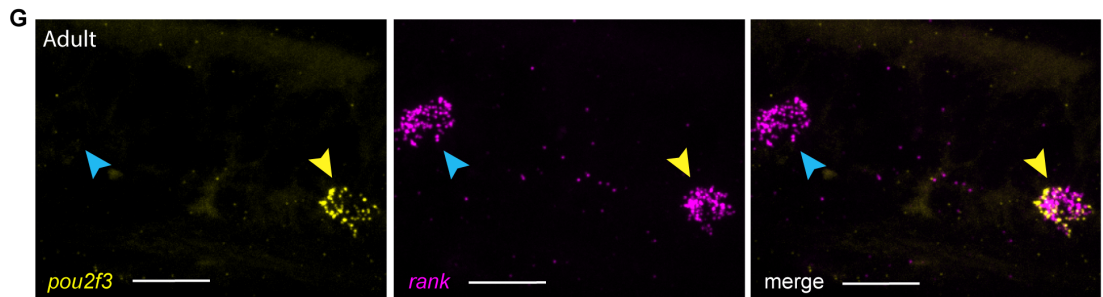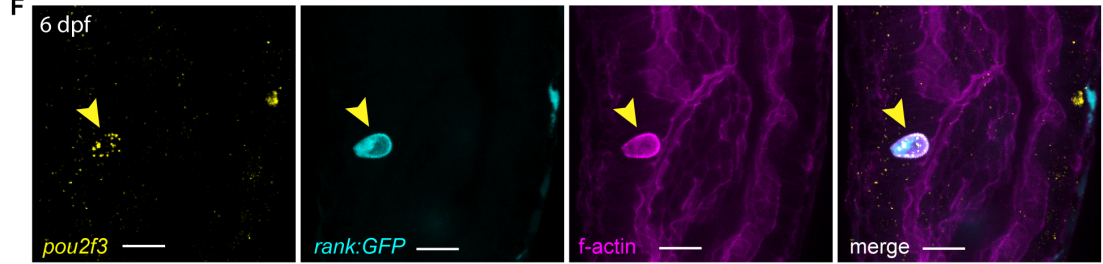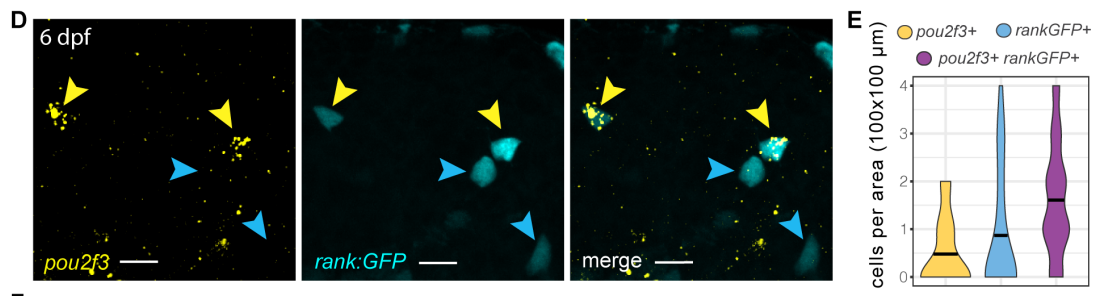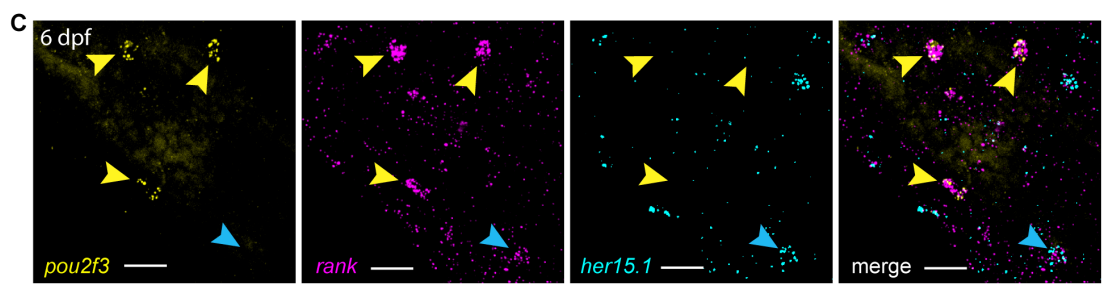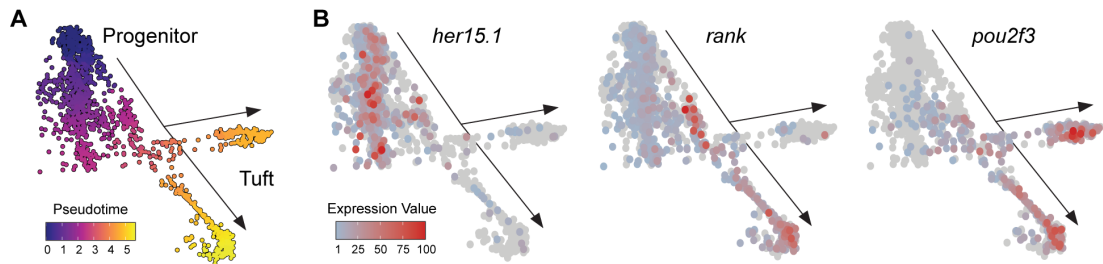
Figure 5.1 *rank* positive cells have variable morphology and express *pou2f3*. A) Monocle lineage trajectory analysis of adult progenitor and tuft-like cells from conventional adult fish (Chapter 3) over pseudotime. B) Relative expression of Notch effector *her15.1*, *rank*, and *pou2f3* in the progenitor to tuft-like cell lineage. C) Visualization of *her15.1*, *rank*, and *pou2f3* mRNA in whole-mounted 6 dpf larval intestines via FISH. Yellow arrowheads point to *pou2f3+ rank+* cells. The blue arrowhead points to a *rank+ her15.1+* cell. Scale bar = 15 µm. D-F) FISH of *pou2f3* in whole-mounted 6 dpf larval intestines from *rank:GFP* zebrafish. (D) Yellow arrowheads point to *pou2f3+ rank:GFP+* cells. Blue arrowheads point to *pou2f3- rank:GFP+* cells. Scale bar = 20 µm. (E) Quantification of *pou2f3+* and *rank:GFP+* single positive and double positive cells within a 100x100 µm area in the anterior-middle intestinal region (n=23 guts). F) A *pou2f3+ rank:GFP+* cell. Scale bar = 15 µm. G) FISH of *pou2f3* and *rank* on a sagittal section of the anterior adult intestine. Yellow arrowhead points to *pou2f3+ rank:GFP+* cell; blue arrowhead points to a *pou2f3- rank:GFP+* cell. Scale bar = 15 µm. H) FISH of *pou2f3* on a sagittal section of a *rank:GFP* adult intestine showing *pou2f3+ rank:GFP+* cells of variable morphology. Yellow arrowheads point to *pou2f3+ rank:GFP+* cells. Scale bar = 15 µm.

5.3 RANK-deficient zebrafish exhibit defective NF-κB signaling and bone development

RANK regulates a broad spectrum of developmental processes, including bone homeostasis (Li et al., 2022), immune cell differentiation (Li et al., 2022), mammary gland epithelial development (Fata et al., 2000), medullary thymic epithelial development (Rossi et al., 2007), and specification of antigen transporting M cells in the intestinal FAE through activation of its effector pathway NF-κB (Knoop et al., 2009; Nakashima et al., 2012). To test RANK function in the gut, I performed a preliminary CRISPR experiment by directly analyzing F0 zebrafish injected with synthetic duplex guide ribonucleoprotein (dgRNP) complexes (Hoshijima et al., 2019; Jacobi et al., 2017) targeting *rank* at the single-cell stage to generate RANK-deficient zebrafish (crispants). With this method, biallelic indel mutations of specified genomic sequences can be achieved at extremely high efficiency (often >90%), where mutagenized F0 crispants are often comparable to true null mutants (Hoshijima et al., 2019). Here, I generated and analyzed *rank* crispant NF-κB reporter fish, where NF-κB:GFP labels an unknown IEC subset (Kanther et al.,

2011). F0 *rank* crispant embryos injected at the single-cell stage exhibited 95% biallelic mutagenesis and 5% monoallelic mutagenesis of the *rank* gene (Table 5.1), indicating that most F0 fish likely possess indel mutations, and that *rank* crispants probably report major phenotypes associated with loss of RANK function. Collectively, *rank* crispants possessed a near 4-fold reduction in cells with active NF-κB (Figure 5.2), supporting a shared role for RANK in NF-κB pathway activation across vertebrates and demonstrating that RANK is a prominent driver of intestinal NF-κB signals in zebrafish. Next, I used the same CRISPR-Cas9 mediated mutagenesis approach to generate stable *rank* mutants by outcrossing dgRNP injected F0 fish, and in-crossing F1 heterozygous progeny from a single F0 parent. In this way, I achieved a stable 5 base pair deletion leading to a frameshift and premature stop codon in the third exon of *rank* (Figure 5.3A) (hereafter referred to as *rank* mutants). The mutated *rank* gene is predicted to produce a truncated protein (residues 1-58 of 574) possessing a small portion of the ligand binding domain, where most of the ligand binding domain and the whole transmembrane domain are absent, rendering the protein non-functional. While mutant development proceeded normally until the juvenile period, *rank* mutants presented with spinal curvature beginning at 12 wpf, where 100% of mutant zebrafish developed scoliosis in adulthood (Figure 5.3B). Abnormal skeletal development in *rank* mutants is consistent with RANK function in mammalian bone formation (Li et al., 2022), though the underlying cause and type of scoliosis engendered by *rank* mutations requires further assessment. Taken together, loss of intestinal NF-κB activation and skeletal defects in RANK-deficient zebrafish indicate that CRISPR-Cas9 editing of the *rank* gene resulted in loss-of-function mutations, and suggest RANK function in NF-κB pathway activation and bone development is shared across vertebrates.

Table 5.1 Cutting efficiencies of *rank* dgRNP in single embryos

	Total	Biallelic mutation	Monoallelic mutation
Embryos (n)	40	38	2
%	-	95	5
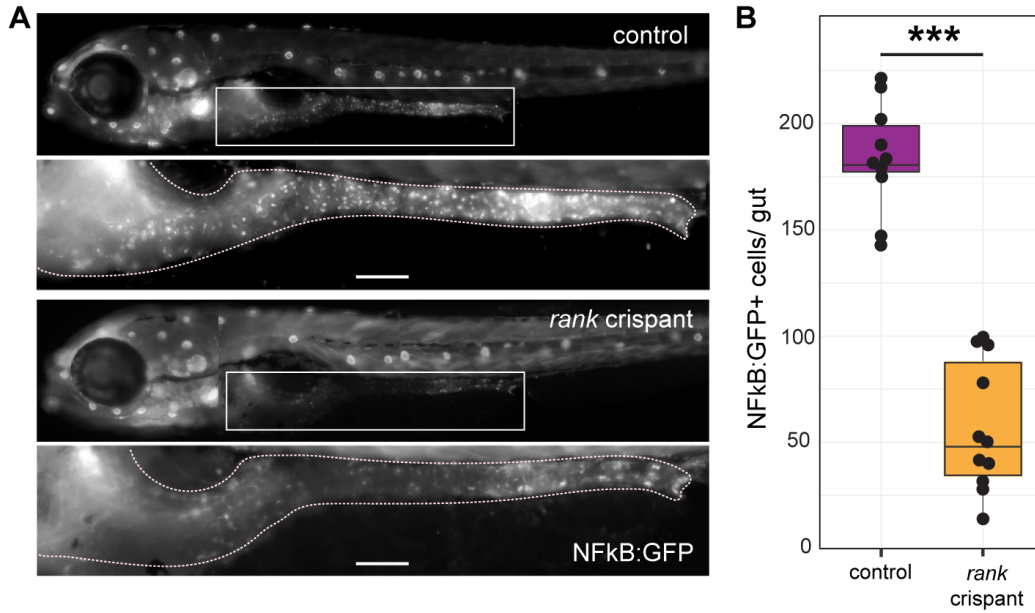
Figure 5.2 RANK drives intestinal NF-κB activity. A) 6 dpf NF-κB:GFP reporter fish (crispants) injected with Cas9 alone (control) or *rank* sgRNA and Cas9. Scale bars = 100 μm. B) Quantification of GFP+ cells in the whole intestines of control and RANK-depleted NF-κB:GFP zebrafish.
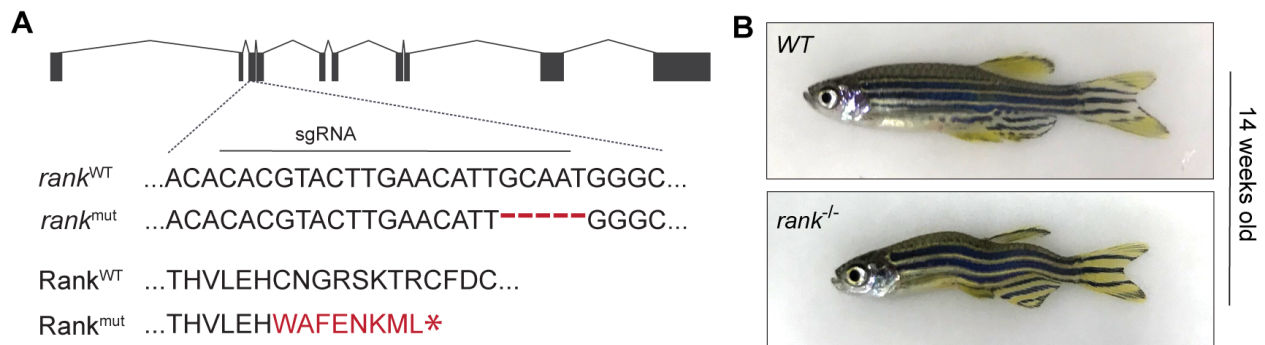
Figure 5.3 *rank* mutants develop scoliosis. A) Schematic for the mutation generated in the zebrafish *rank* gene by CRISPR-Cas9. A 5 bp deletion resulting in a frame shift was confirmed by sanger sequencing, predicted to cause a premature stop codon in the third exon. B) Image of age-matched homozygous *rank* wild-type and mutant siblings (*rank:GFP* background) at 14 wpf.

5.4 *rank* mutants exhibit IEC differentiation defects

Expression of *rank* in the tuft-like lineage implicated RANK in tuft-like cell development. To test this, I first analyzed *rank* mutant larvae for expression of tuft-like cell markers, including *pou2f3*. Quantification of *pou2f3*-expressing cells via FISH revealed a substantial decrease in *pou2f3*+ cells in *rank* mutants (Figure 5.4A), suggesting that RANK acts upstream of *pou2f3* expression. Since *rank* mutants also expressed *rank:GFP*, which reports tuft-like cell localization, I quantified intestinal *rank:GFP*+ cells in larval intestines. Wild-type age-matched siblings possessed >20 GFP+ cells per intestine on average, while *rank* mutant larvae averaged fewer than 5 GFP+ cells (Figure 5.4B). This result reveals that *rank* signals may be required for tuft-like cell production, though the exact mechanism requires clarification. Moreover, given that loss of RANK activity could be expected to increase *rank* gene activation as a compensatory mechanism, loss of *rank:GFP* may signify that RANK regulates survival of *rank*-expressing cells. Next, I assessed cell proliferation levels in 6 dpf larvae via an 8-hour EdU pulse, since loss of tuft-like cells could reflect deficiencies in intestinal proliferation (Figure 5.4C). However, proliferation levels were only slightly decreased in *rank* mutant intestines (Figure 5.4C), which might indicate that loss of *pou2f3*+ and *rank:GFP*+ IECs in *rank* mutants is caused by aberrant cell differentiation, rather than intestinal growth defects, though additional follow-up is required.

Next, I sought to corroborate larval tuft-cell deficiency by assessing morphology and gene expression dynamics in adult *rank* mutants. Consistent with larval analysis, I observed decreased numbers of cells expressing *pou2f3* and *rank* in mutant adults (Figure 5.5D,E). Structurally, mutant intestines appeared comparable to WT age-matched sibling controls (Figure 5.4F), with a slight decrease in fold length (Figure 5.4G) consistent with reduced proliferation in mutant guts (Figure 5.4C). Alcian blue staining revealed fewer mucous-producing cells per fold length in *rank* mutants relative to controls (Figure 5.4F,H), suggesting that *rank* mutants generate fewer goblet cells. Analysis of the *rank:GFP* reporter in WT fish revealed GFP expression in rounded cells at the fold base (putative progenitors), cells with apparent mucous compartments (putative goblet cells), as well as cells with processes extending to the lumen and cells enriched for cortical actin (tuft-like cell subsets) (Figure 5.4I). Subsequent quantification of *rank:GFP* and f-actin positive cells in WT versus *rank* depleted intestines, normalized to fold length, showed 100% loss of f-actin-enriched

IECs (Figure 5.4J), and near-complete ablation of *rank:GFP* expressing cells in *rank* depleted intestines (Figure 5.4K). Taken together, these results align with larval data and suggest that RANK is necessary for tuft-like cell generation across development. Since *rank* and *pou2f3* mRNA, as well as *rank:GFP* signals are diminished in *rank* mutants, it is possible that RANK mediates development or survival of *rank* and *pou2f3*-expressing cells. Moreover, given that *rank:GFP* was evident in adult goblet cells, and that *rank* mutants possessed fewer goblet cells, it is also possible that a goblet cell subset is also derived from *rank+* progenitors. However, given that alcian blue positive cells are still observed in adult mutant intestines (Figure 5.4F,H), I conclude that *rank* is not essential for goblet cell differentiation.
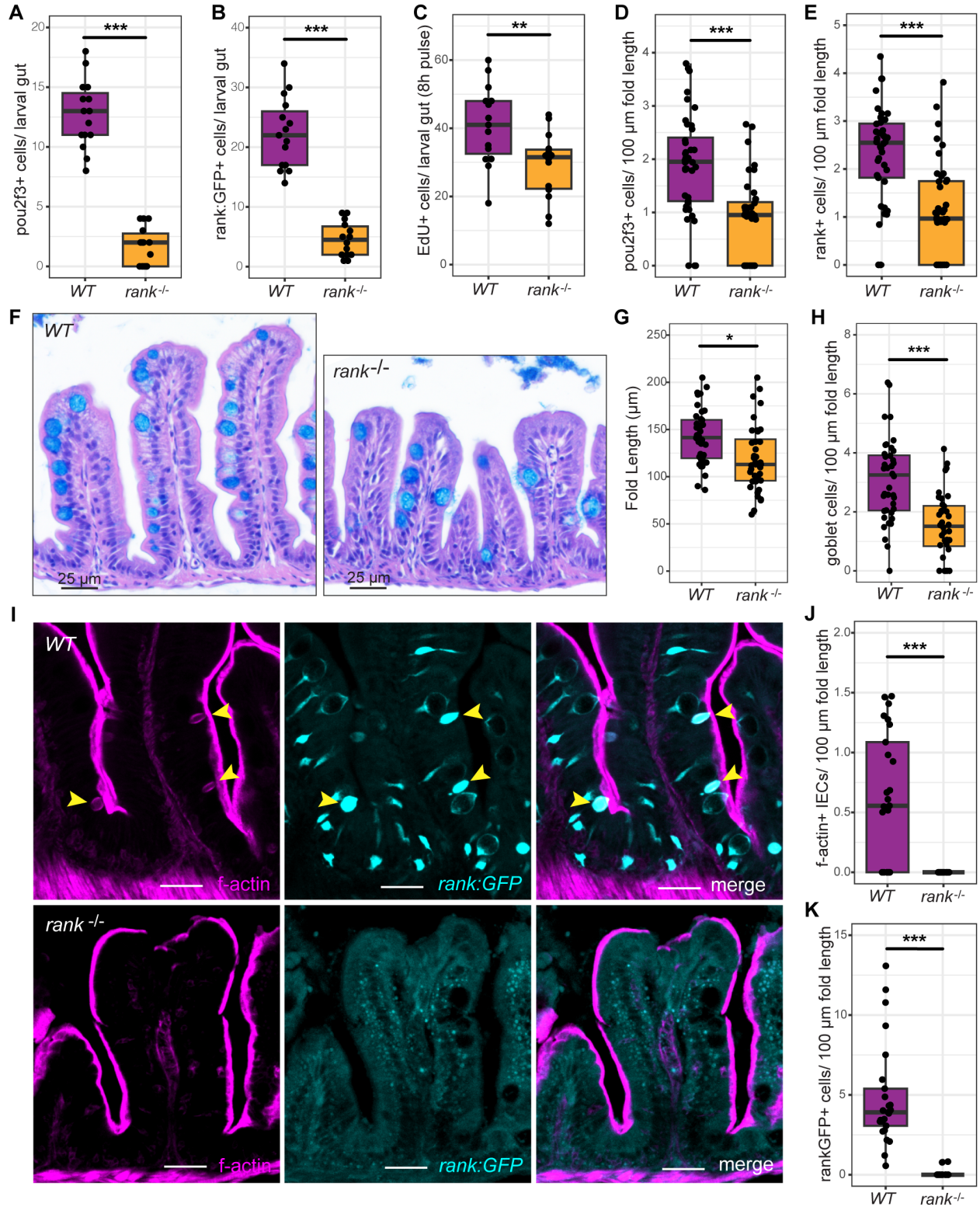
Figure 5.4 Growth and differentiation defects in *rank* mutant intestines. A) Quantification of *pou2f3*-expressing cells per 6 dpf larval gut by FISH on dissected intestines. B) Quantification of

rank:GFP+ cells per intestine in 6 dpf larvae. C) Quantification of EdU+ cells per whole intestine following 8-hour EdU pulse (no chase). D) Quantification of *pou2f3*-expressing cells by FISH, normalized to fold length. n=4 per condition, where 10 folds per anterior middle intestine were quantified. E) Quantification of *rank*-expressing cells by FISH, normalized to fold length. n=4 per condition, where 10 folds per anterior middle intestine were quantified. F) Representative images of intestinal sections stained with hematoxylin, eosin, and alcian blue. G) Quantification of fold length in WT and *rank* mutant adult intestines, based on H&E + alcian blue images. n=4 per condition, where 10 folds per anterior middle intestine were quantified. H) Quantification of alcian blue positive cells (goblets) per 100 μm fold length. I) Representative confocal images of *rank:GFP* and f-actin (phalloidin Alexa Fluor 647) in WT and *rank* mutant intestinal sections. Yellow arrowheads indicate *rank:GFP* and f-actin positive cells. Scale bars = 25 μm. n=5 per condition, where 5 folds per anterior middle intestine were quantified. J) Quantification of f-actin+ IECs normalized to fold length. K) Quantification of *rank:GFP+* IECs normalized to fold length. Significance determined with Student's t-test. *=p<0.01; ** = p<0.001; *** p<0.0001.

To further evaluate tuft-like cell numbers in *rank* mutant intestines, I assessed our adult scRNA-seq dataset for additional tuft-like cell markers that might be useful for visualizing tuft-like cells. To that end, I determined that *annexin A4* (*anxa4*) is most highly expressed in the tuft-like lineage relative to other IEC types (Figure 5.5A), where Anxa4 is a member of the annexin family of calcium-dependent phospholipid binding proteins thought to be involved in endocytosis and exocytosis (Gerke and Moss, 2002). Furthermore, zebrafish Anxa4 is recognized by the monoclonal antibody and putative pan-secretory cell marker 2F11 (Crosnier et al., 2005; Zhang et al., 2014), though I determined that *anxa4* transcripts are also abundant in Best4/Otop2 cells (Figure 5.5A) likely members of the absorptive lineage. Future work will be needed to confirm that Best4/Otop2 cells express *anxa4* and to revisit past conclusions made using the 2F11 antibody, considering this possibility. Notably, a recent study identified 2F11+ cells localized to the adult intestinal fold base (Li et al., 2020), consistent with Best4/Otop2 cell localization as determined by *cftr* mRNA visualization (Figure 3.4).

Anxa4 labeling in controls revealed regular distribution of Anxa4+ cells in the adult fish intestine, where *rank:GFP* was also detected in a subset of Anxa4+ cells (Figure 5.5B). Anxa4 was often irregularly localized or localized in the apical region of tuft-like cells (eg. Figure 5.6), such that quantification of *rank:GFP* and Anxa4 co-expressing cells was challenging. Nevertheless, analysis of *rank* mutant intestines revealed reduced abundance of Anxa4+ cells relative to WT controls (Figure 5.5B,C), consistent with the loss of an *anxa4*-expressing cell subset. Taken together with gene expression, f-actin, and reporter analysis, these data suggest that Anxa4+ tuft-like cells are depleted from *rank* mutants. Moreover, the presence of some Anxa4+ IECs further implicates RANK as an essential and specific mediator of tuft-like lineage development in the zebrafish intestine. Follow-up work will be needed to confirm the presence (or absence) of alternate secretory and absorptive IEC types in *rank* mutant guts.
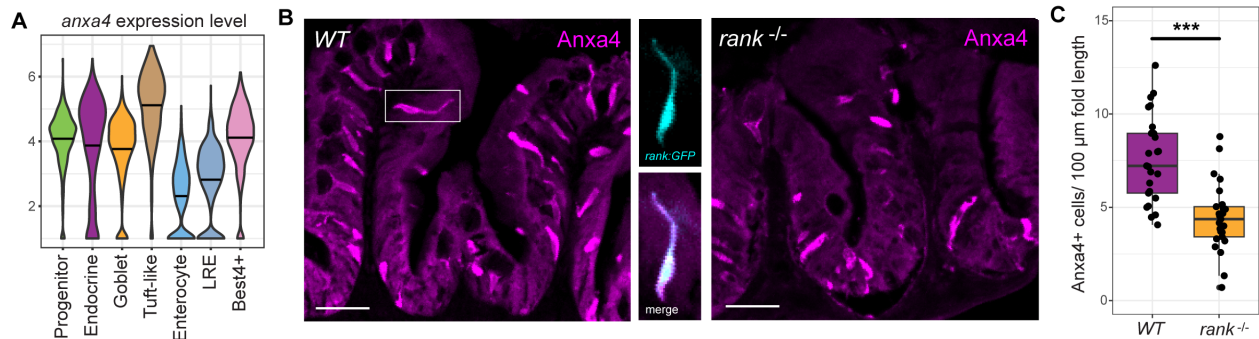
Figure 5.5 Anxa4+ tuft-like cells are diminished in *rank* mutant adult intestines. A) Adult scRNA-seq analysis of *anxa4* expression (putative secretory cell marker) in major IEC types. B) Representative confocal images of Anxa4 immunofluorescence in WT and *rank* mutant intestinal sections. Inset (rotated 90 degrees) showing overlapping *rank:GFP* and anxa4 signal in WT intestine. Scale bars = 25 μm. n=5 per condition, where 5 folds per anterior middle intestine were quantified. C) Quantification of anxa4+ cells normalized to fold length. Significance determined with Student's t-test. *** $p < 0.0001$.

5.5 Morphological analysis of tuft-like cells

Mammalian tuft cells (alternately called Brush cells) have long been characterized by an apical "tuft" of microvilli that extends into the lumen (Rhodin and Dalhman, 1956). Additional morphological features of tuft cells include vesicles and caveolae that comprise a tubulovesicular network (Sato et al., 2002), and lateral cytoplasmic projections of unknown function (Hoover et al., 2017; Luciano and Reale, 1979; Sato et al., 2002). Given these distinct cellular traits, I wondered if I might observe parallel features in zebrafish tuft-like cells. Cytosolic labeling with *rank:GFP*, alongside Anxa4, revealed that Anxa4 is apically-localized in a tuft-like cell subset (Figure 5.6A). Moreover, I observed an apical cell bottleneck with a GFP+ Anxa4+ punctum protruding into the lumen, as well as a lateral cytoplasmic projection interacting with extranuclear DNA in an adjacent cell (Figure 5.6A). While the origin of this extranuclear DNA is uncertain, it could be derived from an internalized protist, consistent with the known role of tuft cells in responding to parasitic protozoans (McGinty et al., 2020). Alternatively, it could represent a viral factory, since some viruses directly target tuft cells to exploit immunomodulatory tuft cell function (Baldridge et al., 2015; Strine and Wilen, 2022; Tomov et al., 2017; Wilen et al., 2018), and zebrafish intestinal epithelia are commonly infected with picornaviruses (Altan et al., 2019; Balla et al., 2020). It will be of great interest to determine the source of such DNA, which may provide insight into the function of zebrafish intestinal tuft-like cells.

To better resolve the structure of the distinct pear shaped tuft-like cell subset, I performed TEM, where I observed similarly shaped, electron dense cells with a thick cell cortex and an apical microvillar tuft (Figure 5.6B), consistent with the punctum observed by confocal imaging (Figure 5.6A). This cell also contained an apical tubular network and large secretory sacs with an electron dense core (Figure 5.6B), consistent with tuft-like cell secretory function. These unique secretory granules are highly similar to rodlets that define teleost rodlet cells (Abd-Elhafeez et al., 2020b; Sayyaf Dezfuli et al., 2022), further substantiating the shared identity of rodlet cells and tuft-like cells. As far as I am aware, this electron micrograph is the first to demonstrate an apical microvillar tuft on a rodlet/ tuft-like cell. Since rodlet cells are thought to exhibit distinct morphological characteristics corresponding to various developmental stages (Abd-Elhafeez et al., 2020b), it is possible that microvillar-possessing tuft-like cells represent a transitory rodlet cell state.

Alternatively, zebrafish intestinal tuft-like cells may be related but distinct from rodlet cells described in other fish species and non-intestinal tissues. Additional work is needed to reconcile the developmental and functional relationships between tuft-like cells and rodlet cells. Furthermore, the relationship between ovoid tuft-like cells and columnar tuft-like cells (described in Figure 5.1) remains unclear, requiring further structural, developmental, genetic and functional clarification. While pear-shaped tuft-like cells therefore possess some features dissimilar to mammalian tuft cells (rodlets and thick cell cortex), they are hallmarked by a similar microvillar tuft, tubular network, and lateral cytoplasmic projections. Given that tuft-like cells also appear to interact with extranuclear DNA in the epithelium, they may also play a role in sensing and responding to foreign microorganisms.
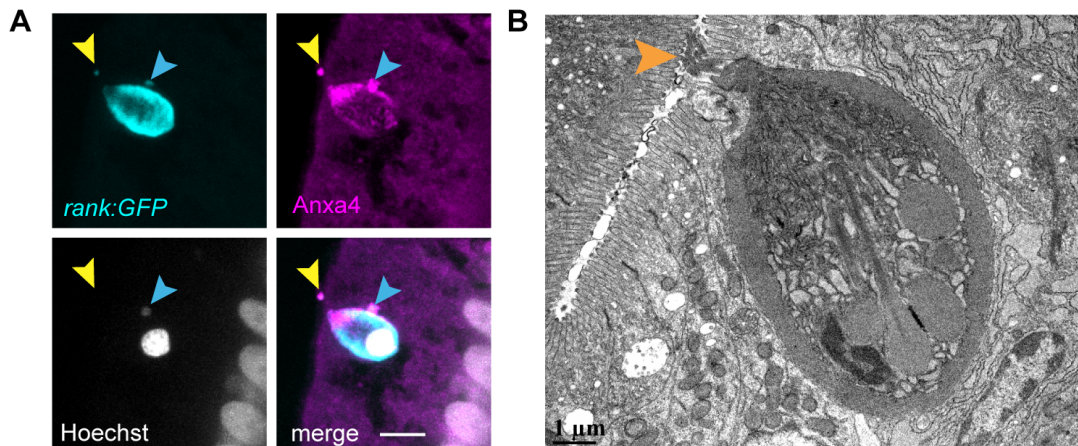
Figure 5.6. Tuft-like cells have an apical tuft and interact with extranuclear DNA. A) Confocal image of *rank:GFP* and anxa4 positive tuft-like cell. Yellow arrowhead indicates apical cell projection protruding into the lumen. Blue arrowhead points to extranuclear DNA overlapping with *rank:GFP* and anxa4 signals. Scale bar = 10 µm. B) Transmission electron microscopy image from adult intestine, showing candidate tuft-like cell with an apical tuft protruding through the brush border.

5.6 Investigating tuft-like cell-microbe interactions

Mammalian tuft cells are well-established sensors of intestinal helminths and protozoans, and are generally non-responsive to pathogenic or commensal microbes (Banerjee et al., 2020; Haber et al., 2017; Wilen et al., 2018). Thus, I reasoned that zebrafish tuft-like cell numbers may be insensitive to microbial colonization, equivalent to the mouse intestinal tuft cells. In agreement with this, scRNA-seq analysis of larval tuft-like cells under GF conditions, or adult tuft-like cells following Vc infection, revealed nominal transcriptional changes (Chapter 4), in contrast to other mature epithelial cell types. To further investigate a role for tuft-like cells in sensing and responding to microbes, I quantified *pou2f3*+ cells in larvae with or without a microbiome. I used *pou2f3* as a tuft-like marker since *rank* is expressed in at least one other cell type (progenitors). Zebrafish raised in the absence of a microbiota slightly elevated intestinal *pou2f3*+ cell numbers, where re-introduction of the parental microbiota (CV) reduced *pou2f3*+ cell numbers back to homeostatic levels (Figure 5.7A). This data indicates that microbes have a moderate restraining influence on tuft-like cell development in the fish gut. It is unclear why this might be, since mammalian tuft cell numbers are unresponsive to most commensal microbes (Banerjee et al., 2020; Lei et al., 2018). Moreover, the fish gut microbiota is an established activator of intestinal NF-κB activity (Kanther et al., 2011); given that *rank* activates intestinal NF-κB (Figure 5.2), and is required for tuft-like cell development, this result seems counterintuitive. Additional work will be necessary to tease apart the role of microbes in moderating RANK activity and tuft-like cell development.

Despite broad microbial insensitivity, mammalian tuft cells express the succinate receptor *Sucnr1*, where the introduction of succinate-producing gut bacteria can trigger tuft cell activation and hyperplasia (Banerjee et al., 2020; Lei et al., 2018). Accordingly, I wondered if larval intestines might develop tuft-like cells hyperplasia in response to succinate treatment, akin to mice (Banerjee et al., 2020; Lei et al., 2018). However, fish larvae immersed in embryo medium supplemented with succinate from 4-6 dpf showed no changes in *pou2f3*-expressing cell numbers at any dose (Figure 5.7B). This result is perhaps unsurprising given that an orthologue to mammalian *Sucnr1* has not yet been identified in zebrafish, though I note that succinate treatment alters metabolic profiles and gut microbial dynamics in adult fish (Ding et al., 2022). It

is possible that tuft-like cells are differentially sensitive to succinate across developmental stages, or that tuft-like cells are not primary sensors of succinate. Measuring tuft-like cell numbers in adult fish exposed to succinate may resolve questions around tuft-like cell sensitivity to succinate in mature animals.
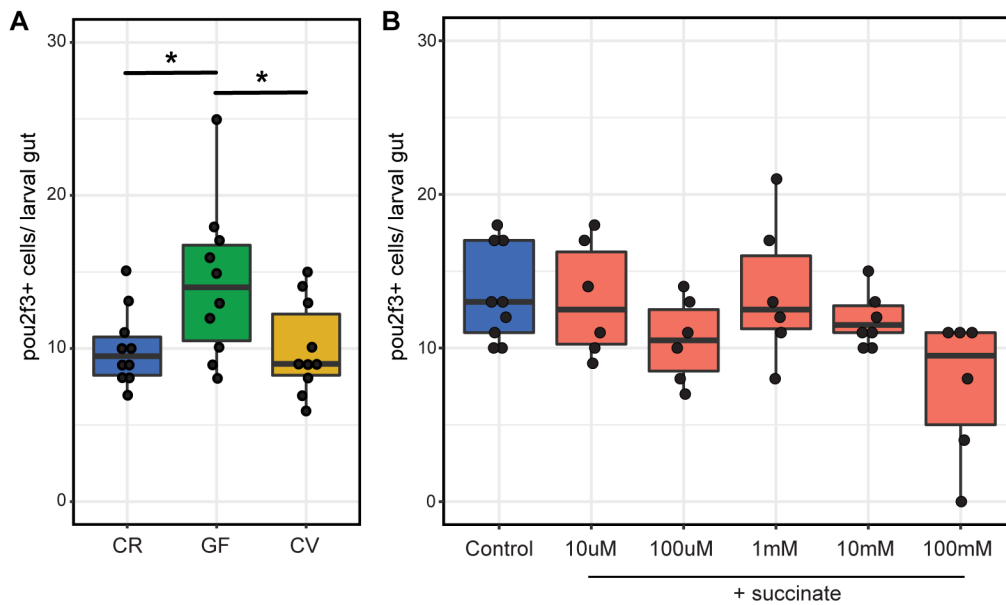
Figure 5.7 Microbial products minimally modulate tuft-like cell development. A) Quantification of *pou2f3*+ cells by FISH in whole dissected intestines from 6 dpf CR (conventionally reared), GF and CV (conventionalized; derived GF then microbiome re-introduced at 3 dpf) zebrafish. Significance determined with Student's t-test. * = p<0.01. B) Quantification of *pou2f3*+ cells by FISH in whole dissected intestines from control fish treated with succinate at the given concentrations. Fish were treated by immersion from 4 dpf through 6 dpf (48-hour treatment). No significant differences were observed across treatments.

Finally, I asked whether RANK-deficient zebrafish acquire unique gut microbial communities. Given that tuft-like cells are expected to associate with microbes and exert immune-modulatory activity, and that *rank* mutants are tuft-like cell deficient, I hypothesized that *rank* mutants experience intestinal dysbiosis. For this experiment, age-matched WT and *rank* mutant siblings were co-housed up to 12 wpf, and then separately housed for 4 weeks, so that I could assess deviations in microbiota composition. To that end, we sequenced bacterial 16S rRNA V4 variable gene region obtained from whole intestinal samples. By principal coordinates analysis (PCoA), we determined that the gut microbiota of *rank* mutants diverged from that of their WT siblings (Figure 5.8A), where the beta-diversity metric analysis of similarity (anosim) revealed significantly different microbial community structure across genotypes (Figure 5.8B). This suggests that the *rank* mutant microbiota diverges from that of WT siblings. Within genotypes, *rank* mutants trended towards lower alpha-diversity index scores relative to WT controls (Figures 5.8C-F), suggesting that RANK-depleted fish possess fewer low-abundance species (chao1), a lower diversity of species (Shannon), and reduced evenness of species distribution (Simpson and dominance metrics). Taken together, this indicates that *rank* mutants possessed a more homogenous intestinal microbiota. While hierarchical clustering of WT and *rank* mutant samples showed intra-group variation in relative bacterial abundance at the phylum level (Figure 5.8G), visualization of relative order abundance revealed differences across genotypes (Figure 5.8H). Corresponding to reduced community diversity, the *rank* mutant microbiota showed increased representation from *Aeromonodales*, common and highly abundant proteobacteria of the fish intestine (Roeselers et al., 2011; Stephens et al., 2016). Previous work showing that several *Aeromonas* species are particularly sensitive to host inflammation in the fish gut (Rolig et al., 2018) indicates that a likely reduction in host inflammatory signals in the absence of RANK and tuft-like cells makes the intestine more hospitable to members of *Aeromonodales*. I also noticed a reduction in the abundance of several core microbiota members such as *Lachnospirales* and *Bacteroidales* (Roeselers et al., 2011; Stephens et al., 2016), where members of *Bacteroidales* are known to encourage IEC production of glycans that determine the spatial arrangement of other gut microbes (Kudelka et al., 2020; Xu and Gordon, 2003). These findings suggest that RANK and tuft-like cell-dependent functions (perhaps innate immune activation) modulate the intestinal

microbiota, facilitating overgrowth of already-prominent microbial colonizers at the expense of less abundant but beneficial microbes. While the direct consequences of *rank* mutant microbiota alterations require further investigation, our data therefore indicate that *rank* mutants experience moderate intestinal dysbiosis. Because RANK WT and mutant fish were only separated for 4 weeks following co-housing, I believe a longer period of group separation would lead to even greater divergence of microbial communities across genotypes.
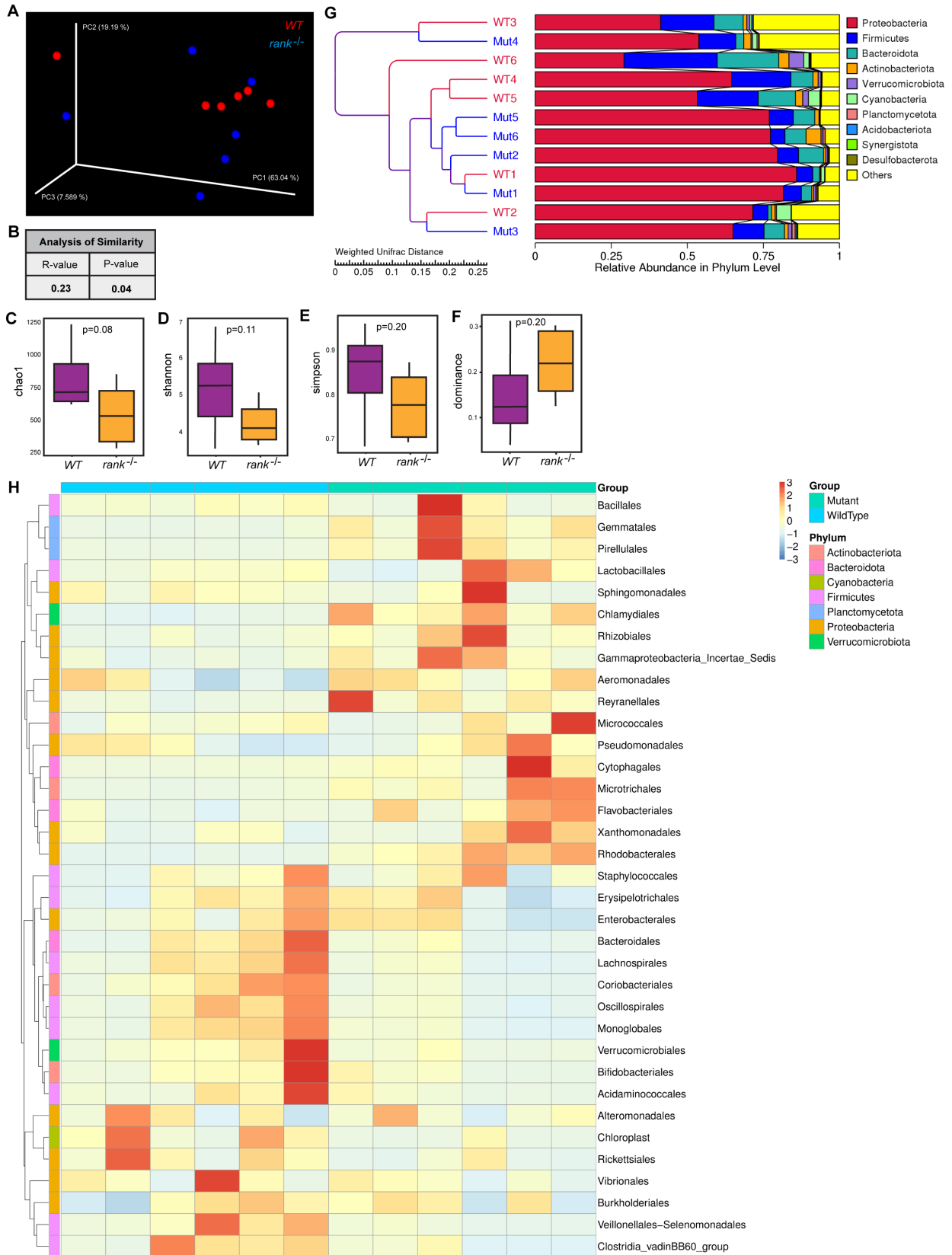
Figure 5.8 Mild gut microbiota alterations in *rank* mutants. A-F) bacterial 16S rRNA gene sequencing of *WT* and *rank* mutant intestines (n=6 per condition). A) Three-dimensional principal coordinates analysis (PCoA) plot comparing microbial communities in *rank* WT and mutant intestines. B) Community difference analysis via the Analysis of Similarity (Anosim) index indicates that microbiota variation between WT and mutants is significantly greater than inner-group variation. C-F) Alpha-diversity indices per genotype including C) Chao1 (species richness), D) Shannon (species diversity), E) Simpson (species evenness/ distribution), and F) dominance (homogeneity). G) Hierarchical clustering of WT and *rank* mutant (Mut) samples using the Unweighted Pair-group Method with Arithmetic Mean (UPGMA), based on the Weighted Unifrac difference matrix (left). The relative abundance of each phylum by sample is shown on the right. H) Heatmap of relative abundance of the top 35 orders for each sample. Respective phyla are represented by coloured bars on the left of the chart, and coloured bars on the top indicate sample group (WT or *rank* mutant).

5.7 Conclusions

In this chapter, I employed earlier-described single-cell profiles of the zebrafish intestine to identify RANK as a candidate regulator of cells with genetic similarity to mammalian microbe-sensing tuft cells. I determined that *rank* is expressed in cell populations resembling both epithelial progenitors and tuft cells, where expression increased along the differentiation axis from *her15.1*+ progenitor-like cells to tuft-like cells. I validated bioinformatic analysis through *in vivo* visualization of *rank* and *pou2f3* mRNA, and a reporter for *rank* gene activation (*rank:GFP*). Given *rank* expression in the tuft-like cell lineage, I surmised that RANK regulates tuft-like cell development. I tested this hypothesis by generating *rank* knockout zebrafish that exhibit characteristics of RANK deficient mammals, namely NF-kB inactivity and aberrant skeletal development (Li et al., 2022). I then used a combination of gene expression and protein visualization assays to determine that *rank* mutants are devoid of tuft-like cell populations, implicating RANK as a critical mediator of tuft-like cell development.

Based on *rank* reporter expression, RANK is likely expressed in progenitors of both tuft-like cells and goblet cells. In mammals, differentiation of both tuft cells and goblet cells is impacted by IL4 and IL13 (Gerbe et al., 2016; von Moltke et al., 2016), though it is yet unclear if these secretory cell subtypes share a common progenitor, and the path for tuft cell differentiation remains unknown (Gehart and Clevers, 2019). Given common IEC types and regulatory infrastructure across vertebrates, it may therefore not be surprising if zebrafish goblet and tuft-like cells share developmental origins, though additional work will be needed to flesh out regulatory pathways at play in these mature IEC types and to understand why RANK only moderately influences goblet cell development. Furthermore, it will be of great interest to determine if RANK also regulates murine and human tuft cell development. Supporting this idea, publicly accessible scRNA-seq analysis of mouse ISC types shows elevated *rank* expression across ISC subtypes (Broad Institute SCP2141) (Biton et al., 2018), where RNA sequencing of RANKL treated murine intestinal organoids revealed increased tuft cell gene signatures relative to untreated controls (Luna Velez et al., 2023). Though researchers did not follow-up on these results, their collective data suggests that RANK activation encourages tuft cell production in murine intestines and provides rationale for exploring RANK-dependent tuft cell development in mammals.

After demonstrating that RANK drives tuft-like cell development in the zebrafish intestinal epithelium, I wondered if zebrafish intestinal tuft-like cells might function similarly to their mammalian counterparts. I began by exploring the morphology of a tuft-like cell subset with distinctive pear-like shape and an actin-rich cortex. Similar to mammalian tuft cells (Hoover et al., 2017; Luciano and Reale, 1979; Sato et al., 2002), this zebrafish tuft-like cell subset possessed a microvillar tuft, a distinctive tubular network that likely facilitates secretory action, and lateral cytoplasmic protrusions. Unexpectedly, I observed the lateral cytoplasmic protrusion interacting with extranuclear DNA in the epithelium. The DNA was a spherical punctum, which could suggest protist identity, or may alternatively represent a viral factory. I did not carry out in-depth high-resolution analysis of tuft-like cells, so the frequency and significance of this cell-DNA interaction requires further follow-up. In addition to features often associated with mammalian tuft cells, zebrafish pear-shaped tuft-like cells possessed a thick cell cortex and sac-like rodlets, features

well-associated with rodlet cells across teleost species (Abd-Elhafeez et al., 2020b; Sayyaf Dezfuli et al., 2022). This data therefore indicates that rodlet cells and my newly identified tuft-like cells share an identity. If true, this study is the first to identify factors (RANK) regulating rodlet cell development (Sayyaf Dezfuli et al., 2022). Given that rodlet cells are known responders to infection, including helminth encounter (Dezfuli et al., 2007; Dezfuli et al., 2016), it may not be surprising that these cells are related to mammalian tuft cells, and share developmental regulators (likely Pou2f3). Furthermore, while I was unable to test tuft-like cell responses to helminth or protist encounter, prior investigations of fish rodlet cells would therefore suggest tuft-like cells mediate immunity to helminthic parasites. This will likely be a productive line of future enquiry.

While murine tuft cells are broadly insensitive to pathogenic or commensal microbes, succinate-producing bacteria induce tuft cell differentiation and activation (Banerjee et al., 2020; Lei et al., 2018). Accordingly, I wondered whether zebrafish tuft-like cells might be responsive to intestinal bacteria. My results (including transcriptional results in Chapter 4) suggest tuft-like cells are only mildly responsive to encounters with both commensal bacterial and the gram-negative pathogen *V. cholerae*. To follow up on this, I then assessed tuft-like cell numbers in response to succinate treatment, where I expected increased tuft-like cell numbers, as observed in succinate-treated mice (Banerjee et al., 2020; Lei et al., 2018). However, I did not observe tuft cell hyperplasia in response to succinate treatment, suggesting that larval tuft-like cells are insensitive to this metabolite. My results may be unsurprising since zebrafish do not encode a succinate receptor. At present, it is unclear if or how tuft-like cells might sense luminal microorganisms, but deeper investigation of genes expressed by tuft-like cells according to our scRNA-seq datasets may provide clues to that effect. Alternatively, intestinal dissociation, sorting, and RNA sequencing of *rank:GFP* positive cells will yield greater sequencing depth and insight into tuft-like cell function.

Lastly, I wondered whether RANK-deficient zebrafish acquire unique gut microbial communities. Since tuft-like cells are expected to provide innate immune signals that influence the luminal microenvironment, I anticipated that *rank* mutants lacking tuft-like cells (and NF-kB signals) would experience intestinal dysbiosis. In line with this prediction, I found that *rank*

mutants possessed diverging microbial communities relative to WT siblings after four weeks of separate housing, including elevated levels of dominant commensals like members of *Aeromonodales* (Roeselers et al., 2011; Stephens et al., 2016). While it will be interesting to independently house WT and *rank* mutants for a longer period before microbiota analysis, these results indicate that the absence of functional RANK and tuft-like cells leads to shifts in the gut microbial community. Future investigation will be necessary to investigate the direct cause of an altered microbiota, and the consequences thereof.

In summary, I identified RANK as a novel regulator of intestinal tuft-like cell development in zebrafish. This work both sheds light on previously unknown RANK function in fish, and identifies a previously undescribed signaling pathway regulating IEC formation in the fish intestine. Additionally, since tuft-like cells exhibit transcriptional overlap to mammalian tuft cells (developmental regulators, leukotriene biosynthesis, etc.), and since other IEC developmental regulators are shared across vertebrates, it is tempting to speculate that RANK is also required for mammalian tuft cell development. This could have important ramifications given current unknowns around tuft cell development in mammals, and may provide a more comprehensive understanding of the role tuft cells play in intestinal homeostasis and disease.

Chapter 6: Discussion

6.1 Cellular characterization of the zebrafish intestinal epithelium

The zebrafish intestine exhibits broad developmental, structural, and functional similarity to the mammalian intestine (Bates et al., 2006; Cheesman et al., 2011; Crosnier et al., 2005; Davison et al., 2017; Ng et al., 2005; Pack et al., 1996; Rawls et al., 2004; Wallace and Pack, 2003; Wallace et al., 2005; Wang et al., 2010b). Like mammals, secretory and absorptive cell subsets arise from a common progenitor cell population at the base of epithelial folds, and comprise the mature IEC population (Crosnier et al., 2005; Ng et al., 2005; Peron et al., 2020; Tavakoli et al., 2022; Wallace et al., 2005). While mammalian IECs have been extensively characterized, we have an incomplete picture of fish IEC composition and arrangement in the gut. For example, the extent of cell heterogeneity among absorptive and secretory cell types is unclear, and we have few genetic markers for future investigation of these cell types. To address these knowledge gaps, I employed scRNA-seq to profile individual cells from larval and adult zebrafish intestines. In this way, I uncovered detailed transcriptional profiles for known cell types, including molecular resolution of variable transcriptional states within a cell type, as well as previously unknown cell types. While my work focused on IECs, I also identified other cells within the zebrafish intestine, or in close association with the gut, including leukocytes, stromal cells, pancreatic cells, hepatocytes, and epidermal cells. I believe these cellular descriptions will drive future gene-level investigations of digestive tract development and function within a relevant vertebrate model.

The largest cell populations in both larval and adult datasets were absorptive IECs that included canonical ECs expressing genes required for nutrient acquisition and metabolism, LREs that mediate protein degradation (Park et al., 2019), and newly discovered Best4/Otop2 cells of unknown function (Busslinger et al., 2021; Parikh et al., 2019; Smillie et al., 2019). Enterocytes are the major drivers of nutrient acquisition and bulwarks protecting the host from microbial intruders. My analysis revealed transcriptionally divergent EC subsets, conserved across development, specialized for these respective tasks. Based on gene expression profiling, most ECs are absorptive generalists, expressing genes that enable carbohydrate, chitin, lipid, and small molecule metabolism. Separately, I identified an EC subset specialized for protein and small molecule metabolism, like LREs. Among cells upregulating EC markers (eg. *fabp2, rbp2a, cd36*), I was most surprised to uncover an enterocyte population that highly expressed interferon-

stimulated genes (eg. *ifit14*, *isg15* and *rsad2*) (Levraud et al., 2019), suggesting that zebrafish intestines possess a dedicated enterocyte population with enhanced anti-viral activity. Future work is needed to ascertain the function of these cells and determine whether ISG-expressing ECs are developmentally specified or arise from a pool of mature ECs. I speculate further on this cell population in section 6.3.

I also identified previously undescribed Best4/Otop2 cells in the zebrafish intestine. Best4/Otop2 cells were first described as members of the absorptive lineage (Parikh et al., 2019), however this has not been definitively demonstrated. Analysis of our adult scRNA-seq data revealed a Best4/Otop2 cell subset with greater EC character, including upregulated expression of EC markers *cd36* and *fabp2*, indicating that Best4/Otop2 cells and ECs are related, and may indeed arise from a common absorptive progenitor. This idea is further supported by enhanced expression of *notch2* and Notch effectors in Best4/Otop2 cells, where Notch activation may solidify absorptive cell fate. Despite these connections, lineage tracing experiments will be required to establish developmental relationships between Best4/Otop2 cells and other IECs. Functionally, human Best4/Otop2 cells are likely regulators of ion-dependent processes, such as high-volume fluid secretion, pH sensing, and electrolyte balance (Busslinger et al., 2021; Parikh et al., 2019; Smillie et al., 2019). A role related to ion transport also appears likely of zebrafish Best4/Otop2 cells, since they express orthologues for several ion channels, including chloride transporter *cftr*. Visualization of Best4/Otop2 cell marker *cftr* revealed that *cftr*-expressor cells are enriched in the basal half of the intestinal barrier, and even within the epithelial fold base. Given the putative basal localization of Best4/Otop2 cells and elevated expression of Notch regulators (with known involvement in ISC maintenance and differentiation), it is intriguing to speculate that Best4/Otop2 cells function as members of the stem cell niche. In support of their putative role as niche cells, I note that zebrafish Best4/Otop2 cells are also marked by expression of orthologue to Wnt pathway component N-Myc downstream-regulated gene 2 (*ndrg2*), a key regulator of mouse IEC differentiation under homeostatic and cancerous conditions (Shen et al., 2018). Given the recent discovery and unconfirmed function of Best4/Otop2 cells in humans, and the lack of a comparable cell type in mice , fish may serve as an excellent model for investigating Best4/Otop2 cell development and function, possibly in a niche-supporting capacity.

In addition to absorptive cell subsets, I uncovered various members of the secretory lineage including endocrine cells, goblet cells, and tuft-like cells. EECs are specialized sensory cells that release various hormones and neurotransmitters in response to both luminal and basolateral stimuli (Gribble and Reimann, 2016). I observed great heterogeneity among endocrine cells, specifically related to peptide hormone expression profiles. This was true in both larvae and adults, though I did not discern a pattern of cell-specific hormone distribution across development. It is possible that I captured too few endocrine cells in the larval stage to make accurate determinations of cell subtypes. It is also possible that captured larval endocrine cells are a mixed pancreatic and intestinal population since I found pancreatic tissue within the larval scRNA-seq dataset, and endocrine cells of the larval intestine and pancreas are transcriptionally alike (Lavergne et al., 2020). Within the adult fish gut, I observed some EECs akin to mammalian EEC subtypes, including cells specialized for proglucagon production, like mammalian L cells (Arora et al., 2018). Thus, our data revealed functional diversity among endocrine subtypes of the larval and adult zebrafish intestines, with some endocrine subtypes demonstrating functional preservation across vertebrates. Future investigation of peptide hormones distributions via FISH, immunolabeling, or transgenic reporter lines will be useful to unravel endocrine cell heterogeneity across intestinal regions and developmental stages.

Goblet cells were the most plentiful secretory cells in our scRNA-seq datasets, reflecting their abundance in the intestine. Goblet cells produce mucous that provides a critical physical and chemical barrier preventing environmental agents from accessing intestinal tissue. In agreement with other recent larval single-cell datasets (Farnsworth et al., 2020; Massaquoi et al., 2023; Wen et al., 2021), I did not identify the canonical intestinal mucin, *muc2*, within putative larval goblet cells. However, the major goblet cell cluster (goblet 1) was enriched for anterior gradient 2 (*agr2*), a well-established goblet cell marker and differentiation factor throughout the larval digestive tract, including the pharynx and esophagus (Chen et al., 2012; Shih et al., 2007). In contrast to larvae, goblet cells identified in adults expressed both *agr2* and *muc2*, indicating that zebrafish begin producing the dominant gel-forming mucin (Grondin et al., 2020) in juvenile or adult stages. In addition to canonical goblet cells, I identified a larval cell subtype, termed goblet 2, that did not express *agr2,* but was otherwise very similar to the goblet 1 cluster. It is possible that goblet

2 cells represent an immature stage of goblet cell development incapable of mucous production, or that these cells reside in a distinct region of the gut. While this would be consistent with prior observations of regionally distinct goblet cell subsets in larval zebrafish (Crosnier et al., 2005), it does not explain why goblet 2 cells (or similar) were not detected in adult intestines. It may be that these cells originated from epidermal tissue that could not be removed during larval intestinal dissection, since the epidermis also possesses mucous-producing cells (Oehlers et al., 2012). In addition to goblet clusters 1 and 2, my larval dataset further revealed an *agr2*-expressing cell subset, termed goblet-like, enriched for markers of foregut secretory cells (*muc5.3* and *pdx1*) (Jevtov et al., 2014; Lavergne et al., 2020), indicating that I uncovered gene expression profiles for mucous-producing cells of the pharynx or esophagus. I uncovered transcriptionally similar goblet-like cells in adult guts, though these cells did not express foregut markers *muc5.3* or *pdx1*. This could suggest that adult goblet-like cells originated from elsewhere in the gut (indeed, little foregut was present in dissected tissue), or that goblet-like cells have distinct functional requirements across developmental stages. Future investigation of mucous requirements and mucous-producing cell subtypes across intestinal regions and tissues will be necessary to build upon the transcriptional heterogeneity observed among goblet-related cells described in this work.

In addition to secretory cells known to inhabit the zebrafish intestine, I uncovered an intriguing cell cluster that resembled mammalian tuft cells. Tuft cells control the epithelial response to helminth encounter, inducing a type 2 immune response characterized by recruitment and activation of group 2 innate lymphoid cells (ILC2) (Gerbe et al., 2016; von Moltke et al., 2016). Tuft cells are additionally distinguished by expression of the taste cell-specific transcription factor *Pou2f3* (Bjerknes et al., 2012; Gerbe et al., 2011; Yamashita et al., 2017), and developmental regulation by Sprouty2 (Schumacher et al., 2021). To my knowledge, tuft cells have not previously been uncovered in any zebrafish tissue. However, my single-cell analysis of both larvae and adults uncovered cells expressing orthologues to various tuft cell markers and differentiation factors (eg. *pou2f3* and *spry2*), suggesting that zebrafish possess an intestinal tuft cell population. Moreover, one subtype of adult zebrafish tuft-like cells expressed orthologues of genes involved in leukotriene biosynthesis and release (eg. *alox5, si:dkey-61f9.1*), where

leukotrienes are required for tuft-cell dependent regulation of intestinal motility, immunity, and inflammatory responses in mammals (Oyesola et al., 2021; Triggiani et al., 2005; Wang and Dubois, 2010). Collectively, these observations suggest overlapping development and function of tuft cells across vertebrates. Future work is needed to validate the presence of tuft-like cell subtypes identified in Chapter 3, and to elucidate functional roles for tuft-like cells in zebrafish. Notably, tuft-like cell subsets distinguished by greater and lesser immune gene signatures are aligned with the two tuft cell subsets identified by single-cell profiling in mice (Haber et al., 2017).

Intriguingly, numerous studies in zebrafish and other teleost fish described an enigmatic cell population, termed the rodlet cell, that is immunologically active and particularly responsive to helminth infection (Abd-Elhafeez et al., 2020a; Reite, 2005; Sayyaf Dezfuli et al., 2018; Sayyaf Dezfuli et al., 2022). Rodlet cells have a distinctive pear-shape and fibrous capsule, and are found in epithelia throughout teleost tissues, including the gill, skin, sensory organs, heart, thymus, kidney, intestine, liver, gonads, and brain (Sayyaf Dezfuli et al., 2022). Moreover, rodlet cells show increased abundance at sites of helminth encounter, where they produce inflammatory peptides and nitric oxide to fight off helminthic parasites (Bosi et al., 2018; Iger and Abraham, 1997; Sayyaf Dezfuli et al., 2022). Despite functional similarities between rodlet and tuft cells, molecular ties between these cells were previously nonexistent. In Chapter 5 of this work, I demonstrate that cells with morphological characteristics of rodlet cells (namely an actin-rich capsule, pear-like shape, and presence of rodlets) express the orthologue of tuft cell differentiation factor *pou2f3*, suggesting that zebrafish rodlet cells and tuft-like cells are one and the same. This would further suggest shared developmental origins of rodlet cells and tuft cells, where rodlet cells may be an ancient tuft cell precursor. Further consistent with this idea, mammalian tuft cells, like rodlets, are ubiquitous throughout epithelial tissues, including the stomach, urethra, pancreas, airway, thymus, and gallbladder (DelGiorno et al., 2020; Luciano and Reale, 1979; Panneck et al., 2014; Perniss et al., 2021; RHODIN and DALHAMN, 1956; Saqui-Salces et al., 2011). Taken together, my analysis suggests that tuft-like cells are the same as rodlet cells, where these cells likely share the functional capacity of mammalian tuft cells to recognize and fight off helminths. In light of these findings, more work will be necessary to reconcile literature around rodlet cells and tuft cells, and

determine overarching similarities and differences (functional and developmental) between these cell types.

Aside from mature IECs, I uncovered cells with progenitor-like qualities in both larval and adult zebrafish intestines. Multipotent ISCs are key to epithelial growth and regeneration, producing regionally specialized mixtures of absorptive and secretory cell types through self-renewing divisions (Barker et al., 2007). While studies in the zebrafish intestine uncovered a cycling basal epithelial cell with stem cell-like properties (Crosnier et al., 2005; Li et al., 2020; Peron et al., 2020; Tavakoli et al., 2022; Wallace et al., 2005; Wang et al., 2010b), a major barrier to harnessing zebrafish as a model for intestinal biology has been the lack of genetic markers and tools to manipulate these cells. One recent study demonstrated that *prmt1*, encoding a histone methyltransferase (Hung and Li, 2004), may mark zebrafish ISCs (Tavakoli et al., 2022), while another showed that cycling IECs are Stat3-responsive (Peron et al., 2020). These studies shed some light on the intestinal progenitor compartment in zebrafish, but do not provide a clear genetic profile for zebrafish ISCs. Here, I uncovered the profile for an IEC subset, conserved across development, expressing classical ISC markers such as Notch pathway components *dld*, *atoh1b*, *ascl1a*, and *hes-related* family members. My identification of Notch pathway components in a putative progenitor cell is not only consistent with the known role for Notch in regulating epithelial progenitors in the zebrafish gut (Crosnier et al., 2005; Flasse et al., 2013; Roach et al., 2013; Troll et al., 2018; Yang et al., 2009), but reveals specific factors that may serve as premier markers for zebrafish ISCs (eg. *her15.1*). Indeed, fluorescent *in situ* hybridization experiments revealed that *her15.1* positive cells are proliferative residents of the fold base in the adult gut, consistent with expected ISC localization. Future work using lineage tracing tools under the control of a *her15.1* promoter (though we tried and failed to isolate a promoter region) will be useful to validate this gene as a marker for multipotent ISCs. Notably, my single-cell analysis also revealed that candidate progenitors and TA cells express the proposed ISC marker *prmt1* (Tavakoli et al., 2022), though *prmt1* was not a precise marker for putative progenitors in either larvae or adults based on my analysis (Broad SCP2141). Furthermore, my observation that candidate progenitors express known Notch regulator *ascl1a* (Flasse et al., 2013; Roach et al., 2013), leads me to speculate that *ascl1a* may be functionally equivalent to mammalian Wnt target and ISC

marker *Ascl2* (Schuijers et al., 2015; van der Flier et al., 2009), though future work is needed to determine if Wnt signals target *ascl1a* in zebrafish, and to ascertain the extent of Wnt activation in progenitors throughout development.

In addition to candidate stem cells, we uncovered basally localized proliferative cells marked by cell cycle regulators such as *pcna*, *mcm5*, and *mki67*, comparable to mammalian transit amplifying cells that expand the number of maturing IECs (Barker et al., 2007; Bjerknes and Cheng, 1999; Haber et al., 2017; Winton and Ponder, 1990). While larval TA cells grouped with the other progenitors during my initial analysis, perhaps due to limited cell numbers, progenitor subtype analysis, as well as integrated analysis of larval and adult datasets, revealed a separate larval TA cell population marked by expression of numerous cell cycle regulators. These data suggest that zebrafish employ intestinal TA cells to amplify mature IEC numbers immediately in the post-embryonic period, though additional work will be needed to validate factors distinguishing TA cells and ISCs.
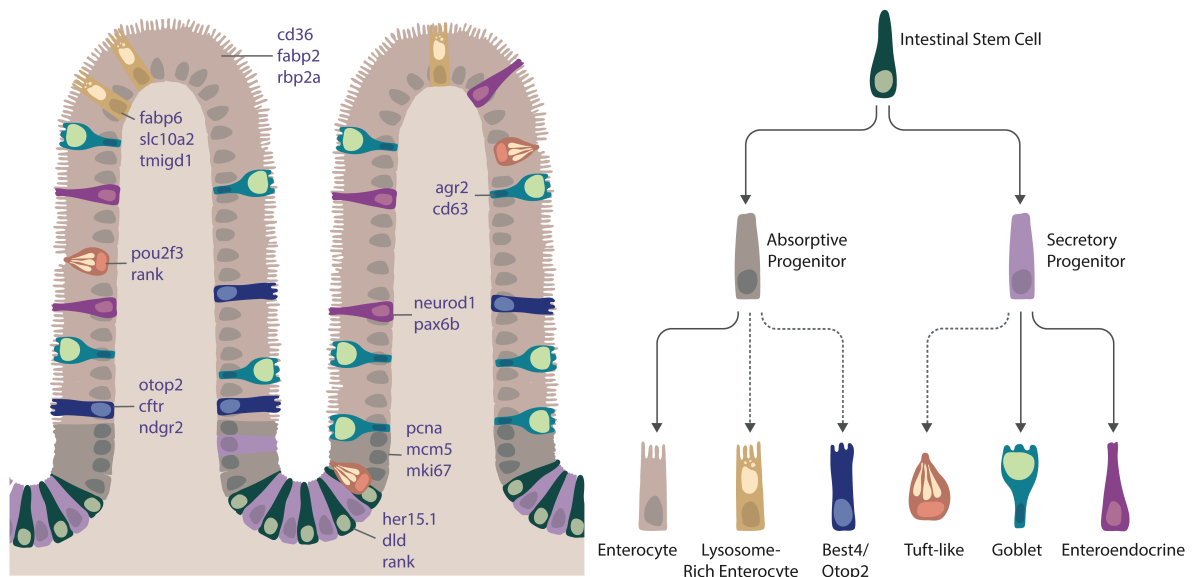
Figure 6.1 Graphic summary of IEC types, markers, and lineages in the zebrafish intestine. Based on single-cell profiling, I propose that zebrafish intestines contain five major IEC types:

enterocytes (including lysosome-rich enterocytes), Best4/Otop2 cells, tuft-like cells, goblet cells, and enteroendocrine cells. Top genetic markers for major cell types (plus LREs and progenitors), shared throughout development, are indicated on the graphic (left). Dotted lines on the right indicate tentative lineages. Note: this graphic does not account for regional cell localization, for which further investigation is required.

6.2 Single-cell profiling of non-IECs

While the focus of this work was IEC characterization, the larval and adult scRNA-seq datasets are further useful for characterization of additional cell types captured in these experiments. For example, I identified significant numbers of stromal, pancreatic, hepatic, and epidermal cells in the larval scRNA-seq experiments, and both larval and adult datasets contained a notable leukocyte fraction (~4% larval cells and ~16% adult cells). Gut-associated leukocytes are critical mediators of intestinal homeostasis and mucosal defense (Mörbe et al., 2021); however, we have limited knowledge of gut-resident immune cells across developmental stages. Accordingly, we produced a comprehensive map of transcriptional states for intestinal leukocytes. In larvae, I identified expected myeloid cell populations of neutrophils and macrophages, where the transcriptional profiles were highly aligned with previous reports (Bennett et al., 2001; Brugman, 2016; Flores et al., 2020; López Nadal et al., 2020; Tang et al., 2017). However, one surprise was the presence of cells expressing classical markers of developing T cells or ILCs (Hernández et al., 2018; Ma et al., 2013). My preferred interpretation is that this cell population represents ILCs that seed the gut by 6 dpf. ILCs are important regulators of tissue homeostasis, tissue repair, defense against parasites, and tolerance to commensal microbes (Saez et al., 2021), functions critical to all post-embryonic stages of intestinal development. Moreover, ILCs seed the mammalian intestine prior to the onset of humoral immunity, so it would not be surprising if ILCs colonize the zebrafish intestine by 6 dpf, before the onset of adaptive responses. Future work is needed to determine the origin of these cells, especially given the presence of extraintestinal tissue in my larval datasets, and to assess possible functional roles for ILCs in the larval gut.

Notably, given that I identified tuft-like cells within the intestine, I am inclined to speculate that ILCs interact with tuft-like cells to mediate the IEC response to protozoan or helminthic encounter.

Within adults, we identified five major cell types including T cells, B cells, macrophages, granulocytes, and dendritic cells, where the T cell population possessed cell subsets expressing markers for conventional CD4+ and CD8+ cells, as well as markers for group 2 and group 3 ILCs (*nitr* genes, *gata3*) (Hernández et al., 2018). Notably, we profiled previously uncharacterized populations of intestinal dendritic cells, B cells, and granulocytes. Little is known of adaptive immune responses in the zebrafish intestine, so these profiles may support future investigation of humoral immunity in adult fish. Combined, our data suggest that both larval and adult zebrafish coordinate intestinal defenses using a combination of myeloid and lymphoid cells, where innate immune cells comprise the major immune cell contingent in larvae, and adults shift to lymphocyte-dominated immunity.

Intestinal stromal and vascular cells are a highly heterogeneous group of cells that support intestinal function by providing growth and inflammatory cues, conducting other cells (such as leukocytes), and by generating matrices that support epithelial structure (Barnhoorn et al., 2020). While I identified a large number of stromal cells in larvae, we captured few stromal cells via adult scRNA-seq. I believe this disparity likely reflects an increasing ratio of epithelial and blood cells to stromal cells over intestinal development, though differential cell-cell adhesion or extracellular matrix properties may make stromal cells more difficult to isolate in adulthood. Despite lower numbers in adults, integrated analysis of larval and adult datasets revealed strongly overlapping stromal cell gene signatures (Chapter 3), suggesting that stromal cells are developmentally and functionally conserved as zebrafish mature. Though I did not conduct further analysis of stromal cell types, I believe the profiles acquired in this work will be useful for determining sources of immune regulators and growth factors, such as Wnt ligands likely to regulate progenitor cell maintenance and growth, and for generating transgenic reporters under the control of cell type-specific promoters. To that end, I have made our datasets publicly accessible for user-friendly visualization on the Broad Single Cell Portal, a web-based resource (see Chapter 2: Materials and Methods).

Collectively, single cell profiling of zebrafish intestines revealed extensive similarities between zebrafish and mammals at cellular and genetic levels. While the full complement of genetic regulators and cell types in the fish epithelium are still under investigation, I believe this study uncovered valuable markers for IEC types and subtypes of the fish gut (Figure 6.1), as well as stromal and leukocyte subsets, and revealed even greater overlap between human and zebrafish intestines than previously thought. Accordingly, I believe the zebrafish intestinal model has immense potential to unlock additional regulators of human intestinal development and function, as well as factors that drive intestinal disease. Among my most notable findings, zebrafish intestines possess Best4/Otop2 cells with extensive genetic similarity to human BEST4/OTOP2 cells. The development and function of BEST4/OTOP2 cells remain speculative, where the zebrafish model will provide an exceptional opportunity to investigate genetic regulators of these cells *in vivo*.

6.3 A cell atlas of microbe-responsive processes in the larval zebrafish intestine

In recent decades, gnotobiotic animal models, combined with functional genomics, have provided tremendous insight into the extensive array of host functions modulated by the microbiota. While various molecular approaches have proven effective in this regard, identifying host signals, signaling pathways, and cell-specific mediators controlling these processes has been an immense challenge. In this work, I reasoned that novel sequencing technologies enabling cell-level transcriptomic analysis would aid in the discovery of molecular regulators of host-microbe interactions in the gut, the epicenter of the animal microbiota. Moreover, in light of the structural, functional, and genetic similarities between zebrafish and mammals, including cell-level similarities uncovered in this study, I reasoned that zebrafish are an excellent model for uncovering common vertebrate responses to the gut microbiota.

While I was able to identify microbe-dependent gene expression changes in every cell type, confirm previously identified microbe-dependent gene expression changes, and identify cellular mediators (some already discussed in Chapter 4), I was most captivated by two minimally discussed phenomena in zebrafish IECs. First, I was struck by overlapping immune responses to the microbiota mediated by dominant intestinal LRE and goblet cell populations, including increased IFN signals, immune cell recruitment, and ROS regulation. Intriguingly, goblet cells and

LREs both inhabit the distal mid-intestinal region, analogous to the mammalian ileum, and are limited within other intestinal regions (Crosnier et al., 2005; Ng et al., 2005; Park et al., 2019; Wallace et al., 2005). This suggests that cells of the distal mid-intestine coordinate immune responses to microbes. While vertebrate ileocytes mediate absorption of bile salts and vitamin B12 (Benoit et al., 2018; Wen et al., 2021), the mammalian ileum also houses intestinal lymphoid tissue that screens trillions of microbes and food antigens to detect and protect against destructive pathogens (Agace and McCoy, 2017; Buettner and Lochner, 2016). Presumably, the 6 dpf zebrafish intestine, devoid of lymphoid tissue but colonized by intestinal microbes (Bates et al., 2006), senses and tolerates bacteria by an alternate mechanism.

Some studies demonstrate that zebrafish IECs in the distal mid-intestine sample bacteria (Korbut et al., 2016; Løkka and Koppang, 2016; Løvmo et al., 2017), analogous to follicle-associated epithelial cells overlying ileal lymphoid tissue. Indeed, LREs contain a supranuclear lysosomal vacuole that captures and degrades luminal material through a combination of scavenger receptors and fluid phase endocytosis (Park et al., 2019; Wallace et al., 2005). Moreover, the present study demonstrated that LREs (in combination with goblet cells) secrete leukocyte recruitment factors in response to bacterial encounter (eg. Saa). Taken together, this suggests that LREs sample bacteria to drive protective inflammatory responses. However, further work is needed to determine if bacterial sampling by LREs or other IECs contributes to tolerance of commensal microbes or pathogen defense. Moreover, despite prior work demonstrating that zebrafish IECs detoxify bacterial LPS via alkaline phosphatase, and that LPS activates MyD88-dependent inflammatory responses (Bates et al., 2007; Galindo-Villegas et al., 2012; Koch et al., 2018; Takeda and Akira, 2005), PRRs mediating the inflammatory response have yet to be uncovered. Indeed, I did not detect significant LRE (or epithelial) PRR expression in either larvae or adults, suggesting that major bacterial sensors are lowly expressed, or that yet unknown sensors are at work in the fish gut.

Why do goblet cells also upregulate immune mediators in response to microbial colonization? Goblet cells are most often appreciated for production of the mucous layer at the epithelial surface (Johansson et al., 2008; Van der Sluis et al., 2006), however recent work in mice demonstrated that goblet cells directly participate in immune activity. Specifically, several studies

revealed that goblet cells also sample luminal antigens by fluid-phase endocytosis, delivering cargo to antigen presenting cells of the lamina propria (Gustafsson et al., 2021; Knoop et al., 2015; McDole et al., 2012). Moreover, a subset of MAMP-sensing colonic goblet cells increase mucin output in response to bacteria, a process dependent on endocytosis of TLR ligands and subsequent ROS production (Birchenough et al., 2016). These results demonstrate that subsets of mouse goblet cells are primed to detect microbes and take protective action. While we do not have evidence of goblet cell antigen sampling and transcytosis in zebrafish, it is possible that similar mechanisms for sensing microbial pattern exist within fish goblet cells. Supporting this idea, I observed reduced expression of enzymatic antioxidants *prdx1* and *gpx1b* (Mukaigasa et al., 2012; Perkins et al., 2014) in germ-free goblet cells, suggesting that bacteria encourage both ROS production and expression of protective ROS regulators in fish goblet cells, perhaps downstream of bacterial sensing. While the total result of bacterial-mediated gene expression changes is unclear, it is likely that these measures culminate in increased production of protective mucous, a familiar intestinal response to bacterial colonization in zebrafish (Bates et al., 2006). While I did not detect *muc2* expression in my dataset, CV goblet cells exhibited increased expression of genes that stimulate intestinal mucin production, such as *sstr5* (Song et al., 2020; Song et al., 2020).

Taken together, I believe that zebrafish intestinal LREs and goblet cells, probable inhabitants of the ileal-like region, mediate protective responses to bacterial colonization, akin to mammalian ileocytes. Aligning my gene expression data with prior studies, I believe that LREs uptake and process bacterial antigen, resulting in production of factors that recruit protective and bactericidal immune cells (macrophages, neutrophils). In support of this effort, goblet cells may also sense bacterial pattern (either directly or indirectly), causing increased expression of factors involved in leukocyte recruitment and mucous production. Given overlapping gene expression changes in LREs and goblet cells, it is likely that these cells employ the same PRRs to mediate bacterial sensing. Future work will be necessary to determine the sensors at work in these cells (and IECs more broadly), as well as the functional consequences of microbe-dependent immune activation in LRE and goblet cell subsets.

In addition to LRE and goblet cell immune activity, I was struck by near-systemic elevation of IFN signals within the CV relative to GF datasets, impacting myeloid cells, progenitors, LREs,

goblet cells, and ECs. This finding aligns with prior studies in mice showing bacterial colonization of the gut stimulates systemic type I IFN activity (Abt et al., 2012; Bradley et al., 2019; Ganal et al., 2012; Steed et al., 2017; Stefan et al., 2020; Van Winkle et al., 2022; Winkler et al., 2020), perhaps through epithelial recognition of bacterial DNA (Lee et al., 2006; Rachmilewitz et al., 2004). Microbe-dependent IFN activity can reduce levels of apoptosis and proliferation, thereby supporting IEC maturation and barrier maintenance (Katlinskaya et al., 2016; Mirpuri et al., 2010). Accordingly, increased IFN activity following bacterial colonization of the zebrafish intestine may reflect efforts to promote barrier integrity and prevent exaggerated inflammatory responses following bacterial colonization. Alternatively, such a response might lower the threshold for IFN activation in the event of pathogenic microbe encounter.

In addition to broad IFN activation in CV IECs, I observed a larger subset of IFN-enriched ECs (IFN-ECs) in CV relative to GF datasets, based on expression of ISGs such as *IFIT2* orthologue *ifit15*, and the fish orthologue to *RSAD2* (*rsad2*), encoding Viperin (Broad SCP1623). It is therefore plausible that a designated EC subset augments viral defenses in response to bacteria, or that bacterial signals promote specification of IFN-ECs from absorptive progenitors. This finding aligns with a recent murine study that found 1-5% of small intestinal ECs express the ISG *IFIT1* under homeostatic conditions, and that microbe-stimulated ISG expression pre-conditions IECs for defense against enteric viruses (Van Winkle et al., 2022). While it is unclear why elevated ISG expression might be localized to certain ECs, this could reflect unique microenvironments and bacterial distribution in the gut, or differential cellular capacities for bacterial sensing. While future work will be necessary to determine the IFN receptor at play in the zebrafish intestine, and to ascertain the role of elevated IFN activity in response to bacteria (systemic and IFN-EC-specific), my findings here demonstrate overlapping vertebrate responses to the microbiota and point to the zebrafish as a superb model for investigating common molecular signals regulated by gut colonization. In the future, I anticipate that advances in GF zebrafish husbandry will enable survival of GF animals into adulthood, and possibly allow for breeding and rearing of GF zebrafish over several generations. Such experiments would further allow researchers to compare cellular responses to the microbiota at a diverse range of developmental stages, and account for stage-specific differences in microbial influences on a host.
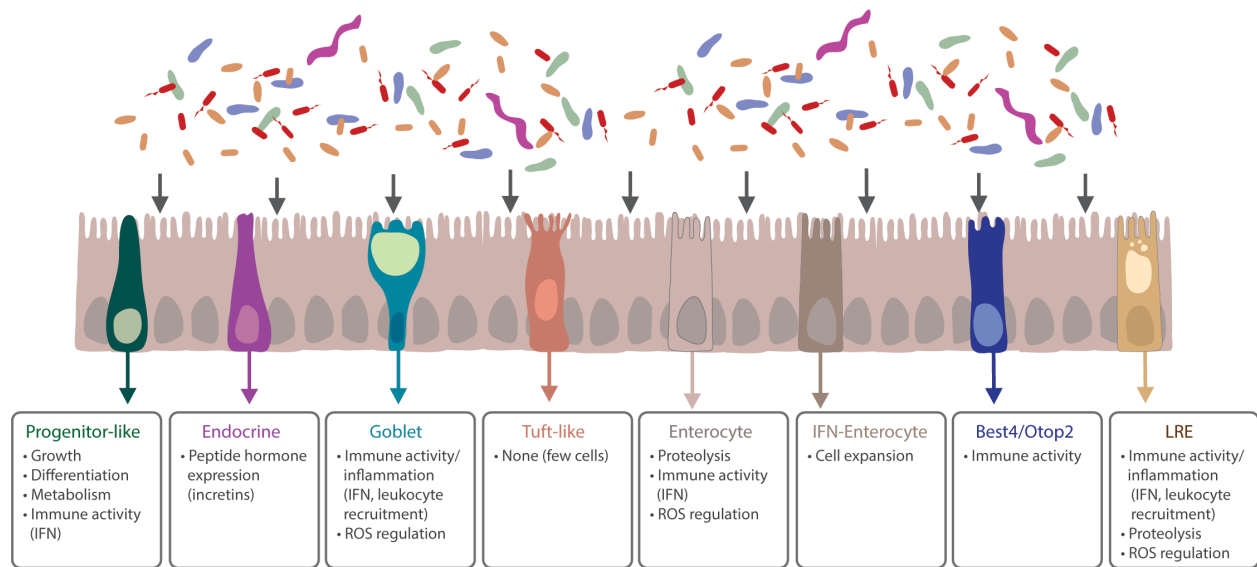
Figure 6.2 Summary of molecular processes encouraged by microbes in larval IEC types, identified by scRNA-seq.

6.4 Single cell resolution of IEC responses to *Vibrio cholerae* infection

Vc, the causative agent of the diarrheal disease cholera, is an aquatic bacterium endemic to wetland areas in over 50 countries, including Nigeria, Sudan, Somalia, Angola, Zimbabwe, and Haiti (WHO, 2010). Humans acquire *V. cholerae* through contaminated drinking water, after which the bacteria become hyper-infectious and highly transmissible (Alam et al., 2005; Butler et al., 2006; Hartley et al., 2006; Merrell et al., 2002; Pukatzki et al., 2006). Following bacterial ingestion, *Vc* traverses the host gastro-intestinal tract, making its way to the small intestine where it penetrates the mucin layer and adheres to the epithelium (Sack et al., 2004). Once there, *Vc* establishes clonal micro-colonies and expresses cholera toxin to induce diarrhea and mild intestinal inflammation (Sack et al., 2004). While disease phenotypes are well-established, determining molecular signals that underly host disease has been a challenge in the field.

Zebrafish are natural hosts for *Vc*, providing an opportunity to investigate molecular mechanisms underlying host disease in a relevant vertebrate model. In our hands *Vc* infection of adult zebrafish caused disease comparable to humans, including disrupted intestinal epithelia, cell shedding into the lumen, and mild inflammation. Using scRNA-seq, we discovered a

coordinated IEC response to infection that included attenuated IFN signaling, reduced expression of ion transporters *clca1* and *cftr*, and a moderate inflammatory response. Beyond reduced ion transporter expression (discussed in Chapter 4), I was particularly struck by reduced IFN signaling in *Vc* infected adults given my observation that IECs of GF zebrafish also exhibit reduced IFN signals. It is plausible that *Vc*-mediated disruption of the commensal microbiota resulted in a germ-free-like IEC phenotype. Under normal circumstances, the commensal microbiota provides a barrier to pathogenic microbes, preventing access to host tissue (Belkaid and Hand, 2014). However, *Vc* employs its type VI secretion system (T6SS) to inject toxic effectors into adjacent bacterial competitors (Pukatzki et al., 2006). In this way, *Vc*, like many gram-negative bacteria, weaponizes the T6SS against commensals within close biophysical proximity (and each other), giving *Vc* clones preferential access to their epithelial niche (Chen et al., 2019a; Joshi et al., 2017; Mougous et al., 2006; Pukatzki et al., 2007; Winkler et al., 2020). Given that we used *Vc* strain V52, which constitutively synthesizes an active T6SS (Pukatzki et al., 2006; Pukatzki et al., 2007), it is tempting to speculate that loss of ISG expression and IFN-ECs in infected fish resulted from the loss of commensal bacteria by T6SS-dependent *Vc* killing. In this way, diminished IFN signals stemming from a reduction in commensal bacterial may mediate barrier disruption that drives disease associated with *Vc* infection. In light of this result, it is possible that prebiotic or probiotic supplementation, with the intent of diversifying the intestinal microflora and increasing abundance of commensal competitors (perhaps T6SS resistant), could stimulate IFN signals and alleviate host disease. Additional work will be necessary to understand how *Vc* facilitates IFN suppression, how *Vc*-mediated IFN suppression disrupts host intestinal function, and how this pathway could be targeted for therapeutic intervention.
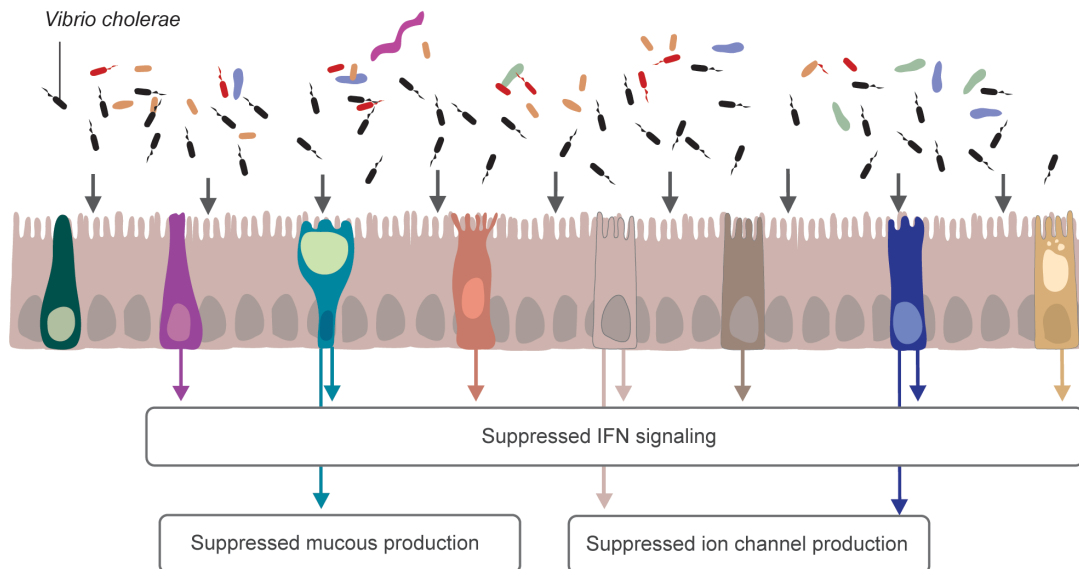
Figure 6.3 Summary of the most notable molecular processes altered by Vc infection in adult zebrafish IECs. Mature IECs (non-progenitors) exhibit globally suppressed IFN activity following Vc infection, perhaps due to T6SS-mediated killing of the commensal microbiota. Goblet cells reduce mucous production, and ECs and Best4/Otop2 cells decrease expression of ion channels.

6.5 RANK-dependent tuft-like cell development in the zebrafish intestine

RANK is a TNF receptor superfamily member and fundamental mediator of developmental processes across animal tissues (Fata et al., 2000; Knoop et al., 2009; Li et al., 2022; Rossi et al., 2007). Within the mammalian intestine, RANK-dependent activation of the NF-κB signaling pathway promotes antigen-capturing M cell development from progenitor compartments adjacent to lymphoid follicles (Debard et al., 2001; Dejardin et al., 2002; Kanaya et al., 2012; Kanaya et al., 2018; Knoop et al., 2009). In this way, RANK mediates formation of a spatially restricted absorptive cell subset, where additional roles for RANK in mammalian IEC development remain unknown.

Single-cell profiling of the zebrafish intestine revealed candidate intestinal progenitors expressing the *rank* orthologue. Bioinformatic lineage trajectory analysis further demonstrated that *rank* expression persists into the tuft-like cell lineage, leading me to hypothesize that RANK

controls tuft-like cell specification. I tested this hypothesis using a combination of mutagenesis and imaging experiments, where I found that zebrafish expressing non-functional RANK fail to generate tuft-like cells. Moreover, I observed *rank* reporter expression in heterogeneous cell populations, including goblet cells, where goblet cell numbers were diminished in *rank* mutant intestines. Taken together, my findings suggest that RANK drives development of the zebrafish intestinal tuft-like cell lineage, where goblet cells and tuft-like cells may share a common progenitor (Figure 6.4).
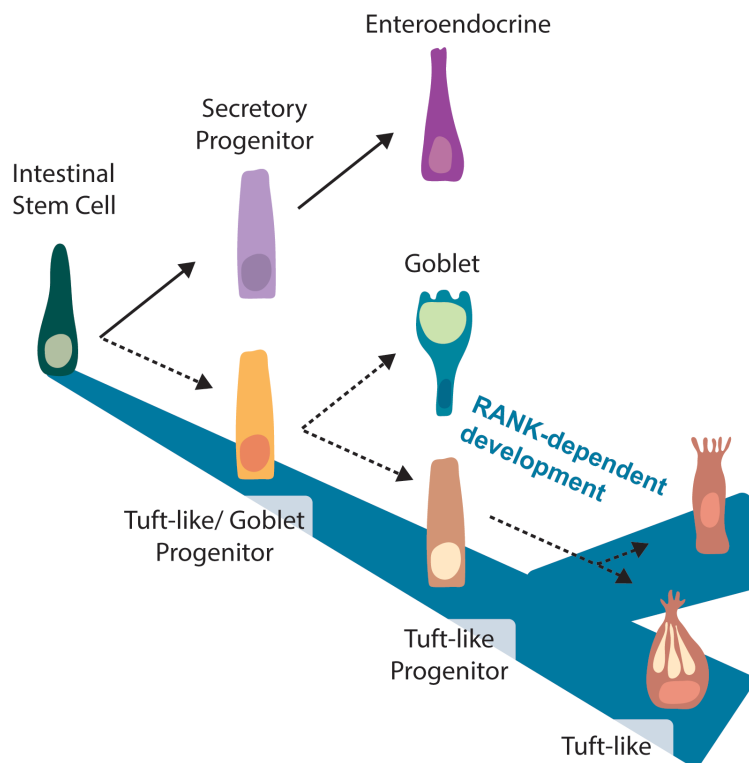
Figure 6.4 Proposed secretory lineage in the zebrafish intestinal epithelium. RANK activity drives tuft-like cell development within the secretory IEC lineage, where tuft-like cells and goblet cells are derived from a common progenitor. I further propose that transcriptionally and morphologically disparate tuft-like cell subsets arise from a common tuft-like progenitor. RANK-dependent NF-κB activation may increasingly provide differentiation or survival cues along the tuft-like lineage, explaining reduced goblet cell abundance in fish depleted of functional RANK.

Dotted lines indicate tentative lineages. The blue path represents increasing *rank* expression and RANK-dependent development along the progenitor to tuft-like cell lineage.

Mammalian tuft cells are generally regarded as secretory in nature since they secrete Il25 (at least in mice) and acetylcholine to potentiate type 2 immune circuits (Gerbe et al., 2016; von Moltke et al., 2016). While the mammalian tuft cell differentiation trajectory remains uncertain, and it is unclear if zebrafish tuft-like cells are of a secretory lineage and nature, several pieces of evidence support zebrafish tuft-like cells as members of secretory lineage. First, *rank* reporter expression in both tuft-like cells and goblet cells, as well as goblet cell loss in *rank* mutants, supports tuft-like cells and goblet cells as members of the same IEC lineage (goblet cells being clear members of the secretory lineage). Because I did not observe significant *rank* expression in goblet cells by scRNA-seq or FISH analysis, *rank* reporter expression in goblet cells may reflect the relatively long half-life of GFP (Kitsera et al., 2007), such that GFP persists during goblet cell specification from *rank*-expressing goblet/ tuft-like progenitors. While it is possible that goblet cell loss in *rank* mutants is a secondary consequence of diminished RANK, or reflects independent RANK function in this cell type, I believe a shared goblet/ tuft-like lineage aligns with developmental studies in mice. Specifically, tuft cell and goblet cell numbers are both significantly increased following IL4 or IL13 exposure (Gerbe et al., 2016; von Moltke et al., 2016) or Sprouty2 depletion (Schumacher et al., 2021), suggesting these cell types share a developmental lineage. Beyond the genetic relatedness of goblet and tuft-like cells, secretory attribution of tuft-like cells is further supported by morphological characteristics. Specifically, TEM analysis revealed one tuft-like cell subset possessing large secretory sacs (rodlets), alongside a dense tubular network, consistent with secretory function. Cells with similar morphological features (identified as rodlet cells), are known to secrete these rodlets, possibly containing alkaline phosphatase, into the lumen (Iger and Abraham, 1997; Sayyaf Dezfuli et al., 2022), perhaps in response to microbial encounter (Sayyaf Dezfuli et al., 2022). Taken together, morphological and lineage analysis therefore support tuft-like cells as secretory in nature.

Is it logical that RANK regulates formation of a secretory cell subtype? At apparent odds with this idea, RANK-dependent NF-κB activity drives absorptive progenitor differentiation into

antigen-transporting M cells (Knoop et al., 2009; Luna Velez et al., 2023). However, shared regulatory infrastructure for development of absorptive M cells and secretory tuft-like (or tuft) cells may be reasonable considering related cell functions, where both cell types sense luminal microbes and relay their findings to underlying lymphocytes. Moreover, variable signals from the lumen and stroma relative to cell localization could easily modulate signals downstream of RANK to alter the developmental outcome of RANK activation. In line with this, RANK can signal through both canonical and non-canonical NF-κB pathways that utilize distinct transcriptional activators to control diverse biological functions (Akiyama et al., 2008; Kanaya et al., 2018; Sun, 2017). It is also plausible that RANK-dependent tuft-like cell function in the zebrafish gut relies on an alternate downstream pathway, since RANK can signal through both MAPK and JNK cascades in other contexts (Ikeda et al., 2008; Lee et al., 2016). While further work is needed to elucidate signals following RANK activation, I demonstrated that RANK-deficient fish lose intestinal NF-κB activity, supporting NF-κB as a downstream mediator of RANK signaling. To provide additional support for this finding, direct demonstration of NF-κB activation in *rank*-expressing cells (perhaps FISH of *rank* in NF-κB reporter fish) will be valuable.

How is RANK activated in the zebrafish intestine? Mammalian RANK orthologues are activated by trimerization that occurs predominantly upon binding with RANKL, a TNF superfamily member (Hikita et al., 2006; Man et al., 2018). It is unclear if RANKL also activates RANK in zebrafish, though work in the medaka fish model identified a role for RANKL-RANK signals in osteoclastogenesis (To et al., 2012), supporting RANKL as a likely RANK activator in fish. Moreover, a recent zebrafish ligand-receptor interactome predicts RANKL-RANK as a likely ligand-receptor pair (Chodkowski et al., 2023), though further work will be needed to identify the mode of RANK activation in the zebrafish intestine. I did not highly detect *rankl* expression in larval or adult scRNA-seq datasets, though small subsets of blood and stromal cells expressed this RANK activator. Moreover, orthologues to the RANKL decoy receptors OPG and LGR4 are both detected in our single-cell datasets, where OPG is highly expressed in a tuft-like cell subset (Broad SCP2141). While non-definitive, the presence of both canonical and decoy receptors within the same IEC lineage hints at a likely role for RANK ligand in tuft-like cells. If RANKL-dependent RANK activation mediates tuft-like cell development, I expect that *rankl* mutant zebrafish will also fail

to develop intestinal tuft-like cells. Alternatively, loss of OPG or Lgr4 might drive tuft-like cell hyperplasia due to increased RANKL availability. Future work using whole-animal or intestine-specific knockouts will enable determination of RANKL and decoy receptor function in the fish gut.

What do zebrafish tuft-like cells do? As discussed in section 6.1, transcriptional analysis of tuft-like cell subsets, as well as prior descriptions of highly similar rodlet cells, indicate that zebrafish tuft-like cells likely share mammalian tuft cell function, sensing luminal parasites and initiating a type 2 immune response. Moreover, one study revealed that adult zebrafish intestines colonized by the parasitic nematode *Pseudocapillaria tomentosa* exhibited increased numbers of cells with pear-shaped morphology (putative tuft-like cells), though these were identified as goblet cells by the authors (Balla et al., 2010). Together, these results suggest that fish tuft-like cells mediate a response to helminths. It makes sense that teleost species such as zebrafish encode a mechanism for anti-helminthic immunity, since fish are highly susceptible to helminthic infection (Dezfuli et al., 2008; Secombes and Chappell, 2004). Future work using transgenic and mutant zebrafish alongside parasitic infection will shed light on the role of tuft-like cells in anti-helminthic immunity. Moreover, our work showing that *rank*-deficient zebrafish possess altered intestinal microbial composition indicates that tuft-like cells may also sense and respond to bacteria. Future work will be needed to pursue these findings in greater detail. In addition to investigating host-microbe interactions from the perspective of the tuft-like cell, it will be further intriguing to explore interactions between tuft-like cells and ILC-like cells identified here, and in sorted blood cells of the adult zebrafish intestine (Hernández et al., 2018). Given the genetic and optical power of the zebrafish for live imaging studies, zebrafish may be an excellent model to investigate tuft cell and blood cell interactions, as well as host-microbe interactions. Because of genetic, structural, and cellular overlap between zebrafish and mammals, zebrafish may reveal shared developmental mediators (eg. RANK) and functional roles for enigmatic tuft cells across vertebrates.

6.6 Concluding remarks

The intestinal epithelium lies at the host-environment interface, forming a single cell layer that harvests dietary nutrients and responds to luminal status, including nutrient availability and microbial composition. Within this thesis, I employed the zebrafish model to investigate intestinal epithelial and microbial interactions at cellular resolution. After characterizing gene expression profiles for zebrafish intestinal cells at two developmental stages, I identified profound transcriptional changes within each cell type of the fish intestine in response to variable luminal stimuli: larval intestinal cells responding to microbiota colonization, and adult intestinal cells countering exposure to pathogenic *Vc*. Together, my findings demonstrate how heterogenous cellular networks in the gut collaborate to maintain organismal health in response to variable environmental agents. During my investigation, I also identified previously undescribed cells of the zebrafish intestine that resemble mammalian tuft cells, and described a role for the TNF receptor superfamily member RANK as a mediator of tuft-like cell development. I believe these findings further establish zebrafish as an outstanding model for host-microbe interaction studies and provide rationale for utilizing zebrafish as a model for tuft cell development and function. Given the importance of tuft cells for fighting parasitic infection, my findings may therefore be beneficial for future investigation of tuft cell-dependent microbe sensing as it relates to human health.

Bibliography

1. Abd-Elhafeez, HH, Abdo, W, Kamal, BM, and Soliman, SA (2020a) Fish telocytes and their relation to rodlet cells in ruby-red-fin shark (rainbow shark) Epalzeorhynchos frenatum (Teleostei: Cyprinidae). Sci Rep, *10*, 18907.

2. Abd-Elhafeez, HH, Abou-Elhamd, AS, Abdo, W, and Soliman, SA (2020b) Migratory Activities and Stemness Properties of Rodlet Cells. Microsc Microanal, *26*, 1035–1052.

3. Abrams, J, Davuluri, G, Seiler, C, and Pack, M (2012) Smooth muscle caldesmon modulates peristalsis in the wild type and non-innervated zebrafish intestine. Neurogastroenterol Motil, *24*, 288–299.

4. Abt, MC, Osborne, LC, Monticelli, LA, Doering, TA, Alenghat, T, Sonnenberg, GF, Paley, MA, Antenus, M, Williams, KL, Erikson, J, Wherry, EJ, and Artis, D (2012) Commensal bacteria calibrate the activation threshold of innate antiviral immunity. Immunity, *37*, 158–170.

5. Agace, WW, and McCoy, KD (2017) Regionalized Development and Maintenance of the Intestinal Adaptive Immune Landscape. Immunity, *46*, 532–548.

6. Aghaallaei, N, Gruhl, F, Schaefer, CQ, Wernet, T, Weinhardt, V, Centanin, L, Loosli, F, Baumbach, T, and Wittbrodt, J (2016) Identification, visualization and clonal analysis of intestinal stem cells in fish. Development, *143*, 3470–3480.

7. Akiyama, T, Shimo, Y, Yanai, H, Qin, J, Ohshima, D, Maruyama, Y, Asaumi, Y, Kitazawa, J, Takayanagi, H, Penninger, JM, Matsumoto, M, Nitta, T, Takahama, Y, and Inoue, J (2008) The tumor necrosis factor family receptors RANK and CD40 cooperatively establish the thymic medullary microenvironment and self-tolerance. Immunity, *29*, 423–437.

8. Alam, A, Larocque, RC, Harris, JB, Vanderspurt, C, Ryan, ET, Qadri, F, and Calderwood, SB (2005) Hyperinfectivity of human-passaged Vibrio cholerae can be modeled by growth in the infant mouse. Infect Immun, *73*, 6674–6679.

9. Ali, M, Nelson, AR, Lopez, AL, and Sack, DA (2015) Updated global burden of cholera in endemic countries. PLoS Negl Trop Dis, *9*, e0003832.

10. Alok, A, Lei, Z, Jagannathan, NS, Kaur, S, Harmston, N, Rozen, SG, Tucker-Kellogg, L, and Virshup, DM (2017) Wnt proteins synergize to activate β-catenin signaling. J Cell Sci, *130*, 1532–1544.

11. Altan, E, Kubiski, SV, Boros, Á, Reuter, G, Sadeghi, M, Deng, X, Creighton, EK, Crim, MJ, and Delwart, E (2019) A Highly Divergent Picornavirus Infecting the Gut Epithelia of Zebrafish (Danio rerio) in Research Institutions Worldwide. Zebrafish, *16*, 291–299.

12. Alvers, AL, Ryan, S, Scherz, PJ, Huisken, J, and Bagnat, M (2014) Single continuous lumen formation in the zebrafish gut is mediated by smoothened-dependent tissue remodeling. Development, *141*, 1110–1119.

13. Anzenberger, U, Bit-Avragim, N, Rohr, S, Rudolph, F, Dehmel, B, Willnow, TE, and Abdelilah-Seyfried, S (2006) Elucidation of megalin/LRP2-dependent endocytic transport processes in the larval zebrafish pronephros. J Cell Sci, *119*, 2127–2137.

14. Aranda, JF, Reglero-Real, N, Marcos-Ramiro, B, Ruiz-Sáenz, A, Fernández-Martín, L, Bernabé-Rubio, M, Kremer, L, Ridley, AJ, Correas, I, Alonso, MA, and Millán, J (2013) MYADM controls endothelial barrier function through ERM-dependent regulation of ICAM-1 expression. Mol Biol Cell, *24*, 483–494.

15. Arora, T, Akrami, R, Pais, R, Bergqvist, L, Johansson, BR, Schwartz, TW, Reimann, F, Gribble, FM, and Bäckhed, F (2018) Microbial regulation of the L cell transcriptome. Sci Rep, *8*, 1207.

16. Auclair, BA, Benoit, YD, Rivard, N, Mishina, Y, and Perreault, N (2007) Bone morphogenetic protein signaling is essential for terminal differentiation of the intestinal secretory cell lineage. Gastroenterology, *133*, 887–896.

17. Bäckhed, F, Ley, RE, Sonnenburg, JL, Peterson, DA, and Gordon, JI (2005) Host-bacterial mutualism in the human intestine. Science, *307*, 1915–1920.

18. Bagnat, M, Navis, A, Herbstreith, S, Brand-Arzamendi, K, Curado, S, Gabriel, S, Mostov, K, Huisken, J, and Stainier, DY (2010) Cse1l is a negative regulator of CFTR-dependent fluid secretion. Curr Biol, *20*, 1840–1845.

19. Baldridge, MT, Nice, TJ, McCune, BT, Yokoyama, CC, Kambal, A, Wheadon, M, Diamond, MS, Ivanova, Y, Artyomov, M, and Virgin, HW (2015) Commensal microbes and interferon-λ determine persistence of enteric murine norovirus infection. Science, *347*, 266–269.

20. Balla, KM, Lugo-Villarino, G, Spitsbergen, JM, Stachura, DL, Hu, Y, Bañuelos, K, Romo-Fewell, O, Aroian, RV, and Traver, D (2010) Eosinophils in the zebrafish: prospective isolation, characterization, and eosinophilia induction by helminth determinants. Blood, *116*, 3944–3954.

21. Balla, KM, Rice, MC, Gagnon, JA, and Elde, NC (2020) Linking Virus Discovery to Immune Responses Visualized during Zebrafish Infections. Curr Biol, *30*, 2092–2103.e5.

22. Banerjee, A, Herring, CA, Chen, B, Kim, H, Simmons, AJ, Southard-Smith, AN, Allaman, MM, White, JR, Macedonia, MC, Mckinley, ET, Ramirez-Solano, MA, Scoville, EA, Liu, Q, Wilson, KT, Coffey, RJ, Washington, MK, Goettel, JA, and Lau, KS (2020) Succinate Produced by Intestinal Microbes Promotes Specification of Tuft Cells to Suppress Ileal Inflammation. Gastroenterology, *159*, 2101–2115.e5.

23. Barker, N (2014) Adult intestinal stem cells: critical drivers of epithelial homeostasis and regeneration. Nat Rev Mol Cell Biol, *15*, 19–33.

24. Barker, N, van Es, JH, Kuipers, J, Kujala, P, van den Born, M, Cozijnsen, M, Haegebarth, A, Korving, J, Begthel, H, Peters, PJ, and Clevers, H (2007) Identification of stem cells in small intestine and colon by marker gene Lgr5. Nature, *449*, 1003–1007.

25. Barker, N, van Oudenaarden, A, and Clevers, H (2012) Identifying the stem cell of the intestinal crypt: strategies and pitfalls. Cell Stem Cell, *11*, 452–460.

26. Barnhoorn, MC, Hakuno, SK, Bruckner, RS, Rogler, G, Hawinkels, LJAC, and Scharl, M (2020) Stromal Cells in the Pathogenesis of Inflammatory Bowel Disease. J Crohns Colitis, *14*, 995–1009.

27. Bastide, P, Darido, C, Pannequin, J, Kist, R, Robine, S, Marty-Double, C, Bibeau, F, Scherer, G, Joubert, D, Hollande, F, Blache, P, and Jay, P (2007) Sox9 regulates cell proliferation and is required for Paneth cell differentiation in the intestinal epithelium. J Cell Biol, *178*, 635–648.

28. Bates, JM, Akerlund, J, Mittge, E, and Guillemin, K (2007) Intestinal alkaline phosphatase detoxifies lipopolysaccharide and prevents inflammation in zebrafish in response to the gut microbiota. Cell Host Microbe, *2*, 371–382.

29. Bates, JM, Mittge, E, Kuhlman, J, Baden, KN, Cheesman, SE, and Guillemin, K (2006) Distinct signals from the microbiota promote different aspects of zebrafish gut differentiation. Dev Biol, *297*, 374–386.

30. Batlle, E, Henderson, JT, Beghtel, H, van den Born, MM, Sancho, E, Huls, G, Meeldijk, J, Robertson, J, van de Wetering, M, Pawson, T, and Clevers, H (2002) Beta-catenin and TCF mediate cell positioning in the intestinal epithelium by controlling the expression of EphB/ephrinB. Cell, *111*, 251–263.

31. Bäumler, AJ, and Sperandio, V (2016) Interactions between the microbiota and pathogenic bacteria in the gut. Nature, *535*, 85–93.

32. Behrens, J, von Kries, JP, Kühl, M, Bruhn, L, Wedlich, D, Grosschedl, R, and Birchmeier, W (1996) Functional interaction of beta-catenin with the transcription factor LEF-1. Nature, *382*, 638–642.

33. Belkaid, Y, and Hand, TW (2014) Role of the microbiota in immunity and inflammation. Cell, *157*, 121–141.

34. Bengmark, S (1998) Ecological control of the gastrointestinal tract. The role of probiotic flora. Gut, *42*, 2–7.

35. Bennet, SMP, Böhn, L, Störsrud, S, Liljebo, T, Collin, L, Lindfors, P, Törnblom, H, Öhman, L, and Simrén, M (2018) Multivariate modelling of faecal bacterial profiles of patients with IBS predicts responsiveness to a diet low in FODMAPs. Gut, *67*, 872–881.

36. Bennett, CM, Kanki, JP, Rhodes, J, Liu, TX, Paw, BH, Kieran, MW, Langenau, DM, Delahaye-Brown, A, Zon, LI, Fleming, MD, and Look, AT (2001) Myelopoiesis in the zebrafish, Danio rerio. Blood, *98*, 643–651.

37. Benoit, CR, Stanton, AE, Tartanian, AC, Motzer, AR, McGaughey, DM, Bond, SR, and Brody, LC (2018) Functional and phylogenetic characterization of noncanonical vitamin B_{12}-binding proteins in zebrafish suggests involvement in cobalamin transport. J Biol Chem, *293*, 17606–17621.

38. Beumer, J, Artegiani, B, Post, Y, Reimann, F, Gribble, F, Nguyen, TN, Zeng, H, Van den Born, M, Van Es, JH, and Clevers, H (2018) Enteroendocrine cells switch hormone expression along the crypt-to-villus BMP signalling gradient. Nat Cell Biol, *20*, 909–916.

39. Birchenough, GM, Nyström, EE, Johansson, ME, and Hansson, GC (2016) A sentinel goblet cell guards the colonic crypt by triggering Nlrp6-dependent Muc2 secretion. Science, *352*, 1535–1542.

40. Biton, M, Haber, AL, Rogel, N, Burgin, G, Beyaz, S, Schnell, A, Ashenberg, O, Su, CW, Smillie, C, Shekhar, K, Chen, Z, Wu, C, Ordovas-Montanes, J, Alvarez, D, Herbst, RH, Zhang, M, Tirosh, I, Dionne, D, Nguyen, LT, Xifaras, ME, Shalek, AK, von Andrian, UH, Graham, DB, Rozenblatt-Rosen, O, Shi, HN, Kuchroo, V, Yilmaz, OH, Regev, A, and Xavier, RJ (2018) T Helper Cell Cytokines Modulate Intestinal Stem Cell Renewal and Differentiation. Cell, *175*, 1307–1320.e22.

41. Bjerknes, M, and Cheng, H (1999) Clonal analysis of mouse intestinal epithelial progenitors. Gastroenterology, *116*, 7–14.

42. Bjerknes, M, Khandanpour, C, Möröy, T, Fujiyama, T, Hoshino, M, Klisch, TJ, Ding, Q, Gan, L, Wang, J, Martín, MG, and Cheng, H (2012) Origin of the brush cell lineage in the mouse intestinal epithelium. Dev Biol, *362*, 194–218.

43. Blache, P, van de Wetering, M, Duluc, I, Domon, C, Berta, P, Freund, JN, Clevers, H, and Jay, P (2004) SOX9 is an intestine crypt transcription factor, is regulated by the Wnt pathway, and represses the CDX2 and MUC2 genes. J Cell Biol, *166*, 37–47.

44. Bolyen, E, Rideout, JR, Dillon, MR, Bokulich, NA, Abnet, CC, Al-Ghalith, GA, Alexander, H, Alm, EJ, Arumugam, M, Asnicar, F, Bai, Y, Bisanz, JE, Bittinger, K, Brejnrod, A, Brislawn, CJ, Brown, CT, Callahan, BJ, Caraballo-Rodríguez, AM, Chase, J, Cope, EK, Da Silva, R, Diener, C, Dorrestein, PC, Douglas, GM, Durall, DM, Duvallet, C, Edwardson, CF, Ernst, M, Estaki, M, Fouquier, J, Gauglitz, JM, Gibbons, SM, Gibson, DL, Gonzalez, A, Gorlick, K, Guo, J, Hillmann, B, Holmes, S, Holste, H, Huttenhower, C, Huttley, GA, Janssen, S, Jarmusch, AK, Jiang, L, Kaehler, BD, Kang, KB, Keefe, CR, Keim, P, Kelley, ST, Knights, D, Koester, I, Kosciolek, T, Kreps, J, Langille, MGI, Lee, J, Ley, R, Liu, YX, Loftfield, E, Lozupone, C, Maher, M, Marotz, C, Martin, BD, McDonald, D, McIver, LJ, Melnik, AV, Metcalf, JL, Morgan, SC, Morton, JT, Naimey, AT, Navas-Molina, JA, Nothias, LF, Orchanian, SB, Pearson, T, Peoples, SL, Petras, D, Preuss, ML, Pruesse, E, Rasmussen, LB, Rivers, A, Robeson, MS, Rosenthal, P, Segata, N, Shaffer, M, Shiffer, A, Sinha, R, Song, SJ, Spear, JR, Swafford, AD, Thompson, LR, Torres, PJ,

Trinh, P, Tripathi, A, Turnbaugh, PJ, Ul-Hasan, S, van der Hooft, JJJ, Vargas, F, Vázquez-Baeza, Y, Vogtmann, E, von Hippel, M, Walters, W, Wan, Y, Wang, M, Warren, J, Weber, KC, Williamson, CHD, Willis, AD, Xu, ZZ, Zaneveld, JR, Zhang, Y, Zhu, Q, Knight, R, and Caporaso, JG (2019) Reproducible, interactive, scalable and extensible microbiome data science using QIIME 2. Nat Biotechnol, *37*, 852–857.

45. Bosi, G, DePasquale, JA, Manera, M, Castaldelli, G, Giari, L, and Sayyaf Dezfuli, B (2018) Histochemical and immunohistochemical characterization of rodlet cells in the intestine of two teleosts, Anguilla anguilla and Cyprinus carpio. J Fish Dis, *41*, 475–485.

46. Bradley, KC, Finsterbusch, K, Schnepf, D, Crotta, S, Llorian, M, Davidson, S, Fuchs, SY, Staeheli, P, and Wack, A (2019) Microbiota-Driven Tonic Interferon Signals in Lung Stromal Cells Protect from Influenza Virus Infection. Cell Rep, *28*, 245–256.e4.

47. Brash, AR (1999) Lipoxygenases: occurrence, functions, catalysis, and acquisition of substrate. J Biol Chem, *274*, 23679–23682.

48. Broderick, NA, Buchon, N, and Lemaitre, B (2014) Microbiota-induced changes in drosophila melanogaster host gene expression and gut morphology. mBio, *5*, e01117–14.

49. Brugman, S (2016) The zebrafish as a model to study intestinal inflammation. Dev Comp Immunol, *64*, 82–92.

50. Bry, L, Falk, PG, Midtvedt, T, and Gordon, JI (1996) A model of host-microbial interactions in an open mammalian ecosystem. Science, *273*, 1380–1383.

51. Buchon, N, Broderick, NA, and Lemaitre, B (2013a) Gut homeostasis in a microbial world: insights from Drosophila melanogaster. Nat Rev Microbiol, *11*, 615–626.

52. Buchon, N, Osman, D, David, FP, Fang, HY, Boquete, JP, Deplancke, B, and Lemaitre, B (2013b) Morphological and molecular characterization of adult midgut compartmentalization in Drosophila. Cell Rep, *3*, 1725–1738.

53. Buettner, M, and Lochner, M (2016) Development and Function of Secondary and Tertiary Lymphoid Organs in the Small Intestine and the Colon. Front Immunol, *7*, 342.

54. Burclaff, J, Bliton, RJ, Breau, KA, Ok, MT, Gomez-Martinez, I, Ranek, JS, Bhatt, AP, Purvis, JE, Woosley, JT, and Magness, ST (2022) A Proximal-to-Distal Survey of Healthy Adult Human

Small Intestine and Colon Epithelium by Single-Cell Transcriptomics. Cell Mol Gastroenterol Hepatol, *13*, 1554–1589.

55. Burgueño, JF, and Abreu, MT (2020) Epithelial Toll-like receptors and their role in gut homeostasis and disease. Nat Rev Gastroenterol Hepatol, *17*, 263–278.

56. Busslinger, GA, Weusten, BLA, Bogte, A, Begthel, H, Brosens, LAA, and Clevers, H (2021) Human gastrointestinal epithelia of the esophagus, stomach, and duodenum resolved at single-cell resolution. Cell Rep, *34*, 108819.

57. Butler, A, Hoffman, P, Smibert, P, Papalexi, E, and Satija, R (2018) Integrating single-cell transcriptomic data across different conditions, technologies, and species. Nat Biotechnol, *36*, 411–420.

58. Butler, SM, Nelson, EJ, Chowdhury, N, Faruque, SM, Calderwood, SB, and Camilli, A (2006) Cholera stool bacteria repress chemotaxis to increase infectivity. Mol Microbiol, *60*, 417–426.

59. Camacho, A, Bouhenia, M, Alyusfi, R, Alkohlani, A, Naji, MAM, de Radiguès, X, Abubakar, AM, Almoalmi, A, Seguin, C, Sagrado, MJ, Poncin, M, McRae, M, Musoke, M, Rakesh, A, Porten, K, Haskew, C, Atkins, KE, Eggo, RM, Azman, AS, Broekhuijsen, M, Saatcioglu, MA, Pezzoli, L, Quilici, ML, Al-Mesbahy, AR, Zagaria, N, and Luquero, FJ (2018) Cholera epidemic in Yemen, 2016-18: an analysis of surveillance data. Lancet Glob Health, *6*, e680–e690.

60. Camp, JG, Frank, CL, Lickwar, CR, Guturu, H, Rube, T, Wenger, AM, Chen, J, Bejerano, G, Crawford, GE, and Rawls, JF (2014) Microbiota modulate transcription in the intestinal epithelium without remodeling the accessible chromatin landscape. Genome Res, *24*, 1504–1516.

61. Cao, J, Spielmann, M, Qiu, X, Huang, X, Ibrahim, DM, Hill, AJ, Zhang, F, Mundlos, S, Christiansen, L, Steemers, FJ, Trapnell, C, and Shendure, J (2019) The single-cell transcriptional landscape of mammalian organogenesis. Nature, *566*, 496–502.

62. Caporaso, JG, Lauber, CL, Walters, WA, Berg-Lyons, D, Lozupone, CA, Turnbaugh, PJ, Fierer, N, and Knight, R (2011) Global patterns of 16S rRNA diversity at a depth of millions of sequences per sample. Proc Natl Acad Sci U S A, *108 Suppl 1*, 4516–4522.

63. Carmon, KS, Gong, X, Lin, Q, Thomas, A, and Liu, Q (2011) R-spondins function as ligands of the orphan receptors LGR4 and LGR5 to regulate Wnt/beta-catenin signaling. Proc Natl Acad Sci U S A, *108*, 11452–11457.

64. Cebra, JJ (1999) Influences of microbiota on intestinal immune system development. Am J Clin Nutr, *69*, 1046S–1051S.

65. Chassaing, B, Van de Wiele, T, De Bodt, J, Marzorati, M, and Gewirtz, AT (2017) Dietary emulsifiers directly alter human microbiota composition and gene expression ex vivo potentiating intestinal inflammation. Gut, *66*, 1414–1427.

66. Cheesman, SE, Neal, JT, Mittge, E, Seredick, BM, and Guillemin, K (2011) Epithelial cell proliferation in the developing zebrafish intestine is regulated by the Wnt pathway and microbial signaling via Myd88. Proc Natl Acad Sci U S A, *108 Suppl 1*, 4570–4577.

67. Chen, C, Yang, X, and Shen, X (2019a) Confirmed and Potential Roles of Bacterial T6SSs in the Intestinal Ecosystem. Front Microbiol, *10*, 1484.

68. Chen, L, Toke, NH, Luo, S, Vasoya, RP, Fullem, RL, Parthasarathy, A, Perekatt, AO, and Verzi, MP (2019b) A reinforcing HNF4-SMAD4 feed-forward module stabilizes enterocyte identity. Nat Genet, *51*, 777–785.

69. Chen, W, Tseng, X, Lin, G, Schreiner, A, Chen, H, Voigt, MM, Yuh, C, Wu, J, Huang, SS, and Huang, J The Ortholog of LYVE-1 Is Required for Thoracic Duct Formation in Zebrafish. CellBio, 228–247.

70. Chen, YC, Lu, YF, Li, IC, and Hwang, SP (2012) Zebrafish Agr2 is required for terminal differentiation of intestinal goblet cells. PLoS One, *7*, e34408.

71. Chen, YH, Lu, YF, Ko, TY, Tsai, MY, Lin, CY, Lin, CC, and Hwang, SP (2009) Zebrafish cdx1b regulates differentiation of various intestinal cell lineages. Dev Dyn, *238*, 1021–1032.

72. Chodkowski, M, Zieleziński, A, and Anbalagan, S (2023) A ligand-receptor interactome atlas of the zebrafish. biorxiv,

73. Chung, WS, Andersson, O, Row, R, Kimelman, D, and Stainier, DY (2010) Suppression of Alk8-mediated Bmp signaling cell-autonomously induces pancreatic beta-cells in zebrafish. Proc Natl Acad Sci U S A, *107*, 1142–1147.

74. Cichy, W, Klincewicz, B, and Plawski, A (2014) Juvenile polyposis syndrome. Arch Med Sci, *10*, 570–577.

75. Claes, AK, Zhou, JY, and Philpott, DJ (2015) NOD-Like Receptors: Guardians of Intestinal Mucosal Barriers. Physiology (Bethesda), *30*, 241–250.

76. Claesson, MJ, Jeffery, IB, Conde, S, Power, SE, O'Connor, EM, Cusack, S, Harris, HM, Coakley, M, Lakshminarayanan, B, O'Sullivan, O, Fitzgerald, GF, Deane, J, O'Connor, M, Harnedy, N, O'Connor, K, O'Mahony, D, van Sinderen, D, Wallace, M, Brennan, L, Stanton, C, Marchesi, JR, Fitzgerald, AP, Shanahan, F, Hill, C, Ross, RP, and O'Toole, PW (2012) Gut microbiota composition correlates with diet and health in the elderly. Nature, *488*, 178–184.

77. Clevers, H (2013) The intestinal crypt, a prototype stem cell compartment. Cell, *154*, 274–284.

78. Crockett, JC, Mellis, DJ, Shennan, KI, Duthie, A, Greenhorn, J, Wilkinson, DI, Ralston, SH, Helfrich, MH, and Rogers, MJ (2011) Signal peptide mutations in RANK prevent downstream activation of NF-κB. J Bone Miner Res, *26*, 1926–1938.

79. Crosnier, C, Vargesson, N, Gschmeissner, S, Ariza-McNaughton, L, Morrison, A, and Lewis, J (2005) Delta-Notch signalling controls commitment to a secretory fate in the zebrafish intestine. Development, *132*, 1093–1104.

80. Cvejic, A, Serbanovic-Canic, J, Stemple, DL, and Ouwehand, WH (2011) The role of meis1 in primitive and definitive hematopoiesis during zebrafish development. Haematologica, *96*, 190–198.

81. Dalum, AS, Kraus, A, Khan, S, Davydova, E, Rigaudeau, D, Bjørgen, H, López-Porras, A, Griffiths, G, Wiegertjes, GF, Koppang, EO, Salinas, I, Boudinot, P, and Rességuier, J (2021) High-Resolution, 3D Imaging of the Zebrafish Gill-Associated Lymphoid Tissue (GIALT) Reveals a Novel Lymphoid Structure, the Amphibranchial Lymphoid Tissue. Front Immunol, *12*, 769901.

82. Darwich, AS, Aslam, U, Ashcroft, DM, and Rostami-Hodjegan, A (2014) Meta-analysis of the turnover of intestinal epithelia in preclinical animal species and humans. Drug Metab Dispos, *42*, 2016–2022.

83. David, LA, Maurice, CF, Carmody, RN, Gootenberg, DB, Button, JE, Wolfe, BE, Ling, AV, Devlin, AS, Varma, Y, Fischbach, MA, Biddinger, SB, Dutton, RJ, and Turnbaugh, PJ (2014) Diet rapidly and reproducibly alters the human gut microbiome. Nature, *505*, 559–563.

84. Davison, JM, Lickwar, CR, Song, L, Breton, G, Crawford, GE, and Rawls, JF (2017) Microbiota regulate intestinal epithelial gene expression by suppressing the transcription factor Hepatocyte nuclear factor 4 alpha. Genome Res, *27*, 1195–1206.

85. Davoodi, S, and Foley, E (2019) Host-Microbe-Pathogen Interactions: A Review of Vibrio cholerae Pathogenesis in Drosophila. Front Immunol, *10*, 3128.

86. de la Pompa, JL, Wakeham, A, Correia, KM, Samper, E, Brown, S, Aguilera, RJ, Nakano, T, Honjo, T, Mak, TW, Rossant, J, and Conlon, RA (1997) Conservation of the Notch signalling pathway in mammalian neurogenesis. Development, *124*, 1139–1148.

87. de Lau, W, Barker, N, Low, TY, Koo, BK, Li, VS, Teunissen, H, Kujala, P, Haegebarth, A, Peters, PJ, van de Wetering, M, Stange, DE, van Es, JE, Guardavaccaro, D, Schasfoort, RB, Mohri, Y, Nishimori, K, Mohammed, S, Heck, AJ, and Clevers, H (2011) Lgr5 homologues associate with Wnt receptors and mediate R-spondin signalling. Nature, *476*, 293–297.

88. Debard, N, Sierro, F, Browning, J, and Kraehenbuhl, JP (2001) Effect of mature lymphocytes and lymphotoxin on the development of the follicle-associated epithelium and M cells in mouse Peyer's patches. Gastroenterology, *120*, 1173–1182.

89. Dejardin, E, Droin, NM, Delhase, M, Haas, E, Cao, Y, Makris, C, Li, ZW, Karin, M, Ware, CF, and Green, DR (2002) The lymphotoxin-beta receptor induces different patterns of gene expression via two NF-kappaB pathways. Immunity, *17*, 525–535.

90. DelGiorno, KE, Naeem, RF, Fang, L, Chung, CY, Ramos, C, Luhtala, N, O'Connor, C, Hunter, T, Manor, U, and Wahl, GM (2020) Tuft Cell Formation Reflects Epithelial Plasticity in Pancreatic Injury: Implications for Modeling Human Pancreatitis. Front Physiol, *11*, 88.

91. den Besten, G, van Eunen, K, Groen, AK, Venema, K, Reijngoud, DJ, and Bakker, BM (2013) The role of short-chain fatty acids in the interplay between diet, gut microbiota, and host energy metabolism. J Lipid Res, *54*, 2325–2340.

92. Dezfuli, BS, Bosi, G, DePasquale, JA, Manera, M, and Giari, L (2016) Fish innate immunity against intestinal helminths. Fish Shellfish Immunol, *50*, 274–287.

93. Dezfuli, BS, Lui, A, Boldrini, P, Pironi, F, and Giari, L (2008) The inflammatory response of fish to helminth parasites. Parasite, *15*, 426–433.

94. Dezfuli, BS, Pironi, F, Shinn, AP, Manera, M, and Giari, L (2007) Histopathology and ultrastructure of Platichthys flesus naturally infected with Anisakis simplex s.l. larvae (Nematoda: Anisakidae). J Parasitol, *93*, 1416–1423.

95. Ding, Q, Lu, C, Hao, Q, Zhang, Q, Yang, Y, Olsen, RE, Ringo, E, Ran, C, Zhang, Z, and Zhou, Z (2022) Dietary Succinate Impacts the Nutritional Metabolism, Protein Succinylation and Gut Microbiota of Zebrafish. Front Nutr, *9*, 894278.

96. Dudakov, JA, Hanash, AM, and van den Brink, MR (2015) Interleukin-22: immunobiology and pathology. Annu Rev Immunol, *33*, 747–785.

97. Eberl, G, Marmon, S, Sunshine, MJ, Rennert, PD, Choi, Y, and Littman, DR (2004) An essential function for the nuclear receptor RORgamma(t) in the generation of fetal lymphoid tissue inducer cells. Nat Immunol, *5*, 64–73.

98. Eden, E, Navon, R, Steinfeld, I, Lipson, D, and Yakhini, Z (2009) GOrilla: a tool for discovery and visualization of enriched GO terms in ranked gene lists. BMC Bioinformatics, *10*, 48.

99. Farnsworth, DR, Saunders, LM, and Miller, AC (2020) A single-cell transcriptome atlas for zebrafish development. Dev Biol, *459*, 100–108.

100. Farrell, JA, Wang, Y, Riesenfeld, SJ, Shekhar, K, Regev, A, and Schier, AF (2018) Single-cell reconstruction of developmental trajectories during zebrafish embryogenesis. Science, *360*,

101. Fast, D, Kostiuk, B, Foley, E, and Pukatzki, S (2018) Commensal pathogen competition impacts host viability. Proc Natl Acad Sci U S A, *115*, 7099–7104.

102. Fast, D, Petkau, K, Ferguson, M, Shin, M, Galenza, A, Kostiuk, B, Pukatzki, S, and Foley, E (2020) Vibrio cholerae-Symbiont Interactions Inhibit Intestinal Repair in Drosophila. Cell Rep, *30*, 1088–1100.e5.

103. Fata, JE, Kong, YY, Li, J, Sasaki, T, Irie-Sasaki, J, Moorehead, RA, Elliott, R, Scully, S, Voura, EB, Lacey, DL, Boyle, WJ, Khokha, R, and Penninger, JM (2000) The osteoclast differentiation factor osteoprotegerin-ligand is essential for mammary gland development. Cell, *103*, 41–50.

104. Ferguson, M, and Foley, E (2022) Microbial recognition regulates intestinal epithelial growth in homeostasis and disease. FEBS J, *289*, 3666–3691.

105. Fiddes, IT, Lodewijk, GA, Mooring, M, Bosworth, CM, Ewing, AD, Mantalas, GL, Novak, AM, van den Bout, A, Bishara, A, Rosenkrantz, JL, Lorig-Roach, R, Field, AR, Haeussler, M, Russo, L, Bhaduri, A, Nowakowski, TJ, Pollen, AA, Dougherty, ML, Nuttle, X, Addor, MC, Zwolinski, S, Katzman, S, Kriegstein, A, Eichler, EE, Salama, SR, Jacobs, FMJ, and Haussler, D (2018) Human-Specific NOTCH2NL Genes Affect Notch Signaling and Cortical Neurogenesis. Cell, *173*, 1356–1369.e22.

106. Flasse, LC, Stern, DG, Pirson, JL, Manfroid, I, Peers, B, and Voz, ML (2013) The bHLH transcription factor Ascl1a is essential for the specification of the intestinal secretory cells and mediates Notch signaling in the zebrafish intestine. Dev Biol, *376*, 187–197.

107. Flores, EM, Nguyen, AT, Odem, MA, Eisenhoffer, GT, and Krachler, AM (2020) The zebrafish as a model for gastrointestinal tract-microbe interactions. Cell Microbiol, *22*, e13152.

108. Flores, MV, Crawford, KC, Pullin, LM, Hall, CJ, Crosier, KE, and Crosier, PS (2010) Dual oxidase in the intestinal epithelium of zebrafish larvae has anti-bacterial properties. Biochem Biophys Res Commun, *400*, 164–168.

109. Flores, MV, Hall, CJ, Davidson, AJ, Singh, PP, Mahagaonkar, AA, Zon, LI, Crosier, KE, and Crosier, PS (2008) Intestinal differentiation in zebrafish requires Cdx1b, a functional equivalent of mammalian Cdx2. Gastroenterology, *135*, 1665–1675.

110. Fre, S, Huyghe, M, Mourikis, P, Robine, S, Louvard, D, and Artavanis-Tsakonas, S (2005) Notch signals control the fate of immature progenitor cells in the intestine. Nature, *435*, 964–968.

111. Galindo-Villegas, J, García-Moreno, D, de Oliveira, S, Meseguer, J, and Mulero, V (2012) Regulation of immunity and disease resistance by commensal microbes and chromatin modifications during zebrafish development. Proc Natl Acad Sci U S A, *109*, E2605–14.

112. Ganal, SC, Sanos, SL, Kallfass, C, Oberle, K, Johner, C, Kirschning, C, Lienenklaus, S, Weiss, S, Staeheli, P, Aichele, P, and Diefenbach, A (2012) Priming of natural killer cells by nonmucosal mononuclear phagocytes requires instructive signals from commensal microbiota. Immunity, *37*, 171–186.

113. Garrett, WS, Gordon, JI, and Glimcher, LH (2010) Homeostasis and inflammation in the intestine. Cell, *140*, 859–870.

114. Gehart, H, and Clevers, H (2019) Tales from the crypt: new insights into intestinal stem cells. Nat Rev Gastroenterol Hepatol, *16*, 19–34.

115. Genander, M, Halford, MM, Xu, NJ, Eriksson, M, Yu, Z, Qiu, Z, Martling, A, Greicius, G, Thakar, S, Catchpole, T, Chumley, MJ, Zdunek, S, Wang, C, Holm, T, Goff, SP, Pettersson, S, Pestell, RG, Henkemeyer, M, and Frisén, J (2009) Dissociation of EphB2 signaling pathways mediating progenitor cell proliferation and tumor suppression. Cell, *139*, 679–692.

116. Gensollen, T, Iyer, SS, Kasper, DL, and Blumberg, RS (2016) How colonization by microbiota in early life shapes the immune system. Science, *352*, 539–544.

117. Gerbe, F, Sidot, E, Smyth, DJ, Ohmoto, M, Matsumoto, I, Dardalhon, V, Cesses, P, Garnier, L, Pouzolles, M, Brulin, B, Bruschi, M, Harcus, Y, Zimmermann, VS, Taylor, N, Maizels, RM, and Jay, P (2016) Intestinal epithelial tuft cells initiate type 2 mucosal immunity to helminth parasites. Nature, *529*, 226–230.

118. Gerbe, F, van Es, JH, Makrini, L, Brulin, B, Mellitzer, G, Robine, S, Romagnolo, B, Shroyer, NF, Bourgaux, JF, Pignodel, C, Clevers, H, and Jay, P (2011) Distinct ATOH1 and Neurog3 requirements define tuft cells as a new secretory cell type in the intestinal epithelium. J Cell Biol, *192*, 767–780.

119. Gerke, V, and Moss, SE (2002) Annexins: from structure to function. Physiol Rev, *82*, 331–371.

120. Gilmore, AP (2005) Anoikis. Cell Death Differ, *12 Suppl 2*, 1473–1477.

121. Glass, TJ, Lund, TC, Patrinostro, X, Tolar, J, Bowman, TV, Zon, LI, and Blazar, BR (2011) Stromal cell-derived factor-1 and hematopoietic cell homing in an adult zebrafish model of hematopoietic cell transplantation. Blood, *118*, 766–774.

122. Glinka, A, Dolde, C, Kirsch, N, Huang, YL, Kazanskaya, O, Ingelfinger, D, Boutros, M, Cruciat, CM, and Niehrs, C (2011) LGR4 and LGR5 are R-spondin receptors mediating Wnt/β-catenin and Wnt/PCP signalling. EMBO Rep, *12*, 1055–1061.

123. Goi, M, and Childs, SJ (2016) Patterning mechanisms of the sub-intestinal venous plexus in zebrafish. Dev Biol, *409*, 114–128.

124. Goldberg, RF, Austen, WG, Zhang, X, Munene, G, Mostafa, G, Biswas, S, McCormack, M, Eberlin, KR, Nguyen, JT, Tatlidede, HS, Warren, HS, Narisawa, S, Millán, JL, and Hodin, RA (2008) Intestinal alkaline phosphatase is a gut mucosal defense factor maintained by enteral nutrition. Proc Natl Acad Sci U S A, *105*, 3551–3556.

125. Gonçalves, AF, Páscoa, I, Neves, JV, Coimbra, J, Vijayan, MM, Rodrigues, P, and Wilson, JM (2012) The inhibitory effect of environmental ammonia on Danio rerio LPS induced acute phase response. Dev Comp Immunol, *36*, 279–288.

126. Gregorieff, A, Stange, DE, Kujala, P, Begthel, H, van den Born, M, Korving, J, Peters, PJ, and Clevers, H (2009) The ets-domain transcription factor Spdef promotes maturation of goblet and paneth cells in the intestinal epithelium. Gastroenterology, *137*, 1333–45.e1.

127. Gribble, FM, and Reimann, F (2016) Enteroendocrine Cells: Chemosensors in the Intestinal Epithelium. Annu Rev Physiol, *78*, 277–299.

128. Grondin, JA, Kwon, YH, Far, PM, Haq, S, and Khan, WI (2020) Mucins in Intestinal Mucosal Defense and Inflammation: Learning From Clinical and Experimental Studies. Front Immunol, *11*, 2054.

129. Grunwald, DJ, and Eisen, JS (2002) Headwaters of the zebrafish -- emergence of a new model vertebrate. Nat Rev Genet, *3*, 717–724.

130. Gubatan, J, Holman, DR, Puntasecca, CJ, Polevoi, D, Rubin, SJ, and Rogalla, S (2021) Antimicrobial peptides and the gut microbiome in inflammatory bowel disease. World J Gastroenterol, *27*, 7402–7422.

131. Gustafsson, JK, Davis, JE, Rappai, T, McDonald, KG, Kulkarni, DH, Knoop, KA, Hogan, SP, Fitzpatrick, JA, Lencer, WI, and Newberry, RD (2021) Intestinal goblet cells sample and deliver lumenal antigens by regulated endocytic uptake and transcytosis. Elife, *10*,

132. Haber, AL, Biton, M, Rogel, N, Herbst, RH, Shekhar, K, Smillie, C, Burgin, G, Delorey, TM, Howitt, MR, Katz, Y, Tirosh, I, Beyaz, S, Dionne, D, Zhang, M, Raychowdhury, R, Garrett, WS, Rozenblatt-Rosen, O, Shi, HN, Yilmaz, O, Xavier, RJ, and Regev, A (2017) A single-cell survey of the small intestinal epithelium. Nature, *551*, 333–339.

133. Hall, CJ, Boyle, RH, Sun, X, Wicker, SM, Misa, JP, Krissansen, GW, Print, CG, Crosier, KE, and Crosier, PS (2014) Epidermal cells help coordinate leukocyte migration during inflammation through fatty acid-fuelled matrix metalloproteinase production. Nat Commun, *5*, 3880.

134. Halpern, M, and Izhaki, I (2017) Fish as Hosts of Vibrio cholerae. Front Microbiol, *8*, 282.

135. Hao, Y, Hao, S, Andersen-Nissen, E, Mauck, WM, Zheng, S, Butler, A, Lee, MJ, Wilk, AJ, Darby, C, Zager, M, Hoffman, P, Stoeckius, M, Papalexi, E, Mimitou, EP, Jain, J, Srivastava, A, Stuart, T, Fleming, LM, Yeung, B, Rogers, AJ, McElrath, JM, Blish, CA, Gottardo, R, Smibert, P, and Satija, R (2021) Integrated analysis of multimodal single-cell data. Cell, *184*, 3573–3587.e29.

136. Haramis, AP, Hurlstone, A, van der Velden, Y, Begthel, H, van den Born, M, Offerhaus, GJ, and Clevers, HC (2006) Adenomatous polyposis coli-deficient zebrafish are susceptible to digestive tract neoplasia. EMBO Rep, *7*, 444–449.

137. Harper, J, Mould, A, Andrews, RM, Bikoff, EK, and Robertson, EJ (2011) The transcriptional repressor Blimp1/Prdm1 regulates postnatal reprogramming of intestinal enterocytes. Proc Natl Acad Sci U S A, *108*, 10585–10590.

138. Hartley, DM, Morris, JG, and Smith, DL (2006) Hyperinfectivity: a critical element in the ability of V. cholerae to cause epidemics. PLoS Med, *3*, e7.

139. He, C, and Chen, X (2005) Transcription regulation of the vegf gene by the BMP/Smad pathway in the angioblast of zebrafish embryos. Biochem Biophys Res Commun, *329*, 324–330.

140. He, XC, Zhang, J, Tong, WG, Tawfik, O, Ross, J, Scoville, DH, Tian, Q, Zeng, X, He, X, Wiedemann, LM, Mishina, Y, and Li, L (2004) BMP signaling inhibits intestinal stem cell self-renewal through suppression of Wnt-beta-catenin signaling. Nat Genet, *36*, 1117–1121.

141. Hennig, B, Meerarani, P, Slim, R, Toborek, M, Daugherty, A, Silverstone, AE, and Robertson, LW (2002) Proinflammatory properties of coplanar PCBs: in vitro and in vivo evidence. Toxicol Appl Pharmacol, *181*, 174–183.

142. Heppert, JK, Davison, JM, Kelly, C, Mercado, GP, Lickwar, CR, and Rawls, JF (2021) Transcriptional programmes underlying cellular identity and microbial responsiveness in the intestinal epithelium. Nat Rev Gastroenterol Hepatol, *18*, 7–23.

143. Hernández, PP, Strzelecka, PM, Athanasiadis, EI, Hall, D, Robalo, AF, Collins, CM, Boudinot, P, Levraud, JP, and Cvejic, A (2018) Single-cell transcriptional analysis reveals ILC-like cells in zebrafish. Sci Immunol, *3*,

144. Herrington, DA, Hall, RH, Losonsky, G, Mekalanos, JJ, Taylor, RK, and Levine, MM (1988) Toxin, toxin-coregulated pili, and the toxR regulon are essential for Vibrio cholerae pathogenesis in humans. J Exp Med, *168*, 1487–1492.

145. Hikita, A, Yana, I, Wakeyama, H, Nakamura, M, Kadono, Y, Oshima, Y, Nakamura, K, Seiki, M, and Tanaka, S (2006) Negative regulation of osteoclastogenesis by ectodomain shedding of receptor activator of NF-kappaB ligand. J Biol Chem, *281*, 36846–36855.

146. Hirose, K, Shimoda, N, and Kikuchi, Y (2011) Expression patterns of lgr4 and lgr6 during zebrafish development. Gene Expr Patterns, *11*, 378–383.

147. Hooper, LV, Stappenbeck, TS, Hong, CV, and Gordon, JI (2003) Angiogenins: a new class of microbicidal proteins involved in innate immunity. Nat Immunol, *4*, 269–273.

148. Hooper, LV, Wong, MH, Thelin, A, Hansson, L, Falk, PG, and Gordon, JI (2001) Molecular analysis of commensal host-microbial relationships in the intestine. Science, *291*, 881–884.

149. Hoover, B, Baena, V, Kaelberer, MM, Getaneh, F, Chinchilla, S, and Bohórquez, DV (2017) The intestinal tuft cell nanostructure in 3D. Sci Rep, *7*, 1652.

150. Horng, JL, Chao, PL, Chen, PY, Shih, TH, and Lin, LY (2015) Aquaporin 1 Is Involved in Acid Secretion by Ionocytes of Zebrafish Embryos through Facilitating CO_2 Transport. PLoS One, *10*, e0136440.

151. Hoshijima, K, Jurynec, MJ, Klatt Shaw, D, Jacobi, AM, Behlke, MA, and Grunwald, DJ (2019) Highly Efficient CRISPR-Cas9-Based Methods for Generating Deletion Mutations and F0 Embryos that Lack Gene Function in Zebrafish. Dev Cell, *51*, 645–657.e4.

152. Howe, JR, Roth, S, Ringold, JC, Summers, RW, Järvinen, HJ, Sistonen, P, Tomlinson, IP, Houlston, RS, Bevan, S, Mitros, FA, Stone, EM, and Aaltonen, LA (1998) Mutations in the SMAD4/DPC4 gene in juvenile polyposis. Science, *280*, 1086–1088.

153. Huang, S, Wang, Y, Luo, L, Li, X, Jin, X, Li, S, Yu, X, Yang, M, and Guo, Z (2019) BMP2 Is Related to Hirschsprung's Disease and Required for Enteric Nervous System Development. Front Cell Neurosci, *13*, 523.

154. Hung, CM, and Li, C (2004) Identification and phylogenetic analyses of the protein arginine methyltransferase gene family in fish and ascidians. Gene, *340*, 179–187.

155. Husebye, E, Hellström, PM, and Midtvedt, T (1994) Intestinal microflora stimulates myoelectric activity of rat small intestine by promoting cyclic initiation and aboral propagation of migrating myoelectric complex. Dig Dis Sci, *39*, 946–956.

156. Iger, Y, and Abraham, M (1997) Rodlet cells in the epidermis of fish exposed to stressors. Tissue Cell, *29*, 431–438.

157. Ikeda, F, Matsubara, T, Tsurukai, T, Hata, K, Nishimura, R, and Yoneda, T (2008) JNK/c-Jun signaling mediates an anti-apoptotic effect of RANKL in osteoclasts. J Bone Miner Res, *23*, 907–914.

158. Isogai, S, Horiguchi, M, and Weinstein, BM (2001) The vascular anatomy of the developing zebrafish: an atlas of embryonic and early larval development. Dev Biol, *230*, 278–301.

159. Jacobi, AM, Rettig, GR, Turk, R, Collingwood, MA, Zeiner, SA, Quadros, RM, Harms, DW, Bonthuis, PJ, Gregg, C, Ohtsuka, M, Gurumurthy, CB, and Behlke, MA (2017) Simplified CRISPR tools for efficient genome editing and streamlined protocols for their delivery into mammalian cells and mouse zygotes. Methods, *121-122*, 16–28.

160. Jenny, M, Uhl, C, Roche, C, Duluc, I, Guillermin, V, Guillemot, F, Jensen, J, Kedinger, M, and Gradwohl, G (2002) Neurogenin3 is differentially required for endocrine cell fate specification in the intestinal and gastric epithelium. EMBO J, *21*, 6338–6347.

161. Jevtov, I, Samuelsson, T, Yao, G, Amsterdam, A, and Ribbeck, K (2014) Zebrafish as a model to study live mucus physiology. Sci Rep, *4*, 6653.

162. Jo-Watanabe, A, Okuno, T, and Yokomizo, T (2019) The Role of Leukotrienes as Potential Therapeutic Targets in Allergic Disorders. Int J Mol Sci, *20*,

163. Johansson, ME, Phillipson, M, Petersson, J, Velcich, A, Holm, L, and Hansson, GC (2008) The inner of the two Muc2 mucin-dependent mucus layers in colon is devoid of bacteria. Proc Natl Acad Sci U S A, *105*, 15064–15069.

164. Johansson, ME, Sjövall, H, and Hansson, GC (2013) The gastrointestinal mucus system in health and disease. Nat Rev Gastroenterol Hepatol, *10*, 352–361.

165. Joshi, A, Kostiuk, B, Rogers, A, Teschler, J, Pukatzki, S, and Yildiz, FH (2017) Rules of Engagement: The Type VI Secretion System in Vibrio cholerae. Trends Microbiol, *25*, 267–279.

166. Jugder, BE, Batista, JH, Gibson, JA, Cunningham, PM, Asara, JM, and Watnick, PI (2022) Vibrio cholerae high cell density quorum sensing activates the host intestinal innate immune response. Cell Rep, *40*, 111368.

167. Jugder, BE, Kamareddine, L, and Watnick, PI (2021) Microbiota-derived acetate activates intestinal innate immunity via the Tip60 histone acetyltransferase complex. Immunity, *54*, 1683–1697.e3.

168. Kanaya, T, Hase, K, Takahashi, D, Fukuda, S, Hoshino, K, Sasaki, I, Hemmi, H, Knoop, KA, Kumar, N, Sato, M, Katsuno, T, Yokosuka, O, Toyooka, K, Nakai, K, Sakamoto, A, Kitahara, Y, Jinnohara, T, McSorley, SJ, Kaisho, T, Williams, IR, and Ohno, H (2012) The Ets transcription factor Spi-B is essential for the differentiation of intestinal microfold cells. Nat Immunol, *13*, 729–736.

169. Kanaya, T, Sakakibara, S, Jinnohara, T, Hachisuka, M, Tachibana, N, Hidano, S, Kobayashi, T, Kimura, S, Iwanaga, T, Nakagawa, T, Katsuno, T, Kato, N, Akiyama, T, Sato, T, Williams, IR, and Ohno, H (2018) Development of intestinal M cells and follicle-associated epithelium is regulated by TRAF6-mediated NF-κB signaling. J Exp Med, *215*, 501–519.

170. Kanazawa, K, and Kudo, A (2005) Self-assembled RANK induces osteoclastogenesis ligand-independently. J Bone Miner Res, *20*, 2053–2060.

171. Kandori, H, Hirayama, K, Takeda, M, and Doi, K (1996) Histochemical, lectin-histochemical and morphometrical characteristics of intestinal goblet cells of germfree and conventional mice. Exp Anim, *45*, 155–160.

172. Kanther, M, Sun, X, Mühlbauer, M, Mackey, LC, Flynn, EJ, Bagnat, M, Jobin, C, and Rawls, JF (2011) Microbial colonization induces dynamic temporal and spatial patterns of NF-κB activation in the zebrafish digestive tract. Gastroenterology, *141*, 197–207.

173. Kao, RM, Rurik, JG, Farr, GH, Dong, XR, Majesky, MW, and Maves, L (2015) Pbx4 is Required for the Temporal Onset of Zebrafish Myocardial Differentiation. J Dev Biol, *3*, 93–111.

174. Karlsson, EK, Harris, JB, Tabrizi, S, Rahman, A, Shlyakhter, I, Patterson, N, O'Dushlaine, C, Schaffner, SF, Gupta, S, Chowdhury, F, Sheikh, A, Shin, OS, Ellis, C, Becker, CE, Stuart, LM, Calderwood, SB, Ryan, ET, Qadri, F, Sabeti, PC, and Larocque, RC (2013) Natural selection in a bangladeshi population from the cholera-endemic ganges river delta. Sci Transl Med, *5*, 192ra86.

175. Katlinskaya, YV, Katlinski, KV, Lasri, A, Li, N, Beiting, DP, Durham, AC, Yang, T, Pikarsky, E, Lengner, CJ, Johnson, FB, Ben-Neriah, Y, and Fuchs, SY (2016) Type I Interferons Control Proliferation and Function of the Intestinal Epithelium. Mol Cell Biol, *36*, 1124–1135.

176. Katzenback, BA (2015) Antimicrobial Peptides as Mediators of Innate Immunity in Teleosts. Biology (Basel), *4*, 607–639.

177. Kawai, T, and Akira, S (2011) Toll-like receptors and their crosstalk with other innate receptors in infection and immunity. Immunity, *34*, 637–650.

178. Kelly, D, Campbell, JI, King, TP, Grant, G, Jansson, EA, Coutts, AG, Pettersson, S, and Conway, S (2004) Commensal anaerobic gut bacteria attenuate inflammation by regulating nuclear-cytoplasmic shuttling of PPAR-gamma and RelA. Nat Immunol, *5*, 104–112.

179. Kim, KA, Kakitani, M, Zhao, J, Oshima, T, Tang, T, Binnerts, M, Liu, Y, Boyle, B, Park, E, Emtage, P, Funk, WD, and Tomizuka, K (2005) Mitogenic influence of human R-spondin1 on the intestinal epithelium. Science, *309*, 1256–1259.

180. Kim, TH, Li, F, Ferreiro-Neira, I, Ho, LL, Luyten, A, Nalapareddy, K, Long, H, Verzi, M, and Shivdasani, RA (2014) Broadly permissive intestinal chromatin underlies lateral inhibition and cell plasticity. Nature, *506*, 511–515.

181. Kitsera, N, Khobta, A, and Epe, B (2007) Destabilized green fluorescent protein detects rapid removal of transcription blocks after genotoxic exposure. Biotechniques, *43*, 222–227.

182. Klose, KE (2000) The suckling mouse model of cholera. Trends Microbiol, *8*, 189–191.

183. Knoop, KA, Kumar, N, Butler, BR, Sakthivel, SK, Taylor, RT, Nochi, T, Akiba, H, Yagita, H, Kiyono, H, and Williams, IR (2009) RANKL is necessary and sufficient to initiate development of antigen-sampling M cells in the intestinal epithelium. J Immunol, *183*, 5738–5747.

184. Knoop, KA, McDonald, KG, McCrate, S, McDole, JR, and Newberry, RD (2015) Microbial sensing by goblet cells controls immune surveillance of luminal antigens in the colon. Mucosal Immunol, *8*, 198–210.

185. Koch, BEV, Yang, S, Lamers, G, Stougaard, J, and Spaink, HP (2018) Intestinal microbiome adjusts the innate immune setpoint during colonization through negative regulation of MyD88. Nat Commun, *9*, 4099.

186. Korbut, R, Mehrdana, F, Kania, PW, Larsen, MH, Frees, D, Dalsgaard, I, and Jørgensen, L (2016) Antigen Uptake during Different Life Stages of Zebrafish (Danio rerio) Using a GFP-Tagged Yersinia ruckeri. PLoS One, *11*, e0158968.

187. Kudelka, MR, Stowell, SR, Cummings, RD, and Neish, AS (2020) Intestinal epithelial glycosylation in homeostasis and gut microbiota interactions in IBD. Nat Rev Gastroenterol Hepatol, *17*, 597–617.

188. Kwan, KM, Fujimoto, E, Grabher, C, Mangum, BD, Hardy, ME, Campbell, DS, Parant, JM, Yost, HJ, Kanki, JP, and Chien, CB (2007) The Tol2kit: a multisite gateway-based construction kit for Tol2 transposon transgenesis constructs. Dev Dyn, *236*, 3088–3099.

189. Lam, SH, Chua, HL, Gong, Z, Lam, TJ, and Sin, YM (2004) Development and maturation of the immune system in zebrafish, Danio rerio: a gene expression profiling, in situ hybridization and immunological study. Dev Comp Immunol, *28*, 9–28.

190. Lavergne, A, Tarifeño-Saldivia, E, Pirson, J, Reuter, AS, Flasse, L, Manfroid, I, Voz, ML, and Peers, B (2020) Pancreatic and intestinal endocrine cells in zebrafish share common transcriptomic signatures and regulatory programmes. BMC Biol, *18*, 109.

191. Le, HTMD, Lie, KK, Giroud-Argoud, J, Rønnestad, I, and Sæle, Ø (2019) Effects of Cholecystokinin (CCK) on Gut Motility in the Stomachless Fish Ballan Wrasse (Labrus bergylta). Front Neurosci, *13*, 553.

192. Lee, J, Rachmilewitz, D, and Raz, E (2006) Homeostatic effects of TLR9 signaling in experimental colitis. Ann N Y Acad Sci, *1072*, 351–355.

193. Lee, K, Chung, YH, Ahn, H, Kim, H, Rho, J, and Jeong, D (2016) Selective Regulation of MAPK Signaling Mediates RANKL-dependent Osteoclast Differentiation. Int J Biol Sci, *12*, 235–245.

194. Lei, W, Ren, W, Ohmoto, M, Urban, JF, Matsumoto, I, Margolskee, RF, and Jiang, P (2018) Activation of intestinal tuft cell-expressed Sucnr1 triggers type 2 immunity in the mouse small intestine. Proc Natl Acad Sci U S A, *115*, 5552–5557.

195. Lenard, A, Daetwyler, S, Betz, C, Ellertsdottir, E, Belting, HG, Huisken, J, and Affolter, M (2015) Endothelial cell self-fusion during vascular pruning. PLoS Biol, *13*, e1002126.

196. Levraud, JP, Jouneau, L, Briolat, V, Laghi, V, and Boudinot, P (2019) IFN-Stimulated Genes in Zebrafish and Humans Define an Ancient Arsenal of Antiviral Immunity. J Immunol, *203*, 3361–3373.

197. Li, B, Wang, P, Jiao, J, Wei, H, Xu, W, and Zhou, P (2022) Roles of the RANKL-RANK Axis in Immunity-Implications for Pathogenesis and Treatment of Bone Metastasis. Front Immunol, *13*, 824117.

198. Li, C, Ma, H, Wang, Y, Cao, Z, Graves-Deal, R, Powell, AE, Starchenko, A, Ayers, GD, Washington, MK, Kamath, V, Desai, K, Gerdes, MJ, Solnica-Krezel, L, and Coffey, RJ (2014) Excess PLAC8 promotes an unconventional ERK2-dependent EMT in colon cancer. J Clin Invest, *124*, 2172–2187.

199. Li, H, Zhang, M, Linghu, E, Zhou, F, Herman, JG, Hu, L, and Guo, M (2018) Epigenetic silencing of TMEM176A activates ERK signaling in human hepatocellular carcinoma. Clin Epigenetics, *10*, 137.

200. Li, HJ, Ray, SK, Singh, NK, Johnston, B, and Leiter, AB (2011) Basic helix-loop-helix transcription factors and enteroendocrine cell differentiation. Diabetes Obes Metab, *13 Suppl 1*, 5–12.

201. Li, J, Prochaska, M, Maney, L, and Wallace, KN (2020) Development and organization of the zebrafish intestinal epithelial stem cell niche. Dev Dyn, *249*, 76–87.

202. Li, Y, Cao, X, Jin, X, and Jin, T (2017) Pattern recognition receptors in zebrafish provide functional and evolutionary insight into innate immune signaling pathways. Cell Mol Immunol, *14*, 80–89.

203. Lickwar, CR, Camp, JG, Weiser, M, Cocchiaro, JL, Kingsley, DM, Furey, TS, Sheikh, SZ, and Rawls, JF (2017) Genomic dissection of conserved transcriptional regulation in intestinal epithelial cells. PLoS Biol, *15*, e2002054.

204. Lin, TY, Liao, BK, Horng, JL, Yan, JJ, Hsiao, CD, and Hwang, PP (2008) Carbonic anhydrase 2-like a and 15a are involved in acid-base regulation and Na+ uptake in zebrafish H+-ATPase-rich cells. Am J Physiol Cell Physiol, *294*, C1250–60.

205. Lin, Z, Luo, M, Zhou, B, Liu, Y, and Sun, H (2021) CFTR regulates embryonic T lymphopoiesis via Wnt signaling in zebrafish. Immunol Lett, *234*, 47–53.

206. Liu, X, Cao, X, Wang, S, Ji, G, Zhang, S, and Li, H (2017) Identification of Ly2 members as antimicrobial peptides from zebrafish Danio rerio. Biosci Rep, *37*,

207. Liu, X, Nagy, P, Bonfini, A, Houtz, P, Bing, XL, Yang, X, and Buchon, N (2022) Microbes affect gut epithelial cell composition through immune-dependent regulation of intestinal stem cell differentiation. Cell Rep, *38*, 110572.

208. Løkka, G, and Koppang, EO (2016) Antigen sampling in the fish intestine. Dev Comp Immunol, *64*, 138–149.

209. López Nadal, A, Ikeda-Ohtsubo, W, Sipkema, D, Peggs, D, McGurk, C, Forlenza, M, Wiegertjes, GF, and Brugman, S (2020) Feed, Microbiota, and Gut Immunity: Using the Zebrafish Model to Understand Fish Health. Front Immunol, *11*, 114.

210. Løvmo, SD, Speth, MT, Repnik, U, Koppang, EO, Griffiths, GW, and Hildahl, JP (2017) Translocation of nanoparticles and Mycobacterium marinum across the intestinal epithelium in zebrafish and the role of the mucosal immune system. Dev Comp Immunol, *67*, 508–518.

211. Luciano, L, and Reale, E (1979) A new morphological aspect of the brush cells of the mouse gallbladder epithelium. Cell Tissue Res, *201*, 37–44.

212. Luna Velez, MV, Neikes, HK, Snabel, RR, Quint, Y, Qian, C, Martens, A, Veenstra, GJC, Freeman, MR, van Heeringen, SJ, and Vermeulen, M (2023) ONECUT2 regulates RANKL-dependent enterocyte and microfold cell differentiation in the small intestine; a multi-omics study. Nucleic Acids Res, *51*, 1277–1296.

213. Luo, J, Yang, Z, Ma, Y, Yue, Z, Lin, H, Qu, G, Huang, J, Dai, W, Li, C, Zheng, C, Xu, L, Chen, H, Wang, J, Li, D, Siwko, S, Penninger, JM, Ning, G, Xiao, J, and Liu, M (2016) LGR4 is a receptor for RANKL and negatively regulates osteoclast differentiation and bone resorption. Nat Med, *22*, 539–546.

214. Ma, D, Wei, Y, and Liu, F (2013) Regulatory mechanisms of thymus and T cell development. Dev Comp Immunol, *39*, 91–102.

215. Macosko, EZ, Basu, A, Satija, R, Nemesh, J, Shekhar, K, Goldman, M, Tirosh, I, Bialas, AR, Kamitaki, N, Martersteck, EM, Trombetta, JJ, Weitz, DA, Sanes, JR, Shalek, AK, Regev, A, and McCarroll, SA (2015) Highly Parallel Genome-wide Expression Profiling of Individual Cells Using Nanoliter Droplets. Cell, *161*, 1202–1214.

216. Macpherson, AJ, Gatto, D, Sainsbury, E, Harriman, GR, Hengartner, H, and Zinkernagel, RM (2000) A primitive T cell-independent mechanism of intestinal mucosal IgA responses to commensal bacteria. Science, *288*, 2222–2226.

217. Maehr, T, Costa, MM, Vecino, JL, Wadsworth, S, Martin, SA, Wang, T, and Secombes, CJ (2013) Transforming growth factor-β1b: a second TGF-β1 paralogue in the rainbow trout (Oncorhynchus mykiss) that has a lower constitutive expression but is more responsive to immune stimulation. Fish Shellfish Immunol, *34*, 420–432.

218. Magalhaes, JG, Rubino, SJ, Travassos, LH, Le Bourhis, L, Duan, W, Sellge, G, Geddes, K, Geddes, K, Reardon, C, Lechmann, M, Carneiro, LA, Selvanantham, T, Fritz, JH, Taylor, BC, Artis, D, Mak, TW, Comeau, MR, Croft, M, Girardin, SE, and Philpott, DJ (2011) Nucleotide oligomerization domain-containing proteins instruct T cell helper type 2 immunity through stromal activation. Proc Natl Acad Sci U S A, *108*, 14896–14901.

219. Man, QW, Zhang, LZ, Zhao, Y, Liu, JY, Zheng, YY, Zhao, YF, and Liu, B (2018) Lymphocyte-derived microparticles stimulate osteoclastogenesis by inducing RANKL in fibroblasts of odontogenic keratocysts. Oncol Rep, *40*, 3335–3345.

220. Massaquoi, MS, Kong, GL, Chilin-Fuentes, D, Ngo, JS, Horve, PF, Melancon, E, Hamilton, MK, Eisen, JS, and Guillemin, K (2023) Cell-type-specific responses to the microbiota across all tissues of the larval zebrafish. Cell Rep, *42*, 112095.

221. Matthews, RP, Lorent, K, Russo, P, and Pack, M (2004) The zebrafish onecut gene hnf-6 functions in an evolutionarily conserved genetic pathway that regulates vertebrate biliary development. Dev Biol, *274*, 245–259.

222. McDole, JR, Wheeler, LW, McDonald, KG, Wang, B, Konjufca, V, Knoop, KA, Newberry, RD, and Miller, MJ (2012) Goblet cells deliver luminal antigen to CD103+ dendritic cells in the small intestine. Nature, *483*, 345–349.

223. McGinty, JW, Ting, HA, Billipp, TE, Nadjsombati, MS, Khan, DM, Barrett, NA, Liang, HE, Matsumoto, I, and von Moltke, J (2020) Tuft-Cell-Derived Leukotrienes Drive Rapid Anti-helminth Immunity in the Small Intestine but Are Dispensable for Anti-protist Immunity. Immunity, *52*, 528–541.e7.

224. Medzhitov, R, Preston-Hurlburt, P, and Janeway, CA (1997) A human homologue of the Drosophila Toll protein signals activation of adaptive immunity. Nature, *388*, 394–397.

225. Meijer, AH, Gabby Krens, SF, Medina Rodriguez, IA, He, S, Bitter, W, Ewa Snaar-Jagalska, B, and Spaink, HP (2004) Expression analysis of the Toll-like receptor and TIR domain adaptor families of zebrafish. Mol Immunol, *40*, 773–783.

226. Melancon, E, Gomez De La Torre Canny, S, Sichel, S, Kelly, M, Wiles, TJ, Rawls, JF, Eisen, JS, and Guillemin, K (2017) Best practices for germ-free derivation and gnotobiotic zebrafish husbandry. Methods Cell Biol, *138*, 61–100.

227. Merrell, DS, Butler, SM, Qadri, F, Dolganov, NA, Alam, A, Cohen, MB, Calderwood, SB, Schoolnik, GK, and Camilli, A (2002) Host-induced epidemic spread of the cholera bacterium. Nature, *417*, 642–645.

228. Micchelli, CA, and Perrimon, N (2006) Evidence that stem cells reside in the adult Drosophila midgut epithelium. Nature, *439*, 475–479.

229. Mirpuri, J, Brazil, JC, Berardinelli, AJ, Nasr, TR, Cooper, K, Schnoor, M, Lin, PW, Parkos, CA, and Louis, NA (2010) Commensal Escherichia coli reduces epithelial apoptosis through IFN-alphaA-mediated induction of guanylate binding protein-1 in human and murine models of developing intestine. J Immunol, *184*, 7186–7195.

230. Mitchell, KC, Breen, P, Britton, S, Neely, MN, and Withey, JH (2017) Quantifying Vibrio cholerae Enterotoxicity in a Zebrafish Infection Model. Appl Environ Microbiol, *83*,

231. Mitchell, KC, and Withey, JH (2018) Danio rerio as a Native Host Model for Understanding Pathophysiology of Vibrio cholerae. Methods Mol Biol, *1839*, 97–102.

232. Molenaar, M, van de Wetering, M, Oosterwegel, M, Peterson-Maduro, J, Godsave, S, Korinek, V, Roose, J, Destrée, O, and Clevers, H (1996) XTcf-3 transcription factor mediates beta-catenin-induced axis formation in Xenopus embryos. Cell, *86*, 391–399.

233. Montoro, DT, Haber, AL, Rood, JE, Regev, A, and Rajagopal, J (2020) A Synthesis Concerning Conservation and Divergence of Cell Types across Epithelia. Cold Spring Harb Perspect Biol, *12*,

234. Moran-Ramos, S, Tovar, AR, and Torres, N (2012) Diet: friend or foe of enteroendocrine cells--how it interacts with enteroendocrine cells. Adv Nutr, *3*, 8–20.

235. Mörbe, UM, Jørgensen, PB, Fenton, TM, von Burg, N, Riis, LB, Spencer, J, and Agace, WW (2021) Human gut-associated lymphoid tissues (GALT); diversity, structure, and function. Mucosal Immunol, *14*, 793–802.

236. Mori-Akiyama, Y, van den Born, M, van Es, JH, Hamilton, SR, Adams, HP, Zhang, J, Clevers, H, and de Crombrugghe, B (2007) SOX9 is required for the differentiation of paneth cells in the intestinal epithelium. Gastroenterology, *133*, 539–546.

237. Mougous, JD, Cuff, ME, Raunser, S, Shen, A, Zhou, M, Gifford, CA, Goodman, AL, Joachimiak, G, Ordoñez, CL, Lory, S, Walz, T, Joachimiak, A, and Mekalanos, JJ (2006) A virulence locus of Pseudomonas aeruginosa encodes a protein secretion apparatus. Science, *312*, 1526–1530.

238. Mouillesseaux, KP, Wiley, DS, Saunders, LM, Wylie, LA, Kushner, EJ, Chong, DC, Citrin, KM, Barber, AT, Park, Y, Kim, JD, Samsa, LA, Kim, J, Liu, J, Jin, SW, and Bautch, VL (2016) Notch regulates BMP responsiveness and lateral branching in vessel networks via SMAD6. Nat Commun, *7*, 13247.

239. Mukaigasa, K, Nguyen, LT, Li, L, Nakajima, H, Yamamoto, M, and Kobayashi, M (2012) Genetic evidence of an evolutionarily conserved role for Nrf2 in the protection against oxidative stress. Mol Cell Biol, *32*, 4455–4461.

240. Muncan, V, Faro, A, Haramis, AP, Hurlstone, AF, Wienholds, E, van Es, J, Korving, J, Begthel, H, Zivkovic, D, and Clevers, H (2007) T-cell factor 4 (Tcf7l2) maintains proliferative compartments in zebrafish intestine. EMBO Rep, *8*, 966–973.

241. Muncan, V, Heijmans, J, Krasinski, SD, Büller, NV, Wildenberg, ME, Meisner, S, Radonjic, M, Stapleton, KA, Lamers, WH, Biemond, I, van den Bergh Weerman, MA, O'Carroll, D, Hardwick, JC, Hommes, DW, and van den Brink, GR (2011) Blimp1 regulates the transition of neonatal to adult intestinal epithelium. Nat Commun, *2*, 452.

242. Murdoch, CC, Espenschied, ST, Matty, MA, Mueller, O, Tobin, DM, and Rawls, JF (2019) Intestinal Serum amyloid A suppresses systemic neutrophil activation and bactericidal activity in response to microbiota colonization. PLoS Pathog, *15*, e1007381.

243. Myers, TJ, and Schat, KA (1990) Intestinal IgA response and immunity to rotavirus infection in normal and antibody-deficient chickens. Avian Pathol, *19*, 697–712.

244. Nag, D, Mitchell, K, Breen, P, and Withey, JH (2018) Quantifying Vibrio cholerae Colonization and Diarrhea in the Adult Zebrafish Model. J Vis Exp,

245. Nakashima, T, Hayashi, M, and Takayanagi, H (2012) New insights into osteoclastogenic signaling mechanisms. Trends Endocrinol Metab, *23*, 582–590.

246. Natividad, JM, and Verdu, EF (2013) Modulation of intestinal barrier by intestinal microbiota: pathological and therapeutic implications. Pharmacol Res, *69*, 42–51.

247. Neish, AS (2009) Microbes in gastrointestinal health and disease. Gastroenterology, *136*, 65–80.

248. Ng, AN, de Jong-Curtain, TA, Mawdsley, DJ, White, SJ, Shin, J, Appel, B, Dong, PD, Stainier, DY, and Heath, JK (2005) Formation of the digestive system in zebrafish: III. Intestinal epithelium morphogenesis. Dev Biol, *286*, 114–135.

249. Nicenboim, J, Malkinson, G, Lupo, T, Asaf, L, Sela, Y, Mayseless, O, Gibbs-Bar, L, Senderovich, N, Hashimshony, T, Shin, M, Jerafi-Vider, A, Avraham-Davidi, I, Krupalnik, V, Hofi, R, Almog, G, Astin, JW, Golani, O, Ben-Dor, S, Crosier, PS, Herzog, W, Lawson, ND, Hanna, JH, Yanai, I, and Yaniv, K (2015) Lymphatic vessels arise from specialized angioblasts within a venous niche. Nature, *522*, 56–61.

250. Nikaido, M, Law, EW, and Kelsh, RN (2013) A systematic survey of expression and function of zebrafish frizzled genes. PLoS One, *8*, e54833.

251. Noah, TK, Kazanjian, A, Whitsett, J, and Shroyer, NF (2010) SAM pointed domain ETS factor (SPDEF) regulates terminal differentiation and maturation of intestinal goblet cells. Exp Cell Res, *316*, 452–465.

252. Nusse, R, and Clevers, H (2017) Wnt/β-Catenin Signaling, Disease, and Emerging Therapeutic Modalities. Cell, *169*, 985–999.

253. Oehlers, SH, Flores, MV, Hall, CJ, Crosier, KE, and Crosier, PS (2012) Retinoic acid suppresses intestinal mucus production and exacerbates experimental enterocolitis. Dis Model Mech, *5*, 457–467.

254. Oehlers, SH, Flores, MV, Okuda, KS, Hall, CJ, Crosier, KE, and Crosier, PS (2011) A chemical enterocolitis model in zebrafish larvae that is dependent on microbiota and responsive to pharmacological agents. Dev Dyn, *240*, 288–298.

255. Ohlstein, B, and Spradling, A (2006) The adult Drosophila posterior midgut is maintained by pluripotent stem cells. Nature, *439*, 470–474.

256. Olden, T, Akhtar, T, Beckman, SA, and Wallace, KN (2008) Differentiation of the zebrafish enteric nervous system and intestinal smooth muscle. Genesis, *46*, 484–498.

257. Olivier, V, Queen, J, and Satchell, KJ (2009) Successful small intestine colonization of adult mice by Vibrio cholerae requires ketamine anesthesia and accessory toxins. PLoS One, *4*, e7352.

258. Ouchi, T, Morimura, S, Dow, LE, Miyoshi, H, and Udey, MC (2021) EpCAM (CD326) Regulates Intestinal Epithelial Integrity and Stem Cells via Rho-Associated Kinase. Cells, *10*,

259. Oyesola, OO, Shanahan, MT, Kanke, M, Mooney, BM, Webb, LM, Smita, S, Matheson, MK, Campioli, P, Pham, D, Früh, SP, McGinty, JW, Churchill, MJ, Cahoon, JL, Sundaravaradan, P, Flitter, BA, Mouli, K, Nadjsombati, MS, Kamynina, E, Peng, SA, Cubitt, RL, Gronert, K, Lord, JD, Rauch, I, von Moltke, J, Sethupathy, P, and Tait Wojno, ED (2021) PGD2 and CRTH2 counteract Type 2 cytokine-elicited intestinal epithelial responses during helminth infection. J Exp Med, *218*,

260. Pack, M, Solnica-Krezel, L, Malicki, J, Neuhauss, SC, Schier, AF, Stemple, DL, Driever, W, and Fishman, MC (1996) Mutations affecting development of zebrafish digestive organs. Development, *123*, 321–328.

261. Panneck, AR, Rafiq, A, Schütz, B, Soultanova, A, Deckmann, K, Chubanov, V, Gudermann, T, Weihe, E, Krasteva-Christ, G, Grau, V, del Rey, A, and Kummer, W (2014) Cholinergic epithelial cell with chemosensory traits in murine thymic medulla. Cell Tissue Res, *358*, 737–748.

262. Parikh, K, Antanaviciute, A, Fawkner-Corbett, D, Jagielowicz, M, Aulicino, A, Lagerholm, C, Davis, S, Kinchen, J, Chen, HH, Alham, NK, Ashley, N, Johnson, E, Hublitz, P, Bao, L, Lukomska, J, Andev, RS, Björklund, E, Kessler, BM, Fischer, R, Goldin, R, Koohy, H, and Simmons, A (2019) Colonic epithelial cell diversity in health and inflammatory bowel disease. Nature, *567*, 49–55.

263. Park, J, Levic, DS, Sumigray, KD, Bagwell, J, Eroglu, O, Block, CL, Eroglu, C, Barry, R, Lickwar, CR, Rawls, JF, Watts, SA, Lechler, T, and Bagnat, M (2019) Lysosome-Rich Enterocytes Mediate Protein Absorption in the Vertebrate Gut. Dev Cell, *51*, 7–20.e6.

264. Patankar, JV, and Becker, C (2020) Cell death in the gut epithelium and implications for chronic inflammation. Nat Rev Gastroenterol Hepatol, *17*, 543–556.

265. Pellegrinet, L, Rodilla, V, Liu, Z, Chen, S, Koch, U, Espinosa, L, Kaestner, KH, Kopan, R, Lewis, J, and Radtke, F (2011) Dll1- and dll4-mediated notch signaling are required for homeostasis of intestinal stem cells. Gastroenterology, *140*, 1230–1240.e1.

266. Perkins, A, Poole, LB, and Karplus, PA (2014) Tuning of peroxiredoxin catalysis for various physiological roles. Biochemistry, *53*, 7693–7705.

267. Perniss, A, Schmidt, P, Soultanova, A, Papadakis, T, Dahlke, K, Voigt, A, Schütz, B, Kummer, W, and Deckmann, K (2021) Development of epithelial cholinergic chemosensory cells of the urethra and trachea of mice. Cell Tissue Res, *385*, 21–35.

268. Peron, M, Dinarello, A, Meneghetti, G, Martorano, L, Facchinello, N, Vettori, A, Licciardello, G, Tiso, N, and Argenton, F (2020) The stem-like Stat3-responsive cells of zebrafish intestine are Wnt/β-catenin dependent. Development, *147*,

269. Perrigoue, J, Das, A, and Mora, JR (2014) Interplay of nutrients and microbial metabolites in intestinal immune homeostasis: distinct and common mechanisms of immune regulation in the small bowel and colon. Nestle Nutr Inst Workshop Ser, *79*, 57–71.

270. Perrone, EE, Chen, C, Longshore, SW, Okezie, O, Warner, BW, Sun, CC, Alaish, SM, and Strauch, ED (2010) Dietary bile acid supplementation improves intestinal integrity and survival in a murine model. J Pediatr Surg, *45*, 1256–1265.

271. Pham, LN, Kanther, M, Semova, I, and Rawls, JF (2008) Methods for generating and colonizing gnotobiotic zebrafish. Nat Protoc, *3*, 1862–1875.

272. Piarroux, R, Moore, S, and Rebaudet, S (2022) Cholera in Haiti. Presse Med, *51*, 104136.

273. Pukatzki, S, Ma, AT, Revel, AT, Sturtevant, D, and Mekalanos, JJ (2007) Type VI secretion system translocates a phage tail spike-like protein into target cells where it cross-links actin. Proc Natl Acad Sci U S A, *104*, 15508–15513.

274. Pukatzki, S, Ma, AT, Sturtevant, D, Krastins, B, Sarracino, D, Nelson, WC, Heidelberg, JF, and Mekalanos, JJ (2006) Identification of a conserved bacterial protein secretion system in Vibrio cholerae using the Dictyostelium host model system. Proc Natl Acad Sci U S A, *103*, 1528–1533.

275. Pyati, UJ, Cooper, MS, Davidson, AJ, Nechiporuk, A, and Kimelman, D (2006) Sustained Bmp signaling is essential for cloaca development in zebrafish. Development, *133*, 2275–2284.

276. Qi, Z, Li, Y, Zhao, B, Xu, C, Liu, Y, Li, H, Zhang, B, Wang, X, Yang, X, Xie, W, Li, B, Han, JJ, and Chen, YG (2017) BMP restricts stemness of intestinal Lgr5^{+} stem cells by directly suppressing their signature genes. Nat Commun, *8*, 13824.

277. Rachmilewitz, D, Katakura, K, Karmeli, F, Hayashi, T, Reinus, C, Rudensky, B, Akira, S, Takeda, K, Lee, J, Takabayashi, K, and Raz, E (2004) Toll-like receptor 9 signaling mediates the anti-inflammatory effects of probiotics in murine experimental colitis. Gastroenterology, *126*, 520–528.

278. Raj, B, Farrell, JA, Liu, J, El Kholtei, J, Carte, AN, Navajas Acedo, J, Du, LY, McKenna, A, Relić, Đ, Leslie, JM, and Schier, AF (2020) Emergence of Neuronal Diversity during Vertebrate Brain Development. Neuron, *108*, 1058–1074.e6.

279. Rajan, AM, Ma, RC, Kocha, KM, Zhang, DJ, and Huang, P (2020) Dual function of perivascular fibroblasts in vascular stabilization in zebrafish. PLoS Genet, *16*, e1008800.

280. Rawls, JF, Samuel, BS, and Gordon, JI (2004) Gnotobiotic zebrafish reveal evolutionarily conserved responses to the gut microbiota. Proc Natl Acad Sci U S A, *101*, 4596–4601.

281. Ray, SK, and Leiter, AB (2007) The basic helix-loop-helix transcription factor NeuroD1 facilitates interaction of Sp1 with the secretin gene enhancer. Mol Cell Biol, *27*, 7839–7847.

282. Rehfeld, JF (2017) Cholecystokinin-From Local Gut Hormone to Ubiquitous Messenger. Front Endocrinol (Lausanne), *8*, 47.

283. Reikvam, DH, Erofeev, A, Sandvik, A, Grcic, V, Jahnsen, FL, Gaustad, P, McCoy, KD, Macpherson, AJ, Meza-Zepeda, LA, and Johansen, FE (2011) Depletion of murine intestinal microbiota: effects on gut mucosa and epithelial gene expression. PLoS One, *6*, e17996.

284. Reinhardt, C, Bergentall, M, Greiner, TU, Schaffner, F, Ostergren-Lundén, G, Petersen, LC, Ruf, W, and Bäckhed, F (2012) Tissue factor and PAR1 promote microbiota-induced intestinal vascular remodelling. Nature, *483*, 627–631.

285. Reite, OB (2005) The rodlet cells of teleostean fish: their potential role in host defence in relation to the role of mast cells/eosinophilic granule cells. Fish Shellfish Immunol, *19*, 253–267.

286. Reuter, AS, Stern, D, Bernard, A, Goossens, C, Lavergne, A, Flasse, L, Von Berg, V, Manfroid, I, Peers, B, and Voz, ML (2022) Identification of an evolutionarily conserved domain in Neurod1 favouring enteroendocrine versus goblet cell fate. PLoS Genet, *18*, e1010109.

287. RHODIN, J, and DALHAMN, T (1956) Electron microscopy of the tracheal ciliated mucosa in rat. Z Zellforsch Mikrosk Anat, *44*, 345–412.

288. Rivera-Chávez, F, Meader, BT, Akosman, S, Koprivica, V, and Mekalanos, JJ (2022) A Potent Inhibitor of the Cystic Fibrosis Transmembrane Conductance Regulator Blocks Disease and Morbidity Due to Toxigenic Vibrio cholerae. Toxins (Basel), *14*,

289. Roach, G, Heath Wallace, R, Cameron, A, Emrah Ozel, R, Hongay, CF, Baral, R, Andreescu, S, and Wallace, KN (2013) Loss of ascl1a prevents secretory cell differentiation within the zebrafish intestinal epithelium resulting in a loss of distal intestinal motility. Dev Biol, *376*, 171–186.

290. Robinette, ML, Fuchs, A, Cortez, VS, Lee, JS, Wang, Y, Durum, SK, Gilfillan, S, Colonna, M, and Immunological, GC (2015) Transcriptional programs define molecular characteristics of innate lymphoid cell classes and subsets. Nat Immunol, *16*, 306–317.

291. Rodman, DM, and Zamudio, S (1991) The cystic fibrosis heterozygote--advantage in surviving cholera. Med Hypotheses, *36*, 253–258.

292. Rodríguez-Fraticelli, AE, Bagwell, J, Bosch-Fortea, M, Boncompain, G, Reglero-Real, N, García-León, MJ, Andrés, G, Toribio, ML, Alonso, MA, Millán, J, Perez, F, Bagnat, M, and Martín-Belmonte, F (2015) Developmental regulation of apical endocytosis controls epithelial patterning in vertebrate tubular organs. Nat Cell Biol, *17*, 241–250.

293. Roeselers, G, Mittge, EK, Stephens, WZ, Parichy, DM, Cavanaugh, CM, Guillemin, K, and Rawls, JF (2011) Evidence for a core gut microbiota in the zebrafish. ISME J, *5*, 1595–1608.

294. Rolig, AS, Parthasarathy, R, Burns, AR, Bohannan, BJ, and Guillemin, K (2015) Individual Members of the Microbiota Disproportionately Modulate Host Innate Immune Responses. Cell Host Microbe, *18*, 613–620.

295. Rolig, AS, Sweeney, EG, Kaye, LE, DeSantis, MD, Perkins, A, Banse, AV, Hamilton, MK, and Guillemin, K (2018) A bacterial immunomodulatory protein with lipocalin-like domains facilitates host-bacteria mutualism in larval zebrafish. Elife, *7*,

296. Rooks, MG, and Garrett, WS (2016) Gut microbiota, metabolites and host immunity. Nat Rev Immunol, *16*, 341–352.

297. Ross, MH, and Pawlina, W. (2006) Histology: A Text and Atlas: with Correlated Cell and Molecular Biology. Lippincott Wiliams & Wilkins).

298. Rossi, SW, Kim, MY, Leibbrandt, A, Parnell, SM, Jenkinson, WE, Glanville, SH, McConnell, FM, Scott, HS, Penninger, JM, Jenkinson, EJ, Lane, PJ, and Anderson, G (2007) RANK signals from CD4(+)3(-) inducer cells regulate development of Aire-expressing epithelial cells in the thymic medulla. J Exp Med, *204*, 1267–1272.

299. Runft, DL, Mitchell, KC, Abuaita, BH, Allen, JP, Bajer, S, Ginsburg, K, Neely, MN, and Withey, JH (2014) Zebrafish as a natural host model for Vibrio cholerae colonization and transmission. Appl Environ Microbiol, *80*, 1710–1717.

300. Sack, DA, Sack, RB, Nair, GB, and Siddique, AK (2004) Cholera. Lancet, *363*, 223–233.

301. Saez, A, Gomez-Bris, R, Herrero-Fernandez, B, Mingorance, C, Rius, C, and Gonzalez-Granado, JM (2021) Innate Lymphoid Cells in Intestinal Homeostasis and Inflammatory Bowel Disease. Int J Mol Sci, *22*,

302. Saqui-Salces, M, Keeley, TM, Grosse, AS, Qiao, XT, El-Zaatari, M, Gumucio, DL, Samuelson, LC, and Merchant, JL (2011) Gastric tuft cells express DCLK1 and are expanded in hyperplasia. Histochem Cell Biol, *136*, 191–204.

303. Sasaki, N, Sachs, N, Wiebrands, K, Ellenbroek, SI, Fumagalli, A, Lyubimova, A, Begthel, H, van den Born, M, van Es, JH, Karthaus, WR, Li, VS, López-Iglesias, C, Peters, PJ, van Rheenen, J, van Oudenaarden, A, and Clevers, H (2016) Reg4+ deep crypt secretory cells function as epithelial niche for Lgr5+ stem cells in colon. Proc Natl Acad Sci U S A, *113*, E5399–407.

304. Sato, A, Hisanaga, Y, Inoue, Y, Nagato, T, and Toh, H (2002) Three-dimensional structure of apical vesicles of tuft cells in the main excretory duct of the rat submandibular gland. Eur J Morphol, *40*, 235–239.

305. Sato, T, van Es, JH, Snippert, HJ, Stange, DE, Vries, RG, van den Born, M, Barker, N, Shroyer, NF, van de Wetering, M, and Clevers, H (2011) Paneth cells constitute the niche for Lgr5 stem cells in intestinal crypts. Nature, *469*, 415–418.

306. Sato, T, Vries, RG, Snippert, HJ, van de Wetering, M, Barker, N, Stange, DE, van Es, JH, Abo, A, Kujala, P, Peters, PJ, and Clevers, H (2009) Single Lgr5 stem cells build crypt-villus structures in vitro without a mesenchymal niche. Nature, *459*, 262–265.

307. Sayyaf Dezfuli, B, Castaldelli, G, and Giari, L (2018) Histopathological and ultrastructural assessment of two mugilid species infected with myxozoans and helminths. J Fish Dis, *41*, 299–307.

308. Sayyaf Dezfuli, B, Pironi, F, Maynard, B, Simoni, E, and Bosi, G (2022) Rodlet cells, fish immune cells and a sentinel of parasitic harm in teleost organs. Fish Shellfish Immunol, *121*, 516–534.

309. Schaefer, L (2014) Complexity of danger: the diverse nature of damage-associated molecular patterns. J Biol Chem, *289*, 35237–35245.

310. Schenkel, AR, Mamdouh, Z, Chen, X, Liebman, RM, and Muller, WA (2002) CD99 plays a major role in the migration of monocytes through endothelial junctions. Nat Immunol, *3*, 143–150.

311. Schindelin, J, Arganda-Carreras, I, Frise, E, Kaynig, V, Longair, M, Pietzsch, T, Preibisch, S, Rueden, C, Saalfeld, S, Schmid, B, Tinevez, JY, White, DJ, Hartenstein, V, Eliceiri, K,

Tomancak, P, and Cardona, A (2012) Fiji: an open-source platform for biological-image analysis. Nat Methods, *9*, 676–682.

312. Schuijers, J, Junker, JP, Mokry, M, Hatzis, P, Koo, BK, Sasselli, V, van der Flier, LG, Cuppen, E, van Oudenaarden, A, and Clevers, H (2015) Ascl2 acts as an R-spondin/Wnt-responsive switch to control stemness in intestinal crypts. Cell Stem Cell, *16*, 158–170.

313. Schumacher, MA, Hsieh, JJ, Liu, CY, Appel, KL, Waddell, A, Almohazey, D, Katada, K, Bernard, JK, Bucar, EB, Gadeock, S, Maselli, KM, Washington, MK, Grikscheit, TC, Warburton, D, Rosen, MJ, and Frey, MR (2021) Sprouty2 limits intestinal tuft and goblet cell numbers through GSK3β-mediated restriction of epithelial IL-33. Nat Commun, *12*, 836.

314. Secombes, CJ, and Chappell, LH (2004) Fish immune responses to experimental and natural infection with helminth parasites. Annu Rev Fish Diseases,

315. Secombes, CJ, Wang, T, Hong, S, Peddie, S, Crampe, M, Laing, KJ, Cunningham, C, and Zou, J (2001) Cytokines and innate immunity of fish. Dev Comp Immunol, *25*, 713–723.

316. Sekirov, I, Russell, SL, Antunes, LC, and Finlay, BB (2010) Gut microbiota in health and disease. Physiol Rev, *90*, 859–904.

317. Senderovich, Y, Izhaki, I, and Halpern, M (2010) Fish as reservoirs and vectors of Vibrio cholerae. PLoS One, *5*, e8607.

318. Shen, L, Qu, X, Li, H, Xu, C, Wei, M, Wang, Q, Ru, Y, Liu, B, Xu, Y, Li, K, Hu, J, Wang, L, Ma, Y, Li, M, Lai, X, Gao, L, Wu, K, Yao, L, Zheng, J, and Zhang, J (2018) NDRG2 facilitates colorectal cancer differentiation through the regulation of Skp2-p21/p27 axis. Oncogene, *37*, 1759–1774.

319. Shih, LJ, Lu, YF, Chen, YH, Lin, CC, Chen, JA, and Hwang, SP (2007) Characterization of the agr2 gene, a homologue of X. laevis anterior gradient 2, from the zebrafish, Danio rerio. Gene Expr Patterns, *7*, 452–460.

320. Shike, H, Shimizu, C, Lauth, X, and Burns, JC (2004) Organization and expression analysis of the zebrafish hepcidin gene, an antimicrobial peptide gene conserved among vertebrates. Dev Comp Immunol, *28*, 747–754.

321. Shin, M, Ferguson, M, Willms, RJ, Jones, LO, Petkau, K, and Foley, E (2022) Immune regulation of intestinal-stem-cell function in Drosophila. Stem Cell Reports, *17*, 741–755.

322. Shroyer, NF, Wallis, D, Venken, KJ, Bellen, HJ, and Zoghbi, HY (2005) Gfi1 functions downstream of Math1 to control intestinal secretory cell subtype allocation and differentiation. Genes Dev, *19*, 2412–2417.

323. Sigloch, C, Spitz, D, and Driever, W (2023) A network of Notch-dependent and -independent her genes controls neural stem and progenitor cells in the zebrafish thalamic proliferation zone. Development, *150*,

324. Smillie, CS, Biton, M, Ordovas-Montanes, J, Sullivan, KM, Burgin, G, Graham, DB, Herbst, RH, Rogel, N, Slyper, M, Waldman, J, Sud, M, Andrews, E, Velonias, G, Haber, AL, Jagadeesh, K, Vickovic, S, Yao, J, Stevens, C, Dionne, D, Nguyen, LT, Villani, AC, Hofree, M, Creasey, EA, Huang, H, Rozenblatt-Rosen, O, Garber, JJ, Khalili, H, Desch, AN, Daly, MJ, Ananthakrishnan, AN, Shalek, AK, Xavier, RJ, and Regev, A (2019) Intra- and Inter-cellular Rewiring of the Human Colon during Ulcerative Colitis. Cell, *178*, 714–730.e22.

325. Sommer, F, and Bäckhed, F (2013) The gut microbiota--masters of host development and physiology. Nat Rev Microbiol, *11*, 227–238.

326. Song, S, Li, X, Geng, C, Li, Y, and Wang, C (2020) Somatostatin stimulates colonic MUC2 expression through SSTR5-Notch-Hes1 signaling pathway. Biochem Biophys Res Commun, *521*, 1070–1076.

327. Spira, WM, Sack, RB, and Froehlich, JL (1981) Simple adult rabbit model for Vibrio cholerae and enterotoxigenic Escherichia coli diarrhea. Infect Immun, *32*, 739–747.

328. Stamataki, D, Holder, M, Hodgetts, C, Jeffery, R, Nye, E, Spencer-Dene, B, Winton, DJ, and Lewis, J (2011) Delta1 expression, cell cycle exit, and commitment to a specific secretory fate coincide within a few hours in the mouse intestinal stem cell system. PLoS One, *6*, e24484.

329. Stappenbeck, TS, Hooper, LV, and Gordon, JI (2002) Developmental regulation of intestinal angiogenesis by indigenous microbes via Paneth cells. Proc Natl Acad Sci U S A, *99*, 15451–15455.

330. Steed, AL, Christophi, GP, Kaiko, GE, Sun, L, Goodwin, VM, Jain, U, Esaulova, E, Artyomov, MN, Morales, DJ, Holtzman, MJ, Boon, ACM, Lenschow, DJ, and Stappenbeck, TS (2017) The

microbial metabolite desaminotyrosine protects from influenza through type I interferon. Science, *357*, 498–502.

331. Stefan, KL, Kim, MV, Iwasaki, A, and Kasper, DL (2020) Commensal Microbiota Modulation of Natural Resistance to Virus Infection. Cell, *183*, 1312–1324.e10.

332. Steiner, AB, Kim, T, Cabot, V, and Hudspeth, AJ (2014) Dynamic gene expression by putative hair-cell progenitors during regeneration in the zebrafish lateral line. Proc Natl Acad Sci U S A, *111*, E1393–401.

333. Stephens, WZ, Burns, AR, Stagaman, K, Wong, S, Rawls, JF, Guillemin, K, and Bohannan, BJ (2016) The composition of the zebrafish intestinal microbial community varies across development. ISME J, *10*, 644–654.

334. Strine, MS, and Wilen, CB (2022) Tuft cells are key mediators of interkingdom interactions at mucosal barrier surfaces. PLoS Pathog, *18*, e1010318.

335. Sullivan, C, Charette, J, Catchen, J, Lage, CR, Giasson, G, Postlethwait, JH, Millard, PJ, and Kim, CH (2009) The gene history of zebrafish tlr4a and tlr4b is predictive of their divergent functions. J Immunol, *183*, 5896–5908.

336. Sumanas, S, Jorniak, T, and Lin, S (2005) Identification of novel vascular endothelial-specific genes by the microarray analysis of the zebrafish cloche mutants. Blood, *106*, 534–541.

337. Sun, SC (2017) The non-canonical NF-κB pathway in immunity and inflammation. Nat Rev Immunol, *17*, 545–558.

338. Supek, F, Bošnjak, M, Škunca, N, and Šmuc, T (2011) REVIGO summarizes and visualizes long lists of gene ontology terms. PLoS One, *6*, e21800.

339. Takeda, K, and Akira, S (2005) Toll-like receptors in innate immunity. Int Immunol, *17*, 1–14.

340. Talbot, K, Kwong, RW, Gilmour, KM, and Perry, SF (2015) The water channel aquaporin-1a1 facilitates movement of CO_2 and ammonia in zebrafish (Danio rerio) larvae. J Exp Biol, *218*, 3931–3940.

341. Tang, Q, Iyer, S, Lobbardi, R, Moore, JC, Chen, H, Lareau, C, Hebert, C, Shaw, ML, Neftel, C, Suva, ML, Ceol, CJ, Bernards, A, Aryee, M, Pinello, L, Drummond, IA, and Langenau, DM

(2017) Dissecting hematopoietic and renal cell heterogeneity in adult zebrafish at single-cell resolution using RNA sequencing. J Exp Med, *214*, 2875–2887.

342. Taniguchi, K, and Karin, M (2018) NF-κB, inflammation, immunity and cancer: coming of age. Nat Rev Immunol, *18*, 309–324.

343. Tavakoli, S, Zhu, S, and Matsudaira, P (2022) Cell clusters containing intestinal stem cells line, the zebrafish intestine intervillus pocket. iScience, *25*, 104280.

344. Thakur, PC, Davison, JM, Stuckenholz, C, Lu, L, and Bahary, N (2014) Dysregulated phosphatidylinositol signaling promotes endoplasmic-reticulum-stress-mediated intestinal mucosal injury and inflammation in zebrafish. Dis Model Mech, *7*, 93–106.

345. Thambyrajah, R, Ucanok, D, Jalali, M, Hough, Y, Wilkinson, RN, McMahon, K, Moore, C, and Gering, M (2016) A gene trap transposon eliminates haematopoietic expression of zebrafish Gfi1aa, but does not interfere with haematopoiesis. Dev Biol, *417*, 25–39.

346. Thélohan, P (1892) Sur des sporozoaires indéterminés parasites des Poissons. J. Anatom. Physiol., *28*, 163–171.

347. Thiagarajah, JR, Donowitz, M, and Verkman, AS (2015) Secretory diarrhoea: mechanisms and emerging therapies. Nat Rev Gastroenterol Hepatol, *12*, 446–457.

348. Thisse, B, and Thisse, C (2004) Fast Release Clones: A High Throughput Expression Analysis. ZFIN Direct Data Submission. (http://zfin.org),

349. Thompson, CA, DeLaForest, A, and Battle, MA (2018) Patterning the gastrointestinal epithelium to confer regional-specific functions. Dev Biol, *435*, 97–108.

350. To, TT, Witten, PE, Renn, J, Bhattacharya, D, Huysseune, A, and Winkler, C (2012) Rankl-induced osteoclastogenesis leads to loss of mineralization in a medaka osteoporosis model. Development, *139*, 141–150.

351. Tomov, VT, Palko, O, Lau, CW, Pattekar, A, Sun, Y, Tacheva, R, Bengsch, B, Manne, S, Cosma, GL, Eisenlohr, LC, Nice, TJ, Virgin, HW, and Wherry, EJ (2017) Differentiation and Protective Capacity of Virus-Specific CD8^{+} T Cells Suggest Murine Norovirus Persistence in an Immune-Privileged Enteric Niche. Immunity, *47*, 723–738.e5.

352. Torraca, V, Otto, NA, Tavakoli-Tameh, A, and Meijer, AH (2017) The inflammatory chemokine Cxcl18b exerts neutrophil-specific chemotaxis via the promiscuous chemokine receptor Cxcr2 in zebrafish. Dev Comp Immunol, *67*, 57–65.

353. Triggiani, M, Granata, F, Giannattasio, G, and Marone, G (2005) Secretory phospholipases A2 in inflammatory and allergic diseases: not just enzymes. J Allergy Clin Immunol, *116*, 1000–1006.

354. Troll, JV, Hamilton, MK, Abel, ML, Ganz, J, Bates, JM, Stephens, WZ, Melancon, E, van der Vaart, M, Meijer, AH, Distel, M, Eisen, JS, and Guillemin, K (2018) Microbiota promote secretory cell determination in the intestinal epithelium by modulating host Notch signaling. Development, *145*,

355. Uribe, A, Alam, M, Midtvedt, T, Smedfors, B, and Theodorsson, E (1997) Endogenous prostaglandins and microflora modulate DNA synthesis and neuroendocrine peptides in the rat gastrointestinal tract. Scand J Gastroenterol, *32*, 691–699.

356. van de Wetering, M, Sancho, E, Verweij, C, de Lau, W, Oving, I, Hurlstone, A, van der Horn, K, Batlle, E, Coudreuse, D, Haramis, AP, Tjon-Pon-Fong, M, Moerer, P, van den Born, M, Soete, G, Pals, S, Eilers, M, Medema, R, and Clevers, H (2002) The beta-catenin/TCF-4 complex imposes a crypt progenitor phenotype on colorectal cancer cells. Cell, *111*, 241–250.

357. van der Flier, LG, and Clevers, H (2009) Stem cells, self-renewal, and differentiation in the intestinal epithelium. Annu Rev Physiol, *71*, 241–260.

358. van der Flier, LG, van Gijn, ME, Hatzis, P, Kujala, P, Haegebarth, A, Stange, DE, Begthel, H, van den Born, M, Guryev, V, Oving, I, van Es, JH, Barker, N, Peters, PJ, van de Wetering, M, and Clevers, H (2009) Transcription factor achaete scute-like 2 controls intestinal stem cell fate. Cell, *136*, 903–912.

359. Van der Sluis, M, De Koning, BA, De Bruijn, AC, Velcich, A, Meijerink, JP, Van Goudoever, JB, Büller, HA, Dekker, J, Van Seuningen, I, Renes, IB, and Einerhand, AW (2006) Muc2-deficient mice spontaneously develop colitis, indicating that MUC2 is critical for colonic protection. Gastroenterology, *131*, 117–129.

360. van Es, JH, van Gijn, ME, Riccio, O, van den Born, M, Vooijs, M, Begthel, H, Cozijnsen, M, Robine, S, Winton, DJ, Radtke, F, and Clevers, H (2005) Notch/gamma-secretase inhibition turns proliferative cells in intestinal crypts and adenomas into goblet cells. Nature, *435*, 959–963.

361. van Soest, JJ, Stockhammer, OW, Ordas, A, Bloemberg, GV, Spaink, HP, and Meijer, AH (2011) Comparison of static immersion and intravenous injection systems for exposure of zebrafish embryos to the natural pathogen Edwardsiella tarda. BMC Immunol, *12*, 58.

362. Van Winkle, JA, Peterson, ST, Kennedy, EA, Wheadon, MJ, Ingle, H, Desai, C, Rodgers, R, Constant, DA, Wright, AP, Li, L, Artyomov, MN, Lee, S, Baldridge, MT, and Nice, TJ (2022) Homeostatic interferon-lambda response to bacterial microbiota stimulates preemptive antiviral defense within discrete pockets of intestinal epithelium. Elife, *11*,

363. Varas, M, Ortíz-Severín, J, Marcoleta, AE, Díaz-Pascual, F, Allende, ML, Santiviago, CA, and Chávez, FP (2017) Salmonella Typhimurium induces cloacitis-like symptomsin zebrafish larvae. Microb Pathog, *107*, 317–320.

364. Venkatachalam, AB, Thisse, C, Thisse, B, and Wright, JM (2009) Differential tissue-specific distribution of transcripts for the duplicated fatty acid-binding protein 10 (fabp10) genes in embryos, larvae and adult zebrafish (Danio rerio). FEBS J, *276*, 6787–6797.

365. Vermeulen, L, and Snippert, HJ (2014) Stem cell dynamics in homeostasis and cancer of the intestine. Nat Rev Cancer, *14*, 468–480.

366. Vidrich, A, Buzan, JM, Brodrick, B, Ilo, C, Bradley, L, Fendig, KS, Sturgill, T, and Cohn, SM (2009) Fibroblast growth factor receptor-3 regulates Paneth cell lineage allocation and accrual of epithelial stem cells during murine intestinal development. Am J Physiol Gastrointest Liver Physiol, *297*, G168–78.

367. von Moltke, J, Ji, M, Liang, HE, and Locksley, RM (2016) Tuft-cell-derived IL-25 regulates an intestinal ILC2-epithelial response circuit. Nature, *529*, 221–225.

368. Wallace, KN, Akhter, S, Smith, EM, Lorent, K, and Pack, M (2005) Intestinal growth and differentiation in zebrafish. Mech Dev, *122*, 157–173.

369. Wallace, KN, and Pack, M (2003) Unique and conserved aspects of gut development in zebrafish. Dev Biol, *255*, 12–29.

370. Wang, D, and Dubois, RN (2010) Eicosanoids and cancer. Nat Rev Cancer, *10*, 181–193.

371. Wang, M, Li, L, Guo, Q, Zhang, S, Ji, D, and Li, H (2016) Identification and expression of a new Ly6 gene cluster in zebrafish Danio rerio, with implications of being involved in embryonic immunity. Fish Shellfish Immunol, *54*, 230–240.

372. Wang, Y, Kaiser, MS, Larson, JD, Nasevicius, A, Clark, KJ, Wadman, SA, Roberg-Perez, SE, Ekker, SC, Hackett, PB, McGrail, M, and Essner, JJ (2010a) Moesin1 and Ve-cadherin are required in endothelial cells during in vivo tubulogenesis. Development, *137*, 3119–3128.

373. Wang, Z, Du, J, Lam, SH, Mathavan, S, Matsudaira, P, and Gong, Z (2010b) Morphological and molecular evidence for functional organization along the rostrocaudal axis of the adult zebrafish intestine. BMC Genomics, *11*, 392.

374. Wen, J, Mercado, GP, Volland, A, Doden, HL, Lickwar, CR, Crooks, T, Kakiyama, G, Kelly, C, Cocchiaro, JL, Ridlon, JM, and Rawls, JF (2021) Fxr signaling and microbial metabolism of bile salts in the zebrafish intestine. Sci Adv, *7*,

375. Westerfield, M. (2000) The zebrafish book. A guide for the laboratory use of zebrafish (Danio rerio). Univ. of Oregon Press, Eugene).

376. WHO, P (2010) Cholera vaccines: WHO position paper-Recommendations. Vaccine, *28*, 4687–4688.

377. Wilen, CB, Lee, S, Hsieh, LL, Orchard, RC, Desai, C, Hykes, BL, McAllaster, MR, Balce, DR, Feehley, T, Brestoff, JR, Hickey, CA, Yokoyama, CC, Wang, YT, MacDuff, DA, Kreamalmayer, D, Howitt, MR, Neil, JA, Cadwell, K, Allen, PM, Handley, SA, van Lookeren Campagne, M, Baldridge, MT, and Virgin, HW (2018) Tropism for tuft cells determines immune promotion of norovirus pathogenesis. Science, *360*, 204–208.

378. Wiles, TJ, Jemielita, M, Baker, RP, Schlomann, BH, Logan, SL, Ganz, J, Melancon, E, Eisen, JS, Guillemin, K, and Parthasarathy, R (2016) Host Gut Motility Promotes Competitive Exclusion within a Model Intestinal Microbiota. PLoS Biol, *14*, e1002517.

379. Willett, CE, Cortes, A, Zuasti, A, and Zapata, AG (1999) Early hematopoiesis and developing lymphoid organs in the zebrafish. Dev Dyn, *214*, 323–336.

380. Winkler, ES, Shrihari, S, Hykes, BL, Handley, SA, Andhey, PS, Huang, YS, Swain, A, Droit, L, Chebrolu, KK, Mack, M, Vanlandingham, DL, Thackray, LB, Cella, M, Colonna, M, Artyomov,

MN, Stappenbeck, TS, and Diamond, MS (2020) The Intestinal Microbiome Restricts Alphavirus Infection and Dissemination through a Bile Acid-Type I IFN Signaling Axis. Cell, *182*, 901–918.e18.

381. Winton, DJ, and Ponder, BA (1990) Stem-cell organization in mouse small intestine. Proc Biol Sci, *241*, 13–18.

382. Wu, SH, Lin, HJ, Lin, WF, Wu, JL, and Gong, HY (2018) A potent tilapia secreted granulin peptide enhances the survival of transgenic zebrafish infected by Vibrio vulnificus via modulation of innate immunity. Fish Shellfish Immunol, *75*, 74–90.

383. Wu, XM, Cao, L, Nie, P, and Chang, MX (2019) Histone H2A cooperates with RIP2 to induce the expression of antibacterial genes and MHC related genes. Dev Comp Immunol, *101*, 103455.

384. Xu, J, and Gordon, JI (2003) Honor thy symbionts. Proc Natl Acad Sci U S A, *100*, 10452–10459.

385. Yamashita, J, Ohmoto, M, Yamaguchi, T, Matsumoto, I, and Hirota, J (2017) Skn-1a/Pou2f3 functions as a master regulator to generate Trpm5-expressing chemosensory cells in mice. PLoS One, *12*, e0189340.

386. Yang, J, Chan, CY, Jiang, B, Yu, X, Zhu, GZ, Chen, Y, Barnard, J, and Mei, W (2009) hnRNP I inhibits Notch signaling and regulates intestinal epithelial homeostasis in the zebrafish. PLoS Genet, *5*, e1000363.

387. Ye, L, Mueller, O, Bagwell, J, Bagnat, M, Liddle, RA, and Rawls, JF (2019) High fat diet induces microbiota-dependent silencing of enteroendocrine cells. Elife, *8*,

388. Yu, C, Jiang, S, Lu, J, Coughlin, CC, Wang, Y, Swietlicki, EA, Wang, L, Vietor, I, Huber, LA, Cikes, D, Coleman, T, Xie, Y, Semenkovich, CF, Davidson, NO, Levin, MS, and Rubin, DC (2010) Deletion of Tis7 protects mice from high-fat diet-induced weight gain and blunts the intestinal adaptive response postresection. J Nutr, *140*, 1907–1914.

389. Zhang, D, Golubkov, VS, Han, W, Correa, RG, Zhou, Y, Lee, S, Strongin, AY, and Dong, PD (2014) Identification of Annexin A4 as a hepatopancreas factor involved in liver cell survival. Dev Biol, *395*, 96–110.

390. Zhang, Q, Widmer, G, and Tzipori, S (2013) A pig model of the human gastrointestinal tract. Gut Microbes, *4*, 193–200.

391. Zitvogel, L, Galluzzi, L, Viaud, S, Vétizou, M, Daillère, R, Merad, M, and Kroemer, G (2015) Cancer and the gut microbiota: an unexpected link. Sci Transl Med, *7*, 271ps1.